INSTYTUT KATALIZY I FIZYKOCHEMII POWIERZCHNI

im. Jerzego Habera

POLSKIEJ AKADEMII NAUK

Nowe estry cukrów i kwasów (R)-3-hydroksyalkanowych – synteza, charakterystyka fizykochemiczna oraz ocena ich potencjału biologicznego

Rozprawa doktorska

mgr Wojciech Snoch

Pierwszy promotor: Dr hab. Maciej Guzik, prof. IKiFP PAN, Instytut Katalizy i Fizykochemii Powierzchni im. Jerzego Habera Polskiej Akademii Nauk

Drugi promotor: Prof. Dr hab. Andrzej Bojarski, Instytut Farmakologii im. Jerzego Maja Polskiej Akademii Nauk

Promotor pomocniczy: Dr Jakub Staroń, Instytut Farmakologii im. Jerzego Maja Polskiej Akademii Nauk

Podziękowania

Pragnę podziękować przede wszystkim moim kochanym rodzicom Andrzejowi Snochowi i Joannie Snoch, którzy zawsze okazują mi wiele wsparcia, a także bratu Marcinowi i siostrze Dorocie.

Ponadto dziękuję mojemu promotorowi, dr. hab. Maciejowi Guzikowi, za ogrom wiedzy i umiejętności, które mi przekazał, życzliwe podejście do wielu spraw, oraz możliwość realizacji prac badawczych pod Jego opieką.

Dziękuję drugiemu promotorowi, prof. dr. hab. Andrzejowi Bojarskiemu, za możliwość realizacji części pracy związanej z syntezami organicznymi w laboratorium Zakładu Chemii Leków Instytutu Farmakologii im. Jerzego Maja PAN, a przede wszystkim za niezwykle cenne wskazówki merytoryczne i stylistyczne, których udzielał w trakcie przygotowywania niniejszej dysertacji.

Słowa wdzięczności chciałbym skierować do dr. Ryszarda Bugno za wszelką pomoc, konsultacje merytoryczne, cierpliwość i przyjazne nastawienie oraz dobre praktyki, jakich mogłem się nauczyć w Zakładzie Chemii Leków.

Dziękuję Prof. dr. hab. Maciejowi Szaleńcowi za pełnienie funkcji promotora i opiekę na początkowym etapie moich studiów doktorskich.

Jestem ogromnie wdzięczny mojemu promotorowi pomocniczemu dr Jakubowi Staroniowi, od którego nauczyłem się i wciąż uczę bardzo wiele, m.in. umiejętności niezbędnych w laboratorium chemii organicznej, a także interpretacji widm spektroskopowych i wyników naukowych. Zawsze mogłem i mogę liczyć na serdeczność, konsultacje merytoryczne, serdeczność, wsparcie na każdym z etapów badań, a także poza laboratorium na wiedzę życiową i twórcze podejście do trudnych zagadnień.

Kieruje słowa wdzięczności i uznania do wszystkich kolegów i koleżanek IKiFP PAN, a w szczególności do członkiń i członków zespołu Biokatalizy Teoretycznej i Eksperymentalnej, z którymi miałem przyjemność dzielić radość i znoje pracy naukowej na co dzień.

Rozprawa doktorska powstała w trakcie realizacji Środowiskowych Studiów Doktoranckich w ramach projektu nr POWR.03.02.00-00-1013/16, „Interdyscyplinarność dla medycyny innowacyjnej: InterDokMed, realizowanych w ramach programu operacyjnego Wiedza Edukacja Rozwój 2014–20 Współfinansowanych ze środków Europejskiego Funduszu Społecznego

Fundusze Europejskie Wiedza Edukacja Rozwój

Unia Europejska Europejski Fundusz Społeczny

NARODOWE CENTRUM NAUKI

Badania zostały przeprowadzone również w ramach realizacji projektów: SONATA no. 2015/17/D/ST4/00514 finansowanego przez Narodowe Centrum Nauki, A także Tango V–A/0013/2021 finansowanego przez Narodowe Centrum Nauki oraz Narodowe Centrum Badań i Rozwoju

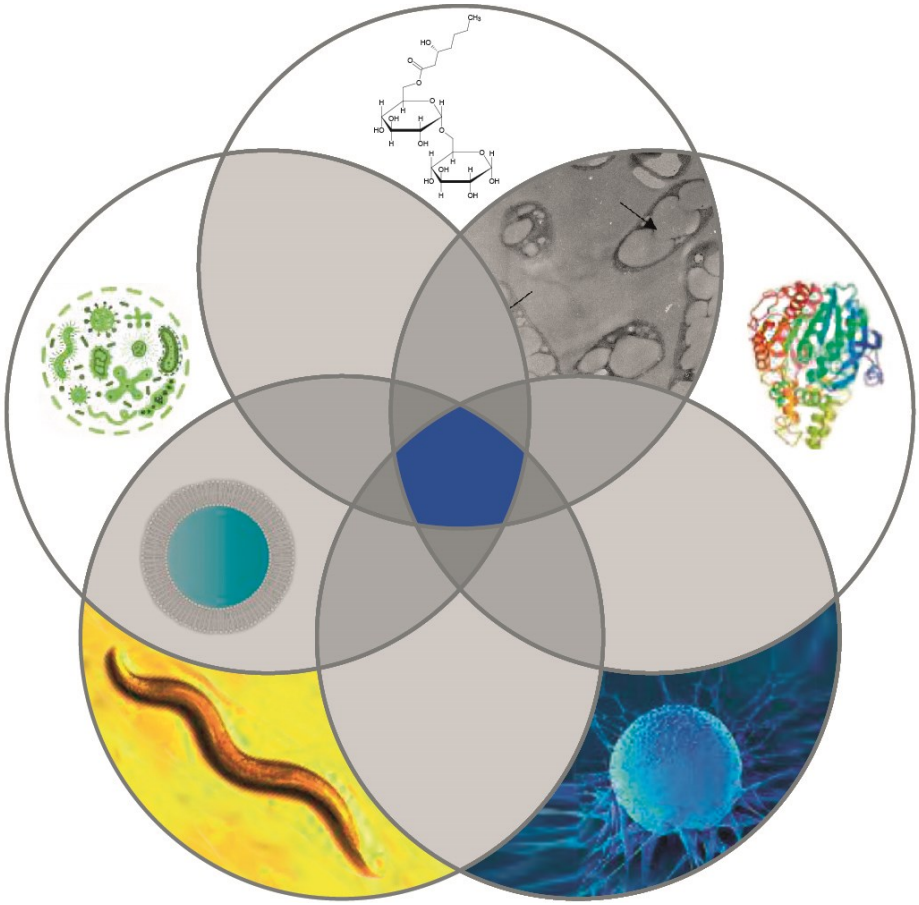

Współpraca

Instytut Farmakologii im. Jerzego Maja Polskiej Akademii Nauk (IF PAN)

Zakład Biologii Komórki, Wydział Biochemii, Biofizyki i Biotechnologii Uniwersytetu Jagiellońskiego (ZBK WBBiB UJ)

Institute of Molecular Genetics and Genetic Engineering (IMGGE), University of Belgrade

Zakład Mikrobiologii Farmaceutycznej i Bioanalityki, Warszawski Uniwersytet Medyczny (ZMF WUM)

Spis treści

Streszczenie (Pl)

W niniejszej pracy ukazany został obecny stan wiedzy na temat zastosowania estrów cukrowych kwasów tłuszczowych (w skrócie: ECKT) w przemyśle spożywczym, kosmetycznym, a także w medycynie i farmacji. Podsumowano dotychczas przebadane i stosowane metody syntezy chemicznej i enzymatycznej ECKT. Następnie omówiono różnorodność komponenty hydrofilowej estrów, tj. samych cukrów, z naciskiem na dostępność tych źródeł w przyrodzie i przemyśle, na przykładzie laktozy (lac). W dalszej części pracy przedstawiono różnorodność oraz samą rolę komponenty hydrofobowej estrów, a także wpływ jej budowy oraz modyfikacji na właściwości ECKT, a co za tym idzie – na ich zastosowanie. Po przedstawieniu tego aspektu zaprezentowano stan wiedzy dotyczący wykorzystania bakteryjnych polihydroksyalkanianów (w skrócie: PHA) nie tylko jako polimery użyteczne w medycynie, ale również jako cenne źródło komponenty hydrofobowej dla ECKT. Podjęta została próba wyjaśnienia, jak ten potencjał może być wzmocniony dzięki wybranym modyfikacjom chemicznym monomerów PHA. Po części teoretycznej przedstawiona została część eksperymentalna, w której omówiono dobór warunków syntezy enzymatycznej ECKT i ich analizy (jakościowa i ilościowa HPLC-MS, GC). By przejść do dalszych etapów i spełnić główne cele aplikacyjne projektu, konieczne było przełożenie procesu syntezy i oczyszczania produktów ze skali analitycznej do miligramowej/gramowej. Dzięki temu możliwe było również określenie struktury uzyskanych związków metodami spektroskopowymi. Dalej, po uzyskaniu większych ilości modyfikowanych i niemodyfikowanych ECKT, istotnym celem było określenie zdolności do tworzenia/stabilizacji emulsji przez uzyskane surfaktanty na podstawie pomiarów wartości: zmian napięcia powierzchniowego w czasie oraz w zależności od stężenia roztworu danego estru, w celu wyliczenia krytycznego stężenia agregacji. Dane te posłużyły do zaprojektowania przykładowych układów emulsyjnych olej/woda na bazie komercyjnie dostępnej oliwki do pielęgnacji skóry oraz skwalanu – stabilizowanych wybranymi estrami. Wyniki te i ich interpretacja są niezbędne do zweryfikowania realnych celów aplikacyjnych – możliwości zastosowania ECKT w przemyśle. Zwieńczenie całego procesu badawczego stanowi weryfikacja potencjału biologicznego nowo wytworzonych ECKT: działania antyproliferacyjnego estrów względem komórek nowotworowych na przykładzie raka prostaty i ludzkiego czerniaka, a także potencjału antybakteryjnego i antygrzybicznego względem popularnych patogenów i organizmów oportunistycznych. Powyższe aspekty biologiczne estrów dodatkowo zostały uzupełnione o ich możliwy wpływ na środowisko na podstawie toksyczności względem

Caenorhabditis elegans. Całość pracy stanowi zestaw czterech artykułów naukowych opublikowanych w trakcie realizacji pracy doktorskiej, cytowanych w odpowiednich miejscach i opatrzonych uzupełnieniami i komentarzami. Autor rozprawy jest zarazem pierwszym współautorem wszystkich publikacji i miał znaczący wkład w ich wykonanie oraz redakcję.

Abstract (Eng)

This work shows the current state of knowledge on the application of sugar esters of fatty acids (ECKT) in the food, cosmetic and pharmaceutical industries. The chemical and enzymatic methods of ECKT synthesis that have been studied and used to date were summarized. This was followed by a discussion of the diversity of the hydrophilic components of the esters, i.e. the sugars themselves, their accessibility in nature and industry, using lactose (lac) as an example. The following part of the paper focuses on the diversity and role of the hydrophobic component of the esters, as well as the influence of its structure and modification on the properties of ECKTs and, consequently, on their application. Having presented this aspect, the state of knowledge regarding the use of bacterial polyhydroxyalkanoates (PHA) not only as polymers useful for medical application, but also as a valuable source of hydrophobic components for ECKT was exposed. An attempt is made to explain how this potential can be enhanced by selected chemical modifications of PHA monomers. After the theoretical part, the experimental part was presented, in which a selection of conditions for the enzymatic synthesis of ECKT and their analysis (qualitative and quantitative HPLC-MS, GC) was discussed. In order to proceed further and meet the main application goals of the project, it was necessary to transfer the process of synthesis and purification of products from the analytical scale to the milligram/gram scale. This also made it possible to determine structures of the obtained compounds using spectroscopic methods. After obtaining larger quantities of modified and unmodified ECKTs, the next important goal was determining the ability of the obtained surfactants to form or stabilize emulsions. In order to do that measurements of surface tension changes in time and as a function of given ester concentration were performed. That allowed to calculate the critical aggregation concentration. These data were used to design sample oil/water emulsion systems based on commercially available skin care oils and squalane – which were stabilized with selected esters. These results and their interpretation are necessary to verify the real application goals – the possibility of using ECKT in the industry. The culmination of the research process is the verification of the biological potential of the newly synthesized ECKTs: antiproliferative effect of the esters against cancer cells, using prostate cancer and human melanoma as examples, as well as the antibacterial and antifungal potential against common pathogens and opportunistic organisms. The aforementioned biological aspects of the esters are further complemented by their possible environmental impact based on toxicity against *Caenorhabditis elegans*. The dissertation is a set of four scientific articles published during the whole research process. The articles were cited and

supplemented by additional comments and discussion. The author of the dissertation is also the first co-author of all the publications and made significant contributions to their editing process.

Lista użytych skrótów

ECKT	Estry cukrowe kwasów tłuszczowych
C9	Kwas nonanowy
C9-Me	Ester etylowy kwasu nonanowego
PHN	poli[(R)-3-hydroksynonanian-ko-(R)3-hydroksyheptanian]
PHPV	poli[(R)-3-hydroksypentanian-ko-(R)-3-hydroksypropionian]
R3OH-C9	Kwas (R)-3-hydroksynonanowy
R3OH-C7	(R)-3-hydroksyheptanowy
mPHN	Mieszanina hydroksykwasów monomerów PHN: (R)-3-hydroksynonanianu i (R)-3-hydroksyheptanianu
mPHN-Me	Mieszanina estrów metylowych monomerów PHN: (R)-3-hydroksynonanianu i (R)-3-hydroksyheptanianu
R3OH-C9-Me	Ester metylowy kwasu (R)-3-hydroksynonanowego
R3OH-C7-Me	Ester metylowy kwasu (R)-3-hydroksyheptanowego
F-mPHN-Me	Mieszanina estrów metylowych fluorowanych monomerów PHN: estry metylowe (R)-3-(2,2,2-trifluoroetoksy)nonanianu i (R)-3-(2,2,2-trifluoroetoksy)heptanianu
glu	α-D-glukopiranoza
gal	β-D-galaktopiranoza
lac	Laktoza: β-D-Galaktopiranozylo-(1→4)-D-Glukopiranoza
C9-glu	Ester glukozowy kwasu nonanowego
C9-gal	Ester galaktozowy kwasu nonaowego
C9-lac	Ester laktozowy kwasu nonanowego
mPHN-glu	Mieszanina estrów glukozy monomerów PHN: (R)-3-hydroksynonanianu i (R)-3-hydroksyheptanianu
mPHN-gal	Mieszanina estrów galaktozy monomerów PHN: (R)-3-hydroksynonanianu i (R)-3-hydroksyheptanianu
mPHN-lac	Mieszanina estrów laktozy monomerów PHN: (R)-3-hydroksynonanianu i (R)-3-hydroksyheptanianu
F-mPHN-glu	Mieszanina estrów glukozy fluorowanych monomerów PHN: (R)-3-(2,2,2–trifluoroetoksy)nonanianu i (R)-3-(2,2,2–trifluoroetoksy)heptanianu
F-mPHN-gal	Mieszanina estrów galaktozy fluorowanych monomerów PHN: (R)-3-(2,2,2–trifluoroetoksy)nonanianu i (R)-3-(2,2,2–trifluoroetoksy)heptanianu
F-mPHN-lac	Mieszanina estrów laktozy fluorowanych monomerów PHN: (R)-3-(2,2,2–trifluoroetoksy)nonanianu i (R)-3-(2,2,2–trifluoroetoksy)heptanianu
CalB	Immobilizowana lipaza B z grzyba *Candida antarctica*
TL-IM	Immobilizowana lipaza z grzyba *Thermomyces lanuginosus*
HTB140	Linia komórkowa ludzkiego czerniaka skóry
Du145	Linia komórkowa ludzkiego raka prostaty
HSF	Linia komórkowa ludzkich fibroblastów skórnych
HaCAT	Linia komórkowa ludzkich keratynocytów skórnych
PNT2	Linia komórkowa ludzkiego nabłonka prostaty
DMSO	Dimetylosulfotlenek
DMF	Dimetyloformamid
THF	Tetrahydrofuran
HLB	Równowaga hydrofilowo-lipofilowa (Hydrophilic-Lipophilic Balance)
CAC	Krytyczne stężenie agregacji
NMP	N-metylopirolidon

Graficzne przedstawienie zakresu prac badawczych

Synteza polimeru – źródła komponenty hydrofobowej estrów

Synteza poli 3–(R)–hydroksynonanianu–ko–heptanianu (PHN)
w procesie fermentacji przy użyciu bakterii:
Pseudomonas putida KT2440

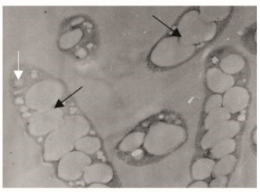

Depolimeryzacja PHN i modyfikacja monomerów

Biokataliza i analiza reagentów

Synteza estrów cukrowych kwasów tłuszczowych (ECKT),
katalizowana immobilizowanymi lipazami

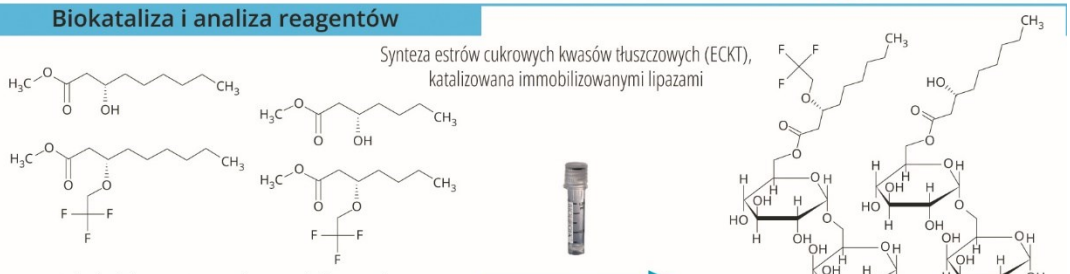

Komponenta hydrofobowa: estry metylowe modyfikowanych
i niemodyfikowanych monomerów (mPHN) lub kwasu nonanowego (C9-Met)

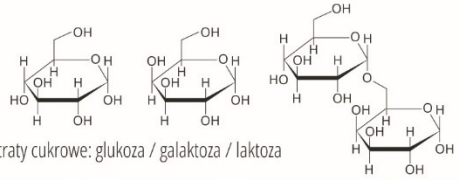

Substraty cukrowe: glukoza / galaktoza / laktoza

Detekcja reagentów za pomocą UHPLC-MS i GC

Zwiększenie skali

Synteza i oczyszczanie modyfikowanych i niemodyfikowanych ECKT
w skali preparatywnej

Oznaczanie struktur ECKT

Analizy struktur za pomocą metod spektroskopowych:
UHPLC–MS, IR, HNMR

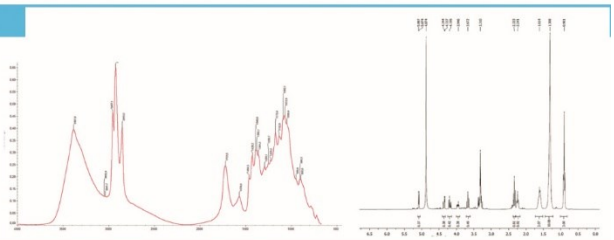

Badania fizykochemiczne

- Pomiary zmiany napięcia powierzchniowego roztworów niemodyfikowanych ECKT
- Wyznaczenie krytycznego stężenia agregacji (CAC)
- Badanie zdolności ECKT do stabilizacji emulsji

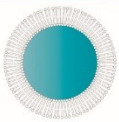

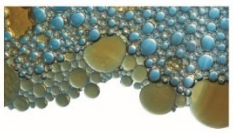

Badania biologiczne in vitro

Oznaczanie
przeciwbakteryjnych
i przeciwgrzybicznych
właściwości wybranych ECKT

Oznaczanie
antyproliferacyjnych
właściwości ECKT
na komórkach rakowych

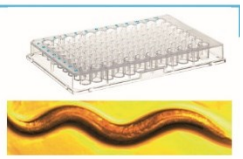

Testy toksyczności na *C. elegans*

1. Wstęp i przybliżenie głównych problemów badawczych

1.1. Problem chorób nowotworowych

Choroby nowotworowe to jedne z najbardziej śmiercionośnych schorzeń na świecie. Według World Human Organization oraz instytucji Globocan w 2021 roku zachorowało ok. 19,29 mln osób. Choroby te spowodowały niemal 10 mln zgonów. Ponadto tego samego roku choroba nowotworowa dotknęła ok. 400 000 dzieci [1]. Rak płuc, prostaty, jelita grubego, żołądka i wątroby to najczęstsze rodzaje nowotworów u mężczyzn, podczas gdy rak piersi, jelita grubego, płuc, szyjki macicy i tarczycy są najczęstsze wśród kobiet [1]. Poniżej zamieszczono statystyki obrazujące skalę i rodzaje chorób nowotworowych.

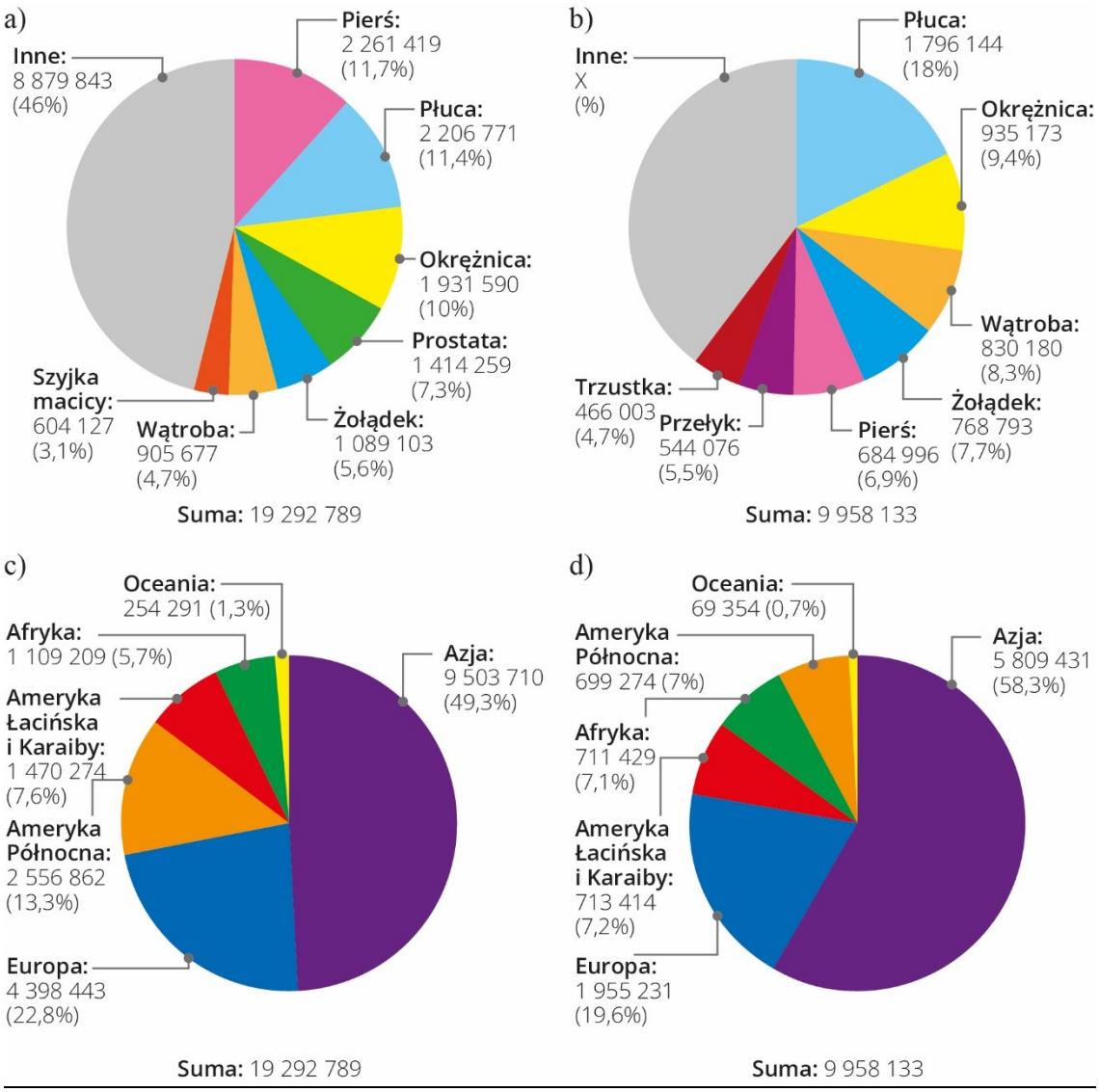

Rys. 1. Statystyki zachorowań i umieralności na choroby nowotworowe w roku 2021: a) nowe przypadki zachorowań na świecie, b) Statystka śmierci, c) Statystyki zachorowań na poszczególnych kontynentach, d) Statystyki śmierci na poszczególnych kontynentach. Zmodyfikowano na podstawie [1]

Ponadto w czasie pandemii spowodowanej wirusem SARS-CoV-2 dostęp do opieki zdrowotnej został ograniczony nawet w krajach rozwiniętych, a osoby w trakcie terapii, mające obniżoną odporność, były dodatkowo wystawione na powikłania związane z infekcją wirusa [2, 3]. Stąd zapotrzebowanie na nowe rodzaje terapii, nowe leki i strategie leczenia nadal rośnie.

Obecnie najpowszechniejsze podejście kliniczne do walki z chorobami nowotworowymi opiera się na terapii skojarzonej, tj. odpowiednim i opcjonalnym doborze i zastosowaniu następujących technik: operacja chirurgiczna usuwająca guz z ciała pacjenta, chemio-, radio-, foto-, termo- i krioterapia. Każda z tych technik jest dobierana indywidualnie i dostosowana do pacjenta w zależności od płci, wieku, zaawansowania choroby i rodzaju nowotworu [4]. Dodatkowo, czasami niezbędne staje się uzupełnienie protokołu o terapię celowaną lub tzw. szczepionki przeciwnowotworowe. Polegają one na podawaniu specjalnie wyhodowanych przeciwciał monoklonalnych znakujących dany typ komórek nowotworowych pobranych od pacjenta/pacjentki bądź immunizowanie pacjenta/pacjentki poprzez podawanie wersji jego/jej komórek nowotworowych w nieszkodliwej formie [5–8]. Do głosu doszła również nanotechnologia, która udostępniła całą paletę różnych nośników: nanocząstek, nanorurek, nanokapsułek zwiększających selektywność leków, ułatwiających dostarczenie leków w konkretne miejsca znajdywania się ognisk przerzutowych oraz ich wchłanianie [9–11].

Dzięki wprowadzeniu i rozpowszechnieniu szczepionek mRNA przeciw wirusowi SARS-CoV-2 dokonano znaczących postępów w rozwoju nowych leków i rozwinięto technologię szczepionek przeciwnowotworowych bazujących na miRNA, siRNA oraz ssDNA. Cząsteczki te podawane są za pomocą wektorów wirusowych bądź nanokapsułek stabilizowanych estrami, w tym ECKT [12, 13].

Jednakże popyt na nowe leki lub ich formy i technologie ich dostarczania nie spada, gdyż komórki nowotworowe mutują i uodparniają się na nowe generacje leków [14, 15]. Ponadto koszty leków i terapii są często duże i limitują powszechność (zwłaszcza w krajach rozwijających się). Dodatkowym problemem, na który należy zwrócić uwagę przemysłu farmaceutycznego, jest cyrkulacja toksycznych cząstek i ugrupowań mutagennych i kancerogennych w środowisku. Zużyte leki, które niszczą komórki nowotworowe bądź ich substraty/produkty uboczne, gdy dostają się do wód, gleb i organizmów zdrowych, same działają mutagennie i kancerogennie [14, 15]. Stąd potrzeba poszukiwania nie tylko samych strategii i nowych związków, lecz także związków o niskiej toksyczności, łatwo

biodegradowalnych i zwiększających wchłanianie już dostępnych komercyjnie leków tak, by móc skutecznie je używać w niższych stężeniach [16, 17].

Ze względu na wyżej wymienione aspekty modyfikowalne ECKT stanowią obiecujący materiał badawczy w procesie poszukiwania alternatywy lub wzmocnienia konwencjonalnych terapii przeciwnowotworowych. Mogą z jednej strony przekazywać konkretne (toksyczne dla komórek nowotworowych) ugrupowania, a z drugiej być łatwo degradowane przez lipazy i esterazy obecne we wszystkich organizmach żywych.

1.2. Estry cukrowe kwasów tłuszczowych

Estry cukrowe należą do klasy związków biodegradowalnych i bioaktywnych, które zwróciły uwagę naukowców i przemysłu w ostatnich dziesięcioleciach [18–20]. Cząsteczki te składają się z hydrofilowej komponenty cukrowej (bogatej w grupy hydroksylowe) połączonej wiązaniami estrowymi z częścią hydrofobową – zwykle kwasem karboksylowym. Liczba i długość tych łańcuchów kwasowych wraz z liczbą grup hydroksylowych danego cukru określają równowagę hydrofilowo-lipofilową (*Hydrophilic-Lypophilic Balance*, w skrócie: HLB) – unikalną właściwość danej cząsteczki estru cukru. Jednocześnie ich budowa chemiczna umożliwia tworzenie miceli i emulsji oraz stabilizację pian dzięki właściwościom powierzchniowo czynnym. Cechy te przekładają się na praktyczne zastosowanie estrów cukrowych kwasów tłuszczowych, dlatego są one szeroko wykorzystywane w przemyśle spożywczym, kosmetycznym i farmaceutycznym (jako dodatki do produktów mlecznych, pasz, kremów, żeli, szamponów, past, maści). ECKT mogą wpływać także na organizmy żywe, np. zwiększają przepuszczalność błon komórkowych i inaktywują białka transbłonowe, narażając w ten sposób drobnoustroje na niekorzystne czynniki zewnętrzne, utratę białek wewnątrzkomórkowych i cennych składników odżywczych, prowadząc do śmierci mikroorganizmu. Wśród estrów cukrów najbardziej popularne są te, które zawierają glukozę, galaktozę, sacharozę lub laktozę ze względu na ich dużą dostępność z zasobów naturalnych.

1.3. Laktoza – odpad przemysłowy źródłem komponenty hydrofilowej dla ECKT

Największymi producentami mleka na świecie są USA i Unia Europejska. Szacuje się, że gospodarka UE wyprodukowała szacunkowo 161,0 mln ton surowego mleka w 2021 r., co oznacza wzrost o 0,7 mln względem poprzedniego roku. Zdecydowana większość mleka

surowego (150,7 mln ton) trafiła do mleczarni, pozostała część została wykorzystana bezpośrednio w gospodarstwach. Mleko to użyto do produkcji zarówno świeżych i przetworzonych produktów mlecznych. Szacuje się, że tego roku mleczarnie wyprodukowały ok. 2,3 mln ton masła i produktów maślanych z 44,4 mln ton pełnego mleka, 10,4 mln ton sera z 61,4 mln ton mleka pełnego i 16,4 mln ton mleka odtłuszczonego, a także 23,2 mln ton mleka spożywczego z 13,0 mln ton mleka pełnego i 10,0 mln ton mleka odtłuszczonego [23]. Z kolei USA w 2019 r. wyprodukowało około 9,9 mln t mleka, które przerobiono głównie na ponad 600 rodzajów sera i mleka w proszku.

Z przemysłu mleczarskiego pozyskuje się dwa główne produkty uboczne: ścieki, w tym woda do mycia i pasteryzacji, oraz serwatkę. Te pierwsze są zmieszane z detergentami i generalnie mają niski wsad organiczny: 2,5 l ścieków na 1 kg przetworzonego mleka. Serwatka natomiast jest silnie obciążającym środowisko produktem przemysłowym, ponieważ na 1 kg sera uzyskuje się 9–10 litrów serwatki. Obecnie około 50% ścieków mleczarskich na świecie jest odprowadzanych do środowiska bez jakiejkolwiek kontroli. Sytuacja ta nie tylko powoduje eutrofizację zbiorników wodnych, lecz także zwiększa koszty oczyszczania wody w oczyszczalniach [24].

Serwatka składa się głównie z laktozy, białka i minerałów (odpowiednio 70–72%, 8–10% i 12–15% suchej masy). Jej pH waha się od 3,3 do 9,0. Zawiera od 0,01 do 1,7 g l^{-1} całkowitego azotu (oznaczanego metodą Kjeldahla NTK); chemiczne zapotrzebowanie na tlen reakcji prowadzących do rozłożenia składników serwatki (COD) to 50–102 g l^{-1}, a biologiczne zapotrzebowanie na tlen mikrorganizmów rozkładających serwatkę (BZT) waha się między 27 a 60 g l^{-1}. Ze względu na te cechy serwatka stanowi atrakcyjny substrat do biologicznego oczyszczania poprzez fermentację beztlenową. Ponadto serwatka może być również wykorzystywana do pozyskiwania między innymi żywności dla niemowląt, wypieków, szczepionek, leków, szamponów i past do zębów. W procesach fermentacji tlenowej przez odpowiednie bakterie można jej użyć nawet do produkcji polihydroksymaślanu (PHB) [25].

Pomimo wysokiej wartości odżywczej około połowa wytworzonej objętości serwatki jest nadal niewłaściwie wykorzystywana lub utylizowana, co powoduje szkody w ekosystemie. Biorąc pod uwagę stały wzrost rocznej produkcji sera, również ilość wytwarzanej serwatki wzrasta, co wymaga nowych strategii w celu poprawy jej wykorzystania i zastosowania. Ze względu na ilość dziennej produkcji, jakość odżywczą i potencjał w przemyśle, cieszy się ona dużym zainteresowaniem branży żywnościowej [24].

Chociaż w ostatnich latach popyt na laktozę się zwiększył, jest mało prawdopodobne, aby istniał zyskowny rynek dla całej potencjalnie dostępnej laktozy. Ponieważ usuwanie serwatki lub odpadów ultrafiltracji przez zrzucanie do dróg wodnych nie jest już dozwolone, poszukiwano sposobów wykorzystania laktozy. Przez wiele lat za najbardziej obiecujące uważano hydrolizę do glukozy i galaktozy, ale inne modyfikacje cieszą się coraz większym zainteresowaniem [26].

Laktoza może być hydrolizowana do glukozy i galaktozy przez enzymy (β-galaktozydazy, powszechnie nazywane laktazą) lub kwasy. Komercyjnymi źródłami β-galaktozydazy są grzyby pleśniowe (zwłaszcza *Aspergillus* spp.), których enzymy mają optymalne kwaśne pH, oraz drożdże (*Kluyveromyces* spp.), które wytwarzają enzymy o optymalnym pH obojętnym [27]. β-galaktozydazy stały się dostępne na rynku i stanowią potencjał komercyjny przy przemysłowym rozwiązywaniu „problemu serwatki" i wyjścia na przeciw ludziom cierpiących na nietolerancję laktozy [27].

Uwzględniając powyższe uwarunkowania, zauważono, że zarówno laktoza, jak i jej składowe mogą być łatwym i tanim do pozyskania na skalę przemysłową substratem do syntezy związków bioaktywnych. Rozszerzenie zaś zakresu wykorzystania tego cukru i jego składowych w farmacji i przemyśle kosmetycznym wpisuje się w idee zielonej gospodarki. Dlatego zdecydowano wykorzystać właśnie te cukry do syntezy ECKT będących przedmiotem omawianej pracy badawczej.

1.4. Źródła komponenty hydrofobowej ECKT

Rodzaj komponenty hydrofobowej ECKT istotnie wpływa na ich właściwości fizykochemiczne. Decydują o nich: długość łańcucha alifatycznego danego kwasu organicznego, obecność lub brak różnych dodatkowych grup funkcyjnych (np. hydroksylowych, fenylowych, halogenków alkilowych itp.), rozgałęzienie łańcuchów węglowych oraz obecność wiązań nienasyconych. Te wszystkie składowe decydują o promieniu cząsteczki ECKT, jej hydrofobowości, ułożeniu przestrzennym, zdolności do formowania micel i agregowania oraz reaktywności. Za nimi idą zdolności do przenikania przez błony komórkowe, toksyczność i oddziaływania z białkami danego organizmu, które są wystawione na działanie ECKT [20, 27]. Jeśli chodzi o inne zastosowania, ECKT pełnią funkcję ochronną podczas procesu krystalizacji, pomiarów mikroskopowych w wysokiej rozdzielczości oraz przechowywania białek w niskich temperaturach. Dodatek surfaktantów

ułatwia również wyodrębnienie fragmentu błon komórkowych, w których zakotwiczone są białka transbłonowe [28, 29].

W procesie projektowania i produkcji ECKT ważny jest dobór komponenty hydrofobowej, a także źródło jej pochodzenia, by odbywało się z możliwie jak najmniejszym obciążeniem dla środowiska naturalnego. Najpopularniejsze źródła to średnio- lub długołańcuchowe kwasy tłuszczowe pochodzące z modyfikacji frakcji ropy naftowej czy też estry metylowe frakcji diesla, tzw. FAME (*Fatty Acid Methyl Esters*). Innym źródłem łańcuchów mogą być kwasy tłuszczowe pochodzące z ekstrakcji i hydrolizy estrów, jakimi są tłuszcze zwierzęce oraz roślinne (efekt produkcji biodiesla). Oleje roślinne to np. olej sojowy (62% rocznej światowej produkcji olejów roślinnych), palmowy (36,5%), rzepakowy (12,5%), słonecznikowy (9%), kukurydziany, lniany, kokosowy, lawendowy, różany, awokado itp. [30, 33, 34].

Najpopularniejsze kwasy tłuszczowe stosowane w przemysłowej produkcji ECKT to: kwas kapronowy (C6), kaprylowy (C8), kaprynowy C10, laurynowy (C12), mirystynowy (C14), palmitynowy (C15), oleinowy (C16) oraz stearynowy (C18) [35–38].

Jednym z najważniejszych powodów przeprowadzenia badań opisanych w niniejszej rozprawie była idea zastosowania nowego, niestandardowego źródła komponenty hydrofobowej ECKT o stosunkowo tanim pochodzeniu, nieobciążającej środowiska technologii pozyskiwania, małej toksyczności, a przede wszystkim możliwości jej modyfikacji chemicznej i enzymatycznej. Takie cechy mają kwasy tłuszczowe pochodzące z depolimeryzacji bakteryjnych poliestrów – polihydroksyalkanianów (PHA).

1.5. Polihydroksyalkaniany

Polihydroksyalkaniany to poliestry zbudowane ze (*R*)-3-hydroksykwasów. Odkładane są w wewnątrzkomórkowych hydrofobowych granulkach przez liczne bakterie, które zazwyczaj mają średnicę od 0,2 μm do 0,7 μm (przykład widoczny na rys. 2a). Przykładowa struktura polimeru została przedstawiona na rysunku 2b. Oprócz 97,7% zawartości PHA, zawierają też 1,8% białek oraz 0,5% innych lipidów [39, 40]. PHA stanowią materiał zapasowy dla komórki bakteryjnej, syntezowany *de novo* w sytuacji nadmiaru źródła węgla i limitu soli nieorganicznych (np. amonowych, fosforanów, siarczanów czy magnezu). PHA może nawet stanowić do 80% suchej masy komórki [40].

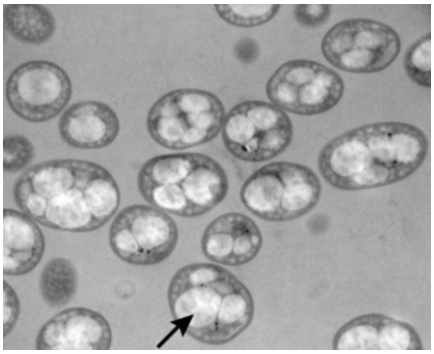

a)

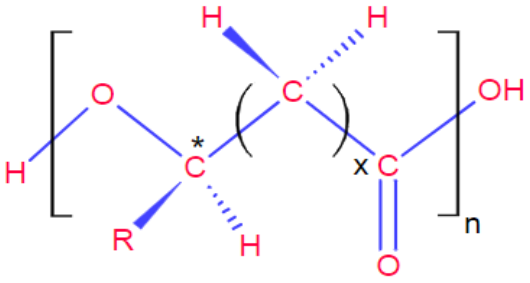

b)

Rys. 2. Przykład PHA: a) granulki PHA zakumulowane w bakteriach *Pseudomonas putida* CA-3 – zmodyfikowano na podstawie [41]; b) wzór półstrukturalny PHA, gdzie n – liczba jednostek monomerycznych w zakresie 100–30 000, * – centrum chiralne, R – reszta z różną liczbą at. C w zakresie 1–18, x – liczba at. C w zakresie 1–3; zmodyfikowano na podstawie [42].

1.5.1. Zastosowania PHA

PHA mają głównie pochodzenie bakteryjne (przynajmniej 119 rodzajów zidentyfikowanych hydroksykwasów), choć są przypadki niektórych genetycznie modyfikowanych roślin zdolnych do ich syntezy [40, 41, 44, 45]. Ich produkcja na skalę przemysłową wspiera rozwój tzw. gospodarki obiegu zamkniętego (*circular economy*), czyli opartej na materiałach odnawialnych i jak najwydajniej wykorzystującej dostępne zasoby naturalne. Źródłem węgla w wielkoskalowych procesach fermentorowych są różne cukry, glicerol z produkcji i obróbki biodiesla, czy oleje i tłuszcze roślinne pozyskane z biorafinerii przetwarzających kukurydzę lub trzcinę cukrową. Nawet odpady z przemysłu zwierzęcego, takie jak łój, też mogą być wykorzystane do produkcji PHA [43, 46, 47]. Ze względu na długość łańcuchów jednostek monomerycznych budujących PHA możemy je podzielić na trzy typy: krótkołańcuchowe, tzw. *short chain length* (scl-PHA C3–C5, włączając w to obecność chiralnego at. C), średniołańcuchowe – *medium chain length* (mcl-PHA, C6–C14) i długołańcuchowe – *long chain length* (lcl-PHA, więcej niż C15) [40, 48]. W zależności od długości, rozgałęzienia łańcuchów bocznych monomerów, obecności kopolimerów, a także obecności grup funkcyjnych, łańcuchy te mogą być różnie upakowywane i dawać różną gęstość, ciężar cząsteczkowy i strukturę polimeru. Powoduje to, że PHA mogą mieć różne właściwości fizyczne i mechaniczne, a co za tym idzie – zastosowanie [41, 49]. Najpopularniejsze zastosowania PHA to folie w rolnictwie, folie spożywcze i kształtki, a w medycynie implanty, stenty i nici chirurgiczne. PHA można też wykorzystać do produkcji układów rozprowadzających leki w tkankach organizmów czy produkcji mikrokapsułek [47–50].

W pracy doktorskiej prezentuję kolejną możliwość zastosowania PHA (na przykładzie polihydroksynonanianu-ko-heptanianu) jako zrównoważonego źródła modyfikowalnych hydroksykwasów do produkcji estrów cukrowych kwasów tłuszczowych.

1.6. Synteza ECKT

1.6.1. Synteza chemiczna

Synteza chemiczna wszystkich estrów cukrowych zachodzi w warunkach bezwodnych. Najlepszymi mediami dla prowadzenia reakcji są takie rozpuszczalniki organiczne, w których można rozpuścić zarówno substrat hydrofobowy, jak i cukier, tj. pirydyna, N-metylopirolidon (NMP), pirolidyna, dimetyloformamid (DMF) oraz dimetylosulfotlenek (DMSO). Jednak z punktu widzenia preparatyki i oczyszczania są to media bardzo trudne do odparowania i odseparowania od produktów. Alternatywą są bezwodne rozpuszczalniki, w których łatwo rozpuścić co prawda jedynie substraty hydrofobowe dla ECKT, za to łatwo je odparować. Przykładami mogą być dichlorometan, metanol, octan etylu, trietyloamina, 2-metylo-2-butanol, tert-butanol. Przy użyciu tego rodzaju mediów reakcyjnych reakcja zachodzi na granicy faz. Substratami hydrofobowymi w tym wypadku są estry metylowe lub winylowe kwasów organicznych, bezwodniki (np. bezwodnik octowy) lub chlorowcowane pochodne kwasów organicznych. Zazwyczaj proces przeprowadza się w obecności sit molekularnych oraz w temperaturze 25–130°C (bardzo rzadko niżej, np. 0°C). Czas trwania tych reakcji – w zależności od katalizatora i warunków – wynosi od kilkunastu sekund do kilku godzin (czasem do 24 h) i pozwala osiągnąć do ok. 90% wydajności.

Co zatem skłania do korzystania z biokatalitycznych dróg otrzymywania ECKT? Jest to przede wszystkim selektywność biokatalizatorów. Ogromne znaczenie ma mniejsza szkodliwość dla środowiska biokatalizatora względem katalizatorów chemicznych, używane media reakcyjne i niższy zakres używanych temperatur w porównaniu do procesów chemicznych. Ponadto, żeby reakcja chemiczna była efektywna, nierzadko trzeba zmodyfikować któryś z substratów (na przykład chlorowanie lub allilowanie substratu kwasowego). Dopiero wtedy można acylować nimi cukry. Ten etap umożliwiają również nie zawsze przyjazne dla środowiska katalizatory np. K_2CO_3, chlorek cynku, chlorek żelaza, H_2/Pd-C, nadchlorek litu, triflat indu czy zeolity. Dla odmiany by uzyskać ECKT z zadowalającą wydajnością przy użyciu enzymów pochodzenia grzybicznego bądź bakteryjnego wystarczy zmetylować jeden z substratów, a niekiedy nawet i to nie jest wymagane. Stąd to enzymy są coraz częściej wybieranymi katalizatorami transestryfikacji. Pełen wachlarz reakcji estryfikacji

zarówno chemicznych, jak i enzymatycznych na przykładzie laktozy został opisany i zestawiony w artykule przeglądowym autorstwa: Staroń, J.; Cichoń, E.; Stefaniak, M.; Guzik, M. [53].

1.6.2. Synteza enzymatyczna ECKT – znaczenie lipaz w procesie syntezy

Spośród ok. 4000 znanych w przyrodzie enzymów, człowiek wykorzystuje w przemyśle ok. 200. W większości są to enzymy pochodzenia bakteryjnego i grzybowego. Ważną funkcję w przemyśle pełnią lipazy, czyli acylohydrolazy triacyloglicerolu (E.C. 3.1.1.3). Mimo, iż są enzymami rozpuszczalnymi w wodzie, hydrolizują wiązania estrowe nierozpuszczalnych w wodzie substratów do bardziej polarnych produktów. Natomiast w warunkach bezwodnych katalizują reakcję odwrotną, tj. syntezę wiązań estrowych, a także transestryfikację, regioselektywne acylowanie alkoholi (np. cukrów, glikoli, metanolu), a także aminowanie, np. syntezę peptydów. Stąd stanowią świetny naturalny katalizator do syntezy ECKT. Lipazy zawierają w centrum aktywnym tzw. triadę katalityczną – sekwencję aminokwasów: seryna-histydyna-kwas asparaginowy (Ser-His-Asp) lub seryna-histydyna-kwas glutaminowy (Ser-His-Glu). Taka budowa centrum aktywnego jest także charakterystyczna dla proteaz serynowych. Znajomość ich struktury odgrywa istotną rolę w projektowaniu i konstruowaniu lipaz do określonych celów [54].

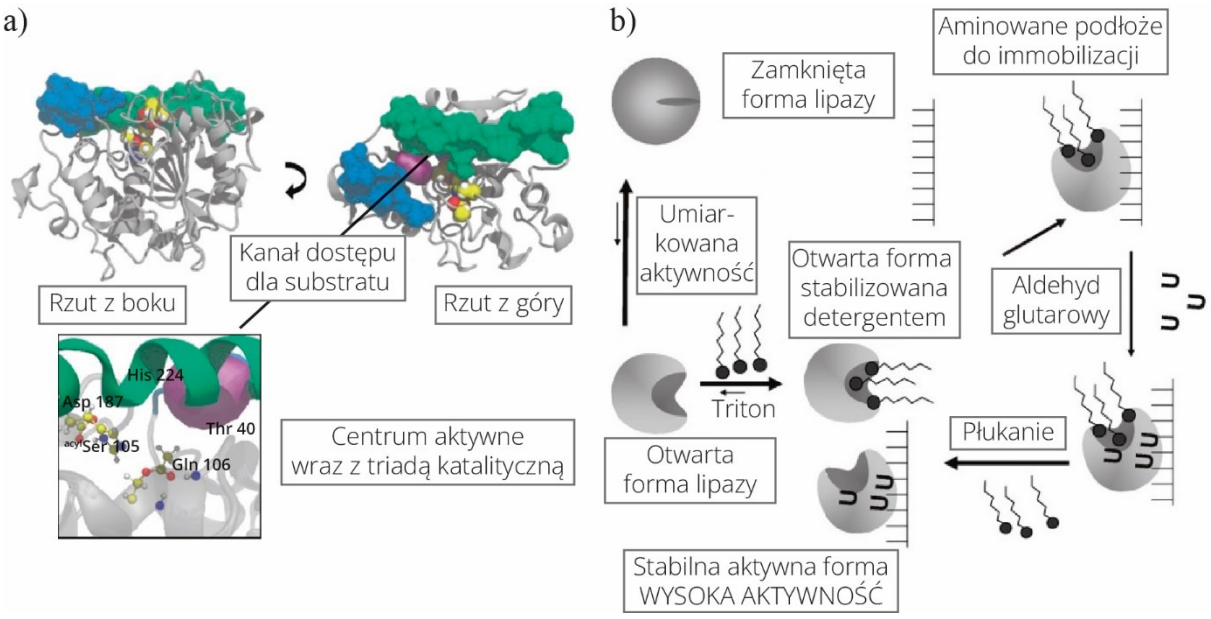

Rys. 3. Schemat działania miejsca aktywnego lipazy: a) struktura lipazy Candida antarctica (CalB): szkielet – kolor szary, wyszczególnione centrum aktywne zawierające triadę katalityczną, w której aminokwas seryna (Ser) sąsiaduje z histydyną (His) i kwasem asparaginowym (Asp): (kolor żółty), wraz z kieszenią przyjmującą substrat (kanał dostępu dla substratu – kolor fioletowy), b) schemat procedury immobilizacji lipazy umożliwiający zwiększenie jej aktywności dzięki stabilizacji detergentem; modyfikowane na podstawie [56, 57].

Immobilizacja zazwyczaj powoduje spadek aktywności enzymów ze względu na agregację i możliwe zasłonięcie dojścia do miejsca aktywnego oraz sam proces nadwyrężający strukturę katalizatora [57]. Z drugiej jednak strony zakotwicza białko oraz stabilizuje fizycznie i termicznie, co pozwala na dłuższe przechowywanie, zwiększa zakres działania (w odniesieniu do pH i temperatury), a także umożliwia ponowne, często kilkukrotne wykorzystanie oraz łatwe odseparowanie od reagentów reakcyjnych. W przypadku lipaz odpowiedni sposób immobilizacji może spowodować wręcz hiperaktywność, gdyż proces umożliwia zmianę konformacji na taką, by spowodować otwarcie miejsca aktywnego (tzw. aktywacja powierzchniowa), a potem unieruchomienie białka (patrz rys. 4). Dlatego zabieg ten jest powszechny przy pracy z lipazami i przy przemysłowym ich wykorzystaniu. Dodatkowo, jeśli chodzi o unieruchomione na złożu lipazy i reakcje estryfikacji, może dochodzić do samoaktywacji enzymów blisko siebie ułożonych [58].

Z powyższych względów, by zsyntezować pożądane ECKT, które są obiektem badawczym tej pracy, użyto katalizatora enzymatycznego, wyżej wymienionego cukru – laktozy (lac) – oraz jej składowych: glukozy (glu) i galaktozy (gal), a jako komponentę hydrofobową wykorzystano estry metylowe kwasu nonanowego (C9), a także mieszaninę estrów metylowych hydroksykwasów pochodzących z depolimeryzacji PHN.

2. Cele pracy

Głównym celem pracy jest synteza, charakterystyka i określenie właściwości biologicznych ECKT. Szczegółowe cele zostały wyróżnione poniżej:

1. Opracowanie metod enzymatycznej syntezy ECKT, a także oznaczania jakościowego, czystości i wydajności procesu. Weryfikacja struktur nowych estrów, a także przeskalowanie procesu z ilości analitycznych do gramowych.
2. Oznaczenie zmian wybranych właściwości fizykochemicznych od stężenia ECKT w wodzie: napięcia powierzchniowego roztworu, krytycznego stężenia agregacji, zdolności do stabilizacji emulsji.
3. Poznanie właściwości przeciwdrobnoustrojowych, w szczególności przeciwbakteryjnych i przeciwdrożdżakowych estrów na bazie glukozy. Przedyskutowanie tych właściwości w kontekście antybiotyków i potencjalnych zastosowań w przemyśle spożywczym i farmaceutycznym.
4. Oznaczenie cytotoksyczności oraz właściwości antyproliferacyjnych modyfikowanych i niemodyfikowanych ECKT względem wybranych linii rakowych oraz komórek referencyjnych. Porównanie tych właściwości z innymi estrami cukrowymi oraz popularnymi cytostatykami. Określenie, jaką rolę w przemyśle i medycynie mogłyby odgrywać nowo zsyntezowane estry.
5. Określenie potencjalnego wpływu badanych związków na środowisko poprzez oznaczenie toksyczności względem modelowych organizmów – nicieni.

3. Wykaz artykułów stanowiących pracę doktorską

(zgodnie z kolejnością ukazania się)

PUBLIKACJA 1 (P1):

Wojciech Snoch, Mateusz Tataruch, Olga Zastawny, Ewelina Cichoń, Mathilde Gosselin, Hubert Cabana, Maciej Guzik "*Hollow silica microspheres as robust immobilization carriers*" 2019, Bioorganic Chemistry 93, 102813; DOI: 10.1016/j.bioorg.2019.02.038

Wkład:
Wykonałem część prac eksperymentalnych dotyczących opracowania ścieżki syntezy estrów cukrowych i ich oznaczania metodami HPLC-MS oraz aktywności badanych lipaz. Przygotowałem wstępną wersję publikacji i metod oraz dyskusji dotyczącej lipaz i syntezy estrów cukrowych.

PUBLIKACJA 2 (P2):

Wojciech Snoch, Karolina Stępień, Justyna Prajsnar, Jakub Staroń, Maciej Szaleniec, Maciej Guzik,*"Influence of Chemical Modifications of Polyhydroxyalkanoate-Derived Fatty Acids on Their Antimicrobial Properties"* 2019, Catalysts, 9(6), 510, DOI: 10.3390/catal9060510

Wkład:
Wykonałem następujące prace eksperymentalne: synteza polimeru – polihydroksynonanianu-ko-heptanianu oraz przeprowadzenie jego oczyszczenia i depolimeryzacji. Dokonałem przeglądu metod modyfikacji hydroksykwasów, w szczególności pod kątem wprowadzenia podstawnika F-alkilowego. Opracowałem metodę jego wprowadzania do grup 3-OH monomerów polihydroksynonanianu-ko-heptanianu. Opracowałem i wykonałem syntezę estrów glukozy za pomocą immobilizowanych lipaz. Przeprowadziłem część analiz UHPLC-MS. Przygotowałem pierwszą wersję całego manuskryptu.

PUBLIKACJA 3 (P3):

Wojciech Snoch, Dawid Wnuk, Tomasz Witko, Jakub Staroń, Andrzej J. Bojarski, Ewelina Jarek, Francisco J. Plou, Maciej Guzik "*In Search of Effective Anticancer Agents–Novel Sugar Esters Based on Polyhydroxyalkanoate Monomers*" 2021, International Journal of Molecular Sciences, 22(13), 7238, DOI: 10.3390/ijms22137238

Wkład:

Opracowałem wstęp manuskryptu na podstawie przeglądu literaturowego. Wykonałem część prac eksperymentalnych: syntezę fermentorową, obróbkę i oczyszczanie polimeru bakteryjnego oraz jego depolimeryzację. Zmodyfikowałem mieszaninę estrów metylowych monomerów wprowadzając fragment alkilowy podstawiony fluorem. Dokonałem syntezy oczyszczenia estrów cukrowych na bazie glukozy, galaktozy i laktozy. Opracowałem metody analityczne UHPLC–MS. Oznaczyłem stężenia i wydajności reakcji. Zinterpretowałem widma IR związków. Uczestniczyłem w procesie interpretacji i dyskusji zdjęć struktur subkomórkowych komórek rakowych z mikroskopu konfokalnego oraz wyników transmigracji. Napisałem pierwszą wersję całego manuskryptu. Opracowałem rysunki, tabele i wykresy oraz suplement. Pełniłem funkcję łącznika pomiędzy współautorami. Odpowiadałem na uwagi recenzentów.

PUBLIKACJA 4 (P4):

Wojciech Snoch, Ewelina Jarek, Dusan Milivojevic, Jasmina Nikodinowic-Runic, Maciej Guzik "*Physicochemical studies of novel sugar fatty acid esters based on (R)-3-hydroxylated acids derived from bacterial polyxydroxyalkanoates and their potential environmental impact"* 2023, Frontiers in Bioengineering and Biotechnology 9(11), 1112053, DOI: 10.3389/fbioe.2023.1112053

Wkład:

Wykonałem większość prac eksperymentalnych (synteza, oczyszczanie, oznaczanie estrów cukrowych, badania fizykochemiczne, część badań toksyczności przeprowadzonych na nicieniach), dokonałem przeglądu literaturowego, napisałem szkic – wersję pierwotną całego manuskryptu, przygotowałem rysunki, wykresy. Opracowałem suplement.

4. Omówienie prac badawczych i publikacji

Wprowadzenie do Publikacji 1

By móc właściwie zrealizować eksperymenty opisane pracy P1 należało dokonać przygotowań polegających na przeglądzie literaturowym dotyczącym metod acylacji różnych dwucukrów (głównie lac i podobnej do niej w budowie sacharozy) łańcuchami alifatycznymi zbliżonymi długością do kwasu nonanowego (to jest C8, C9, C12), za pomocą immobilizowanych lipaz grzybicznych i bakteryjnych. Najważniejsze reakcje estryfikacji i ich warunki (rodzaj rozpuszczalnika, stosunek molowy reagentów, stężenie lipazy, temperatura reakcji, szybkość wytrząsania i czas prowadzenia reakcji) zostały przetestowane a wyniki zebrane w tabeli 1.

Poniższy rysunek 4 przedstawia uproszczony schemat reakcji otrzymywania ECKT na przykładzie modelowego nonanianu glukozy (C9-glu). Reakcja ta była przedmiotem znacznej części badań opisanych w artykule P1.

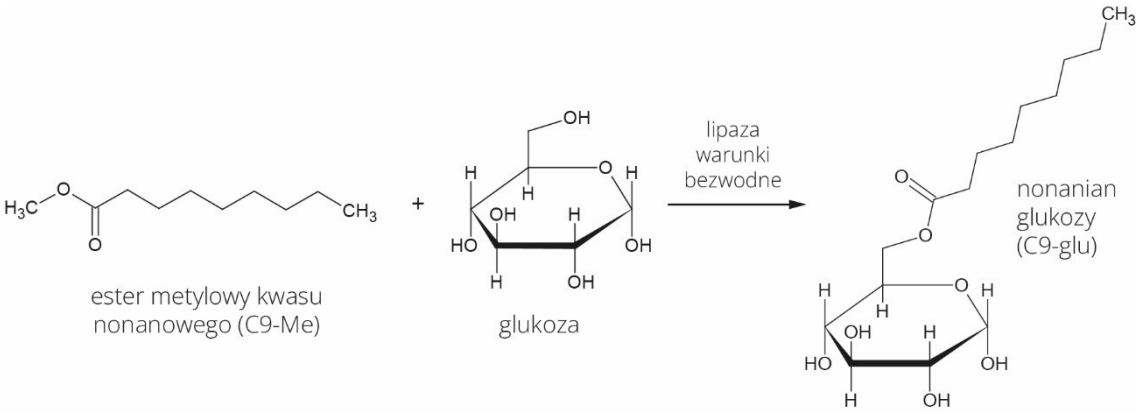

Rys. 4. Schemat reakcji katalizowanej przez lipazę. Adaptacja Panelu B publikacji P1 – lipaza acyluje glukozę nonanianem metylu, tworząc ester cukru i produkt uboczny metanol [59].

Reakcje zostały przeprowadzone z uwzględnieniem warunków zamieszczonych w poniższej tabeli nr 1 po uprzednim zmodyfikowaniu do objętości 1,5 ml. Przygotowano serię reaktorów w szczelnie zakręcanych plastikowych probówkach.

Tabela 1. Zestawienie warunków syntezy enzymatycznej ECKT optymalnych dla uzyskania C9-lac

Nr testowanej metody	Rodzaj/ pochodzenie enzymu	Substrat	Cukier	Medium reakcyjne	Stosunek molowy kwasu do cukieru	Literatura
1	CalB	Kwas octadeka–9–enowy kwas oktadeka 9,12-dienowy	lac	EtOH (99%)	1:1	[58, 59]
2	CalB Amano lipaza PS-IM (Pseudomonas cepacia), Thermomyces lanuginosus amanolipase TL-IM Mucor miehei	monolaurynian winylu	lac, sacharoza	Aceton, MEK, 2M2B	3:1	[60, 61]
3		monolaurynian winylu		Pirydyna	3:1	[65
4	TL–IM	monolaurynian winylu	lac	2M2–But–OH	2:1	[64]
5		monolaurynian winylu	lac	2M2–But–0H 80%/ 20% DMSO	3:1	[65]
6	*Candida rugosa*	kwas kaprowy, kwas laurynowy	lac, ryboza, mannoza	Aceton, EtOH, t–amyl–OH	3:1; 2:1	[66]

Detekcji reagentów dokonano za pomocą wysokosprawnej chromatografii cieczowej sprzężonej ze spektrometrem masowym HPLC-MS (Szimadzu oraz Agilent 6460).

Najbardziej wydajną metodą okazała się być opublikowana przez zespól M. Walsh pt. „*Synthesis of lactose monolaurate as influanced by various lipases and solvents”.* Jej adaptacja to: 22 mg lac [43 mM], użycie 2M2B jako medium reakcyjnego suszonego za pomocą sit molekularnych, 34 mg katalizatora – immobilizowanej lipazy, obecność 10% m/v sit molekularnych (4 Å,150 mg), 130 mM estru czyli odpowiednio C9-Met 1458 µl dla estru C7/C9-Met [67]. Stężenie C9-lac oznaczono metodą standardu wewnętrznego na podstawie krzywej kalibracyjnej dla estru wzorcowego – monolarurenianu sacharozy (C12). Ze względu na niskie wydajności postanowiono rozszerzyć spektrum substratowe o składowe lac,

to jest o glukozę (glu) i galaktozę (gal), a także potwierdzić obecność produktów inną metodą – chromatografią gazową z detektorem płomieniowo-jonizujacym (GC-FID, Varian). By dokonać detekcji GC, mieszaninę reakcyjną należało uprzednio poddać procesowi derywatyzacji za pomocą odczynnika chloro-silanowego TMCS (trimethylchlorosilane). Kluczową rolę w procesie analizy reagentów po reakcji odegrała pirydyna, gdyż umożliwia ona rozpuszczenie zarówno glu, gal, jak i estrów, co jest kluczowe z punktu widzenia derywatyzacji oraz wykreślenia krzywych kalibracyjnych. Dlatego po zatrzymaniu reakcji (poprzez zamrożenie), przed przygotowaniem próbek do analiz, dokonano całkowitej ekstrakcji poprzez dodanie pirydyny do każdego z reaktorów i intensywne mieszanie. Finalnie próbki do analizy HPLC-MS przygotowano według poniższego zoptymalizowanego protokołu. Po wymieszaniu z pirydyną pobrano po 100 µl mieszanin reakcyjnych i rozcieńczano dziesięciokrotnie w roztworze MeOH/H_2O 50%/50% v/v, mieszano przy użyciu mieszadła (typu Vortex), a następnie wirowano. Nadsącz pobrano i rozcieńczono 100 razy w takim samym roztworze MeOH/H_2O. Próbki poddawane analizie GC przygotowano w następujący sposób: po wymieszaniu z pirydyną pobrano po 100 µl mieszanin reakcyjnych i wymieszano z 200 µl odczynnika derywatyzującego (TCMS). Inkubowano przez 30 min w T = 70ºC [68].

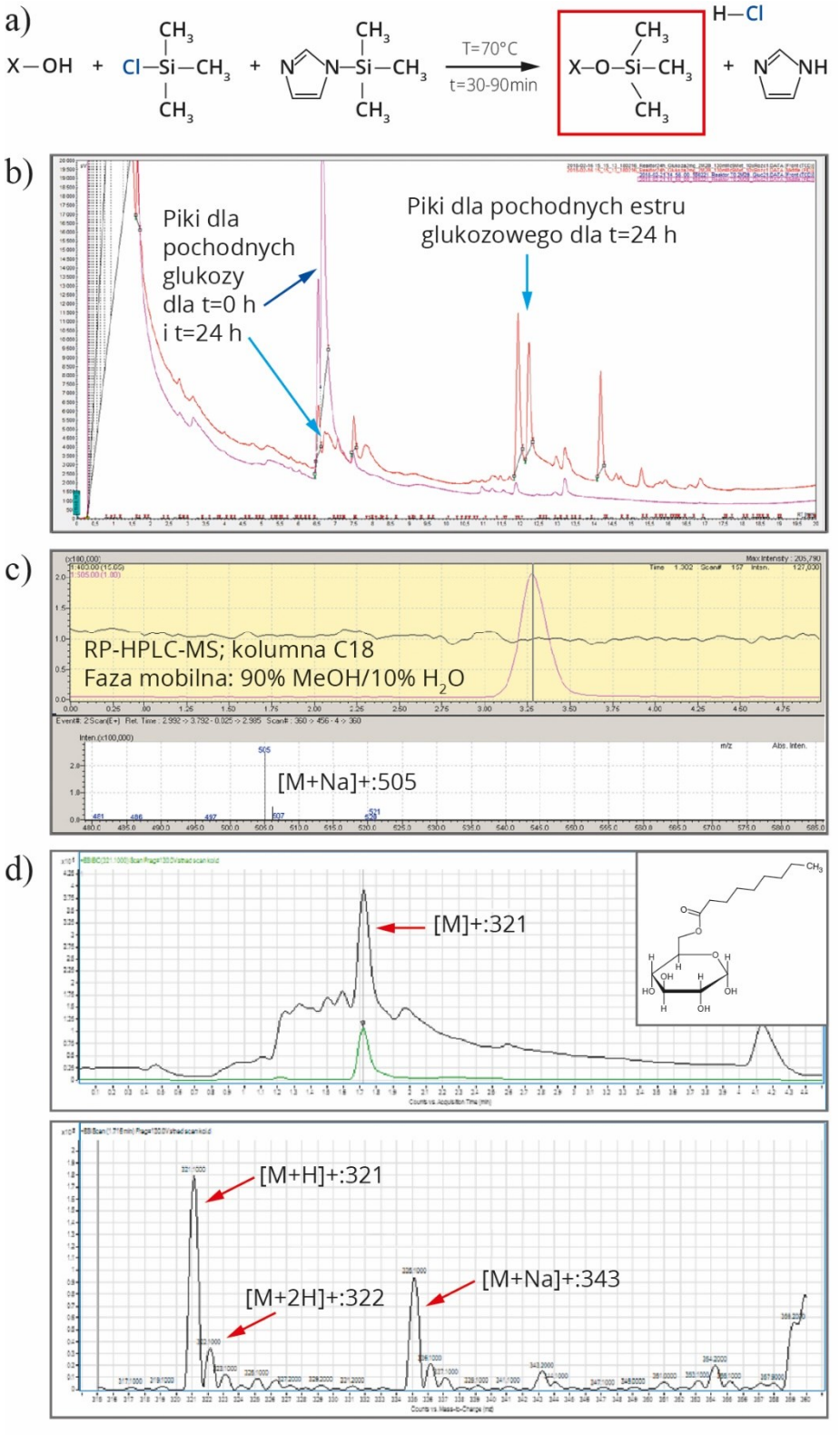

Rys. 5. Chromatogramy ukazujące pierwsze próby detekcji ECKT w trakcie procesu optymalizacji reakcji enzymatycznych: a) schemat procesu derywatyzacji reagentów przed analizą GC-FID, b) chromatogram gazowy C9-glu – GC-FID Varian, c) chromatogram i widmo masowe adduktu $[M+Na]^+$-nonanianu laktozy – HPLC-MS Shimadzu, d) chromatogram i widmo masowe adduktów $[M+H]^+$ i $[M+Na]^+$-nonanianu glukozy – UHPLC-MS Agilent QQQ 6460.

Kiedy upewniono się, że pożądana reakcja zachodzi w warunkach odtworzonych z protokołów opisanych w zestawie publikacji z przeglądu, podjęto próby zwiększenia jej wydajności. Owocem tych prób jest poniższa publikacja.

Publikacja 1 – Bioorganic Chemistry 2019

Bioorganic Chemistry 93 (2019) 102813

Contents lists available at ScienceDirect

Bioorganic Chemistry

journal homepage: www.elsevier.com/locate/bioorg

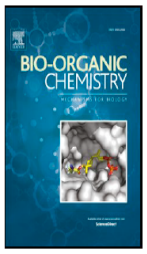

Hollow silica microspheres as robust immobilization carriers

Wojciech Snoch[a], Mateusz Tataruch[a], Olga Zastawny[b], Ewelina Cichoń[c], Mathilde Gosselin[d], Hubert Cabana[e], Maciej Guzik[a,*]

[a] Jerzy Haber Institute of Catalysis and Surface Chemistry Polish Academy of Sciences, Niezapominajek 8, 30-239 Kraków, Poland
[b] Department of Plant Cytology and Embryology, Institute of Botany, Jagiellonian University, Gronostajowa 9, 30-387 Kraków, Poland
[c] Faculty of Material Science and Ceramics, AGH University of Science and Technology, Mickiewicza Av. 30, 30-059 Krakow, Poland
[d] Materium Innovations INC., Boulevard Industriel 790, Granby, J2G 9J5 Quebec, Canada
[e] Department of Civil and Building Engineering, Universite de Sherbrooke, 2500 Boulevard de l'Universite, Sherbrooke, J1K 2R1 Quebec, Canada

Wpływ immobilizacji lipaz na efektywność syntezy ECKT

Dzięki wymienionym w powyższym wprowadzeniu przygotowaniom możliwe było zrealizowanie części badań omawianych w publikacji P1 dotyczących wpływu immobilizacji lipaz na efektywność syntezy ECKT, które wchodzą w zakres niniejszej rozprawy.

Po dobraniu optymalnych warunków i rozpuszczalników dla przeprowadzenia reakcji enzymatycznej syntezy ECKT w skali analitycznej, przy użyciu popularnych i łatwo dostępnych enzymów CalB i TL–IM, postanowiono rozszerzyć wachlarz katalizatorów. W związku z tym została nawiązana współpraca z firmą Eucodis Bioscience produkującą immobilizowane oraz wolne lipazy w celu rozszerzenia spektrum zastosowania możliwych katalizatorów. Przetestowałem serię 26 lipaz, z których jedna – immobilizowana EL70, okazała

się najbardziej obiecująca. Dalej, zespół badawczy pracujący nad P1 nawiązał współpracę z kanadyjską firmą MATSPHERES® produkującą materiały dla biotechnologii, w szczególności dla reaktorów, w tym podłoża do immobilizacji enzymów. Po otrzymaniu porcji podłoży od firmy METSPHERES® we współpracy z dr Eweliną Cichoń i dr inż. Mateuszem Tataruchem dokonaliśmy immobilizacji lipazy EL70 i przetestowaliśmy konwersję glukozy do jej estru kwasu nonanowego. Reakcje przeprowadzin w małych reaktorach typu batch, zgodnie z wcześniej wypracowanymi warunkami reakcji. Testowane podłoża to: Monolit – o gładkiej powierzchni z modyfikowanymi grupami –OH, ażurowe Sphere – zawierające modyfikowane o grupy –OH, jak i –NH_2, oraz mikrocząsteczkowe pianki (*Microcellular foam*), również z modyfikowanymi grupami –OH i –NH_2. Poniżej zestawiono wydajności, które obliczono na podstawie stężenia nieprzereagowanego cukru (tabela 2). Analiz dokonywano metodami UHPLC-MS (QQQ Agilent) oraz GC-FID (Varian).

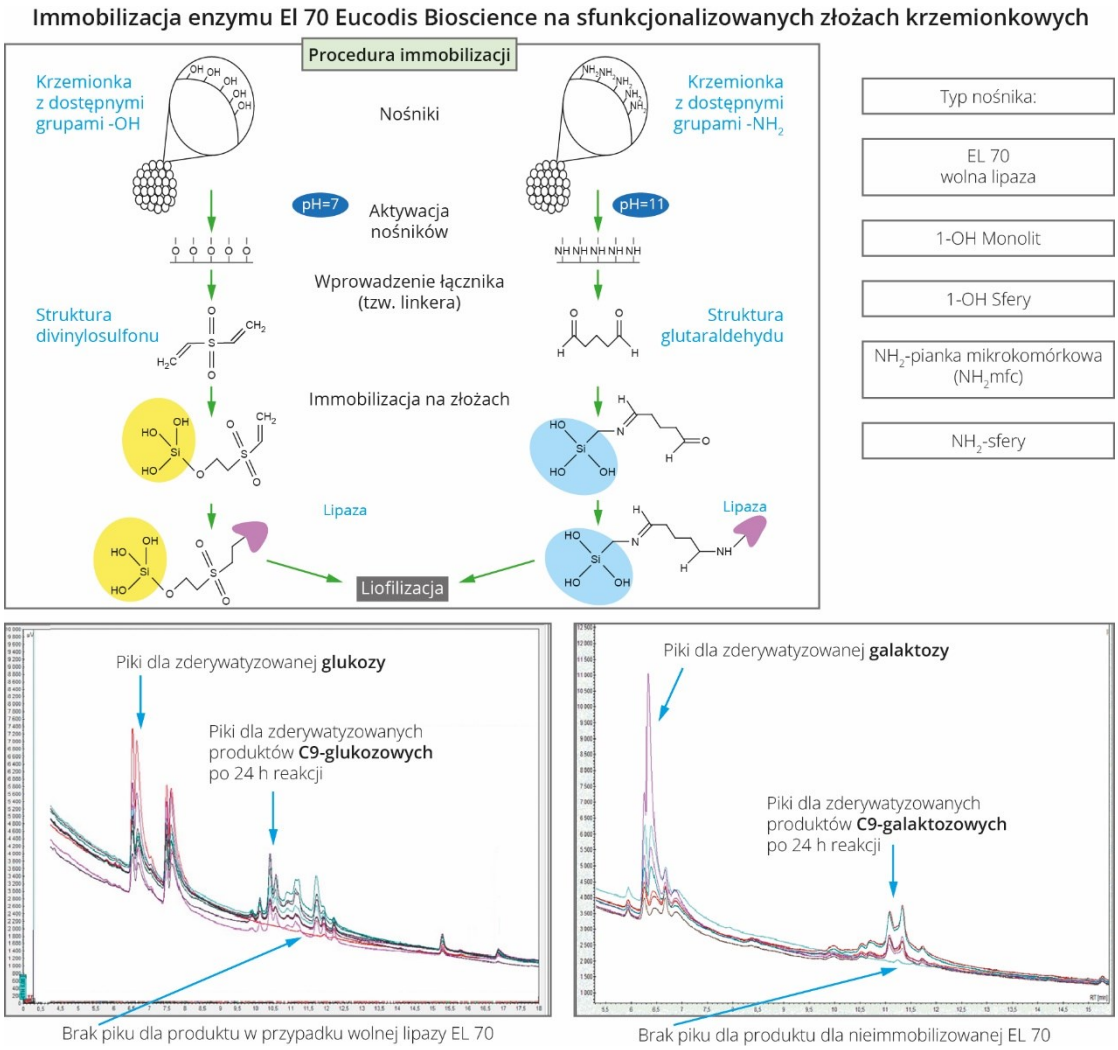

Rys. 6. Schemat immobilizacji enzymów na sfunkcjonalizowanych złożach firmy Matspheres®, oraz wyniki jakościowej analizy GC mieszanin poreakcyjnych.

Eksperyment wykazał brak aktywności wolnej lipazy EL70. Najbardziej preferowanym nośnikiem do dalszych eksperymentów okazały się sfery modyfikowane grupami $–NH_2$.

Tabela 2. Synteza C9-glu w reaktorach z 2M2B jako medium

Nośnik / Enzym	Stężenie glukozy po 24h [mg ml^{-1}]	Konwersja [%]
EL 70 wolna lipaza	3,77	13,5
MATSPHERES®-OH	0,5	88,5
MATSPHERES®-NH_2	0,07	98,4
SBA-OH	0,5	89,1
SBA-NH_2	0,47	83,7
TL-IM	2,53	42,1
CalB	2,72	37,6

Po uzyskaniu wyników reakcji biokatalizy w reaktorach typu batch zdecydowano się na przeprowadzenie eksperymentu angażującego reaktor przepływowy oparty na kolumnie półpreparatywnej, pompie HPLC i termostacie do kolumny, żeby sprawdzić, czy ta forma prowadzenia reakcji może zwiększyć jej wydajność. Schemat reaktora i wyniki umieszczono poniżej. Żeby rozpuścić substrat cukrowy i uniknąć zapchania kolumny oraz pompy, użyto mieszaninę 2M2B:DMSO (8:2, v/v) jako medium reakcyjne. Katalizatorem była lipaza EL70 Eucodis Bioscience immobilizowana na ażurowych podłożach Kanadyjskiej firmy MATSPHERES modyfikowanych grupami –OH lub $–NH_2$.

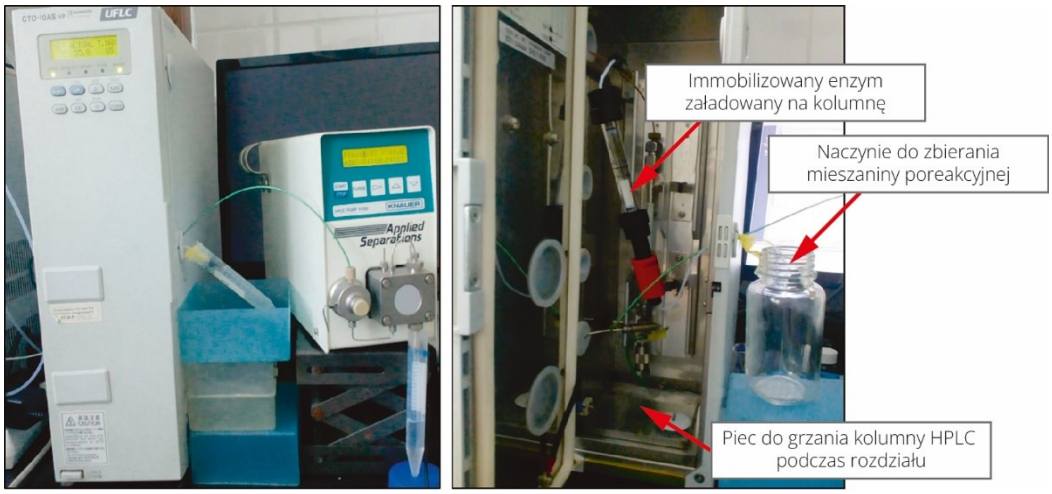

Rys. 7. Schemat reaktora przepływowego w skali analitycznej skonstruowanego we współpracy z dr inż. Mateuszem Tataruchem.

Tabela 3. Zestawienie konwersji uzyskanych w poszczególnych turach rekacji transestryfikacji immobilizowaną lipazą EL70 z wykorzystaniem reaktora przepływowego

	Ponowne wykorzystanie		
Typ nosnika dla enzymu	1	2	3
	Konwersja [%]		
MATSPHERES®-OH	12,9	73,0	51,1
MATSPHERES®-NH2	42,6	88,3	68,1

Tabela 3 pokazuje, jak zmieniały się wydajności reakcji w reaktorze przepływowym za każdym jego wykorzystaniem na podstawie ubytku substratu glukozowego. Ponowne (drugie) wykorzystanie reaktora zwiększyło wydajność reakcji. Jednak trzecie wykorzystanie kolumny z katalizatorem spowodowało spadek wydajności. Eksperyment pokazał nie tylko wzrost wydajności reakcji względem reaktorów typu całkowity wsad tzw. batch z podłożem modyfikowanym grupami $–NH_2$ z 58,7% do 88,3% (wzrost ok. 30%), lecz także możliwość kilkukrotnego wykorzystania katalizatora.

Podsumowanie i wnioski

Niniejszy manuskrypt przedstawia koncepcje rozwoju biokatalitycznej syntezy estrów cukrowych na przykładzie lac, glu, gal, oraz C9-Me. Rozwój ten polegał najpierw na doborze najlepiej działających warunków dla tego układu oraz badaniach przesiewowych serii 26 lipaz firmy Eucodis Bioscience i wyborze jednej najbardziej obiecującej. Okazała się nią EL070. Kolejnym etapem usprawnienia procesu było zastosowanie nośników zarówno gładkich typu SBA, jak i ażurowych firmy MATSPHERES®, modyfikowanych odpowiednio grupami –OH i $–NH_2$. Ostatnim z proponowanych rozwiązań jest synteza za pomocą reaktora przepływowego, zawierającego dobrany w poprzednich etapach katalizator. Wszystkie testy wykonano w skali analitycznej i weryfikowano odpowiednio metodami GC i HPLC-MS.

Powyższe badania wykazały około 7,5-krotne zwiększenie skuteczności działania komercyjnie dostępnej lipazy EL070 po jej zimmobilizowaniu na aminowanych ażurowych nośnikach, a 6,5-krotne w przypadku hydroksylowanych. Dla porównania gładkie nośniki hydroksylowane SBA zwiększyły wydajność reakcji ok. 6,6 krotnie, a aminowane SBA – 6,2 krotnie. Obiecujący okazał się też koncept wykorzystania reaktora przepływowego, gdyż pozwala on na wielokrotne użycie enzymu i prowadzenie reakcji w warunkach ciągłych. Tutaj korzystniejsze rezultaty przyniosły nośniki ażurowe $–NH_2$, dając konwersje co prawda niższą niż w reaktorze typu batch, bo 42,6%, podwajając ją przy następnym użyciu. Jednak po drugim cyklu reakcji wydajność spadła z 88,3% do 68,1%. Zdecydowanie limitującym czynnikiem w tym układzie jest konieczność użycia medium rozpuszczającego cukier (20% DMSO/80%

2M2B), który co prawda zabezpiecza układ przed zatkaniem i umożliwia przepływ substratu przez kolumnę zawierającą katalizator, ale jest trudny do odparowania po reakcji. Zamiast DMSO można w przyszłości przetestować inne rozpuszczalniki, takie jak N-metylopirolidon, pirolidyna czy pirydyna.

Publikacja 2 – Catalysts 2019

catalysts

MDPI

Article

Influence of Chemical Modifications of Polyhydroxyalkanoate-Derived Fatty Acids on Their Antimicrobial Properties

Wojciech Snoch [1], Karolina Stępień [2], Justyna Prajsnar [1], Jakub Staroń [3], Maciej Szaleniec [1] and Maciej Guzik [1,*]

[1] Jerzy Haber Institute of Catalysis and Surface Chemistry, Polish Academy of Sciences, Niezapominajek 8, 30-239 Kraków, Poland; ncsnoch@cyfronet.pl (W.S.); justyna.prajsnar1@gmail.com (J.P.); ncszalen@cyfronet.pl (M.S.)

[2] Medical University of Warsaw, Department of Pharmaceutical Microbiology, 3 Oczki Str. 02-007 Warsaw, Poland; Karolinastepien@windowslive.com

[3] Institute of Pharmacology, Polish Academy of Sciences, Smętna 12, 31-343 Kraków, Poland; jakubstaron@gmail.com

* Correspondence: ncguzik@cyfronet.pl; Tel.: +48-126-395-155

Received: 15 May 2019; Accepted: 30 May 2019; Published: 5 June 2019

check for updates

Po ustaleniu warunków syntezy i detekcji ECKT w P1, kolejnymi etapami stały się: przeskalowanie z ilości analitycznych do miligramowych, modyfikacja komponenty hydrofobowej, a także wstępna weryfikacja właściwości biologicznych estrów na przykładzie bakterii i drożdżaków. W tym celu dokonano biosyntezy estrów: PHN i poli[(R)-3-hydroksypentanian-ko-(R)-3-hydroksypropionianu] (PHPV) za pomocą bakterii, odpowiednio: *Pseudomonas putida* KT2440 i CA3. Następnie polimery poddano kwaśnej metanolizie i uzyskano mieszaniny estrów metylowych odpowiednich 3-hydroksykwasów (w przypadku PHN długości łańcuchów monomerów: C9 i C7, a w przypadku PHPV – C5 i C3). Po przeprowadzeniu szeregu prób i selekcji reakcji chemicznych zabezpieczenia grup 3-OH dopracowano protokół modyfikacji chemicznej monomerów. W konsekwencji do grupy 3-OH monomerów wprowadzono grupę trifluoroetylową poprzez wytworzenie wiązania eterowego przy trzecim atomie węgla monomerów. Reakcja typu SN2 zachodziła w suchym tetrahydrofuranie (THF) suszonym za pomocą glinowodorku litu – $LiAlH_4$. Nukleofilem był wodorek sodu (NaH), a donorem grupy trifluoroetylowej ($–CH_2CF_3$) – trifluorometylosulfonian trifluoroetylu. Po oczyszczeniu i oznaczeniu zmodyfikowanych monomerów założono serię reaktorów preparatywnych, by uzyskać bibliotekę ECKT. Poniżej przedstawiono schemat całego procesu syntezy i modyfikacji monomerów.

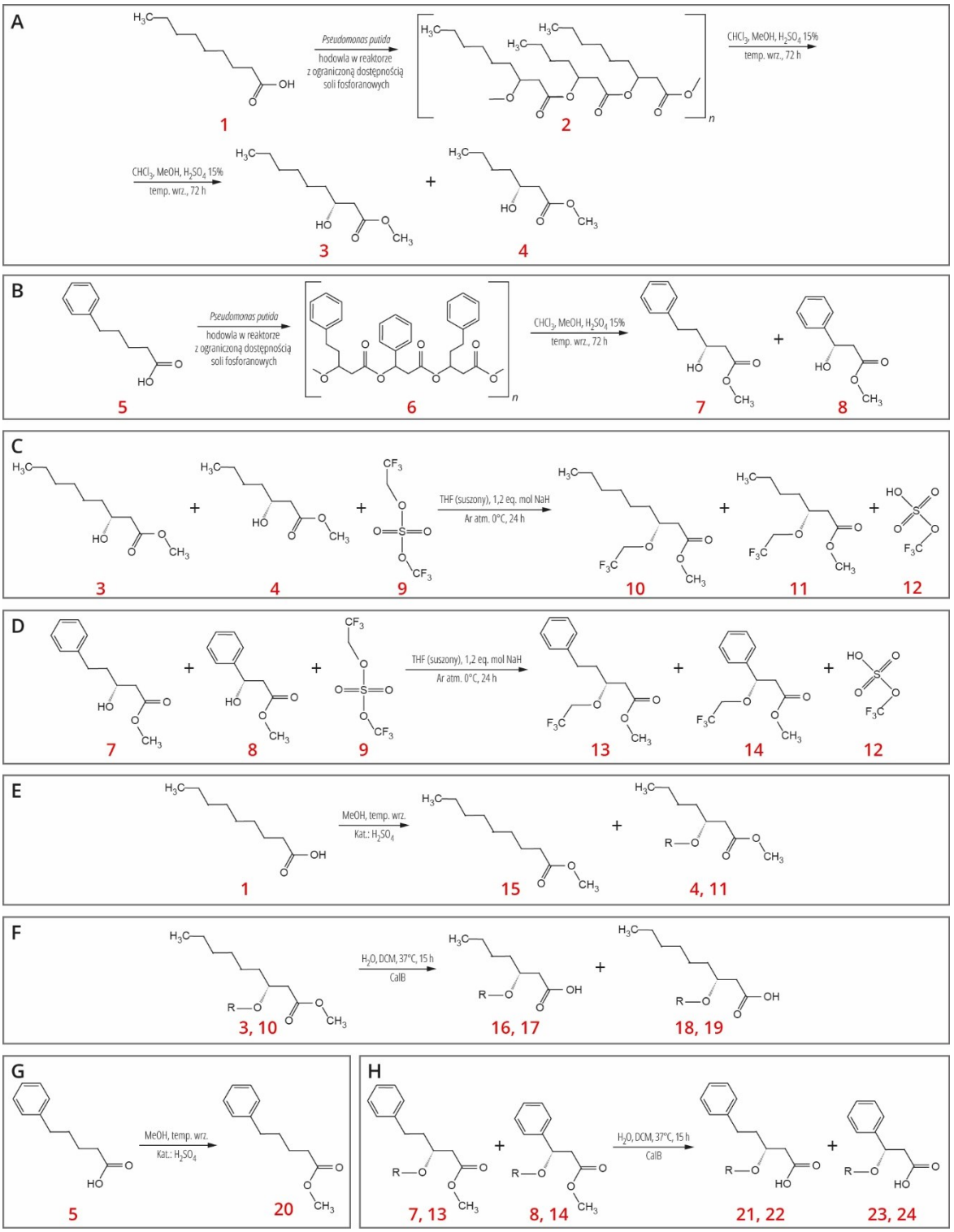

Rys. 8. Wzory oraz schematy biosyntezy bakteryjnych poliestrów, uzyskania z nich metylowanych hydroksykwasów, a także ich modyfikacji chemicznej przed etapem biokatalizy. **A**+**B**: synteza PHN i metanoliza; **C**+**D**: Fluorowanie monomerów; **E**+**G**: synteza estrów metylowych; **F**+**H**: hydroliza substratów przez CalB; **1** – kwas nonanowy (C9); **2** –poli[(R)-3-hydroksynonanian-ko-(R)-3-hydroksyheptanian] (PHN); **3** – ester metylowy PHN (Me-PHN); **4** – ester metylowy (R)-3-hydroksyheptanianu; **5** – kwas 5-fenylopentanowy (C5-Phe); **6** – poli[(R)-3-hydroksypentanian-ko-(R)-3-hydroksyheptanian] (PHPV); **7** – (R)-3-hydroksy-5-fenylopentanian metylu (Me-PHPV); **8** – (R)-3-hydroksy-3-fenylpropionian metylu; **9** – 2,2,2-trifluoroetylo trifluorometyl sulfonian; **10** – (R)-3-(2,2,2-trifluoroethoxy)nonanian metylu; **11** – (3R)-3-(2,2,2-trifluoroetoksy)heptanian metylu; **12** – trifluorometylo

hydroksy sulfonian; **13** – (R)-5-fenylo-3-(2,2,2-trifluoroetoksy)pentanian metylu; **14** – 3-fenylo-3-(2,2,2-trifluoroetoksy)propionian metylu; **15** – nonanian metylu; **16** – kwas (R)-3-hydroksyheptanowy; **17** – kwas 3-(2,2,2-trifluoroetoksy)heptanowy; **18** – (R)-3-kwas hydroksynonanowy; **19** – kwas 3-(2,2,2-trifluoroetoksy)nonanowy; **20** – 5-fenylpentanian metylu; **21** – kwas (R)-3-hydroksy-5-fenylopentanowy; **22** – kwas 5-fenylo-3-(2,2,2-trifluoroetoksy)pentanowy; **23** – kwas (R)-3-hydroksy-3-fenylopropionowy; **24** – kwas 3-fenylo-3-(2,2,2-trifluoroetoksyy)propionowy).

Synteza ECKT – kolejne kroki usprawniania

Na potrzebę preparatywnej produkcji ECKT reakcje z udziałem glukozy, lipazy TL-IM oraz C9-Me, których protokół opracowano w trakcie przygotowania P1, przeskalowano do objętości 10 ml. Tym razem komponentę hydrofobową stanowiły dodatkowo wcześniej wymienione estry metylowe niemodyfikowanych i modyfikowanych monomerów PHN i PHPV.

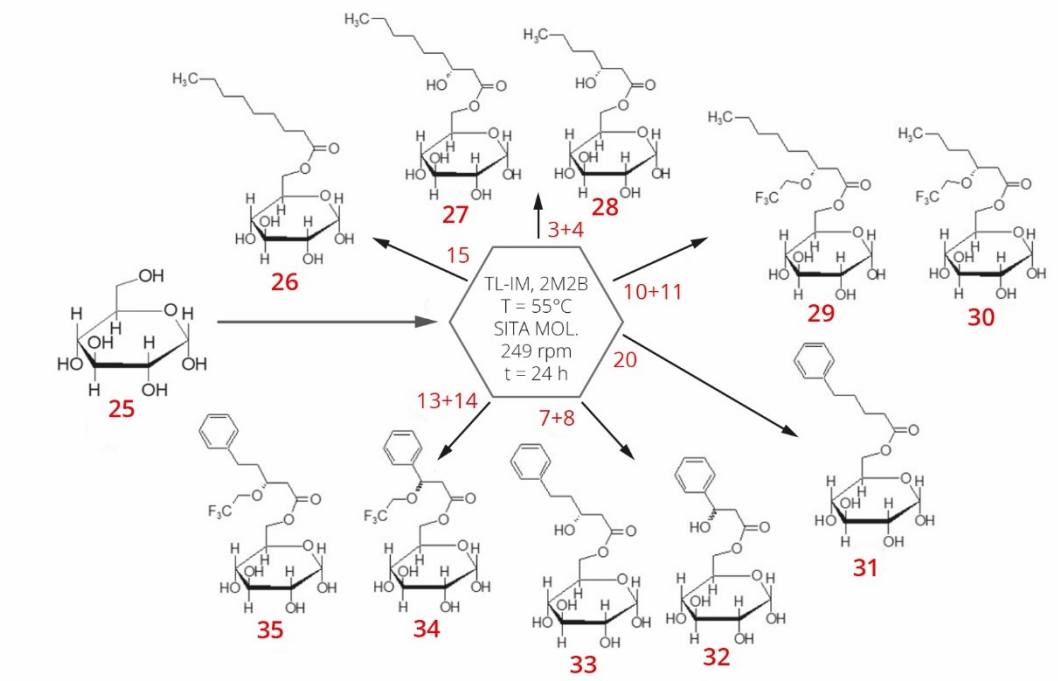

Rys. 9. Wzory półstrukturalne uzyskanych ECKT na bazie glukozy.

Ponadto dopracowano metody analityczne UHPLC-MS. ECKT oznaczono jakościowo. Konwersje wyznaczono na podstawie ilościowej analizy stężenia pozostałej glukozy w próbce. Wyniki umieszczono w poniższej tabeli 4.

Tabela 4. Konwersje uzyskane w reakcjach chemicznych i enzymatycznych

Numer związku w P2:	Skrót nazwy związku:	Konwersja [%]:
15	C9-Me	100
10,11	F-mPHN	48,5
7,8	mPHPV	100
13,14	F-mPHPV	NP
26	C9-glu	42,1*
27,28	mPHN-glu	85*
29,30	F-mPHN-glu	NP
31	C5-Phe-glu	43,3*
32,33	mPHPV-glu	78,7*
34,35	F-mPHPV-glu	NP

* Konwersje przeliczono na podstawie stężenia glu
NP – nie potwierdzono

Opis procesu optymalizacji modyfikacji monomerów PHN

W literaturze można znaleźć cały wachlarz reakcji chemicznych umożliwiających wprowadzenie atomu halogenowca lub podstawnika go zawierającego do łańcucha węglowego, gdyż jest to bardzo popularna praktyka zwiększania potencjału biologicznego leków [68, 69]. Metody te angażują głównie katalizatory metaloorganiczne bądź inne odczynniki niezbyt przyjazne dla środowiska, m.in.: diethylaminosulfur trifluoride (DAST); $BF3/OEt_2$; Olah's reagent (pyridinium poly(hydrogen fluoride) PPHF), N-fluoropyridinium triflate; N-fluorobenzenesulfonimide (NFSI) lub jego metylowany analog (Me-NFSI); BrF_3; czy też katalizatory magnezowe w układzie porfirynowym (trans-difluoro manganese(IV)) [70, 71, 72, 73]. Dodatkowo bywa, że metody te nie są wystarczająco selektywne, gdyż eliminują wszystkie atomy lub ugrupowania danego typu, np. wszystkie atomy H lub całą grupę –OH, bądź mogą być stosowane tylko po to, by podstawić C–H na C–F, nie tworząc układu: C–O–CF [74–76]. Nie dają przez to możliwości wpływania na układy biologiczne za pomocą doboru ilości, lokalizacji tych ugrupowań czy poprzez wykorzystanie chiralności atomu C. Przetestowaliśmy zatem kilka metod fluorowcowania metylowych estrów monomerów PHN z eliminacją atomu H zlokalizowanego jedynie na grupie 3–OH. Testowane związki to: 1-fluoro-3-jodopropan; 1,1-difluoro-2-jodoetan; 1,1,1-trifluoro-3-jodopropan, nukleofile: NaH (60%), diizopropyloamid litu (LDA); media: dimetyloformamid (DMF), dichlorometan (DCM), tetrahydrofuran (THF). Ostatecznie wybrano metodę opisaną w sekcji *Materials and methods* artykułów P2 i P3. Kluczowymi aspektami w tym procesie wydają się warunki bezwodne

(suszenie THF za pomocą $LiAlH_4$; atm. Argonu) decydujące o wydajności oraz obecność łatwo odchodzącej grupy trifluorosulfonowej. Dodatkowo, zaletą tej metody jest nienaruszanie struktury reszty cząsteczki i brak potrzeby używania dodatkowych procedur przygotowania reagentów. Zastosowanie łatwo odchodzącej grupy triflatowej budzi nadzieję na przetestowanie możliwości wprowadzania do monomeru PHN innych układów chemicznych, a przez to wpływanie na ich cytotoksyczność. Ma ona jednak również wadę – zarówno substraty, jak i produkty uboczne wymienionej reakcji alkilacji są mutagenne i kancerogenne oraz lotne. Trzeba zatem zachować szczególną ostrożność oraz odpowiednie procedury przy przeprowadzaniu reakcji, a także utylizacji odpadów po reakcji.

Modyfikacja monomerów PHA, której procedura została szczegółowo opisana w rozdziale 3 (*Materials and methods*) artykułu P2, pozwoliła na otrzymanie 1,26 g (48,5% konwersji) frakcji produktów (**3** i **4**). Wzory półstrukturalne przedstawiono na rys. 9 w panelu A – będącym adaptacją Figury 1 C w artykule P2. Wszystkie konwersje zamieszczone w tabeli 4 zostały zaadaptowane na podstawie artykułu P2 (tabela 1). Analiza spektroskopowa (^{1}H NMR, MS) związków wykazała, że grupy 3–OH estrów metylowych PHN zostały zmodyfikowane (rysunki S4 i S5 w *Supplementary materials* P2).

Zgodnie z naszą najlepszą wiedzą jest to pierwsze doniesienie, które dotyczy zabezpieczania grupy hydroksylowej monomerów PHA lub podstawienia przez podstawnik halogenowy [75, 77–79]. NaH okazał się skutecznym reagentem do usuwania atomów wodoru z grup PHN 3–OH i ich aktywacji w celu ataku ugrupowania trifluoroetylowego, mimo że diizopropyloamidek litu jest znacznie silniejszym nukleofilem. Dodatkowo użycie suchego THF jako medium okazało się kluczowym elementem całego procesu syntezy.

Badania mikrobiologiczne

Badania aktywności przeciwdrobnoustrojowej nowo zsyntezowanych ECKT powstałych z zmodyfikowanych i niemodyfikowanych monomerów PHA przeprowadzono na wybranych bakteriach Gram-dodatnich i Gram-ujemnych i grzybach drożdżopodobnych z kolekcji drobnoustrojów ATCC, NCTC i CIP. Aktywność związków wyrażono jako minimalne stężenie hamujące (MIC). MIC badano metodą dwukrotnego rozcieńczenia seryjnego (w 96-studzienkowych płytkach). Liczebność bakterii w *inokulum* wynosiła 10^6 CFU ml^{-1} (jednostka tworząca kolonię na ml) i 5×10^4 do $2{,}5 \times 10^5$ CFU ml^{-1} dla drożdży. Badane

związki rozpuszczono w DMSO i rozcieńczono w sterylnym podłożu (do maksymalnie 3% zawartości rozpuszczalnika). Stężenia związków wynosiły odpowiednio od 78 do 5000 μg ml^{-1} [80, 81]. Jako kontrole zastosowano cyprofloksacnę (przeciwbakteryjna) i fluxonazol (przeciwgrzybiczny). Eksperyment wykazał, że wartości MIC (lub minimalne stężenie bakteriobójcze – MBC) zarówno niezmodyfikowanych, jak i zmodyfikowanych monomerów PHA i ich estrów glukozy są w większości przypadków wyższe niż 2500 μg ml^{-1}, czyli 50 000 razy wyższe niż powszechnie stosowanych antybiotyków (cyprofloksacyna, flukonazol 0,5 μg ml^{-1}) [80, 82]. Monomery PHA z grupą hydroksylową przy trzecim atomie węgla wykazywały silniejsze działanie przeciwbakteryjne (dla szczepów bakterii takich jak *Staphylococcus aureus* NCTC 4163 i *Bacillus cereus* ATCC 11778) w porównaniu z ich analogami kwasów tłuszczowych bez grupy 3–OH. Podobne wyniki uzyskali Sandoval i współpracownicy, którzy badali wpływ grupy hydroksylowej na właściwości przeciwbakteryjne monomerów PHA [84]. Bakterie wykazały za to pewną wrażliwość na ok. 2–4 razy wyższe stężenia ECKT względem monomerów, z których powstały. Wrażliwość może zależeć od rodzaju użytego węglowodanu, długości kwasów tłuszczowych przyłączonych do cukru oraz ugrupowania związanego z częścią kwasową ECKT [85].

W odniesieniu do działania przeciwgrzybiczego, ester C9-glu (**26**, rys. 10) wykazywał największą aktywność spośród wszystkich badanych ECKT (wartości MIC dla *C. parapsilosis* – 313 μg ml^{-1}, *C. albicans* ATCC 90028 – 625; *C. krusei* ATCC 1023 – 625 μg ml^{-1}). Zaobserwowano również pewne działanie przeciwbakteryjne estrów glukozy mPHN-glu (**27** i **28**, rys. 10) wobec *Staphylococcus spp*. w zakresie MIC 1250–2500 μg ml^{-1}. Po modyfikacji ugrupowaniem fluorowym, estry pochodzące od monomerów PHN (**34** i **35**) wykazały aktywność przeciwdrobnoustrojową wobec *Staphylococcus aureus* NCTC 4163 (MIC 2500 μg ml^{-1}). W przypadku pozostałych badanych par (estry glu vs. testowany szczep) nie zaobserwowano istotnego działania przeciwdrobnoustrojowego. Wyniki te są zgodne z doniesieniami innych, w których estry cukrów glukozy lub maltozy (długość kwasów tłuszczowych n = 8–14) wykazały wartości MIC między 250 a 2000 μg ml^{-1} w testach na szereg szczepów Gram-ujemnych i Gram-dodatnich [88, 89]. Przedstawione w poniższej tabeli 5 wartości MIC zbliżone są do wartości innych, podobnych związków. Doniesienia literaturowe informują, że syntezowana chemicznie przez A. Smith et al. grupa estrów laurynowych α-D-glukozy i β-D-glukozy była toksyczna względem *S. aureus* ATCC 2593 w przedziale odpowiednio 40–310 μmol l^{-1}, estrów oktanoilowych – 2,5 mmol l^{-1}. Względem natomiast *E. coli* ATCC 25922, estry na bazie α-D-glukozy β-D-glukozy były toksyczne

w przedziale odpowiednio 12,5 mmol l^{-1}, dla oktanoilo i 20 mmol l^{-1}, dla estrów laurynowych [88].

Tabela 5. Wartości MIC wybranych kwasów tłuszczowych oraz ECKT względem szczepów kontrolnych [88]

Związek	*S. aureus* ATCC 25923 MIC [mmol ml^{-1}]	*E. coli* ATCC 25922 MIC [mmol ml^{-1}]
Kwas laurynowy (C12)	0,63	10
Monolaurynian	0,04	20
Kwas kaprylowy (C8)	5	12,5
Monokaprylian	2,5	6,25
6-O-lauroilo-α-D–glukopiranozyd metylu	0,31	20
6-O-lauroilo-β-D-glukopiranozyd metylu	0,04	20
6-O-oktanoilo-α-D-glukopiranozyd metylu	2,5	12,5
6-O-dodekanylo-α-D-glukopiranozyd metylu	0,04	20
6-O-dodekanylo-β-D-glukopiranozyd metylu	2,5	20
4,6-di-O-lauroilo-α-D-glukopiranozyd metylu	NDa	ND
6-O-lauroilo-α-D-mannopiranozyd metylu	0,04	20
6-O-lauroilo-α-D-galaktopiranozyd metylu	>10	>20
Monolauroilo pentaerytriol	>10	>20
Dilauroilo pentaerytriol	NO	NO
NO – nie oznaczono NDa – nie oznaczono ze względu na słabą rozpuszczalność		

W innym artykule podano, że syntezowane i badane estry laurynowe i palmitynowe na basie sacharozy wykazały działanie względem popularnych szczepów obecnych w jedzeniu w zakresie MIC = 0,01 do nawet powyżej 5 mg ml^{-1} [89].

Podsumowanie i wnioski

Publikacja P2 opisuje pierwszą próbę modyfikacji grup (*R*)-3-OH monomerów PHA i PHPV oraz enzymatycznej syntezy estrów glukozy powstałych na ich bazie. Procedury ich otrzymywania i oczyszczania wymagają jednak dalszej optymalizacji w kierunku zwiększenia wydajności i czystości. Słabe właściwości antybakteryjne i przeciwgrzybiczne ECKT w porównaniu z antybiotykami nie pozwalają na użycie ich jako przyszłe środki grzybo- lub/i bakteriobójcze, jednak stężenia MIC utrzymują się w przedziale działania i nie odbiegają znacząco od innych dostępnych w literaturze i przemyśle estrów cukrowych.

Trzeba mieć na uwadze, że na etapie tworzenia niniejszej publikacji nie była jeszcze w pełni dopracowana procedura oczyszczania preparatywnego ECKT, co mogło skutkować zanieczyszczeniem resztami cukrowymi. Kolejne etapy pracy i w konsekwencji publikacje pozwoliły na lepsze doczyszczenie badanych związków, rozszerzenie spektrum substratowego

o galaktozę i laktozę, a także zbadanie innych obiektów biologicznych (publikacje P3 i P4). Dodatkowo, interesującym doświadczeniem byłoby zweryfikowanie, czy sama obecność badanych ECKT w hodowli mogłaby wspomagać działanie wybranych antybiotyków, czyniąc drobnoustroje bardziej na nie wrażliwymi. Warto zatem przetestować działanie addytywne czy też synergistyczne otrzymanych ECKT z antybiotykami względem szczepów wzorcowych.

Publikacja 3 – International Journal of Molecular Sciences 2021

International Journal of *Molecular Sciences*

Open Access Article

In Search of Effective Anticancer Agents—Novel Sugar Esters Based on Polyhydroxyalkanoate Monomers

by Wojciech Snoch [1], Dawid Wnuk [2], Tomasz Witko [1], Jakub Staroń [3], Andrzej J. Bojarski [3], Ewelina Jarek [1], Francisco J. Plou [4] and Maciej Guzik [1,*]

[1] Jerzy Haber Institute of Catalysis and Surface Chemistry, Polish Academy of Sciences, Niezapominajek 8, 30-239 Kraków, Poland

[2] Department of Cell Biology, Faculty of Biochemistry, Biophysics and Biotechnology, Jagiellonian University, Gronostajowa 7, 30-387 Kraków, Poland

[3] Maj Institute of Pharmacology, Polish Academy of Sciences, Smętna 12, 31-343 Kraków, Poland

[4] Instituto de Catalisis y Petroleoquimica, CSIC (Spanish National Research Council), Calle de Marie Curie, 2, 28049 Madrid, Spain

[*] Author to whom correspondence should be addressed.

Academic Editor: Hidayat Hussain

Int. J. Mol. Sci. **2021**, *22*(13), 7238; **https://doi.org/10.3390/ijms22137238**

Received: 28 May 2021 / Revised: 28 June 2021 / Accepted: 29 June 2021 / Published: 5 July 2021

Po przebadaniu uzyskanych ECKT pod kątem działania przeciwbakteryjnego i przeciwdrożdżakowego zsyntezowano kolejną porcję ECKT, tym razem dodatkowo z udziałem cukrów lac i gal, oraz podjęto próbę zweryfikowania ich właściwości antyproliferacyjnych względem ludzkich komórek rakowych. W pierwszym etapie konieczne było nie tylko powtórzenie wszystkich syntez w skali preparatywnej, lecz także rozszerzenie z gal i lac. Niezbędne okazało się również zoptymalizowanie procedury oczyszczania badanych związków. W tym celu dokonano uzupełnienia przeglądu literaturowego, w odniesieniu do biokatalitycznej syntezy ECKT na bazie laktozy [19, 91–93]. W konsekwencji, protokoły wypracowane i opisane w P1 i P2 zmodyfikowano w następujący sposób: zmieniono stosunek molowy cukru do komponenty hydrofobowej na 2:1 oraz wydłużono czas prowadzenia reakcji do 48 h. ECKT oczyszczano z wykorzystaniem kolumny preparatywnej RP-C18 VersaPack i układu woda/metanol. Strukturę związków potwierdzono nie tylko za pomocą UHPLC-MS w trybie MRM (jak w P1 i P2), lecz także poprzez metody spektroskopowe ^{1}H NMR, ^{19}F NMR, IR. Procedurę pozyskiwania estrów metylowych monomerów PHN (mPHN-Me) oraz ich fluorowania przeprowadzono zgodnie z protokołem przedstawionym w artykule P2.

Ocena cytotoksyczności ECKT i właściwości antyproliferacyjnych

Dokładny protokół opisano w sekcji *Materials and methods*. W skrócie – przygotowano roztwory wyjściowe o stężeniu po 25 mmol l^{-1} zsyntezowanych związków w DMSO oraz użyto je do otrzymania odpowiednich rozcieńczeń przez dodanie PBS. Serie rozcieńczeń przefiltrowano przez filtry 0,22 μm w warunkach sterylnych i dodano do odpowiednio rozhodowanych komórek rakowych i zdrowych komórek referencyjnych w stężeniach końcowych 0,0624, 0,125, 0,250, 0,50 mg ml^{-1} (tak żeby stężenie DMSO nie przekraczało 2% v/v w studzience pomiarowej). Następnie przeprowadzono test MTT po odpowiednio 24 h, 48 h, 72 h i 120 h. Testowane linie rakowe to rak prostaty (Du145) oraz ludzki czerniak skóry (HTB140). Wybór tych linii jest uzasadniony tym, że rak prostaty jest jedną z najczęściej diagnozowanych chorób nowotworowych (1 414 259 mężczyzn w 2022 r.) [1]. Rak skóry – czerniak, mimo dostępu do szerokiego wachlarzu metod leczenia, potrafi nawracać na skórze nawet w miejscach po wycięciu guza. Stąd potrzeba uzupełniania strategii leczniczych. Z drugiej strony jest interesującym materiałem badawczym ze względu na łatwość w testowaniu na nabłonkach potencjalnych nowych preparatów medycznych.

Tabela 6. Cytotoksyczność ECKT oznaczona za pomocą testu MTT

	Czas [h]	C9-glu	C9-gal	C9-lac	PHN-glu	PHN-gal	PHN-lac	F-mPHN-glu	F-mPHN-gal	F-mPHN-lac
DU145 (rak prostaty)	24	1317,1	1560,5	919,5	932,1	750,9	161,2	–	–	–
	d	66	78	46	146	169	3	–	–	–
	72	658,6	780,3	836,9	541,1	500,0	131,4	100,0	100,0	83,8
	d	33	39	169	159	100	5	5	5	4
	120	1317,1	1560,8	459,8	315,7	304,6	91,3	100,0	100,0	335,0
	d	66	78	23	41	2	3	5	5	17
PNT2 (nabłonek prostaty – kontrola)	24	2491,5	2390,9	1707,2	1507,6	1256,8	421,0	–	–	–
	d	285	120	110	80	32	79	–	–	–
	72	1110,5	1233,3	919,5	1312,2	612,5	199,5	926,8	1183,5	1156,4
	d	207	327	46	115	31	42	127	238	234
	120	2053,1	2355,3	1743,7	1180,2	1838,4	165,2	1075,5	704,9	662,5
	d	538	220	33	247	20	5	296	117	8
HTB140 (ludzki czerniak)	24	1468,8	1659,0	621,6	1767,6	967,3	640,0	63,3	155,9	189,0
	d	46	434	77	253	26	250	24	3	49
	72	1317,1	1560,5	919,5	1195,7	1224,9	283,4	89,3	155,9	216,9
	d	66	78	46	232	61	8	2	3	21
	120	1133,9	1560,5	805,3	1689,4	1496,4	435,0	372,4	247,9	394,2
	d	92	78	51	35	2	10	3	11	70
HaCAT (ludzkie keratynocyty – kontrola)	72	1317,1	1560,5	919,5	1427,3	1200,0	383,9	733,7	580,0	644,1
	d	66	78	46	71	60	25	81	37	17
	120	–	–	–	–	–	–	800,8	945,9	670,0
	d	–	–	–	–	–	–	40	47	33
HSF (ludzkie fibroblasty skórne – kontrola)	72	1317,1	1560,5	919,5	613,4	624,2	445,8	–	–	–
	d	66	78	46	12	322	24	–	–	–
	120	–	–	–	761,2	499,6	631,1	761,2	499,6	631,1
	d	–	–	–	143	25	64	143	25	64

[µmol l^{-1}]: znak „–" – nie oznaczono, d – odchylenie standardowe. Czerwone pola oznaczają najniższe wartości stężeń związków – redukujące populację komórek do 50% (IC50). Informują o najwyższej toksyczności, zielone pola oznaczają najwyższe stężenia IC50. Informują o najniższej toksyczności.

Analizując wpływ ECKT na bazie F-mPHN na linię czerniaka HTB140 po 24 h i 72 h inkubacji, stwierdzono wyższą skuteczność F-mPHN-glu w działaniu antyproliferacyjnym (wartości IC50 odpowiednio ~60 i ~90 μmol l^{-1}) niż F-mPHN-gal (156 μmol l^{-1}). Wydłużenie czasu inkubacji do 120 h nie wpłynęło negatywnie na komórki nowotworowe. Spowodowało to wzrost stężeń IC50 do 370 μmol l^{-1} dla F-mPHN-glu, do 250 μmol l^{-1} dla F-mPHN-gal i 390 μmol l^{-1} dla F-mPHN-lac, odpowiednio. W stosunku do komórek kontrolnych HaCaT i HSF, konieczne było zastosowanie odpowiednio od 2 do 8 razy większych stężeń omawianych związków. Związek mPHN-lac wykazał znacznie wyższą toksyczność wobec linii DU145 niż jego odpowiedniki mPHN-glu i mPHN-gal i mniejszą niż te mające grupy trifluoroetylowe. Wartość IC50 mPHN-lac spadła z 160 μmol l^{-1} po 24 h, przez 130 μmol l^{-1} po 72 h do mniej niż 90 μmol l^{-1} po 120 h. mPHN-lac okazał się mniej szkodliwy dla komórek PNT2, ponieważ ich wartości IC50 spadły z co najmniej 420 μmol l^{-1} po 24 h do 160 μmol l^{-1} po 120 h. Bardziej obiecująca sytuacja była w przypadku komórek czerniaka. IC50 tych związków wynosiło 690 μmol l^{-1} po 24 h; 280 μmol l^{-1} po 72 h i 430 μμmol l^{-1} po 120 h dla komórek HTB140, natomiast IC50 po 72 h dla komórek kontrolnych: HaCaT wynosił 38 μmol l^{-1} i 500 μmol l^{-1} dla HSF.

By dodać bardziej szczegółowy kontekst do dyskusji w publikacji P3, uzupełniono ją o dodatkowy przegląd literaturowy uwzględniający zakresy stężeń cytotoksycznych powszechnie stosowanych chemioterapeutyków oraz innych estrów cukrowych. Na jego podstawie sporządzono poniższą tabelę cytotoksyczności (tabela 7).

Tabela 7. Zestawienie cytotoksyczności wybranych ECKT oraz popularnych chemioterapeutyków względem konkretnych linii rakowych

Związek	IC/EC50 [μmol l^{-1}]	Testowana linia rakowa	Referencja:
cis-platyna	1,14–33	B16F10 czerniak	[94, 95]
	20	Du145	
Paclitaxel/Taxol	0,00126–12,30	Testowane na 397 różnych linii	[94]
SN-38	0,824±0,163	A549 (adenocarcinoma – rak płuc)	[95]
	0,5	H1975 (adenocarcinoma – rak płuc)	
Deaotaxel	0,0056	A549	
	0,0014	H1975	
C8 – Laktoza (caprate)	> 2000	Calu–3/Caco–2 (rak okrężnicy)	[96]
C12 – Laktoza (laurynian)	1069/376		
C16 – Laktoza (palmitynian)	122/60		
C14 – Laktoza (myristynian)	261/112		
(C16) 6-O-palmitoilmaltotriozyd	2,3/3,6	Hep–G2/HeLa	[97]
(C12) (dodecylo)α-D-maltozyd	23		
(C8) 6,6′-di-O-oktanoilo-α,α-trehalozyd	7,4–14,8	BALB/3T3 i KATO III	[98]
(C12) dodecylo-β-D-maltorioza	23		
Fluorowany łańcuch, zawierający grupy triazolowe – C8H17 β-D-glukozydy	1198	Jurkat (ludzki rak limfocytów T)	[99]
C16H33 β-D-glukoza	24		
Fluorowane C14–C19 z F 9–F17 glukopiranozydy	190–600	B16F10 (mysi czerniak skóry)	[73]
Fluorowane C7/C14/C19-gluko-/galakto-/maltopiranozydy	25–250		[75]

Na podstawie zestawionych powyżej wartości można stwierdzić, że estry cukrowe nie mogą konkurować z popularnymi chemioterapeutykami takimi jak cis-Pt, Paclitaxel czy SN-38. Jednak wartości IC50/EC50 są zbliżone do innych estrów takich jak: C14 – Laktoza (myristynian), C16 – Lactoza (palmitynian), C12 – Laktoza (laurynian), a nawet fluorowanych C14–C19 z F9–F17 glukopiranozydów i fluorowanych C7/C14/C19–gluko–/galakto–/maltopiranozydów. Jednocześnie wartość toksycznego stężenia zależy nie tylko od budowy (cukru, długości łańcuch węglowego, obecności i ilości atomów F), lecz także od rodzaju komórek. Na przykładzie komórek Calu–3/Caco–2 (rak okrężnicy) widać, że wzrost łańcucha alifatycznego estru laktozowego powoduje zmniejszenie wartości IC50 odpowiednio z 1069 μmol l^{-1} do 122/60 μmol l^{-1} i 261/112 μmol l^{-1}. Ponadto inne komórki typu BALB/3T3 i KATO III czy Hep-G2/HeLa są 100 razy bardziej czułe na związki o podobnej długości łańcucha. Jest to sugestia, by rozszerzyć zakres badanych obiektów o różne linie komórkowe. Dodatkowo zaobserwowano, że obecność wielu ugrupowań C–F w łańcuchach alifatycznych fluorowanych C14–C19 z F9–F17 glukopiranozydów i fuorowanych C7/C14/C19-gluko-/galakto-/maltopiranozydów nie czyni ich o rząd lub dwa rzędy wielkości bardziej toksycznymi względem komórek czerniaka w porównaniu z fluorowanymi ECKT opisywanymi w P3.

Podsumowanie i wnioski

Pomimo stosunkowo wysokich wartości IC50 (60–170 μmol l^{-1}) zsyntetyzowanych ECKT względem komórek rakowych Du145 i HTB140, w porównaniu z powszechnie stosowanymi chemioterapeutykami, badane związki mogą konkurować z innymi ECKT opisanymi już w literaturze. Surfaktanty na bazie PHA mogłyby tworzyć mikroemulsje lub mikroemulsyjne systemy dostarczania leków, które dalej pomagałyby w stabilizacji i dystrybucji stosowanych komercyjnie leków w leczeniu raka lub terapii genowej. Takie nośniki na bazie ECKT stanowią potencjalne narzędzie do współpracy z chemioterapeutykami także dzięki ich własnym właściwościom cytotoksycznym [101–103]. Ciekawym ich aspektem są również potencjalne właściwości antyprzerzutowe. Dalsze zbadanie tego zjawiska w rozszerzonym programie badawczym dostarczyłoby wielu istotnych informacji. Przesłanką do tego jest widoczny wpływ badanych EKCT na cytoszkielet i włókna pośrednie komórki [103]. Wreszcie panel testowanych linii komórkowych w eksperymentach cytotoksyczności powinien zostać poszerzony o inne linie, które mogą być bardziej wrażliwe na syntetyzowane związki. Podsumowując, dane zawarte w tym manuskrypcie stanowią punkt odniesienia dla przyszłych badań związanych z tworzeniem SMEDDS w oparciu o zsyntetyzowany ECKT do celowanych terapii przeciwnowotworowych.

Publikacja 4 – Frontiers in Bioengineering and Biotechnology 2023

"Physicochemical studies of novel sugar fatty acid esters based on (R)-3-hydroxylated acids derived from bacterial polyhydroxyalkanoates and their environmental impact"

frontiers | Frontiers in Bioengineering and Biotechnology

TYPE Original Research
PUBLISHED 09 February 2023
DOI 10.3389/fbioe.2023.1112053

OPEN ACCESS

EDITED BY
Kevin Edward O Connor,
University College Dublin, Ireland

REVIEWED BY
Anastasia Zerva,
Agricultural University of Athens, Greece
Eduardo J. Gudiña,
University of Minho, Portugal

*CORRESPONDENCE
Maciej Guzik,
maciej.guzik@ikifp.edu.pl

SPECIALTY SECTION
This article was submitted to Industrial Biotechnology, a section of the journal Frontiers in Bioengineering and Biotechnology

RECEIVED 30 November 2022
ACCEPTED 16 January 2023
PUBLISHED 09 February 2023

Physicochemical studies of novel sugar fatty acid esters based on (*R*)-3-hydroxylated acids derived from bacterial polyhydroxyalkanoates and their potential environmental impact

Wojciech Snoch[1], Ewelina Jarek[1], Dusan Milivojevic[2], Jasmina Nikodinovic-Runic[2] and Maciej Guzik[1]*

[1]Jerzy Haber Institute of Catalysis, Surface Chemistry Polish Academy of Sciences, Kraków, Poland, [2]Institute of Molecular Genetics and Genetic Engineering, University of Belgrade, Belgrade, Serbia

Po zweryfikowaniu właściwości przeciwrakowych opisanych ECKT koniecznymi dalszymi etapami w procesie potencjalnego użycia danego związku lub jego formulacji w przemyśle jest charakterystyka fizykochemiczna i orientacyjne określenie potencjalnego wpływu badanych związków na środowisko. W tym wypadku badania ograniczone zostały tylko do niemodyfikowanych ECKT, gdyż ze względu na ich budowę (oraz brak fluoroalkilu) estry te mogą stanowić odpowiednik lub zamiennik surfaktantów niejonowych używanych powszechnie w kremach, maściach czy emulsjach.

Protokoły opracowane w ramach realizacji publikacji P3 zostały zmodyfikowane tak, by umożliwić dalszy proces usprawniania otrzymywania ECKT. Zwiększono objętość całkowitą reaktorów do 100 ml, żeby ułatwić rozpuszczanie się substratów cukrowych. Ponadto usprawniono proces oczyszczania poprzez zwiększenie liczby próbek nakładanych na kolumnę. Było to możliwe dzięki zastosowaniu złoża krzemionkowego modyfikowanego ugrupowaniami oktadecylowanymi w układzie fazy odwróconej (RP-C18) firmy KARL ROTH, które samemu można nałożyć na szklaną kolumnę o większej objętości i wypłukać

z niej pozostałe ECKT. Umożliwiło to również rozpoczęcie wzrostu gradientu od 10% fazy A (H_2O). Zabiegi te pozwoliły na zwiększenie całkowitej masy produktów eluowanych z kolumny preparatywnej odpowiednio nawet do 118–600 mg przy zachowaniu podobnego poziomu wydajności względem wyników opisanych w publikacji P3. Zwiększyły one jednak udział diestrów w badanych mieszaninach ECKT i nie rozwiązały problemu rozdziału mono- od diestrów. Kwestia ta istotnie wpływa na charakterystykę właściwości fizykochemicznych ECKT (dynamiczne napięcie powierzchniowe, CMC, zdolność do stabilizacji emulsji). Ponadto zwrócono uwagę na istotny aspekt dotyczący metody detekcji i oznaczenia jakościowego i ilościowego reagentów. Usprawniono czułość detekcji substratów cukrowych (UHPLC-MS tryb MRM), co pozwoliło na wykreślenie krzywych kalibracyjnych i oznaczenie zawartości pozostałych cukrów. Czystości badanych ECKT oznaczono metodą UHPLC-MS i wynosiły one odpowiednio 84–94%. Dodatkowo, estry cukrowe, ze względu na niejonowy charakter, mają ograniczoną zdolność rozpadu na jony potomne w trybie MRM, dając dużą intensywność pików w trybie SIM i znacznie niższą w trybie MRM. Niektóre z mono- oraz diestrów zawierające łańcuchy C7 (mPHN-glu C7C7, mPHN-gal C7 oraz C9C7, a także mPHN-lac C7, C7C7, C9C7) w ogóle nie ulegały rozpadowi w celce kolizyjnej (Q2). Porównano zatem pola powierzchni pików zarówno w trybie SIM, jak i MRM oraz uznano za trafniejsze posługiwanie się powierzchniami pików uzyskanych z trybu SIM przy wyznaczeniu średnich mas molowych otrzymanych mieszanin i kalkulacji procentowego udziału monoestrów (tabela 1 P4 przedstawiająca skład i masy związków, tabela S1 P4 zawierająca czystości i wydajności otrzymywania ECKT).

Na podstawie zmian napięcia powierzchniowego w czasie, roztworów wodnych zawierających różne stężenia ECKT, wykreślono krzywe, stężenia równowagowe (rys. 2 i 3 w artykule P4) oraz krytyczne stężenia agregacji (CAC; tabela 2 P4). Krzywe dla różnych stężeń (w pełni omówione w P4), ale o podobnym profilu i niewielkiej różnicy wartości, wskazują na agregację związku lub tworzenie miceli. W przypadku C9-glu, mPHN-glu, mPHN-gal i mPHN-lac zaobserwowano po dwa takie profile (rys. S1 P4).

Porównując wartości CAC badanych mieszanin ECKT oraz wartości napięć międzyfazowch ich roztworów z wartościami napięć i krytycznych stężeń micelizacji (CMC) związków o podobnej strukturze i/lub stosowanymi w przemyśle, można zaobserwować pewne zależności. Przedstawiono je w tabeli 8 i omówiono poniżej.

Tabela 8. Właściwości fizykochemiczne badanych ECKT zebrane razem i zestawione ze związkami referencyjnymi

Badane związki									
Nazwa związku	**CAC [mmol l^{-1}]**	**CAC [g l^{-1}]**	**Napięcie powierzchniowe γ [mN m^{-1}]**	**Teoretyczne wartości HLB (Griffin) w zależności od składu**					**pH**
				C9	**C7**	**C9C9**	**C7C7**	**C9C7**	
C9-glu	2,7	0,864	31,5–24,5	11,25	–	7,83	–	–	5,39
C9-gal	2,0	0,64	25,2–23,5	11,25	–	7,83	–	–	5,33
C9-lac	0,56	0,27	29,2–25,8	14,20	–	11,00	–	–	6,29
mPHN-glu	1,4	0,471	35–26	11,72	12,79	8,70	9,81	9,22	3,92
mPHN-gal	0,56	0,188	37–32	11,72	12,79	8,70	9,81	9,22	4,12
mPHN-lac	0,016	0,0079	39–28,5	14,41	15,27	11,49	12,57	12,01	6,8

Związki referencyjne				
Nazwa związku	**CMC [mmol l^{-1}]**	**Napięcie powierzchniowe γ [mN m^{-1}]**	**HLB (Griffin)**	**REF**
β -D-glukozyd oktylowy	21,2	31	12,32	[104]
β -D-glukozyd nonylowy	6,9	29,6	11,7	
Monooktanian glukozy (C8)	10,15	26,37	11,76	[105]
Monodekanian glukozy (C10)	0,71	30,49	10,77	
Monodekanian glukozy (C10)	1,5	25,5	10,77	[106]
Kaprynian laktozy (C10)	2,5	40,6	14,8	[107]
Laurynian laktozy (C12)	0,55	40,4	14,1	[108]
Laurynian sacharozy (C12)	1,2	19,7	8,19	[109]
Oleinian sacharozy (C18)	0,0345	29,6	10,1	
Tween 80	0,01	38	15	
Laurynian α-D-glukozy (C12)	0,13	41,2	3,8	[110] [111]
Laurynian α-D-maltozy (C12)	0,12	35,9	4,5	
Tetradekanian laktozy (C14)	0,041	38,6	4,3	
Monooktanian sacharozy (C8) SM-800 ®	6,0	28,7	15,8	[112]
SM-1000 ®	0,57	32,9		
SM-1200 ®	0,27	33,5		

Biorąc pod uwagę skład badanych mieszanin i udział diestrów, oczekiwalibyśmy niższych zakresów stężeń CAC, podobnych do przedstawionych w tabeli 8, m.in. oleinianu sacharozy. Wartości te odpowiadają jednak w przybliżeniu wartościom innych estrów czy eterów zawierających dłuższe łańcuchy węglowe (również zestawionych w tej tabeli). Przykładami mogą być: monodekanian glukozy (C10), kaprynian laktozy (C10), laurynian laktozy (C12) oraz laurynian sacharozy (C12). Dodatkowo wartości napięć powierzchniowych badanych ECKT ($\gamma = 39$–$24{,}5$ mN m^{-1}) również mieszczą się w zakresie porównywanych estrów ($\gamma = 40{,}6$–$19{,}7$ mN m^{-1}). Jak widać, obecność dodatkowych łańcuchów C9 lub C7 w składniku hydrofobowym nie przekłada się bezpośrednio na właściwości porównywalne z dwukrotnie dłuższymi łańcuchami alifatycznymi innych estrów. Nie wiemy dokładnie, czy diestry na bazie monomerów PHN powstają głównie przez łączenie się z ich grupami 3–OH, czy z grupami cukrowymi –OH. Połączenie łańcuchów C7 i C9 monomerów PHN lub reszt kwasu nonanowego, odpowiednio z różnymi grupami –OH cukrów, powoduje rozgałęzienie całej cząsteczki, co ma wpływ na jej właściwości fizykochemiczne. Co więcej, sama obecność 3–OH monomerów może również wpływać na rozgałęzienie całej cząsteczki i zakłócać hydrofobowość łańcucha węglowego [106]. Nie mamy jednak wystarczających danych, aby przeprowadzić szczegółową analizę ich struktury. By rozwiązać ten problem, należałoby rozdzielić monomery C9 od C7 przed reakcjami, następnie ponownie przeprowadzić reakcje enzymatyczne w skali preparatywnej, a na etapie oczyszczania zwiększyć rozdzielczość, manipulując zmianą gradientu MeOH względem H_2O, objętościami zbieranych frakcji i szybkością przepływu. Po rozdziale preparatywnym badane frakcje należy dokładnie osuszyć i poddać analizie ^{1}H NMR, ^{12}C NMR, 3D NMR i HR-MS. Otrzymane spektra należy ze sobą zestawić i przedyskutować intensywności i stosunki poszczególnych sygnałów.

Stabilizacja emulsji

Kolejnym ważnym etapem dla charakterystyki i przydatności nowych ECKT w przemyśle kosmetycznym i farmaceutycznym było określenie zdolności do stabilizacji emulsji. W tym celu sporządzono serię układów woda/olej (W/O), gdzie fazą wodną były roztwory ECKT w stężeniach odpowiednio 0,5 × CAC, 1,0 × CAC i 1,5 × CAC, a fazą olejową stanowił popularny w kosmetykach skwalan lub oliwka do pielęgnacji skóry dzieci Bambino® (zawierająca kosurfaktanty). Po wytrząsaniu układy filmowano przez pierwsze 5 min, a potem robiono zdjęcia w czasach t = 30 min, 1 h, 3 h, 5 h i 24 h. Na podstawie konsystencji i formy emulsji dobrano skalę oceniającą ich stabilność.

Na podstawie serii filmów i zdjęć wykonanych dla 48–godzinnych układów W/O zawierających różne stężenia badanych ECKT nie można było zmierzyć grubości warstwy emulsji, a tym samym określić wskaźnika stabilności emulsji (*Emulsion Stability Index*, w skrócie: ESI). Wynikało to z krótkiego czasu życia emulsji. Jednak w zależności od rodzaju estru, jego stężenia i składu fazy olejowej układy emulsyjne tworzyły się i utrzymywały od kilku minut do 1 h. Emulsje zawierające skwalan były mniej stabilne. Układy referencyjne W/O niezawierające estrów rozmywają się już po kilku minutach. Z kolei systemy zawierające ECKT na bazie olejku do pielęgnacji ciała okazały się bardziej trwałe, ponieważ miały zróżnicowany skład i zawierały kosurfaktanty, takie jak długołańcuchowe alkohole. Ponadto w większości przypadków można było zaobserwować różnice w trwałości i konsystencji emulsji, zależne od stężenia ECKT w fazie wodnej. Im wyższe stężenie ECKT, tym stabilniejszy i bardziej jednorodny układ. Najbardziej stabilne okazały się systemy zawierające C9-glu i C9-gal. Najmniej stabilny system zawierał C9-lac. Emulsje na bazie estrów mPHN-glu i mPHN-gal okazały się mniej stabilne niż te z kwasu nonanowego. Natomiast emulsje zawierające mPHN-lac wykazywały wyższą trwałość niż mPHN-glu, mPHN-gal i C9-lac.

Idealny system W/O stosowany w przemyśle kosmetycznym lub farmaceutycznym pochodzi z naturalnych źródeł. Emulsje muszą być wystarczająco stabilne, aby można je było przechowywać w temperaturze pokojowej. Z drugiej strony, powinny być biodegradowalne i biokompatybilne. Natomiast w przypadku systemów dostarczania leków nie jest również wskazane, by czas ich istnienia w organizmie był dłuższy niż 48–72 h. Zbyt długo cyrkulujące w tkankach układy micelarne, mikro i nanokapsułki, czy same surfaktanty mogą zwiększyć wchłanianie przez błony komórkowe innych, niepożądanych substancji. Innym ważnym czynnikiem jest biodostępność emulsji. Oznacza to łatwe wchłanianie przez powierzchnie nabłonka, przechodzenie przez błony komórkowe, ale nieuszkadzanie ich [113]. Micele chroniące strukturę leku przed enzymami i zmiany pH powinny umożliwiać stopniowe uwalnianie go do tkanek [114]. Składniki budujące micele powinny być łatwo rozkładane w organizmie lub z niego usuwane oraz degradowane w środowisku, w którym potem ewentualnie mogą się znajdywać [116–122]. Niewątpliwie badane ECKT wykazują pewne właściwości stabilizujące emulsję, ale w celu nadania układom W/O pożądanej jakości wymagana jest ich dalsza optymalizacja, w tym stężenia ECKT, składu fazy olejowej, metod mieszania i dodatku kosurfaktantów [122].

Na uwagę zasługuje również fakt, że chociaż zdolność ECKT do stabilizacji emulsji nie jest spektakularna, wykazują one właściwości przeciwnowotworowe (P3), co zwiększa ich możliwości zastosowania w przemyśle [123].

Potencjalny wpływ ECKT na środowisko

Caenorhabiditis elegans to wielokomórkowy, niepasożytniczy organizm modelowy, który jest cennym obiektem badawczym do testowania działania różnych przemysłowych substancji chemicznych, takich jak leki przeciwnowotworowe i antybiotyki [125, 126]. Każdego roku ludzkość wytwarza ogromne ilości ścieków przemysłowych, a wraz z nimi środków powierzchniowo czynnych [114, 115, 127, 128]. Dlatego istnieje potrzeba ciągłego monitorowania ich wpływu na organizmy żyjące w glebie i wodach gruntowych [129, 130]. Przydatność przedstawicieli Nematoda przejawia się w szybkim cyklu życiowym, łatwym rozmnażaniu i uzyskiwaniu dużej liczby osobników w kolejnych pokoleniach (są hermafrodytami) oraz możliwości długotrwałego przechowywania larw i jaj w warunkach laboratoryjnych. Nie wymagają ciągłej hodowli, a procedura synchronizacji cykli życiowych osobników w populacji jest prosta. Ponadto nicienie żywią się łatwo dostępnym źródłem pożywienia – bakteriami *E. coli*. Najważniejsza z ludzkiego punktu widzenia, jest obecność prostych układów narządów: nerwowego (pierścień nerwowy), krwi, protonefrydialnego, gonad oraz umiejętność oceny nie tylko liczebności populacji pod mikroskopem, lecz także zdolności do aktywnego przemieszczania poszczególnych osobników w populacji. Dlatego nicienie mogą być pośrednim bioindykatorem wpływu badanych substancji na środowisko naturalne [131, 132].

Stosowanie estrów w formulacjach atopowych prowadzi do ich uwolnienia do środowiska naturalnego. Z tego powodu postanowiono przeprowadzić badania wstępne określające ich cytokotoksyczność. W tym celu badano wpływ estrów cukrów na nicieniach – oceniano ich przeżywalność po 48-godzinnej ekspozycji na wybrane stężenia ECTK. Na podstawie mobilności organizmów wyciągnięto wnioski dotyczące ich żywotności. Liczba osobników na studzienkę wynosiła 6–42. Każde stężenie związku badano w trzech powtórzeniach (1 stężenie na 3 studzienki) i wyniki uśredniano. Organizmy aktywnie poruszające się uważano za żywe, ledwo poruszające się – za żywe (mając na uwadze, że związki te mogą mieć negatywny wpływ na organizmy), a organizmy nieruchome – za martwe. Wyniki badań przeprowadzonych na nicieniach przedstawione są na rysunku nr 4 w publikacji P4, który został zaadaptowany i widnieje w tej pracy jako rys. 10.

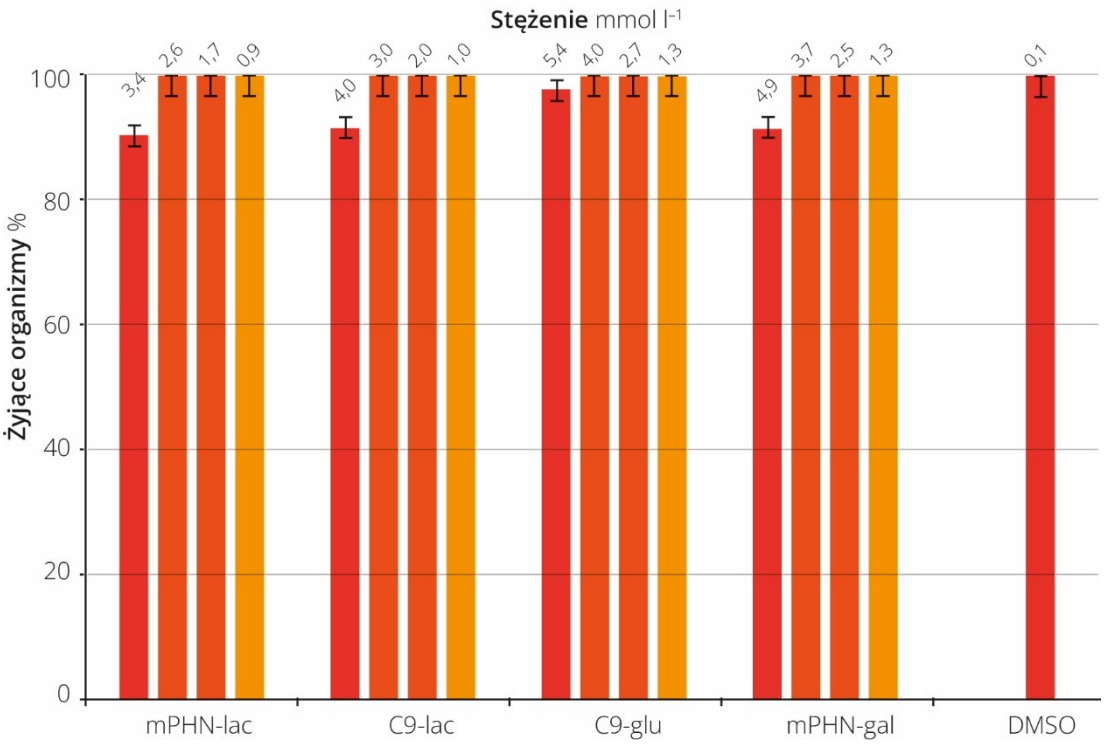

Rys. 10. Wykres przedstawiający toksyczności wybranych niemodyfikowanych ECKT, testowanych na *C. elegans*.

Przeprowadzone badania pozwoliły stwierdzić, że uzyskane ECKT nie stanowią większego zagrożenia dla badanych nicieni w tym czasie ekspozycji. Dopiero najwyższe ich stężenia (2,0 mg ml^{-1}) zmniejszyły populacje organizmów nawet o 15%, ale 1,5 mg ml^{-1} nie wpłynęło na nie, co również świadczy o ich niskiej szkodliwości. Stężenia estrów na studzienkę mieściły się w przedziale 0,0625–2,0 mg ml^{-1}, co odpowiada ich stężeniom molowym: C9-glu 0,186– 5,690 mmol l^{-1}; C9-gal 0,162– 5,312 mmol l^{-1}; C9-lac 0,125– 4,0 mmol l^{-1}; mPHN-glu 0,142– 4,544 mmol l^{-1}; mPHN-gal 0,148– 4,744 mmol l^{-1}; mPHN-lac 0,119– 3,816 mmol l^{-1}.

W porównaniu z wynikami omówionymi w artykule P3, poziomy wszystkich niemodyfikowanych estrów (opartych na monomerach PHN) redukujących populację komórek nowotworowych: Du145 i HTB140 o 50% (IC50) w okresie 24–72 h nie przekroczyły stężeń: 0,25 mg ml^{-1} (zakres IC50 odpowiednio 0,090–1,500 mmol l^{-1} dla komórek nowotworowych i 0,500–2,5 mmol l^{-1} odpowiednio dla zdrowych komórek odniesienia). Innymi słowy, zakres stężeń badanych związków wykazujących działanie przeciwnowotworowe jest znacznie niższy niż stężeń toksycznych dla nicieni, co sugeruje, że dalsze badania ECKT pod kątem zastosowania w medycynie nie powinny wykazywać charakteru ekotoksycznego [123].

Zaletą badanych w tej pracy ECKT jest brak w ich strukturze wiązań eterowych, które często występują w popularnych surfaktantach takich jak: glikol polietylenowy (PEG), betaina

kokamidopropylowa (CAPB) i hydroksysultaina kokamidopropylowa (CAPHS), Tween 20, Tween 80 [132], alkoholowy eter polioksyetylenowy (AEO) lub obecność innych możliwie toksycznych grup jak w przypadku eteru polioksyetylenowego alcylofenolu (APEO). To sprawia, że badane ECKT są łatwiej rozkładane przez enzymy w organizmach jedno- i wielokomórkowych [133]. Dodatkowo hydrofobowe składniki badanego ECKT nie przekraczają 9 atomów węgla, co może być kolejną zaletą w porównaniu z innymi powszechnie stosowanymi estrami: monolaurynianem sorbitanu (Span 20, Span 80), monolaurynianem PEG 20-Sorbitan (SPEG, Tween 20, Tween 80) na bazie kwasów o długości łańcucha odpowiednio C12, C16 i C18, ponieważ zwiększenie długości łańcucha składnika hydrofobowego zwiększa również toksyczność ECKT [134]. Dla porównania, toksyczność innych strukturalnie podobnych estrów allozy do *C. elegans* o różnych długościach łańcucha węglowego n = 2, 4, 6, 8 mieściła się w przedziale 0,2–1 mmol l^{-1} [135].

Weryfikując potencjalne zastosowanie danego związku, kosmetyku lub nośnika leku w przemyśle, zanim trafi on do badań przedklinicznych, konieczna jest ocena toksykologiczna na każdym z możliwych etapów (najmniejsza, największa szkodliwa dawka i przewlekłe podawanie związku), nie tylko komórkowym, ale także na bardziej złożonych organizmach żywych [137, 138]. Najwyższe testowane w niniejszej pracy poziomy ECKT (2,0 mg ml^{-1} około 6,0–8,0 mmol l^{-1}), które zmniejszały populacje *C. elegans* o około 15%, były znacznie powyżej ich wartości CAC. Jednocześnie zakres stężeń surfaktantów stosowanych w fazie wodnej do projektowania modelowych układów emulsyjnych wynosi 0,5–1,5-krotności CAC. Informacja o braku negatywnego wpływu estrów na badane nicienie w tym zakresie stężeń otwiera możliwość dalszych prób aplikacyjnych. Należy jednak pamiętać, że cząsteczki ECKT budujące micele mają inne stężenia i organizację niż te rozproszone w buforach, w których żyły badane organizmy. Mogą się zatem zachowywać inaczej i wykazywać inny poziom toksyczności [135, 139–141].

Podsumowanie i wnioski

Właściwości fizykochemiczne otrzymanych estrów cukrów nie zostały w pełni scharakteryzowane, ale są wystarczające do oceny ich potencjału aplikacyjnego. Aby dokładnie odpowiedzieć na pytanie, dlaczego ECKT wykazują tak wysokie poziomy CAC przy niskich wartościach napięcia międzyfazowego, należałoby oddzielić PHN C7 od monomerów C9, oddzielnie zsyntetyzować estry, a następnie oddzielić mono- od diestrów. Jest to proces czasochłonny i bardziej kosztowny w skali preparatywnej niż próba wytworzenia układów emulsyjnych opartych na mieszaninach opisanych powyżej. Niemniej jednak uzyskane wartości CAC i γ odpowiadają związkom o podobnej strukturze z literatury (takim jak SM-1000, tj. dekanian sacharozy, laurynian laktozy czy monodekanian glukozy). Również możliwość tworzenia systemów wodno-olejowych na bazie popularnych składników kosmetycznych – skwalanu i popularnej oliwki do pielęgnacji skóry dzieci – potwierdziła potencjał aplikacyjny badanych estrów. Jednak proces tworzenia i testowania tych emulsji powinien być dalej optymalizowany. Konieczne byłoby przetestowanie szeregu różnych składników olejów, a także kosurfaktantów w celu porównania ich wskaźników stabilności emulsji oraz wielkości i zachowania miceli.

W przyszłości warto skoncentrować się na ocenie toksyczności nie tylko samych związków, lecz także układów emulsyjnych opartych na ECKT. Rozszerzenie tych eksperymentów o takie aspekty jak wpływ ECKT na zwiększenie podatności *C. elegans* na działanie różnych niesprzyjających warunków glebowych (obecność pestycydów, soli nieorganicznych, niskie pH, substancje osmotycznie czynne). Badanie to mogłoby stanowić symulację tego, czy i jak układy W/O stabilizowane badanymi ECKT rzeczywiście zwiększają wchłanianie niekorzystnych substancji przez organizmy z otoczenia oraz zwiększają ich toksyczność. Cenna byłaby nawet ocena podatności na organizmy oportunistyczne. Z farmaceutycznego i medycznego punktu widzenia kluczowym krokiem jest odpowiedź na pytanie dotyczące mechanizmów działania estrów, w tym utraty łączności błon wewnątrzkomórkowych [96]. Nicienie należy zbadać bardziej szczegółowo pod kątem wpływu ECKT (i stabilizowanych przez nie układów emulsyjnych) na ich narządy wewnętrzne, takie jak układ hormonalny i nerwowy, a także zdolność do rozmnażania [130, 142].

5. Podsumowanie i wnioski końcowe

Niniejsza rozprawa stanowi klamrę dla cyklu czterech publikacji, których jestem pierwszym współautorem i do których powstania znacząco się przyczyniłem. Przedstawiają pierwsze próby syntezy ECKT na bazie laktozy, glukozy i galaktozy oraz hydroksykwasów pochodzących z depolimeryzacji bakteryjnego PHN pozyskanego na drodze kontrolowanej fermentacji. Wszystkie pięć celów wymienionych w rozdziale 2 zostało zrealizowane. Potwierdzone zostały struktury nowo wytworzonych estrów, dopracowane metody ich syntezy, detekcji oraz oczyszczania w skali analitycznej i preparatywnej. Te ostatnie wymagają dalszych prac, w szczególności zwiększenia wydajności w kierunku wybranych: mono– lub diestrów i wydajnej ich separacji w skali preparatywnej.

Podwaliny dla całego procesu badawczego dały eksperymenty przesiewowe pozwalające na ustalenie optymalnych warunków reakcji syntezy ECKT za pomocą lipaz, a także warunków detekcji jakościowej produktów i ilościowej substratu cukrowego. Pozwoliło to na zrealizowanie publikacji P1, w której wykazano zasadność nie tylko testowania nowych, komercyjnych lipaz ale również ich immobilizacji na nowych podłożach ażurowych modyfikowanymi grupami –OH i $–NH_2$ (firma MATSPHERES®, współpraca z dr inż. Eweliną Cichoń). We współpracy z dr inż. Mateuszem Tataruchem (IKiFP PAN) skonstruowano i przedstawiono użycie reaktora przepływowego w skali miligramowej, z kolumną zawierającą immobilizowaną lipazę EL70 Eucodis Bioscience®. Okazał się on być konkurencyjny względem reaktorów typu całkowity wsad i daje możliwość nawet trzykrotnego użycia. Jednak by skorzystać w pełni z jego możliwości należy dokonać dalszych optymalizacji m.in. medium reakcyjnego (użyć np. DMF, lub NMP, zamiast DMSO).

We współpracy z promotorem pomocniczym dr. Jakubem Staroniem (IF PAN) opracowana została po raz pierwszy metoda wprowadzania fluorowcoalkilu do estrów metylowych monomerów PHN (P2 i P3). Nową metodę modyfikacji monomerów PHN warto spróbować adaptować w kierunku wprowadzania innych wartościowych dla farmakologii ugrupowań, np. fenylowych, metoksylowych czy trifluorofenylowych.

We współpracy z dr. Dawidem Wnukiem (ZBK WBBiB UJ) zweryfikowane zostały właściwości antyproliferacyjne uzyskanych ECKT względem komórek ludzkiego czerniaka HTB140 i raka prostaty Du145. Wartości IC50 będące wynikiem tych pierwszych badań nie wskazują, że badane ECKT mogą stanowić konkurencję dla leków wykorzystywanych w terapiach przeciwnowotworowych, jednak działają one w podobnym zakresie, co inne

opisane w literaturze ECKT. Wykazano natomiast większą cytotoksyczność fluorowanych ECKT (P3) względem niemodyfikowanych, a te z kolei – większą cytotoksyczność niż estry posiadające jedynie łańcuchy alifatyczne C9. Zamysł zatem wzmocnienia potencjału biologicznego ECKT poprzez udekorowanie komponenty hydrofobowej ugrupowaniami fluorowcoalkilu za pośrednictwem wiązania eterowego okazał się trafny. We współpracy z mgr Karoliną Stępień (ZMF WUM) zweryfikowane zostały bakteriostatyczne i przeciwdrożdżakowe właściwości wybranych estrów glukozy (P2). Okazały się one niesatysfakcjonujące do zastosowań przemysłowych. Natomiast we współpracy z dr. Dusanem Milivojevicem (IMGGE UB) wykazaliśmy potencjalnie niski negatywny wpływ na środowisko za pomocą testów toksyczności przeprowadzanych na modelowym organizmie *Caenorhabitis elegans* (P4). Oznaczenie podstawowych właściwości fizykochemicznych wybranych ECKT (HLB, pH, γ, CAC) oraz ich zdolności do stabilizacji emulsji (we współpracy dr Eweliną Jarek) pozwoliło na określenie szans wykorzystania badanych ECKT w przemyśle kosmetycznym i farmaceutycznym (P4).

Ponadto owocem niniejszych badań oprócz cytowanych i omawianych publikacji jest zgłoszenie patentowe nr P.437233 o tytule: „Zastosowanie estrów cukrowych kwasów tłuszczowych o komponencie kwasowej będącej mieszaniną monomerów uzyskanych z bakteryjnego polihydroksynonaniano-ko-heptanianu do hamowania proliferacji komórek nowotworowych w leczeniu i profilaktyce chorób” [142].

Wypracowane rozwiązania i uzyskane wyniki wykazują na tyle duży potencjał, że są wykorzystywane dalej – w projekcie NCN i NCBR Tango V–A/0013/2021 pt. „Opracowanie funkcjonalnej formy aplikacji estrów cukrowych kwasów tłuszczowych na bazie bakteryjnych polihydroksyalkanianów hamujących rozwój komórek nowotworowych”, dotowanym w wysokości 250 tys. PLN, którego jestem głównym wykonawcą. W projekcie tym skupiam się na opracowaniu lepiej działających formulacji, a co za tym idzie – aplikacji badanych modyfikowanych i niemodyfikowanych ECKT. Planowane do uzyskania formulacje, oprócz samych czystych mieszanin ECKT, to układy mikroemulsyjne oraz nano/mikrokapsułki. Wszystkie uzyskane układy będą testowane na szerokim panelu linii komórkowych raka jelita grubego oraz czerniaka. Najlepiej działająca formulacja jednego z estrów przejdzie do dalszych etapów. Są nimi: weryfikacja działania synergistycznego wraz z powszechnie wykorzystywanymi chemioterapeutykami, badania toksykologiczne na myszach oraz testy z ksenograftami tkankowymi pochodzącymi od pacjentów onkologicznych (układami PDX –

Patient Derived Xentograms). Badania te nie byłyby możliwie bez opracowanych metodologii syntezy i charakterystyki przedstawionych w niniejszej rozprawie doktorskiej.

Dalsze kierunki badań, jakie należy przeprowadzić w zakresie omawianej tematyki badawczej, można podzielić na dwa główne nurty: badania podstawowe i aplikacyjne. Badania podstawowe winny skupić się na doprecyzowaniu mechanizmu i dróg działania modyfikowanych i niemodyfikowanych ECKT na układy żywe oraz uściśleniu, czy i jak dokładnie ECKT oddziałują z błonami komórkowymi oraz strukturami subkomórkowymi; z jakimi receptorami się wiążą i jak wpływają na genom komórek; czy i jak aktywują szlak apoptotyczny; czy wpływają na wiązanie się komórek do podłoża, czy też zaburzają glikolizę [143]. W tym celu należałoby zsyntezować i wprowadzić do komórek/organizmów formy deuterowane badanych związków [144]. Warto również skorzystać z badań proteomicznych z wykorzystaniem metod western blot, spektrometrii masowej, mikroskopii fluorescencyjnej oraz cytometrii przepływowej [145]. Ponadto warto spróbować alternatywnych możliwości alkilacji grup 3-OH monomerów PHN tak, żeby móc wprowadzić inne ugrupowania np. fenylowe, metoksylowe, trifluoroetylowe. W szczególności ważnym aspektem wydaje się enzymatyczna droga alkilacji hydroksykwasów czy utworzonych z nich ECKT [146, 147]. Badania aplikacyjne z kolei winny się skupić na zwiększeniu wydajności modyfikacji monomerów oraz syntezy estrów cukrowych na większą skalę, a także na zwiększeniu efektywności separacji mono- od diestrów przed samą modyfikacją i acylacją nimi cukrów. Ponadto dalszej optymalizacji wymaga otrzymywanie stabilnych układów W/O, mikroemulsji/mikrokapsułek jako potencjalnych nośników leków.

Podsumowując, bazując na wymienionych publikacjach, patencie, projektach, a przede wszystkim wynikach badań, można stwierdzić, że nowo zsyntezowane i scharakteryzowane ECKT oraz ich modyfikacje stanowią nowy, cenny materiał badawczy i nadają się do podjęcia dalszych etapów weryfikacji możliwości ich zastosowań w medycynie, przemyśle farmaceutycznym i kosmetycznym. Przedstawione metody syntezy i oczyszczania, mimo stosunkowo niskich wydajności, okazały się wystarczające, aby można było zidentyfikować, wstępnie scharakteryzować i zbadać właściwości biologiczne ECKT. Tym niemniej autor jest świadomy, iż jest to dopiero wierzchołek góry lodowej w odniesieniu do badań nad tą interesującą grupą związków.

6. Bibliografia

[1] "WHO Cancer," 2021. [Online]. Available: https://www.who.int/health-topics/cancer. [Accessed: 15-Mar-2021].

[2] J. J. Tuech *et al.*, "Strategy for the practice of digestive and oncological surgery during the Covid-19 epidemic," *J. Visc. Surg.*, vol. 157, no. 3, pp. S7–S12, 2020, doi: 10.1016/j.jviscsurg.2020.03.008.

[3] W. Liang *et al.*, "Cancer patients in SARS-CoV-2 infection: a nationwide analysis in China," *Lancet Oncol.*, vol. 21, no. 3, pp. 335–337, 2020, doi: 10.1016/S1470-2045(20)30096-6.

[4] "Treatment for Cancer - NCI." [Online]. Available: https://www.cancer.gov/about-cancer/treatment.

[5] K. Alpaugh and M. Von Mehren, "Monoclonal antibodies in cancer treatment: A review of recent progress," *BioDrugs*, vol. 12, no. 3, pp. 209–236, 1999, doi: 10.2165/00063030-199912030-00004.

[6] T. F. Galvão, A. Livinalli, L. C. Lopes, I. R. Zimmermann, and M. T. Silva, "Biosimilar monoclonal antibodies for cancer treatment," *Cochrane Database Syst. Rev.*, vol. 2020, no. 2, 2020, doi: 10.1002/14651858.CD013539.

[7] F. J. Esteva, V. M. Hubbard-Lucey, J. Tang, and L. Pusztai, "Immunotherapy and targeted therapy combinations in metastatic breast cancer," *Lancet Oncol.*, vol. 20, no. 3, pp. e175–e186, 2019, doi: 10.1016/S1470-2045(19)30026-9.

[8] and R. R. D. Cody Barbari, Tyler Fontaine, Priyanka Parajuli, Narottam Lamichhane, Silvia Jakubski, Purushottam Lamichhane, "Immunotherapies and Combination Strategiesfor Immuno-Oncology." .

[9] A. Aghebati-Maleki *et al.*, "Nanoparticles and cancer therapy: Perspectives for application of nanoparticles in the treatment of cancers," *Journal of Cellular Physiology*, vol. 235, no. 3. pp. 1962–1972, 2020, doi: 10.1002/jcp.29126.

[10] W. Park, Y. J. Heo, and D. K. Han, "New opportunities for nanoparticles in cancer immunotherapy," *Biomaterials Research*, vol. 22. 2018, doi: 10.1186/s40824-018-0133-y.

[11] L. N. Borgheti-Cardoso *et al.*, "Nanotechnology approaches in the current therapy of skin cancer," *Adv. Drug Deliv. Rev.*, 2020, doi: 10.1016/j.addr.2020.02.005.

[12] N. Sobhani *et al.*, "Therapeutic cancer vaccines: From biological mechanisms and engineering to ongoing clinical trials," *Cancer Treat. Rev.*, vol. 109, no. May, p. 102429, 2022, doi: 10.1016/j.ctrv.2022.102429.

[13] A. L. Huff, E. M. Jaffee, and N. Zaidi, "Messenger RNA vaccines for cancer immunotherapy: progress promotes promise," *J. Clin. Invest.*, vol. 132, no. 6, 2022, doi: 10.1172/JCI156211.

[14] R. A. Ward, S. Fawell, N. Floc'H, V. Flemington, D. McKerrecher, and P. D. Smith, "Challenges and Opportunities in Cancer Drug Resistance," *Chem. Rev.*, vol. 121, no. 6, pp. 3297–3351, 2021, doi: 10.1021/acs.chemrev.0c00383.

[15] N. Chatterjee and T. G. Bivona, “Polytherapy and Targeted Cancer Drug Resistance,” *Trends in Cancer*, vol. 5, no. 3, pp. 170–182, 2019, doi: 10.1016/j.trecan.2019.02.003.

[16] A. P. C. Araújo, C. Mesak, M. F. Montalvão, Í. N. Freitas, T. Q. Chagas, and G. Malafaia, “Anti-cancer drugs in aquatic environment can cause cancer: Insight about mutagenicity in tadpoles,” *Sci. Total Environ.*, vol. 650, pp. 2284–2293, 2019, doi: 10.1016/j.scitotenv.2018.09.373.

[17] C. G. Alimba, K. O. Adekoya, and O. O. Soyinka, “Exposure to effluent from pharmaceutical industry induced cytogenotoxicity, hematological and histo-pathological alterations in clarias gariepinus (Burchell, 1822),” *EXCLI Journal*, vol. 18. pp. 63–78, 2019, doi: 10.17179/excli2018-1916.

[18] V. P. Torchilin, “Micellar nanocarriers: Pharmaceutical perspectives,” *Pharm. Res.*, vol. 24, no. 1, pp. 1–16, 2007, doi: 10.1007/s11095-006-9132-0.

[19] T. Tong *et al.*, “Smart nanocarriers as therapeutic platforms for bladder cancer,” *Nano Research*. 2021, doi: 10.1007/s12274-021-3753-9.

[20] A. Kato, K. Ando, G. Tamura, G. Jamura, and K. Arima, “Effects of Some Fatty Acid Esters on the Viability and Transplantability of Ehrlich Ascites Tumor Cells Effects of Some Fatty Acid Esters on the Viability and Transplantability of Ehrlich Ascites Tumor Cells,” *Cancer Res.*, vol. 31, no. 5, pp. 501–504, 1971.

[21] M. Y. Liang, M. G. Banwell, Y. Wang, and P. Lan, “Effect of Variations in the Fatty Acid Residue of Lactose Monoesters on Their Emulsifying Properties and Biological Activities,” *J. Agric. Food Chem.*, vol. 66, no. 47, pp. 12594–12603, 2018, doi: 10.1021/acs.jafc.8b05794.

[22] Y. Teng, S. G. Stewart, Y. W. Hai, X. Li, M. G. Banwell, and P. Lan, “Sucrose fatty acid esters: synthesis, emulsifying capacities, biological activities and structure-property profiles,” *Crit. Rev. Food Sci. Nutr.*, vol. 0, no. 0, pp. 1–21, 2020, doi: 10.1080/10408398.2020.1798346.

[23] “Stable raw milk production in 2021.” [Online]. Available: https://ec.europa.eu/eurostat/en/web/products-eurostat-news/-/ddn-20221114-2.

[24] C. Fernanda and V. De Souza, “Whey butter : a promising perspective for the dairy industry,” pp. 1–9, 2022.

[25] P. Zikmanis, S. Kolesovs, and P. Semjonovs, “Production of biodegradable microbial polymers from whey,” *Bioresour. Bioprocess.*, vol. 7, no. 1, 2020, doi: 10.1186/s40643-020-00326-6.

[26] S. R. Cabral, B. M. De Brito De Azevedo, M. P. Da Silva, A. S. Figueiredo, A. P. L. Martins, and M. N. De Pinho, “Optimization of cheese whey ultrafiltration/diafiltration for the production of beverage liquid protein concentrates with lactose partially removed,” *J. Membr. Sci. Res.*, vol. 5, no. 2, pp. 171–177, 2019, doi: 10.22079/JMSR.2018.92367.1208.

[27] P. F. Fox, T. Uniacke-Lowe, P. L. H. McSweeney, and J. A. O’Mahony, *Enzymology of Milk and Milk Products*. 2015.

[28] P. Zhang *et al.*, “Fatty acid-conjugated radiopharmaceuticals for fibroblast activation protein-targeted radiotherapy,” *Eur. J. Nucl. Med. Mol. Imaging*, vol. 49, no. 6, pp. 1985–1996, 2022, doi: 10.1007/s00259-021-05591-x.

[29] K. Imamura *et al.*, “Characteristics of sugar surfactants in stabilizing proteins during freeze-thawing and freeze-drying,” *J. Pharm. Sci.*, vol. 103, no. 6, pp. 1628–1637, 2014, doi: 10.1002/jps.23988.

[30] S. Le Guenic, L. Chaveriat, V. Lequart, N. Joly, and P. Martin, “Renewable Surfactants for Biochemical Applications and Nanotechnology,” *Journal of Surfactants and Detergents*, vol. 22, no. 1. pp. 5–21, 2019, doi: 10.1002/jsde.12216.

[31] S. P. Singh and D. Singh, “Biodiesel production through the use of different sources and characterization of oils and their esters as the substitute of diesel: A review,” *Renewable and Sustainable Energy Reviews*, vol. 14, no. 1. pp. 200–216, 2010, doi: 10.1016/j.rser.2009.07.017.

[32] H. Brännström, H. Kumar, and R. Alén, “Current and Potential Biofuel Production from Plant Oils,” *Bioenergy Res.*, vol. 11, no. 3, pp. 592–613, 2018, doi: 10.1007/s12155-018-9923-2.

[33] T. Inovia, “Sun flower in the global vegetable oil system: situation, specificities and perspectives,” 2020.

[34] E. C. Voutsas *et al.*, “Solubility measurements of fatty acid glucose and sucrose esters in 2-methyl-2-butanol and mixtures of 2-methyl-2-butanol with dimethyl sulfoxide,” *J. Chem. Eng. Data*, vol. 47, no. 6, pp. 1517–1520, 2002, doi: 10.1021/je0200970.

[35] M. Verboni, S. Lucarini, and A. Duranti, “6’ -O-lactose ester surfactants as an innovative opportunity in the pharmaceutical field: From synthetic methods to biological applications,” *Pharmaceuticals*, vol. 14, no. 12, 2021, doi: 10.3390/ph14121306.

[36] Nurhayati Binti Yusof, “Synthesis of Surface - Active Maltodextrin Laurates By Enzymatic Transesterification,” no. July, 2019.

[37] F. J. Plou *et al.*, “Enzymatic acylation of di- and trisaccharides with fatty acids: choosing the appropriate enzyme, support and solvent,” *J. Biotechnol.*, vol. 96, no. 1, pp. 55–66, 2002, doi: 10.1016/S0168-1656(02)00037-8.

[38] K. Sudesh, H. Abe, and Y. Doi, “Synthesis, structure and properties of polyhydroxyalkanoates: biological polyesters,” *Prog. Polym. Sci.*, vol. 25, no. 10, pp. 1503–1555, 2000.

[39] M. Koller, “Modern biotechnological polymer synthesis: {A} review,” *Food Technol. Biotechnol.*, vol. 48, no. 3, pp. 255–269, 2010.

[40] I. Chodak, “Polyhydroxyalkanoates: Origin, properties and applications,” *Monomers, Polym. Compos. from Renew. Resour.*, pp. 451–477, 2008, doi: 10.1016/B978-0-08-045316-3.00022-3.

[41] P. Ward, G. de Roo, and K. E. O’Connor, “Accumulation of polyhydroxyalkanoate from styrene and phenylacetic acid by {Pseudomonas} putida {CA}-3,” *Appl Env. Microbiol*, vol. 71, no. 4, pp. 2046–2052, 2005, doi: 10.1128/aem.71.4.2046-2052.2005.

[42] G. Jiang *et al.*, “Carbon sources for polyhydroxyalkanoates and an integrated biorefinery,” *Int. J. Mol. Sci.*, vol. 17, no. 7, 2016, doi: 10.3390/ijms17071157.

[43] H. Lu *et al.*, “Reconfiguring Plant Metabolism for Biodegradable Plastic Production,” *BioDesign Res.*, vol. 2020, pp. 1–13, 2020, doi: 10.34133/2020/9078303.

[44] J. Kaparapu, “Polyhydroxyalkanoate (PHA) production by genetically engineered microalgae: a review,” *J. New Biol. Reports*, vol. 7, no. 2, pp. 68–73, 2018.

[45] M. H. A. Ibrahim and A. Steinbüchel, “Zobellella denitrificans strain {MW}1, a newly isolated bacterium suitable for poly(3-hydroxybutyrate) production from glycerol,” *J. Appl. Microbiol.*, vol. 108, no. 1, pp. 214–225, 2009.

[46] A. M. Cromwick, T. Foglia, and R. W. Lenz, “The microbial production of poly(hydroxyalkanoates) from tallow,” *Appl. Microbiol. Biotechnol.*, vol. 46, no. 5–6, pp. 464–469, 1996, doi: 10.1007/s002530050845.

[47] M. Zinn and R. Hany, “Tailored {Material} {Properties} of {Polyhydroxyalkanoates} through {Biosynthesis} and {Chemical} {Modification},” *Adv. Eng. Mater.*, vol. 7, no. 5, pp. 408–411, 2005, doi: 10.1002/adem.200500053.

[48] K. Sofińska *et al.*, “Structural, topographical, and mechanical characteristics of purified polyhydroxyoctanoate polymer,” *J. Appl. Polym. Sci.*, vol. 136, no. 4, 2019, doi: 10.1002/app.47192.

[49] G. F. Bunster, “Polyhydroxyalkanoates: Production and Use,” *Encycl. Biomed. Polym. Polym. Biomater.*, no. August, pp. 6412–6421, 2016, doi: 10.1081/E-EBPP-120049915.

[50] M. Guzik, T. Witko, A. Steinbüchel, M. Wojnarowska, M. Sołtysik, and S. Wawak, “What Has Been Trending in the Research of Polyhydroxyalkanoates? A Systematic Review,” *Front. Bioeng. Biotechnol.*, vol. 8, no. September, 2020, doi: 10.3389/fbioe.2020.00959.

[51] S. Kabilan, M. Ayyasamy, S. Jayavel, and G. Paramasamy, “Pseudomonas sp. as a source of medium chain length polyhydroxyalkanoates for controlled drug delivery: Perspective,” *Int. J. Microbiol.*, no. February 2012, 2012, doi: 10.1155/2012/317828.

[52] A. R. Boccaccini, “Biomedical applications of polyhydroxyalkanoates , an overview of animal Biomedical applications of polyhydroxyalkanoates , an overview of animal testing and in vivo responses,” no. May, 2014, doi: 10.1586/17434440.3.6.853.

[53] J. Staroń, J. M. Dąbrowski, E. Cichoń, and M. Guzik, “Lactose esters: synthesis and biotechnological applications,” *Crit. Rev. Biotechnol.*, vol. 38, no. 2, pp. 245–258, 2018, doi: 10.1080/07388551.2017.1332571.

[54] R. Sharma, Y. Chisti, and U. C. Banerjee, “Production, purification, characterization, and applications of lipases,” *Biotechnol. Adv.*, vol. 19, no. 8, pp. 627–662, 2001, doi: 10.1016/S0734-9750(01)00086-6.

[55] H. F. Carvalho, V. Ferrario, and J. Pleiss, “Molecular Mechanism of Methanol Inhibition in CALB-

Catalyzed Alcoholysis: Analyzing Molecular Dynamics Simulations by a Markov State Model," *J. Chem. Theory Comput.*, vol. 17, no. 10, pp. 6570–6582, 2021, doi: 10.1021/acs.jctc.1c00559.

[56] C. Mateo, J. M. Palomo, G. Fernandez-Lorente, J. M. Guisan, and R. Fernandez-Lafuente, "Improvement of enzyme activity, stability and selectivity via immobilization techniques," *Enzyme Microb. Technol.*, vol. 40, no. 6, pp. 1451–1463, 2007, doi: 10.1016/j.enzmictec.2007.01.018.

[57] B. Stauch, S. J. Fisher, and M. Cianci, "Open and closed states of Candida Antarctica lipase B: Protonation and the mechanism of interfacial activation," *J. Lipid Res.*, vol. 56, no. 12, pp. 2348–2358, 2015, doi: 10.1194/jlr.M063388.

[58] M. Kramer, J. C. Cruz, P. H. Pfromm, M. E. Rezac, and P. Czermak, "Enantioselective transesterification by Candida antarctica Lipase B immobilized on fumed silica," *J. Biotechnol.*, vol. 150, no. 1, pp. 80–86, 2010, doi: 10.1016/j.jbiotec.2010.07.018.

[59] W. Snoch *et al.*, "Hollow silica microspheres as robust immobilization carriers," *Bioorg. Chem.*, vol. 93, no. March, p. 102813, 2019, doi: 10.1016/j.bioorg.2019.02.038.

[60] N. do A. S. Neta *et al.*, "Enzymatic synthesis of sugar esters and their potential as surface-active stabilizers of coconut milk emulsions," *Food Hydrocoll.*, vol. 27, no. 2, pp. 324–331, 2012, doi: 10.1016/j.foodhyd.2011.10.009.

[61] N. S. Neta, J. A. Teixeira, and L. R. Rodrigues, "Sugar Ester Surfactants: Enzymatic Synthesis and Applications in Food Industry," *Crit. Rev. Food Sci. Nutr.*, vol. 55, no. 5, pp. 595–610, 2015, doi: 10.1080/10408398.2012.667461.

[62] A. Wagh, "Characterization of Lactose Monolaurate for its Antimicrobial and Emulsification Properties and its Effect on Crystallization Behavior of Anhydrous Milk Fat Committee Member," p. 146, 2013.

[63] M. K. Walsh, R. A. Bombyk, A. Wagh, A. Bingham, and L. M. Berreau, "Synthesis of lactose monolaurate as influenced by various lipases and solvents," *J. Mol. Catal. B Enzym.*, vol. 60, no. 3–4, pp. 171–177, 2009, doi: 10.1016/j.molcatb.2009.05.003.

[64] S.-M. Lee, G. Sandhu, and M. K. Walsh, "Growth inhibitory properties of lactose fatty acid esters," *Saudi J. Biol. Sci.*, 2015, doi: 10.1016/j.sjbs.2015.10.013.

[65] X. Zhang, F. Song, M. Taxipalati, W. Wei, F. Feng, and C. S. Chen, "Comparative study of surface-active properties and antimicrobial activities of disaccharide monoesters," *PLoS One*, vol. 9, no. 12, pp. 1–19, 2014, doi: 10.1371/journal.pone.0114845.

[66] U. H. Zaidan *et al.*, "Biocatalytic production of lactose ester catalysed by mica-based immobilised lipase," *Food Chem.*, vol. 131, no. 1, pp. 199–205, 2012, doi: 10.1016/j.foodchem.2011.08.060.

[67] M. K. Walsh, R. A. Bombyk, A. Wagh, A. Bingham, and L. M. Berreau, "Synthesis of lactose monolaurate as influenced by various lipases and solvents," *J. Mol. Catal. B Enzym.*, vol. 60, no. 3–4, pp. 171–177, 2009, doi: 10.1016/j.molcatb.2009.05.003.

[68] F. Orata, “Derivatization Reactions and Reagents for Gas Chromatography Analysis,” *Adv. Gas Chromatogr. - Prog. Agric. Biomed. Ind. Appl.*, 2012, doi: 10.5772/33098.

[69] K. Müller, C. Faeh, and F. Diederich, “Fluorine in pharmaceuticals: Looking beyond intuition,” *Science (80-.).*, vol. 317, no. 5846, pp. 1881–1886, 2007, doi: 10.1126/science.1131943.

[70] K. L. Kirk, “Fluorine in medicinal chemistry : Recent therapeutic applications of fluorinated small molecules,” vol. 127, pp. 1013–1029, 2006, doi: 10.1016/j.jfluchem.2006.06.007.

[71] D. E. Yerien, S. Bonesi, and A. Postigo, “Fluorination methods in drug discovery,” *Org. Biomol. Chem.*, vol. 14, no. 36, pp. 8398–8427, 2016, doi: 10.1039/c6ob00764c.

[72] W. Liu and J. T. Groves, “Manganese-catalyzed oxidative benzylic C-H fluorination by fluoride ions,” *Angew. Chemie - Int. Ed.*, vol. 52, no. 23, pp. 6024–6027, 2013, doi: 10.1002/anie.201301097.

[73] X. Li *et al.*, “Synthesis and biocompatibility evaluation of fluorinated, single-tailed glucopyranoside surfactants,” *New J. Chem.*, vol. 32, no. 12, pp. 2169–2179, 2008, doi: 10.1039/b805015e.

[74] I. Ben-David, D. Rechavi, E. Mishani, and S. Rozen, “A novel synthesis of trifluoromethyl ethers via xanthates, utilizing BrF3,” *J. Fluor. Chem.*, vol. 97, no. 1–2, pp. 75–78, 1999, doi: 10.1016/S0022-1139(99)00031-7.

[75] X. Li *et al.*, “Hydrophobic tail length, degree of fluorination and headgroup stereochemistry are determinants of the biocompatibility of (fluorinated) carbohydrate surfactants,” *Colloids Surfaces B Biointerfaces*, vol. 73, no. 1, pp. 65–74, 2009, doi: 10.1016/j.colsurfb.2009.04.023.

[76] J. Radivojevic *et al.*, “Polyhydroxyalkanoate-based 3-hydroxyoctanoic acid and its derivatives as a platform of bioactive compounds,” *Appl Microbiol Biotechnol*, pp. 1–12, 2015, doi: 10.1007/s00253-015-6984-4.

[77] C. H. Chiang *et al.*, “Regioselective hydroxylation of C 12 -C 15 fatty acids with fluorinated substituents by cytochrome P450 BM3,” *Chem. - A Eur. J.*, vol. 19, no. 41, pp. 13680–13691, 2013, doi: 10.1002/chem.201302402.

[78] V. M. Dembitsky and M. Srebnik, “Natural halogenated fatty acids: Their analogues and derivatives,” *Prog. Lipid Res.*, vol. 41, no. 4, pp. 315–367, 2002, doi: 10.1016/S0163-7827(02)00003-6.

[79] S. O. Connor *et al.*, “Biomaterials The anti-cancer activity of a cationic anti-microbial peptide derived from monomers of polyhydroxyalkanoate,” *Biomaterials*, vol. 34, no. 11, pp. 2710–2718, 2013, doi: 10.1016/j.biomaterials.2012.12.032.

[80] M. Constantin, C. I. Simionescu, A. Carpov, E. Samain, and H. Driguez, “Chemical modification of poly (hydroxyalkanoates). Copolymers bearing pendant sugars,” vol. 94, no. 2, pp. 91–94, 1999.

[81] Clinical and Laboratory Standards Institute (CLSI) and B. L. Z. F. R. C. M. A. W. J. A. M. N. D. G. M. E. M. J. F. D. J. H. D. W. H. J. A. H. J. B. P. M. P. J. M. S. R. B. T. M. M. T. J. D. T. M. P. Weinstein, *Methods for Dilution Antimicrobial Susceptibility Tests for Bacteria That Grow Aerobically ; Approved*

Standard — Ninth Edition, vol. 32, no. 2. 2012.

[82] M. C. Arendrup, J. Meletiadis, J. W. Mouton, K. Lagrou, P. Hamal, and J. Guinea, "J Guinea 7 (Scientific Secretary, Spain), P Hamal 6 (Steering Committee," *Czech Republic), H Järv*, vol. 12, no. 3, p. 4, 2017.

[83] A. Wagh, M. K. Walsh, and S. Martini, "Effect of lactose monolaurate and high intensity ultrasound on crystallization behavior of anhydrous milk fat," *JAOCS, J. Am. Oil Chem. Soc.*, vol. 90, no. 7, pp. 977–987, 2013, doi: 10.1007/s11746-013-2244-x.

[84] Á. Sandoval *et al.*, "Production of 3-hydroxy-n-phenylalkanoic acids by a genetically engineered strain of Pseudomonas putida," *Appl. Microbiol. Biotechnol.*, vol. 67, no. 1, pp. 97–105, 2005, doi: 10.1007/s00253-004-1752-x.

[85] C. H. Pohl, J. L. F. Kock, and V. S. Thibane, "Antifungal free fatty acids: a review," *Sci. against Microb. Pathog. Curr. Res. Technol. Adv.*, vol. 1, no. January 2011, pp. 61–71, 2011.

[86] L. Zhao, H. Zhang, T. Hao, and S. Li, "In vitro antibacterial activities and mechanism of sugar fatty acid esters against five food-related bacteria," *Food Chem.*, vol. 187, pp. 370–377, 2015, doi: 10.1016/j.foodchem.2015.04.108.

[87] M. Ferrer *et al.*, "Synthesis of sugar esters in solvent mixtures by lipases from Thermomyces lanuginosus and Candida antarctica B, and their antimicrobial properties," *Enzyme Microb. Technol.*, vol. 36, no. 4, pp. 391–398, 2005, doi: 10.1016/j.enzmictec.2004.02.009.

[88] A. Smith, P. Nobmann, G. Henehan, P. Bourke, and J. Dunne, "Synthesis and antimicrobial evaluation of carbohydrate and polyhydroxylated non-carbohydrate fatty acid ester and ether derivatives," vol. 343, pp. 2557–2566, 2008, doi: 10.1016/j.carres.2008.07.012.

[89] N. Park and M. K. Walsh, "Microbial inhibitory properties of maltodextrin fatty acid esters against food-related microorganisms," *Lwt*, vol. 147, no. May, p. 111664, 2021, doi: 10.1016/j.lwt.2021.111664.

[90] N. R. Khan and V. K. Rathod, "Enzyme catalyzed synthesis of cosmetic esters and its intensification: A review," *Process Biochem.*, vol. 50, no. 11, pp. 1793–1806, 2015, doi: 10.1016/j.procbio.2015.07.014.

[91] U. H. Zaidan *et al.*, "Biocatalytic production of lactose ester catalysed by mica-based immobilised lipase," *Food Chem.*, vol. 131, no. 1, pp. 199–205, 2012, doi: 10.1016/j.foodchem.2011.08.060.

[92] M. Enayati, Y. Gong, J. M. Goddard, and A. Abbaspourrad, "Synthesis and characterization of lactose fatty acid ester biosurfactants using free and immobilized lipases in organic solvents," *Food Chem.*, vol. 266, no. June, pp. 508–513, 2018, doi: 10.1016/j.foodchem.2018.06.051.

[93] A. L. R. LazarAA-n, A. Zugasti Cruz, G. A. de la PeAAa, S. Y. S. Belmares, and C. A. Sierra Rivera, "Synergistic cytotoxic effect of sodium dichloroacetate combined with chemotherapeutic drugs on B16F10 murine melanoma cell line.," *Biomed. Res.*, vol. 30, no. 1, pp. 179–185, 2019, doi: 10.35841/biomedicalresearch.30-19-030.

[94] U. McDermott, “Genomics of drug sensitivity in cancer,” *Eur. Biotechnol. Sci. Ind. News*, vol. 9, no. 9–10, pp. 40–42, 2010, doi: 10.32388/podf8k.

[95] Y. Wang *et al.*, “Downregulation of breast cancer resistance protein by long-term fractionated radiotherapy sensitizes lung adenocarcinoma to SN-38,” *Investigational New Drugs*, vol. 39, no. 2. pp. 458–468, 2021, doi: 10.1007/s10637-020-01003-3.

[96] S. Lucarini *et al.*, “Synthesis, structure–activity relationships and in vitro toxicity profile of lactose-based fatty acid monoesters as possible drug permeability enhancers,” *Pharmaceutics*, vol. 10, no. 3, pp. 1–18, 2018, doi: 10.3390/pharmaceutics10030081.

[97] V. Castell, M. Ferrer, G. Perez, F. J. Plou, and A. Ballesteros, “Antitumour activity of fatty acid maltotriose esters obtained by enzymatic synthesis,” vol. 39, pp. 35–39, 2005, doi: 10.1042/BA20040122.

[98] S. Okabe *et al.*, “Disaccharide esters screened for inhibition of tumor necrosis factor-α release are new anti-cancer agents,” *Japanese J. Cancer Res.*, vol. 90, no. 6, pp. 669–676, 1999, doi: 10.1111/j.1349-7006.1999.tb00799.x.

[99] E. D. Oldham *et al.*, “Cytotoxic activity of triazole-containing alkyl β-D-glucopyranosides on a human T-cell leukemia cell line,” *Chem. Cent. J.*, vol. 9, no. 1, pp. 1–12, 2015, doi: 10.1186/s13065-014-0072-1.

[100] Y. Zhao *et al.*, “Effects of sucrose ester structures on liposome-mediated gene delivery,” *Acta Biomater.*, vol. 72, pp. 278–286, 2018, doi: 10.1016/j.actbio.2018.03.031.

[101] Y. Guan, H. Chen, and Q. Zhong, “Nanoencapsulation of caffeic acid phenethyl ester in sucrose fatty acid esters to improve activities against cancer cells,” *J. Food Eng.*, vol. 246, pp. 125–133, 2019, doi: 10.1016/j.jfoodeng.2018.11.008.

[102] J. Richard, “Challenges and opportunities in the delivery of cancer therapeutics,” *Ther. Deliv.*, vol. 2, no. 1, pp. 107–121, 2011, doi: 10.4155/tde.10.89.

[103] K. Upadhyaya *et al.*, “Identification of gallic acid based glycoconjugates as a novel tubulin polymerization inhibitors,” *Org. Biomol. Chem.*, vol. 14, no. 4, pp. 1338–1358, 2016, doi: 10.1039/c5ob02113h.

[104] T. Gaudin *et al.*, “Impact of the chemical structure on amphiphilic properties of sugar-based surfactants: A literature overview,” *Adv. Colloid Interface Sci.*, vol. 270, pp. 87–100, 2019, doi: 10.1016/j.cis.2019.06.003.

[105] X. Zhang, W. Wei, X. Cao, and F. Feng, “Characterization of enzymatically prepared sugar medium-chain fatty acid monoesters,” *J. Sci. Food Agric.*, vol. 95, no. 8, pp. 1631–1637, 2015, doi: 10.1002/jsfa.6863.

[106] R. Hollenbach *et al.*, “Interfacial and Foaming Properties of Tailor-Made Glycolipids—Influence of the Hydrophilic Head Group and Functional Groups in the Hydrophobic Tail,” *Molecules*, vol. 25, no. 17.

2020, doi: 10.3390/molecules25173797.

[107] S.-M. Lee, A. Wagh, G. Sandhu, and M. K. Walsh, “Emulsification Properties of Lactose Fatty Acid Esters,” *Food Nutr. Sci.*, vol. 09, no. 12, pp. 1341–1357, 2018, doi: 10.4236/fns.2018.912096.

[108] S. Lucarini *et al.*, “Synthesis, structure–activity relationships and in vitro toxicity profile of lactose-based fatty acid monoesters as possible drug permeability enhancers,” *Pharmaceutics*, vol. 10, no. 3. 2018, doi: 10.3390/pharmaceutics10030081.

[109] R. Ye, D. G. Hayes, R. Burton, A. Liu, F. M. Harte, and Y. Wang, “Solvent-free lipase-catalyzed synthesis of technical-grade sugar esters and evaluation of their physicochemical and bioactive properties,” *Catalysts*, vol. 6, no. 6. 2016, doi: 10.3390/catal6060078.

[110] G. Garofalakis, B. S. Murray, and D. B. Sarney, “Surface {Activity} and {Critical} {Aggregation} {Concentration} of {Pure} {Sugar} {Esters} with {Different} {Sugar} {Headgroups},” *J. Colloid Interface Sci.*, vol. 229, no. 2, pp. 391–398, doi: 10.1006/jcis.2000.7035.

[111] “Pharmaceutical composition for nasal delivery- US 10.729.687 B1.” .

[112] G. Garofalakis, B. S. Murray, and D. B. Sarney, “Surface activity and critical aggregation concentration of pure sugar esters with different sugar headgroups,” *J. Colloid Interface Sci.*, vol. 229, no. 2, pp. 391–398, 2000, doi: 10.1006/jcis.2000.7035.

[113] “Production of green surfactants: Market prospects | Elsevier Enhanced Reader.” .

[114] I. Felzenszwalb *et al.*, “Toxicological evaluation of nail polish waste discarded in the environment,” *Environmental Science and Pollution Research*, vol. 26, no. 27. pp. 27590–27603, 2019, doi: 10.1007/s11356-018-1880-y.

[115] M. Dhaval *et al.*, “Lipid-based emulsion drug delivery systems — a comprehensive review,” *Drug Delivery and Translational Research*, vol. 12, no. 7. pp. 1616–1639, 2022, doi: 10.1007/s13346-021-01071-9.

[116] L. Y. Kok *et al.*, “Development and pharmacokinetic evaluation of a self-nanoemulsifying drug delivery system for the oral delivery of cannabidiol,” *Eur. J. Pharm. Sci.*, vol. 168, no. November 2021, p. 106058, 2022, doi: 10.1016/j.ejps.2021.106058.

[117] M. Smoleński, B. Karolewicz, A. M. Gołkowska, K. P. Nartowski, and K. Małolepsza-Jarmołowska, “Emulsion-based multicompartment vaginal drug carriers: From nanoemulsions to nanoemulgels,” *International Journal of Molecular Sciences*, vol. 22, no. 12. 2021, doi: 10.3390/ijms22126455.

[118] Z. Sun, Q. Zhao, R. Haag, and C. Wu, “Responsive Emulsions for Sequential Multienzyme Cascades,” *Angewandte Chemie - International Edition*, vol. 60, no. 15. pp. 8410–8414, 2021, doi: 10.1002/anie.202013737.

[119] R. Shkreli, R. Terziu, L. Memushaj, and K. Dhamo, “Formulation and stability evaluation of a cosmetics emulsion loaded with different concentrations of synthetic and natural preservative,” vol. 5, no. 1, pp.

38–51, 2022.

[120] F. Baratta, E. Peira, C. Maza, M. Gallarate, and P. Brusa, “Cannabis-Based Oral Emulsion for Medical Purposes to Meet the Needs of Patients: Formulation, Quality and Stability,” *Pharmaceutics*, vol. 14, no. 3. 2022, doi: 10.3390/pharmaceutics14030513.

[121] J. Jampilek, J. Kos, and K. Kralova, “Potential of nanomaterial applications in dietary supplements and foods for special medical purposes,” *Nanomaterials*, vol. 9, no. 2. 2019, doi: 10.3390/nano9020296.

[122] M. Silva and J. Chandrapala, “Ultrasonic Emulsification of Milk Proteins Stabilized Primary and Double Emulsions: A Review,” *Food Rev. Int.*, vol. 00, no. 00, pp. 1–23, 2021, doi: 10.1080/87559129.2021.1934006.

[123] W. Snoch *et al.*, “In search of effective anticancer agents—novel sugar esters based on polyhydroxyalkanoate monomers,” *Int. J. Mol. Sci.*, vol. 22, no. 13, 2021, doi: 10.3390/ijms22137238.

[124] P. Wittkowski *et al.*, “Caenorhabditis elegans As a Promising Alternative Model for Environmental Chemical Mixture Effect Assessment - A Comparative Study,” *Environ. Sci. Technol.*, vol. 53, no. 21, pp. 12725–12733, 2019, doi: 10.1021/acs.est.9b03266.

[125] J. D. Judy *et al.*, “Microplastics in municipal mixed-waste organic outputs induce minimal short to long-term toxicity in key terrestrial biota,” *Environ. Pollut.*, vol. 252, pp. 522–531, 2019, doi: 10.1016/j.envpol.2019.05.027.

[126] S. Akbari, N. H. Abdurahman, R. M. Yunus, F. Fayaz, and O. R. Alara, “Biosurfactants—a new frontier for social and environmental safety: a mini review,” *Biotechnol. Res. Innov.*, vol. 2, no. 1, pp. 81–90, 2018, doi: 10.1016/j.biori.2018.09.001.

[127] A. Tovar-Sanchez, E. Sparaventi, A. Gaudron, and A. Rodriguez-Romero, “A new approach for the determination of sunscreen levels in seawater by ultraviolet absorption spectrophotometry,” *PLoS ONE*, vol. 15, no. 12 December. 2020, doi: 10.1371/journal.pone.0243591.

[128] B. S. Rathi, P. S. Kumar, and D. V. N. Vo, “Critical review on hazardous pollutants in water environment: Occurrence, monitoring, fate, removal technologies and risk assessment,” *Sci. Total Environ.*, vol. 797, 2021, doi: 10.1016/j.scitotenv.2021.149134.

[129] A. J. Ebele, M. Abou-Elwafa Abdallah, and S. Harrad, “Pharmaceuticals and personal care products (PPCPs) in the freshwater aquatic environment,” *Emerg. Contam.*, vol. 3, no. 1, pp. 1–16, 2017, doi: 10.1016/j.emcon.2016.12.004.

[130] P. R. Hunt, “The C. elegans model in toxicity testing,” *J. Appl. Toxicol.*, vol. 37, no. 1, pp. 50–59, 2017, doi: 10.1002/jat.3357.

[131] K. A. Fagan and D. S. Portman, “Sexual modulation of neural circuits and behavior in caenorhabditis elegans,” *Semin. Cell Dev. Biol.*, vol. 33, no. April, pp. 3–9, 2014, doi: 10.1016/j.semcdb.2014.06.007.

[132] M. Place, “In vivo eco-toxicological assessment of some cationic and amphoteric surfactants in

transgenic Caenorhabditis elegans CICÎRMA Marius 1,2* , de POMERAI David 3," vol. 25, pp. 19–32, 2020.

[133] M. Zheng, L. Mo, R. Qin, L. Liang, and F. Zhang, "Research progress of surfactant," *AIP Conference Proceedings*, vol. 1794. 2017, doi: 10.1063/1.4971930.

[134] K. Bunchongprasert and J. Shao, "Effect of fatty acid ester structure on cytotoxicity of self-emulsified nanoemulsion and transport of nanoemulsion droplets," *Colloids Surfaces B Biointerfaces*, vol. 194, no. March, p. 111220, 2020, doi: 10.1016/j.colsurfb.2020.111220.

[135] H. Sakoguchi, T. Shintani, H. Ishiyama, R. C. Yanagita, Y. Kawanami, and M. Sato, "Nematocidal activity of 6-O-octanoyl- And 6-O-octyl-D-allose against larvae of Caenorhabditis elegans," *Biosci. Biotechnol. Biochem.*, vol. 83, no. 12, pp. 2194–2197, 2019, doi: 10.1080/09168451.2019.1648206.

[136] S. K. Bopp *et al.*, "Regulatory assessment and risk management of chemical mixtures: challenges and ways forward," *Crit. Rev. Toxicol.*, vol. 49, no. 2, pp. 174–189, 2019, doi: 10.1080/10408444.2019.1579169.

[137] M. Dent *et al.*, "Principles underpinning the use of new methodologies in the risk assessment of cosmetic ingredients," *Computational Toxicology*, vol. 7. pp. 20–26, 2018, doi: 10.1016/j.comtox.2018.06.001.

[138] A. I. Rusanov, "Theory of surfactant diffusion in micellar systems with variable aggregation numbers," *Colloids and Surfaces A: Physicochemical and Engineering Aspects*, vol. 551. pp. 158–164, 2018, doi: 10.1016/j.colsurfa.2018.04.065.

[139] P. Kaur, T. Garg, G. Rath, R. S. R. Murthy, and A. K. Goyal, "Surfactant-based drug delivery systems for treating drug-resistant lung cancer," *Drug Deliv.*, vol. 23, no. 3, pp. 727–738, 2016, doi: 10.3109/10717544.2014.935530.

[140] G. S. Khamkar, "Self Micro Emulsifying Drug Delivery System (SMEED) o/w microemulsion for BCS class II drugs: An approach to enhance an oral bioavailability," *Int. J. Pharm. Pharm. Sci.*, vol. 3, no. SUPPL. 3, pp. 1–3, 2011.

[141] M. A. Alfhili *et al.*, "Non-ionic surfactants antagonize toxicity of potential phenolic endocrine-disrupting chemicals, including triclosan in caenorhabditis elegans," *Molecules and Cells*, vol. 41, no. 12. pp. 1052–1060, 2018, doi: 10.14348/molcells.2018.0378.

[142] Pokr, "Kancelaria Ogólna POTWIERDZENIE Urząd Patentowy RP stwierdza , że dnia 2020-06-30 przyjęto w formie elektronicznej wniosek o udzielenie patentu na wynalazek : Urządzenie do kontrolowanego warstwowego nalewania cieczy," 2020.

[143] C. Arrest and D. U. Human, "Lipophilized Epigallocatechin Gallate Derivative Exerts Anti-Proliferation Efficacy through Induction of Cell Cycle Arrest and Apoptosis on DU145 Human Prostate Cancer Cells," *Nutrients*, vol. 12(1), p. 92, 2020, doi: doi: 10.3390/nu12010092.

[144] L. Zhong, C. Hou, L. Zhang, J. Zhao, F. Li, and W. Li, "Synthesis of deuterium-enriched sorafenib derivatives and evaluation of their biological activities," *Molecular Diversity*, vol. 23, no. 2. pp. 341–

350, 2019, doi: 10.1007/s11030-018-9875-7.

[145] M. K. Ediriweera, K. H. Tennekoon, and S. R. Samarakoon, “In vitro assays and techniques utilized in anticancer drug discovery,” *Journal of Applied Toxicology*, vol. 39, no. 1. pp. 38–71, 2019, doi: 10.1002/jat.3658.

[146] S. Simić, E. Zukić, L. Schmermund, K. Faber, C. K. Winkler, and W. Kroutil, “Shortening Synthetic Routes to Small Molecule Active Pharmaceutical Ingredients Employing Biocatalytic Methods,” *Chem. Rev.*, vol. 122, no. 1, pp. 1052–1126, 2022, doi: 10.1021/acs.chemrev.1c00574.

[147] Q. Xu *et al.*, “Stereodivergent Synthesis of Epoxides and Oxazolidinones via the Halohydrin Dehalogenase-Catalyzed Desymmetrization Strategy,” *ACS Catalysis*, vol. 12, no. 11. pp. 6285–6293, 2022, doi: 10.1021/acscatal.2c00718.

7. Załączniki

Bioorganic Chemistry 93 (2019) 102813

Contents lists available at ScienceDirect

Bioorganic Chemistry

journal homepage: www.elsevier.com/locate/bioorg

Hollow silica microspheres as robust immobilization carriers

Wojciech Snoch[a], Mateusz Tataruch[a], Olga Zastawny[b], Ewelina Cichoń[c], Mathilde Gosselin[d], Hubert Cabana[e], Maciej Guzik[a,*]

[a] Jerzy Haber Institute of Catalysis and Surface Chemistry Polish Academy of Sciences, Niezapominajek 8, 30-239 Kraków, Poland
[b] Department of Plant Cytology and Embryology, Institute of Botany, Jagiellonian University, Gronostajowa 9, 30-387 Kraków, Poland
[c] Faculty of Material Science and Ceramics, AGH University of Science and Technology, Mickiewicza Av. 30, 30-059 Krakow, Poland
[d] Materium Innovations INC., Boulevard Industriel 790, Granby, J2G 9J5 Quebec, Canada
[e] Department of Civil and Building Engineering, Universite de Sherbrooke, 2500 Boulevard de l'Universite, Sherbrooke, J1K 2R1 Quebec, Canada

ARTICLE INFO

Keywords:
Hollow silica microspheres
Immobilization
Lipase
Ethylbenzene dehydrogenase
Biocatalysis
Batch reactor
Flow reactor

ABSTRACT

Hollow silica microspheres provide an ideal solid support for enzyme immobilization. We tested one of the newest development, namely MATSPHERES®, a silica openwork material as a carrier for the covalent immobilization of enzymes used to synthesize bioactive compounds. Two model enzymes – ethylbenzene dehydrogenase and EL070 lipase – were considered. They belong to two different enzyme classes and catalyse reactions taking place in various environments (aqueous and non-aqueous, aerobic and anaerobic). The enzymes were immobilized by covalent bonds (*via* divinyl sulfone and glutaraldehyde) on new silica material. Effectiveness of immobilization processes on the spheres grafted with amine groups and on the analogues without functionalization was determined for both enzymes. Microspheres were characterized morphologically and also their mechanical stability was examined during exposure to varying physical conditions. It was shown that MATSPHERES® due to their openwork structure and relative stability under batch and flow conditions can be a competitive SBA support for enzyme immobilization and production of bioactive compounds.

1. Introduction

In the era of frightening industrial growth, it became necessary to look for solutions that are less harmful to the environment, in either the production of new goods or waste management. Therefore, acquisition of new biologically active compounds with the aid of biocatalysis is gaining more and more popularity. *Green Chemistry* employing enzymes in compound processing offers a wide range of advantages over traditional ways: reduction in energy and water consumption, minimizing the use of hazardous, toxic chemicals and solvents as well as decrease in waste emission and pollution [1,2]. Enzymes used in biocatalysis allow to obtain a wide range of compounds, including those applied in food and pharmaceutical industries, in an extremely selective manner. Moreover, recent developments in biocatalysis open new routes for utilisation of compounds originating from various resources, also those constituting as a waste. Enzymes can be applied either in the synthesis of new drugs or intermediate products exhibiting desired properties. However, despite huge advantages, enzymes, as products of living organisms, have small tolerance to a range of physicochemical and biological parameters (i.e. temperature, pH, solvents and proteolytic enzymes etc.) [3]. Thus, studies elucidating improvements of the enzyme efficiency, reaction optimisation routes or a search for the most optimal reaction conditions are essential. To overcome the problem of their vulnerability, enzymes may be immobilized on a range of different supports. Immobilization increases their stability and activity, which has a significant impact on improving the overall efficiency of catalysed reaction [4]. The conversion rate for immobilized enzymes is also found to be higher compared to their free forms (only in case of lipases) [5] and organic solvent resistance is significantly increased [6]. Moreover, immobilization greatly facilitates the re-use of the catalysts [7–9].

Due to a huge number of potential applications of enzyme immobilization there is a growing interest in searching for and testing new supports which meet the requirements of specific enzymes or reactions conducted by them [10]. For example, silica based microspheres constitute a new interesting group of enzymes attaching carriers. Silica capacities to bind an enzyme on its surface were already widely studied [11–13]. Most importantly, silica as a support is chemically versatile; it offers great variation of its chemical surface modification enabling different approaches for covalent binding of a given enzyme [14]. Further, recent developments in material design enable creation of 3D spheres of different sizes and architecture [15–17]. Openwork spheres for example not only provide greater surface for immobilisation of an

* Corresponding author.
E-mail address: ncguzik@cyfronet.pl (M. Guzik).

https://doi.org/10.1016/j.bioorg.2019.02.038
Received 14 December 2018; Received in revised form 15 February 2019; Accepted 18 February 2019
Available online 02 March 2019

enzyme when compared to simple granules but also support reduction on operating pressure in flow bioreactors enabling higher flows for particular applications. In the presented work we have focused on one of such new developments – on MATSPHERES® – hollow silica microsphere of sophisticated 3D architecture for immobilisation of two distinct enzymes – a dehydrogenase and a lipase, which perform their catalytic reactions in two different reaction media – aqueous and non-aqueous.

Both enzymes selected for this study are of pharmaceutical and chemical importance. Both are used to synthesize bioactive compounds with a variety of applications. The first enzyme considered in this study is an ethylbenzene dehydrogenase (EbDH) belonging to DMSO reductase family [18]. It was firstly isolated from *Aromatoleum aromaticum* (EbN1 *Azoarcus* sp.) where it is responsible for anaerobic ethylbenzene mineralization and converts wide range of substrates into chiral secondary alcohols [14–24], which are considered as Active Pharmaceutical Ingredients (APIs). EbDH is one of the few enzymes conducting synthesis of secondary chiral alcohols by enantioselective hydroxylation of hydrocarbon substrates structurally similar to ethylbenzene. What is especially noteworthy is the fact that out of 34 known EbDH substrates, 21 result exclusively in (*S*) enantiomer [25–27]. For example, natural product of EbDH transformation of ethylenbenzene, that is 1-phenylethanol, is found to be utilized as a synthon for i.e. selective A1 adenosine receptor antagonists synthesis, a stimulating agent of the central nervous system [28,29] or in synthesis of dopamine transporter ligands (DAT) as a novel potential cocaine-abuse therapeutic agent [30]. The other enzyme used in this study is a lipase, commercially available from Eucodis Bioscience GmbH (Austria) under trade name EL070. Lipases (EC 3.1.1.3.) are a subclass of the hydrolases that under physiological conditions play crucial role in hydrolysis of triacylglycerols, while in the absence of water are prone to catalyze reversed reactions (i.e. esterification). It was reported that lipases promote efficient synthesis of sugar fatty acids (SFAEs) [6,31–33]. SFAEs constitute a novel group of non-ionic sugar-based surfactants increasingly used as emulsifiers in pharmaceutical, cosmetic, food and detergent formulae. Biodegradability and biocompatibility, no irritating effect and lack of toxicity of those compounds are favourable features that raise the great interest of their additional broad applications in food and pharmaceutical industries [34]. They were shown to bare antibacterial properties resulting from surfactant interactions with bacterial cell membrane [35] and also they can be potentially implemented as anticancer agents [36,37].

Having the above in mind, we have conducted a systematic study that encompassed characterisation of MATSPHERES® hollow silica microspheres, their application for two types of enzymes immobilisation, which was followed by catalytic testes in both batch and flow modes.

2. Materials and methods

2.1. Materials

Commercial lipase EL070 (EC 3.1.1.3) of prokaryotic origin (highly purified lyophilized powder) was obtained from Eucodis Bioscience (Austria). Ethylbenzene dehydrogenase (EbDH) (EC 1.17.99.2) was obtained as described elsewhere in detail [27]. Briefly, *Aromatoleum aromaticum* was cultivated under anaerobic conditions, cells were collected and free cell extract was submitted to column purification (Sepharose DEAE, Hydroxapatite). Purity of enzyme was assayed by SDS-PAGE (data not shown). Immobilisation carriers were provided by Materium Innovations (Canada) and referred to in this manuscript as MATSPHERES®–OH (non-modified) and MATSPHERES®–NH_2 (modified as described below). SBA-15-ultra-2 carriers were obtained as described in [38] and referred to in this manuscript as SBA-OH (non-modified) and SBA-NH_2 (modified as described below). Other chemicals were of reagent grade and purchased from Merck (Poland) and VWR (Poland).

2.2. Physical characterisation of silica spheres

The size of MATSPHERES® was confirmed by light microscopy observations (Nikon ECLIPSE E200; 7 photos, magnification 400x, sample size 136 objects) and analysed with ImageJ 1.49 v software. The shape of the microspheres after short activity assays and long-term reactions was also examined with an optical microscope in order to evaluate the influence of reaction conditions on the structural integrity of the carriers. Similarly, the effect of freezing immobilization support (−20 °C, 2 weeks period) was also determined by microscopic observations. The effect of the flow rate was studied with Agilent 1100 Series binary pump by varying the flow up to 5 ml min^{-1} for PrepRPC FPLC column (Pharmacia Biotech, Sweden) packed with 0.5 ml of each of the supports studied. Specific surface area (S_{BET}), pore volume (V_{tot}) and pore diameter of SBA were obtained as described elsewhere [38]. SBA grain size was determined based on electron microscope measurements (JEOL JSM-7500F). MATSPHERES® characteristics were provided by the supplier (including S_{BET}, V_{tot}, pore diameter and density of functional groups). The interaction of spheres with of media components was verified by appropriate HPLC measurement as described below. Each component (i.e. glucose, methyl nonanoate, 1- (*S*)-phenylethanol, $K_3[Fe(CN)_6]$ in respective reaction media was incubated over appropriate time which depended on the assay performed and its concentration was analysed.

2.3. Enzyme immobilization

Enzymes immobilization was carried out accordingly to scheme at Fig. 1. Immobilization of each enzyme (EbDH or lipase) was conducted with 0.5 ml of each carrier (MATSPHERES®–OH and MATSPHERES®–NH_2 silica microspheres, SBA-OH or SBA-NH_2).

2.3.1. EbDH immobilization

The carriers (0.5 ml) were rinsed twice with distilled water and then with 20 ml of buffer appropriate to the type of surface activation, i.e. 1 M Na_2CO_3 (pH 11) for silica-OH carriers, 0.1 M KH_2PO_4/Na_2HPO_4 (pH 7.0) for silica-NH_2 carriers. Next the surface of the carriers were activated according to the following procedures: i) silica-OH carriers were slowly agitated with 0.5 ml of 3% divinyl sulfone (DVS) in 1 M Na_2CO_3 for 1 h at room temperature using laboratory orbital shaker. ii) silica-NH_2 carriers were stirred with 0.5 ml 2.5% glutaraldehyde (GA) in 0.1 M KH_2PO_4/Na_2HPO_4 for 1 h at room temperature. After activation with DVS and GA the supports were rinsed with distilled water and subsequently with 0.1 M Na_2HPO_4 (pH 8.0) or 0.1 M KH_2PO4/Na_2HPO_4 (pH 7.0), respectively. Moreover, in order to protect the enzyme during immobilization all buffers were supplemented with 3 mM $K_3[Fe(CN)_6]$. For each type of the carrier 0.5 ml of the purified EbDH (3.67 mg/mL, activity: 27.18 mU/mL) was added and gently stirred for 1 h at room temperature after which it was cooled to 4 °C and left at this temperature for 3 h. The excess of unbound protein was filtered off and carriers were washed with 0.1 M KH_2PO_4/Na_2HPO_4 (pH 7.0) to remove the excess of unbound protein. All eluates were collected and analyzed for the presence of the unbound protein. Finally, in order to endcap the free active groups of the carrier, the supports were submerged in 0.5 M Tris/HCl buffer pH 7.5 for 3 h at 4 °C. At this stage immobilization of EbDH was completed and each carrier-EbDH was left at 4 °C.

2.3.2. Lipase immobilization

For each ml of carrier 100 mg of lipase was prepared. 10 mg of lipase was weighed for control sample used in protein activity assay. Lipase was dissolved in buffer solutions pH = 8.0 and pH = 7.0, respectively for silica-OH and silica-NH_2. Lipase concentration in each of

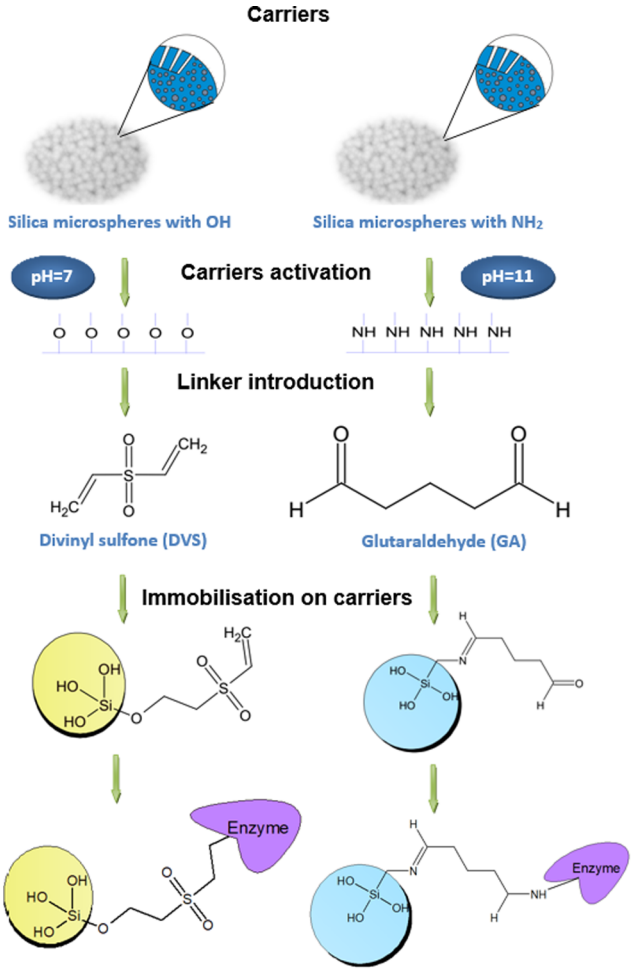

Fig. 1. Schematic representation of immobilization procedures used in this work.

the buffers was 50 mg ml^{-1} or 30.2 mg ml^{-1} for MATSPHERES® or SBA, respectively. The carriers (0.25 ml) were rinsed twice with 0.5 ml of the buffer appropriate to the type of surface activation, i.e. 1 M Na_2CO_3 (pH 11.0) for silica-OH carriers, 0.1 M KH_2PO4/Na_2HPO_4 (pH 7.0) for silica-NH_2 carriers. Next, in order to activate the carriers surface, the following procedures were conducted: i) silica-OH carriers were slowly agitated with 0.5 ml of 3% DVS in 1 M Na_2CO_3 for 1 h at room temperature using laboratory orbital shaker; ii) silica-NH_2 carriers were stirred with 0.5 ml 2.5% GA in 0.1 M KH_2PO_4/Na_2HPO_4 for 1 h at room temperature. After activation, each carrier was rinsed six times with deionized water in order to remove the excess of the linker. Then, each was suspended in a buffer solution (0.1 M Na_2HPO_4, pH = 8.0) and stored for 3 h at 4 °C. After that time, silica-OH and silica-NH_2 carriers were rinsed twice with 0.1 M Na_2HPO_4 (pH 8.0) or 0.1 M KH_2PO4/Na_2HPO_4 (pH 7.0), respectively. For each type of the carrier 0.5 ml of the lipase solution was added and gently stirred for 1 h at room temperature after which it was cooled to 4 °C and left at this temperature overnight (Note: enzyme was dissolved/suspended in 0.1 M Na_2HPO_4 (pH 8.0) or 0.1 M KH_2PO4/Na_2HPO_4 (pH 7.0), respectively for silica-OH and silica-NH_2 carriers). The excess of unbound protein was filtered off and carriers were rinsed four times with 0.1 M KH_2PO_4/Na_2HPO_4 (pH 7.0). All eluates were collected and analyzed for the presence of the unbound protein. Finally, in order to endcap the free active groups of the carrier, the supports were submerged in 0.5 M Tris/HCl buffer pH 7.5 and gently stirred at room temperature for 1 h. Next, each carrier was rinsed with deionized water and freeze-dried overnight.

The success of immobilization process for each enzyme was described by "enzyme loading" and "retained activity" parameters as described in Eqs. (1) and (2).

$$\textbf{Enzyme Loading}(\%) = \frac{\text{immobilized protein [mg]}}{\text{initial amount of protein [mg]}} \times 100\% \quad (1)$$

$$\textbf{Retained Activity}\ (\%) = \frac{\text{observed activity [U]}}{\text{initial activity [U]}} \times 100\% \quad (2)$$

2.4. Reagents sorption studies

Reagents used for EbDH: 0.25 ml (66 mg MATSPHERES®–OH and 63 mg MATSPHERES® –NH_2) of a carrier was suspended in 10 ml of 100 mM MES buffer (pH 5.5) containing 1.55 mM 1-(*S*)-phenylethanol (PhEtOH) or 1 mM electron acceptor potassium ferricyanide (III) $K_3[Fe(CN)_6]$. The mixture was continuously shaken (temp. 30 °C, 250 rpm) for 3 days and 0.25 ml samples were removed periodically. Samples were centrifuged (13,000 rpm) and submitted for quantitative HPLC and UV–vis analysis. Reagents used for EL070: 0.25 ml (66 mg MATSPHERES®–OH and 63 mg MATSPHERES®–NH_2) of a carrier was suspended in 10 ml of reaction medium (80% v/v of 2-methyl-2-butanol and 20% v/v DMSO) containing 4 mg ml^{-1} glucose. The mixture was continuously shaken (temp. 30 °C, 250 rpm) for 3 days and 0.25 ml samples were removed. Samples were centrifuged (13,000 rpm) and submitted for quantitative HPLC-MS analysis.

2.5. Determination of protein concentration

The amount of protein in the supernatant was determined by Bradford method using Bovine Serum Albumin as a standard [39]. The amount of bound protein was determined indirectly by the difference between the amount of protein introduced into the coupling reaction mixture and the amount of protein in the filtrates. Measurement were performed using spectrophotometer microplate reader (Epoch, BioTek, Instruments, Inc.) controlled with a Gen5 Data Analysis software interface. Immobilization efficiency was calculated by subtracting the concentration of the tested supernatants from the initial concentration of the enzyme solution.

2.6. Determination of EbDH activity

Enzymatic tests were carried out in three modes: batch, fed-batch and continuous flow, under aerobic and anaerobic conditions. 0.5 ml of homogenous or immobilized EbDH enzyme (carrier suspension) was added into 10 ml (batch mode, aerobic conditions) or 20 ml (fed-batch mode, anaerobic conditions) of 0.1 M Tris/HCl buffer (pH 7.5) with 6 mM $K_3[Fe(CN)_6]$. Reaction buffer was preheated to 30 °C. The reactions were initiated by addition of ethylbenzene stock solution in *tert*-butyl alcohol (C = 1.5 mM). The initial activity was determined under aerobic conditions. An EbDH activity unit (U) was defined as the amount of enzyme liberating 1 μmol of 1-(*S*)-phenylethanol per minute under the assay conditions. Activity was calculated in U/mL of settled immobilized preparation or in U/mg of immobilized enzyme. Degree of reaction conversion was calculated as the ratio of the product concentration at the end of the reaction to the initial substrate concentration. Long term fed-batch enzymatic experiments were carried out under anaerobic conditions in order to extend the enzyme operation stability [27]. The substrate and re-oxidant were supplemented whenever depletion was observed by HPLC or UV–Vis (420 nm), respectively. HPLC determination of substrate and product was conducted as described elsewhere [27]. Immobilized EbDH was tested in the flow regime under anaerobic conditions by measuring the concentration of the product obtained at a specific flow rate. The range of flow rates varied from 0.05 to 1.5 ml min^{-1} and reactions were carried out in the same conditions as described above. Based on these measurements, the

Table 1
Physical analysis of immobilization supports.

Carrier	Particle shape and size	S_{BET} [$m^2 g^{-1}$]	V_{tot} [$cm^3 g^{-1}$]	Amine group density [mmol g^{-1}]	Vinyl group density [mmol g^{-1}]	Pore diameter [Å]	Mass of 0.5 ml of carrier [mg]
SBA-OH	Cube,	692	1.95	—	—	140	52
SBA-NH_2		490	1.62	1.0	—	140	74
	190 ± 49 nm by 580 ± 144 nm						
MATSPHERES® –OH	Sphere,	212	1.52	—	—	150–300	132
MATSPHERES® –NH_2		189	1.41	0.5	0.5	150–300	125
	30 ± 10 µm						

dependence of substrate conversion to residence time was determined. Residence time was calculated as the ratio of the bed volume (including the volume of the carrier being compared) to the flow rate. Having the above in mind, the most optimum flow rate was selected.

2.7. Determination of free and immobilised lipases enzymatic activity towards tributyrin

Enzymatic activity was determined by employing a modified protocols [40–42]. Briefly, tributyrin solution was prepared in HEPES buffer (pH 7.2) with addition of 25 µl–50 µl of Triton X per 20 ml of the reaction mixture. Lipase *Thermomyces lanuginosus* (TL-IM, Science Technics Sdn Bhd; Malaysia), *Candida antarctica* lipase B (CalB, Novozym 435; 10,000 PLU/g; Denmark) and EL070 (free and immobilized on different supports) were incubated in the solution with constant stirring (150 rpm) at 55 °C. Samples were withdrawn at specific intervals, diluted 10x with acetonitrile and analysed at Shimadzu Prominence HPLC equipped with UV–Vis detector set to 210 nm and Eclipse XDB-C18 column 4.6 × 100 um Agilent Technologies (depletion of tributyrin, increase of acetic acid signal). An isocratic elution of 15% water and 85% acetonitrile was applied. The injection interval was 4.5 min. Lipase activity unit (U) was defined as the amount of the enzyme that catalyzes the conversion of 1 µmol of tributyrin per minute under the specified conditions of the assay method.

2.8. Determination of EL070 activity in SFAE synthesis

Enzymatic reactions were carried out either in 100% v/v 2-methyl-2-butanol (2M2B) or in 2M2B/DMSO (80:20, v/v). Glucose was supplemented to yield 4 mg ml^{-1}, whereas methyl nonanoate to 11 mg ml^{-1}. 50 mg of molecular sieves (4 Å) was added to withdraw forming water. Reactions were initiated by addition of 12 mg of an enzyme (TL-IM, CalB or EL070 free or in immobilized form). Reactions were conducted at 55 °C either in a batch mode (24 h, rotation in a BINDER thermostat oven MASON Technology) or in a continuous flow mode. PrepRPC FPLC packed column was connected to HPLC pump Applied Separations K-500). Samples were collected at set intervals and were analysed on HPLC-MS system as described below. Lipase activity unit (U) was defined as the amount of the enzyme that catalyzes the conversion of 1 µmol of glucose per minute under the specified conditions of the assay method.

2.9. HPLC measurement

Glucose qualitative analysis was performed by HPLC measurements on Agilent 1290 Infinity System with automatic autosampler and MS Agilent 6460 Triple Quad Detector equipped with Agilent Zorbax Eclipse Plus C18 column (2.1 × 50 mm, 1.8 µm). For separation of sugar fatty acid esters (SFAE) the column was eluted at 30 °C at a flow rate of 0.4 ml min^{-1} and developed with gradient elution of mixture of water (A) and methanol (B) given as follows: 0.00 min (95% A/5% B) to 1.00 min (0% A/100% B) to 3.50 min (0% A/100% B) to 3.51 min (95% A/5% B) to 4.50 min (0% A/100% B). The injection interval was 4.5 min. MS Agilent 6460 Triple Quad tandem mass spectrometer with Agilent Jet Stream ESI interface was used in negative ion mode. Nitrogen at a flow rate of 10 L min^{-1} was used as the drying gas and for collision-activated dissociation. Drying gas and sheath gas temperatures were set to 350 °C. Capillary voltage was set to 3500 V, whereas the nozzle voltage was set to 500 V. Glucose was monitored by MRM transition of 179 → 89 *m/z* in negative ion mode and its depletion was calculated from calibration curve. MassHunter software (Agilent) was used for HPLC-MS system control, data acquisition, and data processing.

3. Results and discussion

3.1. Physicochemical characterisation of immobilisation supports

It is well known that grain size, pore architecture and carrier surface functionalization are very important factors that affect the applicability of a carrier. Therefore, we have performed basic physical analysis of MATSPHERES® and compared them with standard Santa Barbara Amorphous (SBA-15) immobilization carriers (Table 1). Microscopic observations revealed that the MATSPHERES® supports are hollow micrometric spheres, whereas SBA, a commonly used enzyme immobilization support, is a powder consisting of nanometric cubes. Nitrogen adsorption studies showed that the available surface area of the hollow spheres was 2.6 to 3.4 fold lower than these of SBA (for details see supplementary material). There was also lower coverage of the ammonium immobilisation on the spheres. However, the spheres are characterised with up to 2 fold larger pores with greater variety in sizes due to the openwork architecture, which positively influences enzyme immobilization by enabling its penetration and encapsulation in the sphere's core. Mechanistic studies revealed that the hollow spheres are not resistant to mechanical stirring with magnetic bar, however they withstand prolonged rotation (i.e. application in batch type reactors) and elevated pressures obtained by relatively high flows (up to 5 ml min^{-1}) (Fig. 2). In addition, the pressure generated by a column filled with 0.5 ml MATSPHERES® at a flow rate of 3 ml min^{-1} corresponds to the pressure that generates the same volume of SBA-15 at three times lower flow rate (Fig. 2E). Thus, the hollow microspheres outperform the standard SBA supports for applications in flow through reactors. Neither lyophilisation nor cycle of freezing the wet supports at −20 °C and thawing had any effect on the spheres architecture. Finally, storing of MATSPHERES® at −20 °C in aqueous solution for two weeks did not destruct their structure (Fig. 2G). Such stability may be due to perforated structure of this material.

3.2. Carriers' interactions with the reaction components

For the purpose of demonstrating the universality of hollow microspheres in biocatalysis, we have chosen two distinct enzymes of interest for pharmaceutical and food industries that carry out their catalytic reactions in different media, i.e. aqueous and non-aqueous, ethylbenzene dehydrogenase (EbDH) and a lipase (EL070) respectively. These two enzymes greatly differ in the mode of action (Fig. 3) – EbDH

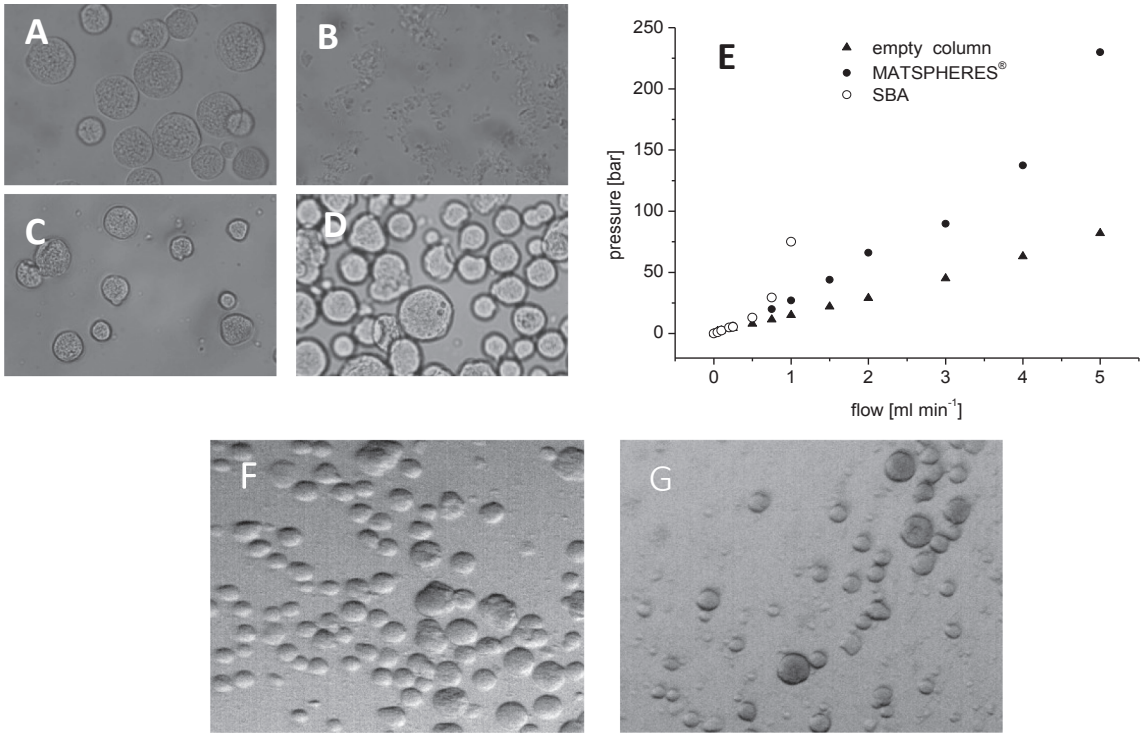

Fig. 2. Mechanistic performance of hollow spheres. Microscopic observations of spheres under different condition (magnification 400 X): (A) unmodified carrier material, (B) material after 24 h stirring in solution with magnetic bar, (C) material after constant rotation for 48 days, (D) material after quadruple flow of solvent at 0.05 ml min^{-1}, (E) pressure as a function of the flow rate generated by the empty column and a column filled with 0.5 ml of silica. Microscopic image of MATSPHERES® before (F) and after (G) 14 days of storing at −20 °C.

converts ethylbenzene in buffered water solution to 1-(*S*)-phenylethanol and requires an artificial electron acceptor ($K_3[Fe(CN)_6]$) for its action *in vitro*, whereas lipase is capable of generating of a novel ester bond in non-aqueous environment without aid of any mediator. Therefore, we have conducted several experiments in order to determine whether the hollow spheres interact with any given component of both reactions. Firstly, we verified whether the hollow spheres display any interaction with both enzymatic substrates under the reaction condition employed in this study. We did not observe any relevant physical nor chemical interplay for any of the tested compounds, with exception to $K_3[Fe(CN)_6]$. When potassium ferricyanide(III) was contacted with MATSPHERES®–OH and SBA-OH in EbDH reaction buffer (1 mM $K_3[Fe(CN)_6]$) remained on the same concentration level over 312 h. However that was not the case for the spheres with NH_2 and vinyl functionalities (MATSPHERES®–NH_2 or SBA-NH_2), where a rapid decrease to depletion was observed (Fig. 4). This can be explained by the $K_3[Fe(CN)_6]$ oxidation reaction of distal –NH_2 groups, and therefore we conclude the MATSPHERES®–NH_2 are less desirable in use for EbDH biocatalysis.

3.3. Enzymes immobilization on the hollow spheres and their enzymatic performance

Enzymatic preparation of ethylbenzene dehydrogenase obtained from a native strain *Aromatoleum aromaticum* EbN1, as well as commercial EL070 lipase powder, were used for immobilization on two types of spheres – non-functionalized (MATSPHERES®–OH) and functionalized with vinyl and amino groups (MATSPHERES®–NH_2). For

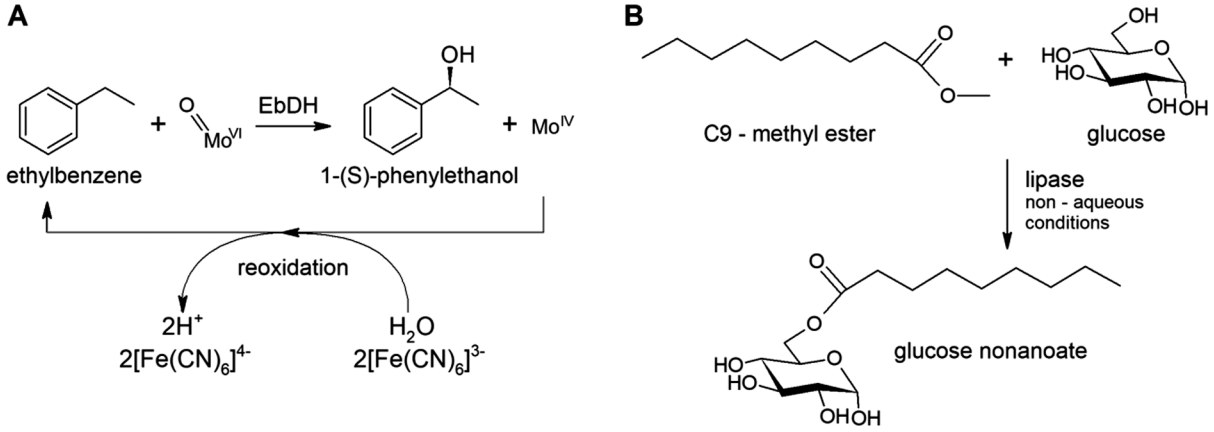

Fig. 3. Reactions performed by enzymes in this study. Panel A – ethylbenzene dehydrogenase converts ethylbenzene to 1-(S)-phenylethanol while transferring an electron to an artificial electron acceptor $K_3[Fe(CN)_6]$. Panel B – lipase EL070 acylates glucose with methyl nonanoate to form sugar ester and a side product methanol.

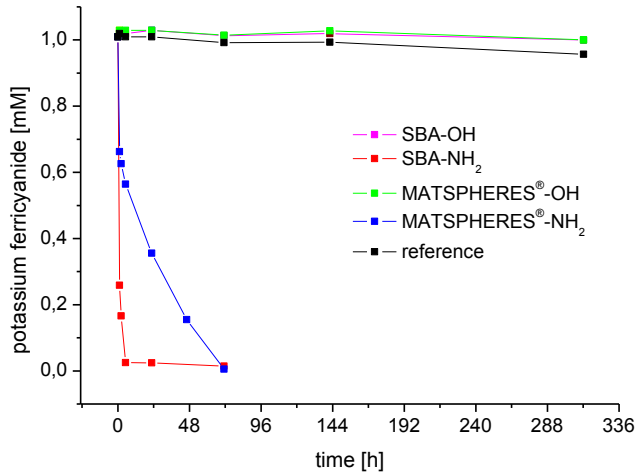

Fig. 4. Interaction of potassium ferricyanide (III) with hollow microspheres. Buffer with electron acceptor without silica stands as a reference.

further comparisons SBA-OH and SBA-NH_2 analogous preparations were also made (Table 2).

3.3.1. EbDH

It is known that EbDH class of enzymes is oxygen sensitive [21,43] and therefore these conditions seem to be more favorable for long-term EbDH operation. We have confirmed this phenomenon by performing a batch type reactors under both atmospheres. After immobilization process, there was high protein coverage of both types of spheres, ranging from 88 to 90% or 3.2 – 3.3 mg of bound protein per ml of carrier. Under aerobic conditions and independently of sphere's modification we observed a progressing enzyme inactivation due to the presence of oxygen. Under these conditions, free and immobilized formulation of EbDH were inactivated after about 20 h of continues work [27]. Still, they were able to produce similar amounts of product for all carries (from the lowest for SBA-NH_2 – 0.14 mM up to 0.17 mM for MATSPHERES®–NH_2) of 1-(*S*)-phenylethanol before its complete inactivation. It needs to be stressed that the activity of each functionality under aerobic condition was similar among carries with the same functionality (see Tables 2 and 3).

In the absence of oxygen, a more active immobilized biocatalyst can be rapidly selected. Under anaerobic conditions, the enzyme operated for over 580 h (24 days), with residual activity still remaining for further 21 days, being able to convert several batches of substrate to achieve final 2.84 mM (56.5 µmol) (MATSPHERES®–OH) and 1.56 mM (31.2 µmol) (MATSPHERES®–NH_2) product concentrations (Fig. 5, Table 3). The average process activity determined as a change in product concentration from the start of the experiment until 580 h of reaction (the end of the linear rate of product formation) was 1.6 mU, 0.8 mU and 2.9 mU for the reactors with MATSPHERES®–OH, MATSPHERES®–NH_2 and free enzyme, respectively. For comparisons, the SBA preparations proved to be only slightly better than MATSPHERES® by 1.1 and 1.2 fold for SBA-OH and SBA-NH_2, respectively. Noteworthy, enzyme lifetime elongated almost 30 fold (from 20 h in aerobic conditions to over 580 h in anaerobic conditions).

Under the anaerobic conditions, the best results in terms of reaction efficiency were obtained with activation of –OH groups (for both of MATSPHERES® and SBA), which is in agreement with Tataruch et al., 2014 [27]. Moreover, enzymatic preparations on carriers with OH functionalities under aerobic conditions resulted in higher activity when compared to the –NH_2 supports. This could be the combined effect of two factors: i) presence of the DVS activator ii) lack of electron acceptor interaction with microsphere surface. In case of MATSPHERES®–NH_2, the electron acceptor depletion is probably caused by its reduction by reactive amine groups. This phenomenon may lead to serious decline in the activity of the enzyme immobilized on MATSPHERES®–NH_2.

Recently we have reported EbDH immobilisation on a cellulosic support [27], however, when flow reactors are concerned this type of carrier is inadequate due to its physical performance (gluing of grains thus clogging the column). MATSPHERES® however seems to be suitable for this type of applications and even outperforms standard SBA carrier used widely in immobilization studies with regards to their flow

Table 2
Catalytic characterization of immobilized and homogenous enzymes – EbDH and EL070.

Carrier	Activating agent	activity [mU] per mL (per mg) of carrier or homogenous enzyme*	Retained activity [%]	Bound protein** [mg ml^{-1}]	Enzyme loading (protein) [%]	Specific initial activity [mU mg^{-1}]
EbDH						
Homogenous EbDH	—	27.18	100	—	—	7.40
MATSPHERES® –OH	DVS	10.88 (0.041)	40	3.30	90	3.29
MATSPHERES® –NH_2	GA	9.60 (0.038)	35	3.23	88	2.98
SBA-OH	DVS	11.00 (0.106)	40	3.35	91	3.28
SBA-NH_2	GA	9.32 (0.063)	34	3.2	87	2.91
Lipase EL070						
Homogenous EL070	—	(274160.0)	100	—	—	274160.0
MATSPHERES® –OH	DVS	427920 (1620)	4.6	33.6	67	12735.7
MATSPHERES® –NH_2	GA	685450 (2740)	5.6	44.2	88	15507.9
SBA-OH	DVS	468738 (4521)	8.6	19.9	65	23554.7
SBA-NH_2	GA	279232 (1887)	3.7	27.3	89	10228.3

Where: DVS – divinyle sulphone, GA – glutaraldehyde.

* EbDH was obtained in liquid formulation from bacterial strain in our laboratory (see materials and methods), whereas lipase was purchased in powdered form. Therefore for homogenous EbDH the activity was given only "per ml", whereas in case of homogenous lipase "per mg".

** The amount of bound protein was calculated by subtracting the washed off protein quantity from this used for immobilization and recalculated per 1 ml of the carrier. Protein concentration for native EbDH (all supports) was 3.67 mg ml^{-1}, for lipase EL070 was 50 mg ml^{-1} and 30.2 mg ml^{-1} for MATSPHERES® and SBA, respectively.

Table 3
Synthesis of 1-(*S*)-phenylethanol under aerobic and anaerobic conditions.

Type of carrier	Final product concentration in the reactor [mM]	Reaction efficiency (based on max. product conc.) [%]	Final product concentration in the reactor [mM]	Reaction efficiency (based on max. product conc.) [%]
Reaction condition	anaerobic		aerobic	
Homogenous EbDH	4.90	100	0.40	100
MATSPHERES® –OH	2.84	58	0.16	40
MATSPHERES® –NH_2	1.56	32	0.17	43
SBA-OH	3.12	64	0.15	38
SBA-NH_2	2.17	44	0.14	35

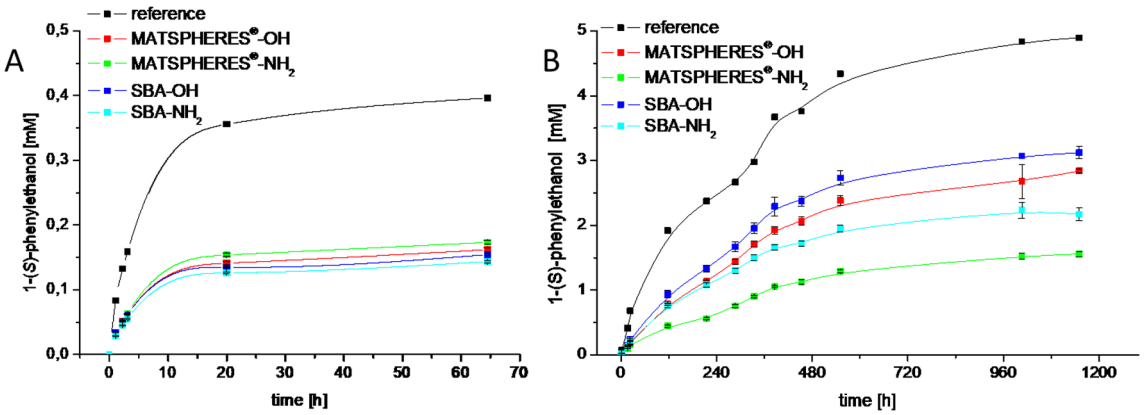

Fig. 5. Profiles of changes in product concentration in reaction catalysed by immobilized and native EbDH in aerobic (Panel A) and anaerobic (Panel B) atmosphere.

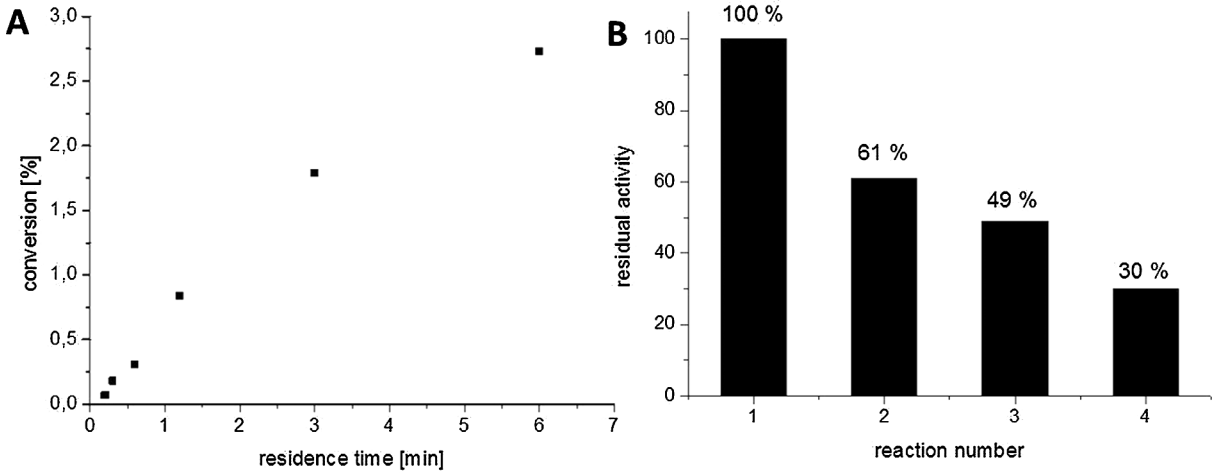

Fig. 6. Performance of immobilized EbDH in flow reactor. A – effect of residence time on acetophenone conversion; B – subsequent cycles in flow reactor.

characteristics (Fig. 2). We have tested the most promising enzyme formulation (EbDH immobilized on MATSPHERES®–OH) in the flow regime under anaerobic conditions by measuring the concentration of the product obtained at a specific flow rate. Fig. 6A shows the variation of product concentration with a change in flow rate in a single pass flow through the 0.5 ml of bed with EbDH immobilised on MATSPHERES®–OH in the reactor. In order to determine the reusability of the immobilised EbDH preparation (MATSPHERES®–OH), we performed a consecutive enzymatic test under a flow regime of 0.05 ml min^{-1}. 20 ml of the reaction medium with an initial concentration of 1.5 mM substrate was pumped through the silica bed in four reactor cycles under anaerobic conditions at a rate of 0.05 ml min^{-1} (6 h 20 min). After each charge, the column with the immobilized enzyme was washed with a fresh reaction buffer without substrate and stored under anaerobic atmosphere at 7 °C. The product concentration achieved after the first reaction reached 41 μM and was defined as 100% of activity. A drop in the activity was observed when consecutive cycle of enzymatic reaction were performed in the flow-through reaction (Fig. 6B). In the fourth charge, 30% of the residual activity was achieved in comparison to the first charge. 2.1 μmoles of the product was obtained in combined four charges in less than 27 h.

3.3.2. *EL070 lipase*

Mesoporous silica micro/nanoparticles, among other siliceous supports, also proved to be reliable carriers for lipases immobilisation [44–46]. However, little is known about the employment of hollow microspheres functionalised by DVS/GA with available –OH/–NH_2 surface active groups for lipase immobilisation and particularly for their use in sugar fatty acids ester (SFAE) synthesis. Therefore we have immobilised a commercial lipase on both types of carriers and tested the preparations for their usefulness in SFAE production. Based on tributyrin lipase activity assay and Bradford protein concentration

assay it was determined that 0.127 mg of EL070 lipase was loaded on 1 mg of MATSPHERES®–OH giving finally 12.6U of enzyme activity, whereas 0.177 mg of lipase was loaded on 1 mg MATSPHERES®–NH_2 resulting in 15.5U of final enzyme activity (Table 2). Enzyme loading of the protein loading reached 67% for MATSPHERES®–OH and 88% for MATSPHERES®–NH_2. This may be due to the fact that silica inherently has hydroxyl groups on the surface, while by introducing additional NH_2 groups, the possibilities for the enzyme to be incorporated into the carrier are increased [37]. Immobilisation efficiency of EL070 on SBA was comparable to these obtained for spheres, namely 65% for SBA-OH and 88% for SBA-NH_2. Specific initial activity of SBA-OH preparation was 23.5 U mg^{-1} (1.8 fold greater than spheres), whereas for SBA-NH_2 we obtained 10.2 U mg^{-1} (0.6 fold lower than spheres). However, when specific activity values of the resulting preparations were compared with homogenous EL070 activity (274.2 U mg^{-1}), the efficiency of the whole process was only 4.6% and 5.7% for MATSPHERES®–OH and MATSPHERES®–NH_2, respectively; whereas for SBA-OH – 8.6% and SBA-NH_2 – 3.7%. These results suggest that during the immobilization procedure the enzyme was partially inaccessible. This may be due to covalent bond formation between functional groups of the protein and linking agents DVS or GA respectively, resulting in changes of the enzyme conformation that dislocates its active site [47–50].

Consecutively, we have employed free EL070 and its immobilised variants for biocatalytic synthesis of sugar esters in non-aqueous environments. Following protocols of others [23,41] the enzymatic reactions were performed in 2-methyl-2-butanol (2M2B) on its own (batch processes) or supplemented with 20% dimethyl sulfoxide (DMSO), in order to facilitate complete glucose solubilisation in the reaction medium during the flow type reactors. The free enzyme was found to poorly convert methyl nonanoate and glucose to its corresponding sugar ester in the batch tests (maximum of 13.5% glucose conversion, Table 4). However once immobilised on MATSPHERES®–OH and MATSPHERES®–NH_2, the lipase was able to produce glucose nonanoate in 2M2B with 88.5% and 98.4% efficiency, respectively (Table 4). Similar enhancement of SFAE synthesis was achieved, when lactose and palmitic acid were catalysed with immobilised *Candida antarctica* lipase B to form lactose palmitate [6]. For a benchmark comparison the EL070 immobilised on SBA supports and two other commercial immobilised lipase preparations were tested. We found that our two MATSPHERES® preparations of EL070 outperformed immobilised *Thermomyces lanuginosus* Amano lipase (TLIM) by 2.1–2.3 fold and *C. antarctica* lipase B (CalB) by 2.4–2.6 fold. When MATSPHERES®–OH where compared to their SBA counterparts conversions were at the same level. However, MATSPHERES®–NH_2 proved to be 1.2 fold more efficient than SBA-NH_2 (Table 4). It is also worth to notice that glucose nonanoate is not commercially available, therefore all conversion calculations were made taking into consideration the depletion of glucose in the reaction medium. However, the glucose nonanoate formation was confirmed by ESI-MS, ^{1}H NMR and IR measurements (see supplementary information).

Having in mind good performance of the hollow microspheres under different flow conditions, we set up flow type reactors in order to produce sugar esters in this mode. Being aware that sugar ester synthesis is a much slower process than EbDH biocatalysis, we decided to conduct experiments under the slowest flow possible under our experimental setup (0.02 ml min^{-1}). In order to avoid clogging of the reactor, we used 2M2B:DMSO (8:2, v/v) medium, as it allowed for a total glucose solubilisation. The column was packed with 250 µl of enzymatic bed and reactions were conducted 3 times at 55 °C and a flow rate of 0.05 ml min^{-1} (6 h 20 min). We have observed that MATSPHERES®–NH_2 enabled faster sugar conversion to glucose nonanoate after 1st and 2nd charges by 3.3 and 1.2 fold respectively when compared to MATSPHERES®–OH (final 88.3% versus 73.0% conversion, Table 5). The observed drop in the conversion for the 3rd round when the hollow microspheres were used can be explained by water sorption from the surrounding environment and ester hydrolysis (each round lasted for 6 h, set-up was not sealed and medium contained hygroscopic DMSO). Nevertheless, the investigated continuous flow system outperformed some of the previously reported SFAE continuous reactor setups [51–55].

Table 4
Synthesis of glucose nonanoate in 2-methyl-2-butanol in batch mode.

	Glucose after 24 h [mg ml^{-1}]	Conversion [%]
EL 070 homogenous	3.77	13.5
MATSPHERES® –OH	0.50	88.5
MATSPHERES® –NH_2	0.07	98.4
SBA-OH	0.50	89.1
SBA-NH_2	0.47	83.7
TLIM	2.53	42.1
CalB	2.72	37.6

Table 5
Performance of immobilised lipases in the flow reactors.

	Turnover	Conversion [%]			
		0	1	2	3
Type of support	MATSPHERES® –OH	0	12.9	73.0	51.1
	MATSPHERES® –NH_2	0	42.6	88.3	68.1

4. Conclusions

In the process of immobilization of ethylbenzene dehydrogenase on MATSPHERES® and SBA carriers with the same functionalization similar values of activity and bound protein were obtained, and thus the parameters characterizing the process of immobilization (enzyme loading, retained activity). At this stage there were no major differences between the spheres and the SBA carriers. Apart from the residual enzyme activity in the final phase of the reaction, it was shown that under anaerobic conditions the enzymatic preparations were able to operate for about 24 days (580 h), which corresponds to results reported already in the literature [27]. A prolonged operation (days) of enzymatic preparations in anaerobic conditions clearly indicated that for both supports without additional amino group (spheres or SBA) the immobilised enzyme operated more efficiently and differences in the final product concentrations or average process activities were very small.

Immobilisation of lipase enabled efficient production of sugar ester in either batch or flow-through regime. For immobilized lipase, the percentage of retained activity was significantly lower than in the case of EbDH (in the range of 3.7–8.6%). However, only the use of the immobilized formulation of this enzyme allowed effective glucose nonanoate synthesis. Within the silicas with amine groups, the retained activity for MATSPHERES® was 50% higher than for SBA, whereas this dependence was inverse for the NH_2-silica.

Silica carriers are widely used for immobilisation of a variety of enzymes. We have shown that hollow microspheres are also suitable for this type of applications. The MATSPHERES® are durable materials due to their openwork architecture that withstands harsh physical conditions (prolonged rotational mixing, freeze/thawing cycles, lyophilisation, etc.) revealing their broad applications in biocatalysis. Moreover, the hollow spheres enabled acceptable enzymes immobilisation, which are comparable to the gold standard in mesoporous silica immobilization – Santa Barbara Amorphous carriers.

Acknowledgements

Maciej Guzik, Wojciech Snoch and Ewelina Cichoń greatly acknowledge the financial support of National Science Centre, Poland [grant SONATA no. 2015/17/D/ST4/00514]. Mateusz Tataruch

acknowledges partial financial support of the project by the statutory research fund of Jerzy Haber Institute of Catalysis and Surface Chemistry Polish Academy of Sciences. Wojciech Snoch also acknowledges the support of InterDokMed project no. POWR.03.02.00-00-I013/16. We thank Anna Miłaczewska for preparing graphical abstract.

Conflict of interest

Mathilde Gosselind is an employee of Materium Innovations INC.

Appendix A. Supplementary material

Supplementary data to this article can be found online at https://doi.org/10.1016/j.bioorg.2019.02.038.

References

[1] V. Ferreira-Leitão, M. Cammarota, E. Gonçalves Aguieiras, L. Vasconcelos de Sá, R. Fernandez-Lafuente, D. Freire, The protagonism of biocatalysis in green chemistry and its environmental benefits, Catalysts 7 (2017) 9.
[2] R.A. Sheldon, S. van Pelt, Enzyme immobilisation in biocatalysis: why, what and how, Chem. Soc. Rev. 42 (2013) 6223–6235.
[3] G.W. Huisman, S.J. Collier, On the development of new biocatalytic processes for practical pharmaceutical synthesis, Curr. Opin. Chem. Biol. 17 (2013) 284–292.
[4] J.N. Talbert, L.S. Wang, B. Duncan, Y. Jeong, S.M. Andler, V.M. Rotello, J.M. Goddard, Immobilization and stabilization of lipase (CaLB) through hierarchical interfacial assembly, Biomacromolecules 15 (2014) 3915–3922.
[5] S.M. Andler, L.S. Wang, V.M. Rotello, J.M. Goddard, Influence of hierarchical interfacial assembly on lipase stability and performance in deep eutectic solvent, J. Agric. Food Chem. 65 (2017) 1907–1914.
[6] M. Enayati, Y. Gong, J.M. Goddard, A. Abbaspourrad, Synthesis and characterization of lactose fatty acid ester biosurfactants using free and immobilized lipases in organic solvents, Food Chem. 266 (2018) 508–513.
[7] C. Mateo, J.M. Palomo, G. Fernandez-Lorente, J.M. Guisan, R. Fernandez-Lafuente, Improvement of enzyme activity, stability and selectivity via immobilization techniques, Enzyme Microb. Technol. 40 (2007) 1451–1463.
[8] K. Labus, A. Turek, J. Liesiene, J. Bryjak, Efficient Agaricus bisporus tyrosinase immobilization on cellulose-based carriers, Biochem. Eng. J. 56 (2011) 232–240.
[9] K. Labus, I. Gancarz, J. Bryjak, Immobilization of laccase and tyrosinase on untreated and plasma-treated cellulosic and polyamide membranes, Mat. Sci. Eng. C 32 (2012) 228–235.
[10] A. Sikander, W. Zafar, S. Shafiq, M. Manzoor, Enzymes immobilization: an overview of techniques, support materials and its applications, Int. J. Sci. Technol. Res. 6 (2017) 64–72.
[11] B. Chen, C. Lei, Y. Shin, J. Liu, Probing mechanisms for enzymatic activity enhancement of organophosphorus hydrolase in functionalized mesoporous silica, Biochem. Biophys. Res. Commun. 390 (2009) 1177–1181.
[12] N. Adiram-filiba, A. Schremer, E. Ohaion, M. Nadav-tsubery, T. Lublin-tennenbaum, K. Keinan-adamsky, G. Goobes, Ubiquitin immobilized on mesoporous MCM41 silica surfaces – analysis by solid-state NMR with biophysical and surface characterization, Biointerphases 12 (2017) 1–9.
[13] E. Onoja, S. Chandren, F.I.A. Razak, R.A. Wahab, Extraction of nanosilica from oil palm leaves and its application as support for lipase immobilization, J. Biotechnol. 283 (2018).
[14] S. Shioji, M. Hanada, Y. Hayashi, Continuous surface modification of silica particles for enzyme immobilization, Adv. Powder Technol. 14 (2003) 231–245.
[15] X. Chen, K. Wilgosz, K. Cendrowski, T. Tang, P.K. Chu, R.J. Kalenczuk, E. Mijowska, Facile synthesis of hollow silica spheres with nanoholes, Dalt. Trans. 42 (2013) 6381–6385.
[16] M.N. Gorsd, L.R. Pizzio, M.N. Blanco, Synthesis and characterization of hollow silica spheres, Proc. Mat. Sci. 8 (2015) 567–576.
[17] Y. Bao, C. Shi, T. Wang, X. Li, J. Ma, Recent progress in hollow silica: template synthesis, morphologies and applications, Micropor. Mesopor. Mater. 227 (2016) 121–136.
[18] H.A. Johnson, D.A. Pelletier, Isolation and characterization of anaerobic ethylbenzene dehydrogenase, a novel Mo-Fe-S enzyme, J. Bacteriol. 183 (2001) 4536–4542.
[19] R. Rabus, Æ.M. Kube, Æ.J. Heider, The genome sequence of an anaerobic aromatic-degrading denitrifying bacterium, strain EbN1, Arch. Microbiol. 183 (2005) 27–36.
[20] D.P. Kloer, C. Hagel, J. Heider, G.E. Schulz, Crystal structure of ethylbenzene dehydrogenase from *Aromatoleum aromaticum*, Structure 14 (2006) 1377–1388.
[21] M. Szaleniec, C. Hagel, M. Menke, P. Nowak, M. Witko, J. Heider, Kinetics and mechanism of oxygen-independent hydrocarbon hydroxylation by ethylbenzene dehydrogenase, Biochemistry 46 (2007) 7637–7646.
[22] H.A. Johnson, A.M. Spormann, In vitro studies on the initial reactions of anaerobic ethylbenzene mineralization, J. Bacteriol. 181 (1999) 5662–5668.
[23] R. Rabus, F. Widdel, Anaerobic degradation of ethylbenzenes and other aromatic hydrocarbons by new denitrifying bacteria, Arch. Microbiol. 163 (1995) 96–103.
[24] R. Rabus, J. Heider, Initial reactions of anaerobic metabolism of alkylbenzenes in denitrifying and sulfate reducing bacteria, Arch. Microbiol. 170 (1998) 377–384.
[25] D. Knack, C. Hagel, M. Szaleniec, A. Dudzik, A. Salwinski, J. Heider, Substrate and inhibitor spectra of ethylbenzene dehydrogenase: perspectives on application potential and catalytic mechanism, Appl. Environ. Microbiol. 78 (2012) 6475–6482.
[26] A. Dudzik, B. Kozik, M. Tataruch, A. Wójcik, D. Knack, T. Borowski, J. Heider, M. Witko, M. Szaleniec, The reaction mechanism of chiral hydroxylation of p -OH and p -NH 2 substituted compounds by ethylbenzene dehydrogenase, Can. J. Chem. 91 (2013) 775–786.
[27] M. Tataruch, J. Heider, J. Bryjak, P. Nowak, D. Knack, A. Czerniak, J. Liesiene, M. Szaleniec, Suitability of the hydrocarbon-hydroxylating molybdenum-enzyme ethylbenzene dehydrogenase for industrial chiral alcohol production, J. Biotechnol. 192 (2014) 400–409.
[28] F. Aeckersberg, F.A. Rainey, Growth, natural relationships, cellular fatty acids and metabolic adaptation of sulfate-reducing bacteria that utilize long-chain alkanes under anoxic conditions, Arch. Microbiol. 170 (1998) 361–369.
[29] F. Bondavalli, M. Botta, O. Bruno, A. Ciacci, F. Corelli, P. Fossa, A. Lucacchini, F. Manetti, C. Martini, G. Menozzi, L. Mosti, A. Ranise, S. Schenone, A. Tafi, M.L. Trincavelli, Synthesis, molecular modeling studies, and pharmacological activity of selective A1 receptor antagonists, J. Med. Chem. (2002) 4875–4887.
[30] L. Hsin, C.M. Dersch, M.H. Baumann, D. Stafford, J.R. Glowa, R.B. Rothman, A.E. Jacobson, K.C. Rice, Development of long-acting dopamine transporter ligands as potential cocaine-abuse therapeutic agents: chiral hydroxyl-containing derivatives of 1-[2-[bis(4-fluorophenyl)methoxy]ethyl]-4-(3-phenylpropyl)piperazine and 1-[2-(diphenylmethoxy)ethyl]-4-(3-phenylpropyl)piperazine, J. Med. Chem. 45 (6) (2002) 1321–1329.
[31] M.K. Walsh, R.A. Bombyk, A. Wagh, A. Bingham, L.M. Berreau, Synthesis of lactose monolaurate as influenced by various lipases and solvents, J. Mol. Catal. B Enzym. 60 (2009) 171–177.
[32] D.R. Perinelli, S. Lucarini, L. Fagioli, R. Campana, D. Vllasaliu, A. Duranti, L. Casettari, Lactose oleate as new biocompatible surfactant for pharmaceutical applications, Eur. J. Pharm. Biopharm. 124 (2018) 55–62.
[33] S. Siebenhaller, J. Gentes, A. Infantes, C. Muhle-Goll, F. Kirschhöfer, G. Brenner-Weiß, K. Ochsenreither, C. Syldatk, Lipase-catalyzed synthesis of sugar esters in honey and agave syrup, Front. Chem. 6 (2018) 1–9.
[34] I.J.A. Baker, B. Matthews, H. Suares, I. Krodkiewska, D.N. Furlong, F. Grieser, C.J. Drummond, Sugar fatty acid ester surfactants: structure and ultimate aerobic biodegradability, J. Surf. Deterg. 3 (2000) 1–11.
[35] L. Zhao, H. Zhang, T. Hao, S. Li, *In vitro* antibacterial activities and mechanism of sugar fatty acid esters against five food-related bacteria, Food Chem. 187 (2015) 370–377.
[36] S. Okabe, M. Suganuma, Y. Tada, Y. Ochiai, E. Sueoka, H. Kohya, A. Shibata, M. Takahashi, M. Mizutani, Disaccharide esters screened for inhibition of tumor necrosis factor- α release are new anti-cancer agents, Japan. J. Cancer Res. (1999) 669–676.
[37] X. Wang, S. Miao, P. Wang, S. Zhang, Bioresource technology highly efficient synthesis of sucrose monolaurate by alkaline protease Protex 6L, Bioresour. Technol. 109 (2012) 7–12.
[38] A. Rugor, M. Tataruch, J. Staroń, A. Dudzik, E. Niedzialkowska, P. Nowak, A. Hogendorf, A. Michalik-Zym, D.B. Napruszewska, A. Jarzębski, K. Szymańska, W. Białas, M. Szaleniec, Regioselective hydroxylation of cholecalciferol, cholesterol and other sterol derivatives by steroid C25 dehydrogenase, Appl. Microbiol. Biotechnol. 101 (2017) 1163–1174.
[39] M.M. Bradford, A rapid and sensitive method for the quantitation of microgram quantities of protein utilizing the principle of protein-dye binding, Anal. Biochem. 72 (1976) 248.
[40] H.S. Wu, M.J. Tsai, Kinetics of tributyrin hydrolysis by lipase, Enzyme Microb. Technol. 35 (2004) 488–493.
[41] A. Hochkoeppler, S. Palmieri, A spectrophotometric lipase activity assay by coupled lipase-lipoxygenase in reverse micelles, Biocatal. Biotransformation. 3 (1990) 357–365.
[42] J.M. Fasciano, F.R. Mansour, N.D. Danielson, Ion-exclusion high-performance liquid chromatography of aliphatic organic acids using a surfactant-modified C18 column, J. Chromatogr. Sci. 54 (2016) 958–970.
[43] O. Kniemeyer, J. Heider, Ethylbenzene dehydrogenase, a novel hydrocarbon-oxidizing molybdenum/iron-sulfur/heme enzyme, J. Biol. Chem. 276 (2001) 21381–21386.
[44] Z. Ali, L. Tian, P. Zhao, B. Zhang, N. Ali, M. Khan, Q. Zhang, Immobilization of lipase on mesoporous silica nanoparticles with hierarchical fibrous pore, J. Mol. Catal. B Enzym. 134 (2016) 129–135.
[45] D. Cazaban, L. Wilson, L. Betancor, Lipase immobilization on siliceous supports : application to synthetic reactions, Current Organ. Chem. (2017) 85–92.
[46] J. Zdarta, A. Meyer, T. Jesionowski, M. Pinelo, A general overview of support materials for enzyme immobilization: characteristics, properties, practical utility, Catalysts 8 (2018) 92.
[47] P. Adlercreutz, Immobilisation and application of lipases in organic media, Chem. Soc. Rev. 42 (2013) 6406.
[48] J.A. Laszlo, M. Jackson, R.M. Blanco, Active-site titration analysis of surface influences on immobilized *Candida antarctica* lipase B activity, J. Mol. Catal. B, Enzym. 69 (2011) 60–65.
[49] F. Secundo, Conformational changes of enzymes upon immobilisation, Chem. Soc. Rev. 42 (2013) 6250–6261.
[50] F.J. Plou, M.A. Cruces, M. Ferrer, G. Fuentes, E. Pastor, M. Bernabé, M. Christensen, F. Comelles, J.L. Parra, A. Ballesteros, Enzymatic acylation of di- and trisaccharides with fatty acids: choosing the appropriate enzyme, support and solvent, J. Biotechnol. 96 (2002) 55–66.
[51] F.K. Sutili, H.S. Ruela, D.D.O. Nogueira, I.C.R. Leal, L.S.M. Miranda, R.O.M.A. De Souza, Enhanced production of fructose ester by biocatalyzed continuous flow

process, Sus. Chem. Proc. 3 (6) (2015) 8–11.
[52] H.S. Ruela, F.K. Sutili, I.C.R. Leal, N.M.F. Carvalho, L.S.M. Miranda, R.O.M.A. de Souza, Lipase-catalyzed synthesis of secondary glucose esters under continuous flow conditions, Eur. J. Lipid Sci. Technol. 4 (115) (2015) 464–467.
[53] J. Piao, S. Adachi, Enzymatic preparation of fatty acid esters of sugars alcohols by condensation in acetone using a packed-bed reactor with immobilized Candida antarctica lipase, Biocatal. Biotransform. 22 (2004) 269–274.
[54] F.M. Xavier, H.R. Reyes, H.S. Garcia, C.G. Hill, Immobilized lipase reactors for modification of fats and oils-a review, J. Am. Oil Chem. Soc. 67 (1990) 890–910.
[55] X. Xu, T. Porsgaard, H. Zhang, J. Adler-nissen, C. Høy, Production of structured lipids in a packed-bed reactor with *Thermomyces lanuginosa* Lipase, J. Am. Oil Chem. Soc 79 (2002) 561–565.

catalysts

MDPI

Article

Influence of Chemical Modifications of Polyhydroxyalkanoate-Derived Fatty Acids on Their Antimicrobial Properties

Wojciech Snoch [1], Karolina Stępień [2], Justyna Prajsnar [1], Jakub Staroń [3], Maciej Szaleniec [1] and Maciej Guzik [1,*]

1 Jerzy Haber Institute of Catalysis and Surface Chemistry, Polish Academy of Sciences, Niezapominajek 8, 30-239 Kraków, Poland; ncsnoch@cyfronet.pl (W.S.); justyna.prajsnar1@gmail.com (J.P.); ncszalen@cyfronet.pl (M.S.)

2 Medical University of Warsaw, Department of Pharmaceutical Microbiology, 3 Oczki Str. 02-007 Warsaw, Poland; Karolinastepien@windowslive.com

3 Institute of Pharmacology, Polish Academy of Sciences, Smętna 12, 31-343 Kraków, Poland; jakubstaron@gmail.com

* Correspondence: ncguzik@cyfronet.pl; Tel.: +48-126-395-155

Received: 15 May 2019; Accepted: 30 May 2019; Published: 5 June 2019

Abstract: Sugar esters are bioactive compounds derived from renewable resources. They consist of a sugar moiety with attached non-polar part – usually a fatty acid. These compounds find uses in cosmetic, food and pharmaceutical industries as surfactants due to their physicochemical and antimicrobial activities. In this study we have produced fatty acids for sugar ester synthesis from bacterially derived polyesters, namely polyhydroxyalkanoates (PHAs). We have developed methodology to decorate PHA monomers with a fluorinated moiety. With aid of biocatalysis a series of glucose esters was created with unmodified and modified PHA monomers. All synthesised compounds showed moderate antimicrobial activity.

Keywords: polyhydroxyalkanoate; (*R*)-3-hydroxyacids; biocatalysis; sugar esters; antimicrobial

1. Introduction

Sugar esters represent a class of biodegradable and bioactive compounds that brought attention of scientists and industries in recent decades [1]. These molecules are composed of a hydrophilic sugar component (rich in hydroxyl groups) connected via ester bonds to a hydrophobic part, usually a carboxylic acid. The number and the length of these acid derived chains, together with the number of hydroxyl groups of the particular sugar determine the hydrophilic-lipophilic balance (HLB) - a unique property of a given molecule of sugar ester. At the same time their chemical structures enable them to form micelles, emulsions, stabilize foams thanks to their surface active properties [2,3]. These features bring practical importance of sugar fatty acids esters (SFAEs), hence they are widely used in the food, cosmetic and pharmaceutical industries (as additives for dairy products, feeds, creams, gels, shampoos, pastes, ointments) [3–7]. SFAE not only have interesting physicochemical properties, but also are biologically active [8,9], increase the cell membrane permeability of microorganisms and inactivate transmembrane proteins, thus exposing microbes to adverse external factors, loss of intracellular proteins and valuable nutrients leading to an immediate inactivation [10,11].

The most popular among the sugar esters are those which contain glucose, galactose, sucrose or lactose because of their availability from natural resources [12–16]. The hydrophobic component is commonly derived from plant or animal biomass, e.g., butyric (C4), caprylic (C8), pelargonic (C9), lauric (C12), palmitic (C16) and stearic (C18) acids [5,8,9,17,18]. Depending on the length of aliphatic

chain, its branching and existence of additional functional groups SFAE molecules may be more or less available for a given organism (due to variations in cell membrane transfer) and also faster or slower decomposed by enzymes (lipases, glycosidases). The presence of additional functional groups in the aliphatic chain modifies both the physical properties and therapeutic effect of SFAE, thus enhancing its biological effectiveness and spectrum [19–22]. These include phenyl, hydroxyl, amino, hydroxyphenyl, methoxy-phenyl and halogen-containing moieties, e.g., phenyl-fluorine, or alkyl halides [23–26]. Out of the mentioned modifiers, the fluorine most profoundly alters the molecule's biological functions (i.e., increases the free-radical production; influences bio-retention due to increased hydrophobicity of a given molecule) [27–29].

In order to aid in the search for new modifiers of the hydrophobic component of SFAE we tapped into monomeric units that build bacterially derived polymers. Bacteria synthesise polyhydroxyalkanoates (PHAs) in response to unfavourable environmental conditions employing sophisticated biochemical apparatus [30]. PHAs are composed of 3-hydroxylated fatty acids, where the hydroxyl group is always in an absolute *R* configuration [31]. Existence of this hydroxyl group on the carboxylic acid moiety opens interesting paths for modifications [32]. For example, it can be readily used to form an ether bond between oxygen atom and a halogenated alkyl group, which may influence their potential therapeutic effect. In recent years similar modifications of PHA monomers have been performed. However, they relied on the elimination of the hydroxyl group on chiral 3rd carbon atom and its exchange to 3-chloro, 3-fluorobenzyl, 3-bromo, 3-fluoro or amino group, which led to the loss of chirality of the molecule, but improved bacteriostatic properties [33,34].

Our study presents the development of a biocatalytic synthesis method for the preparation of unique glucose esters based on PHA derived monomers, namely mixtures of (*R*)-3-hydroxynonanoic and (*R*)-3-hydroxyheptanoic acids or (*R*)-3-hydroxy-5-phenylpentanoic and (*R*)-3-hydroxy-3-phenylpropionic acids arising from two types of PHA polymers obtained in bacterial fermentation process grown on, respectively, nonanoic or 5-phenylvaleric acids. The PHA derived acids were further functionalised with a 2,2,2-trifluoroethyl trifluoromethyl sulphate moiety. The virgin mixtures or their modified counterparts were attached to glucose via lipase mediated biocatalytic reaction in a water-free organic solvent systems. The resulting novel SFAEs were purified and characterised, and submitted to antimicrobial studies in order to elucidate their potential antimicrobial characteristics.

2. Results and Discussion

2.1. Synthesis of Polyhydroxyalkanoates

P. putida CA-3 was cultured on 5-phenylpentanoic acid (40 mM) in a shake flask for 5 days, which yielded 2.43 g/L of cell dry weight (CDW) mass with 57% (*w*/*w*) of PHA. The extracted PHA polymer (PHPV) composed of (*R*)-3-hydroxy-5-phenylpentanoic and (*R*)-3-hydroxy-3-phenylpropionic acids in a 94:6 molar ratio. In case of polyhydroxynonanoate (PHN) fermentation, *P. putida* KT244 strain was grown on nonanoic acid and accumulated 71% of the polymer in CDW, while the molar ratio of obtained (*R*)-3-hydroxynonanoic and (*R*)-3-hydroxyheptanoic acid monomers was 7:3.

2.2. Modification of PHA Monomers

The procedure described in Section 3 allowed us to obtain 1.26 g (48.5% conversion) of a pure fraction of desired products (**3,4**) – PHN derived mixture of hydroxyacids methyl esters. Structural analysis (^{1}H NMR, MS) of compounds revealed that 3-OH groups of PHN methyl esters were successfully protected (Figures S4 and S5 in Supplementary Material). Product **10** lost the methyl group during the ionization in MS, therefore it was identified as acid ([M-H]$^-$ 255 *m*/*z*) at retention time (Rt) of 2.3 min. An analogous situation occurred with the shorter protected PHA monomer (product **11**), (227 *m*/*z*, Rt = 1.9 min). Additionally, we observed a fragmentation ion (162.9 *m*/*z*), which, in accordance with the theoretical predictions of the fragmentation of compound **11** (Figure S5 in Supplementary Materials). The remaining chromatography fractions contained either dimers or trimers of **10+11** or

their fluorinated counterparts. Unfortunately all trials for P3HPV derived fatty acid modifications ended without significant results. ^{14}C NMR confirmed that an etheric bond between C–O^- at the 3rd carbon atom of the P3HPV monomer aliphatic chain and trifluorethyl group was created. However purity of the collected fractions was unsatisfying, thus not allowing us from further biocatalytic steps with the mixture of **34+35**. Results of all were gathered and summarized in Table 1.

Table 1. Summary of PHA modifications and their sugar esters synthesis.

Compound Number:	Conversion [%]:
15	100
10,11	48.5
7,8	100
13,14	n.c.
26	42.1 *
27,28	85 *
29,30	n.c.
31	43.3 *
32,33	78.7 *
34,35	n.c.

* Conversions calculated from glucose concentrations.

To the best of our knowledge this is a first report that concerns protection of the hydroxyl group of a PHA monomers without its removal or its substitution by a halogen substituent [24,33–35]. NaH turned out to be an efficient reactant for hydrogen atoms removal of PHN 3-OH groups and their activation for an attack of trifluoroethyl moiety, even though lithium diisopropylamide is a much stronger nucleophil. Most importantly, an extra dry THF as a medium turned out to be the key element of the whole synthetic process.

Conversion of glucose to its corresponding esters (SFAE) via *Thermomyces lanuginosus* lipase (TL-IM) was confirmed by MS/MS analysis (Table 2). Compound **26** was identified as $[M+Cl^-]^-$ adduct 355 *m*/*z* in a scan mode, whereas in Product Ion Scan mode its precursor $[M-H]^-$ ion (319 *m*/*z*) produced fragmentation ion 228.9 *m*/*z* (Figure S6 in Supplementary Materials). PHN glucose esters (**27,28**) - both C9 and C7 were detected as $[M + Cl^-]^-$ ions in the scan mode, where their signals were 371 and 343 *m*/*z* respectively. In Product Ion Scan mode the precursor and fragmentation ions were observed at 335 and 307 *m*/*z*. Compound **27** in Product Ion Scan was characterized by fragmentation signals at 334.7, 172.8, 58.7 *m*/*z*. Such fragmentation was consistent with results of the theoretical analysis of the breakdown of the compound (Figures S7 and S8 in Supplementary Materials). Glucose esters of aromatic compounds have been synthesized with success, as indicated by their spectra in MS analysis. The product **31** was detected as the $[M-H]^-$ ion (339 *m*/*z*). In the case of PHPV sugar esters, only the MS spectrum with (R)-3-hydroxy-5-phenylpentanoic acid (compound **33**) was obtained. The compound was detected in the scan mode as the mass with the chlorine adduct, ($[M+Cl^-]^-$ = 391 *m*/*z*) with retention time of 1.4 min. In Product Ion Scan mode the **33** precursor ion $[M-H]^-$ (355 *m*/*z*) did not fragmented within the range of scanned energy collisions. The yield obtained within our study are comparable to these obtained for acylation of glucose by others [36,37].

2.3. Antimicrobial Testing

The initial microbial experiment showed that MIC (or Minimum bactericidal concentration—MBC) values of both unmodified and modified PHA monomers and their glucose esters are in most cases higher than 500 μg mL^{-1}, which is 50,000 fold higher than commonly used antibiotics (Ciplofloxan, Fluxonazole) [38,39]. Nevertheless, the literature reports and our results show that SFAEs in general have a bacteriostatic effect if present in higher concentrations, which can be used for other than therapeutic purposes (e.g., in the cosmetic or food industries, as surfactants/emulsifiers) [20,21,40,41]. Therefore, we increased the tested concentrations up to 5000 μg mL^{-1} (Table 3).

Table 2. Precursor ions and Product ions of tested compounds in product ion scan mode.

Compound	Precursor Ion (*m*/*z*)	Product Ions (*m*/*z*)	Collision Energies (eV)	Retention Time (min)
1	157	157.1	5	1.6
3	173	173.1, 59	5	1.9
4	145	145.1, 59	5	1.8
5	191	114.8, 190.6	5	1.6
7	207	176.9, 206.9	5	1.6
8	179	n.c	-	-
12	255	255	5	2.3
13	227	226.7, 162.9	5	1.9
26	319	318.5, 228.9	5	1.7
27	335	334.7, 172.8, 58.7	10	1.4
28	307	n.c. *	-	-
29	417	417.1	25	1.6
30	389	n.c	-	-
31	339	338.9	5	1.7
33	356	354.9	5	1.4
32	n.c.	n.d. *	-	-

* n.c.—not confirmed, n.d.—not determined.

The results obtained during this study prove that microorganisms exhibit different sensitivity to antimicrobial agents, which strongly depends on the type of carbohydrate used, length of fatty acids attached to the sugar and moiety linked to the fatty acid part of SFAE. 5-phenylvaleric acid proved to be more effective against the tested bacteria at lower concentrations compared to aliphatic nonanoic acid. The antibacterial action of acids with the phenyl group has been known before—phenylpropionic or phenylacetic acid have a strong antibacterial effect on various types of bacteria such as *S. aureus*, *C. albicans* and *E. coli* at 1000 μg mL^{-1} [42]. The opposite situation was observed in the case of inhibition of *Candida* growth, where nonanoic acid was more effective at 10 times lower concentrations compared to aromatic acids [43]. It has been reported that nonanoic acid could be active against some dermatophytes and non-dermatophyte fungi. Some of other saturated fatty acids (i.e., capric and lauric) have been also reported to possess the inhibitory effect against *Candida* spp. Fungicidal activity of fatty acids could be determined by mechanisms focused on yeast membrane disruption [43]. Sugar fatty acids esters also tend to be biologically beneficial in combating fungi. Their emulsifying properties could be successful implement in detergents and cosmetic production.

PHA monomers with a hydroxyl group at the 3rd carbon atom showed a stronger antibacterial activity (for bacteria strain such as *Staphylococcus aureus* NCTC 4163 and *Bacillus cereus* ATCC *11778)*, when compared to their fatty acids analogues without the 3-OH group. Similar results were obtained by Sandoval and colleagues, who tested the effect of the hydroxyl group on the antibacterial properties of PHA monomers [44]. For other strains tested no improvement of antibacterial activity was observed in the MIC between 5-phenylvaleric acid and PHPV derived monomer mixture. Attachment of the fluorinated moiety to PHN derived monomers did not significantly influenced their biological activity against tested strains.

Table 3. Activity of modified and unmodified PHA monomers and their SFAE against standard bacteria and fungi strains – minimal inhibitory concentrations (MIC, μg mL^{-1}).

Ciprofloxacin/ Fluxonazole	[34,35]	[32,33]	[27,28]	[31]	[26]	[10,11]	[7,8]	[3,4]	[5]	[1]	Compound [ug mL^{-1}]:
4	2500	>5000	2500	5000	5000	2500	2500	1250	1250	2500	*Staphylococcus aureus NCTC 4163*
0.5	5000	>5000	1250	>5000	5000	2500	2500	2500	1250	2500	*Staphylococcus aureus* ATCC 6538
0.5	>5000	>5000	>5000	>5000	5000	2500	2500	2500	1250	2500	*Staphylococcus epidermidis* ATCC 12228
0.5	5000	>5000	1250	>5000	5000	2500	1250	2500	1250	2500	*Staphylococcus epidermidis* RP 62A
0.5	>5000	>5000	>5000	>5000	5000	2500	2500	2500	2500	2500	*Enterococcus hirae ATCC 10541*
0.5	>5000	>5000	>5000	>5000	2500	2500	2500	1250	1250	2500	*Bacillus cereus* ATCC *11778*
0.5	>5000	>5000	>5000	>5000	5000	2500	2500	2500	1250	2500	*Bacillus subtilis* ATCC *6633*
0.5	>5000	>5000	>5000	>5000	>5000	2500	5000	5000	2500	5000	*Escherichia coli* ATCC 25922
0.5	>5000	>5000	>5000	>5000	>5000	5000	5000	5000	2500	5000	*Pseudomonas aeruginosa* ATCC 27853
0.5	>5000	>5000	>5000	>5000	5000	2500	2500	5000	2500	2500	*Salmonella enterica* subsp. f*nterica* CIP 108115
0.5	>5000	>5000	5000	>5000	5000	2500	1250	2500	2500	2500	*Listeria monocytogenes*
0.5	>5000	>5000	>5000	>5000	313	5000	>5000	>5000	625	156	*Candida parapsilosis* ATCC 22019
0.5	>5000	>5000	>5000	>5000	625	5000	>5000	2500	1250	313	*Candida albicans* ATCC 90028
0.5	>5000	>5000	>5000	>5000	625	>5000	>5000	5000	1250	156	*Candida krusei* ATCC 6258
0.5	>5000	>5000	>5000	>5000	1250	5000	>5000	5000	1250	156	*Candida albicans* ATCC 10231

Sugar esters synthetized in this work revealed weak antibacterial to moderate antifungal activities (Table 3). C9-glucose ester (**26**) exhibited the highest antifungal activity of all studied sugar esters (MIC values of 313; 625; 625 μg mL^{-1} for *C. parapsilosis*; *C. albicans ATCC 90028*; *C. crusei ATCC 1023*, respectively). We observed also some antibacterial activity of PHN glucose esters (**27,28**) towards *Staphylococcus* spp. in MIC range of 1250–2500 μg mL^{-1}. When modified with fluorine moiety, the PHN derived esters (**34,35**) retained their antimicrobial activity for *Staphylococcus aureus* NCTC 4163 (MIC 2500 μg mL^{-1}). For other tested pairs (glucose esters vs. tested strain) we did not observe significant antimicrobial action. These findings are in line with reports of others, where glucose or maltose sugar esters (fatty acid carbon atoms n = 8–14) revealed MIC values between 250 to 2000 μg mL^{-1}, when tested against a range of Gram negative and positive strains [10,45].

3. Materials and Methods

3.1. Synthesis of Polyhydroxyalkanoates

Polyhydroxynonanoate (PHN; **2**) was produced with *Pseudomonas putida* KT2440 strain with nonanoic acid (**1**) in the fermentation feed as the sole energy and carbon source (Figure 1A) as described in our previous study [46]. Polyhydroxyphenylvalerate (PHPV; **6**, Figure 1B) was obtained in shake flask cultures with *Pseudomonas putida* CA-3 (50 mL total medium volume in 250 mL Erlenmeyer flasks, 30 °C, 250 rpm, 5 day fed-batch cultivation) in Minimal Salt Medium (containing (g L^{-1}): $Na_2HPO_4{\cdot}12H_2O$, 9.0; KH_2PO_4, 1.5; $MgSO_4{\cdot}7H_2O$, 0.2; NH_4Cl, 1.0; $CaCl_2{\cdot}2H_2O$, 0.02; Fe(III)NH_4-citrate, 0.0012) with sodium phenylvalerate (total 80 mM). Polymers were extracted with ethyl acetate and characterised as described previously [46]. The polymers were degraded to their monomeric units via an acidic methanolysis (15% H_2SO_4 in methanol) to yield hydroxy fatty acid methyl esters according to previously established protocol [34].

3.2. Modification of PHA Monomers

Several methods of the 3-OH PHA methyl esters groups' halogenation were tested. Briefly different fluorinated alkyl iodes (1-fluoro-3-iodopropane; 1,1-difluoro-2-iodoethane; 1,1,1-trifluoro-3-iodopropane), various nucleophiles (sodium hydride (NaH; 60%), lithium diisopropylamide (LDA)) and different media (dimethylformamide (DMF), dichloromethane (DCM), tetrahydrofuran (THF)) were tested. Finally one method was chosen and was as follows. To stirred solution of 2.26 g PHN (**2**; 1 eq. mol) in anhydrous THF (20 mL), NaH (1.2 eq. mol) was added under argon atmosphere. After 30 min 2,2,2 -trifluoroethyl trifluoromethyl sulfate (**9**; 1.2 eq. mol) was added (Figure 1C). The reaction mixture was stirred on ice overnight. After acidification, an extraction in ethyl acetate (Et-Ac)/H_2O was performed. TLC in Ac 1:7 H confirmed that no PHN (**2**) was left in the reaction mixture. Versa flash chromatography purification gave fraction of 1.5 g fluorinated PHN methyl esters (**10,11**) mixture (^{1}H NMR spectra are available in supplementary materials). PHPV modification followed under the same procedure (Figure 1D). After modifications a part of all of the obtained monomers was converted into their acidic forms using *Candida antractica* lipase B (CalB) in water environment (Figure 1F,H). Briefly 300 mg of a given methyl ester was dissolved in 2 mL of dichloromethane. To 5 mL of H_2O, 85 mg of lipase was added. Both mixtures were combined and vigorously shaken (240 rpm, 35°C) overnight. Mixtures were acidified to pH 4 with HCl, and brine was added followed by the addition of 7 mL of ethyl acetate in order to extract (3×) the desired fatty acid.

3.3. SFAE Synthesis

Enzymatic reactions were carried out in water free 2-methyl-2-butanol (2M2B) in 10 mL total volume. Glucose was supplemented to yield 4 mg mL^{-1} (1 eq. mol), whereas methyl nonaoate (**15**) to 11 mg mL^{-1}; PHN methyl esters (**3**, **4**) 9.5 mg mL^{-1}; fluorinated PHN methyl esters (**10,11**) 11.46 mg mL^{-1}; 5-phenylpentanoic methyl esters (**20**) to 8.3 mg mL^{-1}; PHPV methyl esters (**7,8**) 9.02 mg (to 2 eq. mol). A quantity of 100 mg mL^{-1} of molecular sieves (4Å) was added to withdraw the water

formed. Reactions were initiated by addition of 12 mg mL^{-1} of an enzyme (*Thermomyces lanuginosus* lipase herein referred to as TL-IM), with shaking (240 rpm), at 55 °C for 24 h (New Brunswick Scientific Exella E24 Incubator Shaker Series; (Figure 2)) [36,37,47]. Samples were collected at set intervals and were analysed on HPLC-MS system.

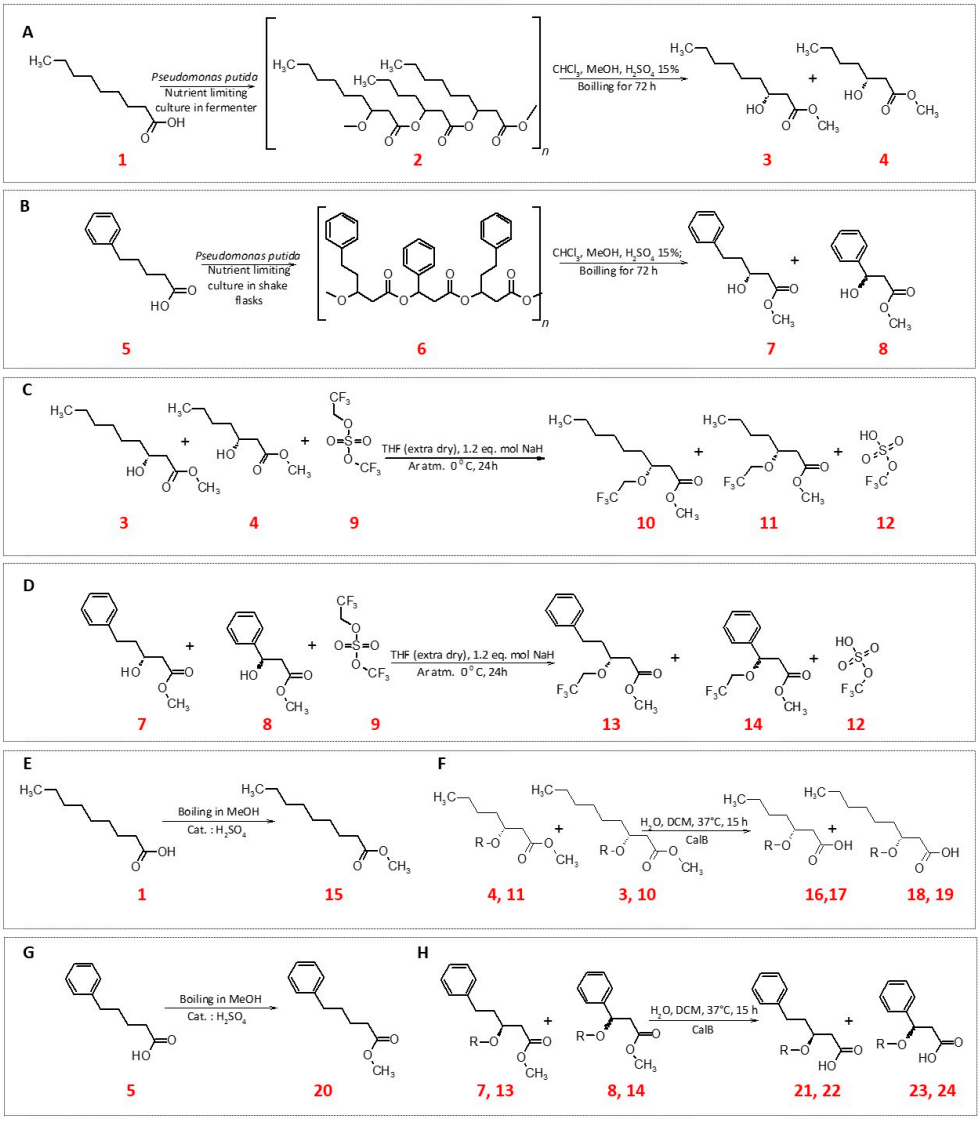

Figure 1. Scheme of synthesis PHA and modifications their monomers (**A**+**B**: PHN synthesis and methanolysis; **C**+**D**: Fluorination of PHN monomers **E**+**G**: methyl ester synthesis; **F**+**H**: demethylation of substrates with CalB); **1.** nonanoic acid; **2.** poly-3-hydroxyhydroxynonaoate; **3.** methyl (3R)-3-hydroxynonanoate; **4.** methyl (3R)-3-hydroxyheptanoate; **5.** 5-phenylpentanoic acid; **6.** poly-3-hydroxypentanoate; **7.** methyl (3R)-3-hydroxy-5-phenylpentanoate; **8.** methyl (3R)-3-hydroxy-3-phenylpropanoate; **9.** 2,2,2-trifluoroethyl trifluoromethyl sulfate; **10.** methyl (3R)-3-(2,2,2-trifluoroethoxy)nonanoate; **11.** methyl (3R)-3-(2,2,2-trifluoroethoxy)heptanoate; **12**. trifluoromethyl hydrogen sulfate; **13.** methyl (3R)-5-phenyl-3-(2,2,2-trifluoroethoxy)pentanoate; **14**. methyl 3-phenyl-3-(2,2,2-trifluoroethoxy)propanoate; **15.** methyl nonanoate; **16**. (R)-3-hydroxyheptanoic acid; **17.** 3-(2,2,2-trifluoroethoxy)heptanoic acid; **18.** (R)-3-hydroxynonanoic acid; **19.** 3-(2,2,2-trifluoroethoxy)nonanoic acid; **20.** methyl 5-phenylpentanoate; **21**. (R)-3-hydroxy-5-phenylpentanoic acid; **22**. 5-phenyl-3-(2,2,2-trifluoroethoxy)pentanoic acid; **23**. (R)-3-hydroxy-3-phenylpropanoic acid; **24**. 3-phenyl-3-(2,2,2-trifluoroethoxy)propanoic acid.

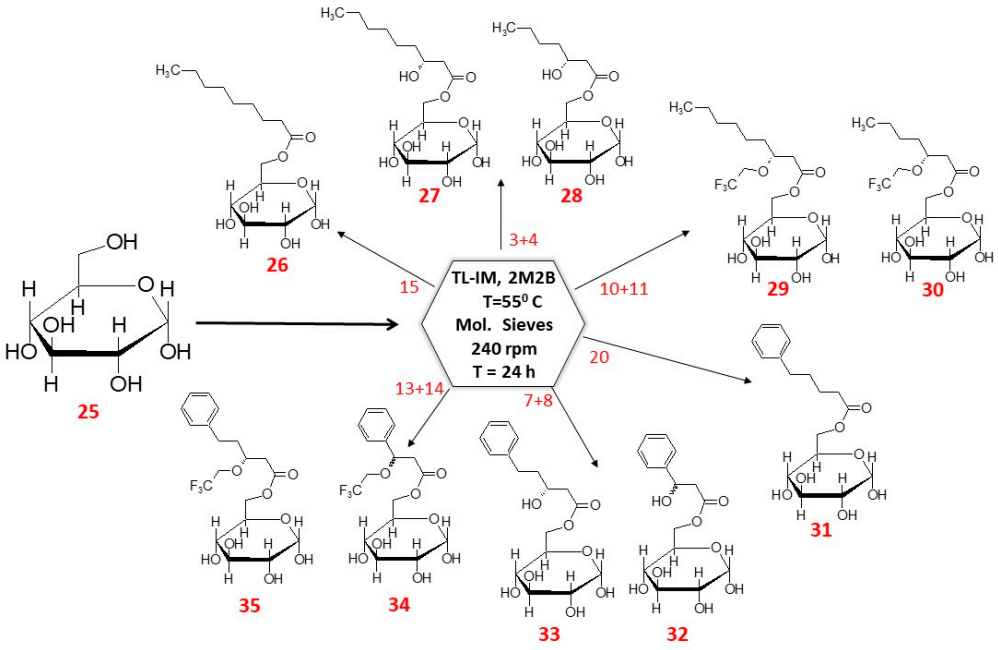

Figure 2. Scheme of synthesis SFAE. 25. Glucose [(2*S*,5*S*)-6-(hydroxymethyl) oxane-2,3,4,5-tetrol]; **26.** [(3*S*,6*S*)-3,4,5,6- tetrahydroxyoxan-2-yl] methyl nonanoate]; **27.** [(3*S*,6*S*)-3,4,5,6-tetrahydroxyoxan-2-yl] methyl (3*R*)-3-hydroxynanonoate; **28.** [(3*S*,6*S*)-3,4,5,6-tetrahydroxyoxan-2-yl] methyl (3*R*) -3-hydroxyheptanoate; **29.** [(3*S*,6*S*)-3,4,5,6-tetrahydroxyoxan-2-yl] methyl(3*R*)-3-(2,2,2-trifluoroethoxy) nonanoate; **30.** [(3*S*,6*S*)-3,4,5,6-tetrahydroxyoxan-2-yl] methyl (3*R*)-3-(2,2,2-trifluoroethoxy) heptanoate; **31.** [(3*S*,6*S*)-3,4,5,6-tetrahydroxyoxan-2-yl] methyl 5-phenylpentanoate; **32.** [(3*S*,6*S*)-3,4,5,6-tetrahydroxyoxan-2-yl]methyl (3*R*) -3-hydroxy-3-phenylpropanoate; **33.** [(3*S*,6*S*)-3,4,5,6-tetrahydroxyoxan-2-yl] methyl (3*R*)-3-hydroxy-5-phenylpentanoate; **34.** [(3*S*,6*S*)-3,4,5,6-tetrahydroxyoxan-2-yl] methyl (3*R*)-3-phenyl-3-(2,2,2-trifluoroethoxy) propanoate; **35.** [(3*S*,6*S*)-3,4,5,6-tetrahydroxyoxan-2-yl] methyl (3*R*) -3-phenyl-3-(2,2,2-trifluoroethoxy) pentanoate.

3.4. LC-MS

The analyses were performed by UHPLC measurements on Agilent 1290 Infinity System with automatic autosampler and MS Agilent 6460 Triple Quad Detector (Santa Clara, CA, USA) equipped with Agilent Zorbax Eclipse Plus C18 column (2.1 × 50 mm, 1.8 µm). Separations were conducted at 30 °C at in a gradient of water (A) and methanol (B) according to the eluent program 0.00 min (95% A/5% B) to 1.00 min (100% B) to 3.51 min (95% A/5% B) to 4.50 min (95% A/5% B) using a flow rate of 0.4 mL min^{-1}. The 5 µl injections of samples were applied in duplicates. An MS Agilent 6460 Triple Quad tandem mass spectrometer with an Agilent Jet Stream ESI interface was used in negative ion polarization using either the Scan (MS2 scan) or Product Ion Scan modes. The optimum collision energy was 5 eV for all of the products. Nitrogen at a flow rate of 10 L min^{-1} was used as the drying gas and for collision-activated dissociation. The drying gas and sheath gas temperatures were set to 350 °C. The capillary voltage was set to 3500 V, whereas the nozzle voltage was set to 500 V. All compounds were monitored in scan and product ion modes with different collision energies (5–30 eV) (*m*/*z* values of products in the Table 2). MassHunter software (Version B.05.00, Agilent, Santa Clara, CA, USA) was used for HPLC-MS system control, data acquisition, and data processing.

3.5. Antimicrobial Testing

The studies of antimicrobial activity were conducted for modified and non-modified PHA monomers (acids) and their SFAE derivatives using clinical and reference strains of bacteria and yeast-like fungi from international microbe collections: ATCC (American Type Culture Collection), NCTC (National Collection of Type Culture) and CIP (The Collection de l'Institut Pasteur). Among

reference strains, there were seven Gram-positive bacteria (*Staphylococcus aureus* NCTC 4163, *S. aureus* ATCC 6538, *S. epidermidis* ATCC 12228, *S. epidermidis* ATCC 35984, *Enterococcus hirae* ATCC 10541, *Bacillus cereus* ATCC 17778 and *B. subtilis* ATCC 6633) and four Gram-negative bacteria (*Pseudomonas aeruginosa* ATCC 27853, *Escherichia coli* ATCC 25922, *Salmonella enterica* subsp. *enterica* CIP 108115 and clinical isolate of *Listeria monocytogenes*). The yeast-like fungi used in this study were *Candida* spp. (*C. parapsilosis* ATCC 22019, *C. krusei* ATCC 6258, *C. albicans* ATCC 90028 and *C. albicans* ATCC 10231). Compounds antimicrobial activity was expressed as minimum inhibitory concentration (MIC) according to The European Committee on Antimicrobial Susceptibility Testing (EUCAST) and The Clinical & Laboratory Standards Institute (CLSI) reference procedures with some modification. MIC was tested by the twofold serial microdilution method (in 96-well microtiter plates) on MH II liquid medium for bacteria or RPMI- 1640 medium for *Candida* species. The final inoculum of all studies bacteria was $10^{6\circ}$ CFU/mL (colony forming unit per mL) and 5×10^4 to 2.5×10^5 CFU mL^{-1} for yeast. The stock solutions of tested compounds were prepared in DMSO and diluted in sterile medium (to maximum 3% of solvent content). The concentrations of compounds were from 78 to 5000 μg mL^{-1}. The MIC value was the lowest concentration of the researched compound at which bacteria growth was no longer observed after 18 h. Yeast growth was evaluated by absorbance measurement at 530 nm after at least 24 h of incubation. The MIC was defined as a 50% or more reduction in growth compared to the control well [38,48]. As controls, two antimicrobial compounds were used: ciprofloxacin (antibacterial) and fluxonazole (antifungal).

4. Conclusions

This work provides an insight into synthesis of novel range of compounds derived from bacterial polyesters – polyhydroxyalkanoates. Firstly, we have established a methodology for protection of hydroxyl group of PHA derived monomers by introducing a fluorinated moiety via an etheric bond. Secondly, we developed a protocol for biocatalytic acylation of glucose with these bacterially derived fatty acids. Further in the study we have tested antimicrobial potential of these unmodified and modified PHA derivatives. The obtained compounds revealed moderate antibacterial and antifungal activities. Further research is needed in order to increase the antimicrobial activity of either PHA monomers or their sugar esters by introduction of other bioactive structural components to their moieties.

Supplementary Materials: The following are available online at http://www.mdpi.com/2073-4344/9/6/510/s1.

Author Contributions: Conceptualization, M.G.; Data curation, J.S.; Formal analysis, W.S.; Investigation, W.S., K.S. and J.P.; Supervision, J.S., M.S. and M.G.; Visualization, J.P.; Writing—original draft, W.S., K.S. and J.P.; Writing—review & editing, J.S., M.S. and M.G.

Funding: This work was supported by the National Science Centre, Poland [grant SONATA no. 2015/17/D/ST4/00514]. JP and WS acknowledge the support of InterDokMed project no. POWR.03.02.00-00-I013/16. We greatly acknowledge the joint consortium "Interdisciplinary Centre of Physical, Chemical and Biological Sciences" of ICSC PAS and INP PAS for providing access to the Agilent 1290 Infinity System with an automatic autosampler and an MS Agilent 6460 Triple Quad Detector. The research on antimicrobial activity was carried out with the use of CePT infrastructure financed by the European Union—the European Regional Development Fund within the Operational Programme "Innovative economy" for 2007–2013.

Conflicts of Interest: The authors declare no conflicts of interest.

References

1. Staroń, J.; Dąbrowski, J.M.; Cichoń, E.; Guzik, M. Lactose esters: Synthesis and biotechnological applications. *Crit. Rev. Biotechnol.* **2018**, *38*, 245–258. [CrossRef] [PubMed]
2. Hidayat, C.; Fitria, K.; Hastuti, P. Enzymatic synthesis of bio-surfactant fructose oleic ester using immobilized lipase on modified hydrophobic matrix in fluidized bed reactor. *Agric. Agric. Sci. Procedia* **2016**, *9*, 353–362. [CrossRef]

3. Jeromin, G.E.; Zoor, A.; Stergiou, P.-Y.; Foukis, A.; Filippou, M.; Koukouritaki, M.; Parapouli, M.; Theodorou, L.G.; Hatziloukas, E.; Afendra, A.; et al. Enzymatic esterification of tapioca maltodextrin fatty acid ester. *Carbohydr. Polym.* **2001**, *99*, 2079–2090.
4. Maag, H. Fatty acid derivatives: Important surfactants for household, cosmetic and industrial purposes. *J. Am. Oil Chem. Soc.* **1984**, *61*, 259–267. [CrossRef]
5. Hill, K.; Rhode, O. Sugar-based surfactants for consumer products and technical applications. *Lipid/Fett* **1999**, *101*, 25–33. [CrossRef]
6. Neta, N.D.A.S.; Santos, J.C.S.D.; Sancho, S.D.O.; Rodrigues, S.; Gonçalves, L.R.B.; Rodrigues, L.R.; Teixeira, J.A. Enzymatic synthesis of sugar esters and their potential as surface-active stabilizers of coconut milk emulsions. *Food Hydrocoll.* **2012**, *27*, 324–331. [CrossRef]
7. Zhao, T.-H.; Gu, J.-Y.; Pu, W.-F.; Dong, Z.-M.; Liu, R. Study on the synthesis and properties of an eco-friendly sugar-based anionic–nonionic surfactant. *RSC Adv.* **2016**, *6*, 70165–70173. [CrossRef]
8. El-Laithy, H.M.; Shoukry, O.; Mahran, L.G. Novel sugar esters proniosomes for transdermal delivery of vinpocetine: Preclinical and clinical studies. *Eur. J. Pharm. Biopharm.* **2011**, *77*, 43–55. [CrossRef]
9. Szuts, A.; Szabó-Révész, P. Sucrose esters as natural surfactants in drug delivery systems—A mini-review. *Int. J. Pharm.* **2012**, *433*, 1–9. [CrossRef]
10. Zhao, L.; Zhang, H.; Hao, T.; Li, S. In vitro antibacterial activities and mechanism of sugar fatty acid esters against five food-related bacteria. *Food Chem.* **2015**, *187*, 370–377. [CrossRef]
11. Xiao, D.; Ye, R.; Davidson, P.M.; Hayes, D.G.; Golden, D.A.; Zhong, Q. Sucrose monolaurate improves the efficacy of sodium hypochlorite against escherichia coli O157: H7 on spinach. *Int. J. Food Microbiol.* **2011**, *145*, 64–68. [CrossRef] [PubMed]
12. Ferla, B.L.; Lay, L.; Poletti, L.; Russo, G.; Panza, L. Easy chemo-enzymatic synthesis of human milk trisaccharides from a common selectively protected lactose building block. *J. Carbohydr. Chem.* **2000**, *19*, 331–343. [CrossRef]
13. Rencurosi, A.; Poletti, L.; Panza, L.; Lay, L. Improvement on lipase catalysed regioselective O-acylation of lactose: A convenient route to 2-O-fucosyllactose. *J. Carbohydr. Chem.* **2001**, *20*, 761–765. [CrossRef]
14. Desbois, A.P. Potential applications of antimicrobial fatty acids in medicine, agriculture and other industries. *Recent Pat. Antiinfect. Drug Discov.* **2012**, *7*, 111–122. [CrossRef] [PubMed]
15. Karlova, T.; Poláková, L.; Šmidrkal, J.; Filip, V. Antimicrobial effects of fatty acid fructose esters. *Czech J. Food Sci.* **2010**, *28*, 146–149. [CrossRef]
16. Das, B.; Sarkar, S.; Sarkar, A.; Bhattacharjee, S.; Bhattacharjee, C. Recovery of whey proteins and lactose from dairy waste: A step towards green waste management. *Process Saf. Environ. Prot.* **2016**, *101*, 27–33. [CrossRef]
17. Huang, C.B.; George, B.; Ebersole, J.L. Antimicrobial activity of n-6, n-7 and n-9 fatty acids and their esters for oral microorganisms. *Arch. Oral Biol.* **2010**, *55*, 555–560. [CrossRef]
18. Blanchfield, J.; Toth, I. Lipid, Sugar and Liposaccharide based delivery systems 2. *Curr. Med. Chem.* **2012**, *11*, 2375–2382. [CrossRef]
19. Zheng, C.J.; Yoo, J.S.; Lee, T.G.; Cho, H.Y.; Kim, Y.H.; Kim, W.G. Fatty acid synthesis is a target for antibacterial activity of unsaturated fatty acids. *FEBS Lett.* **2005**, *579*, 5157–5162. [CrossRef]
20. Smith, A.; Nobmann, P.; Henehan, G.; Bourke, P.; Dunne, J. Synthesis and antimicrobial evaluation of carbohydrate and polyhydroxylated non-carbohydrate fatty acid ester and ether derivatives. *Carbohydr. Res.* **2008**, *343*, 2557–2566. [CrossRef]
21. Watanabe, T.; Katayama, S.; Matsubara, M.; Honda, Y.; Kuwahara, M. Antibacterial carbohydrate monoesters suppressing cell growth of streptococcus mutans in the presence of sucrose. *Curr. Microbiol.* **2000**, *41*, 210–213. [CrossRef] [PubMed]
22. Galbraith, H.; Miller, T.B. Effect of metal cations and PH on the antibacterial activity and uptake of long chain fatty acids. *J. Appl. Bacteriol.* **1973**, *36*, 635–646. [CrossRef] [PubMed]
23. Fernandez-Lorente, G.; Palomo, J.M.; Cocca, J.; Mateo, C.; Moro, P.; Terreni, M.; Fernandez-Lafuente, R.; Guisan, J.M. Regio-selective deprotection of peracetylated sugars via lipase hydrolysis. *Tetrahedron* **2003**, *59*, 5705–5711. [CrossRef]
24. Dembitsky, V.M.; Srebnik, M. Natural halogenated fatty acids: Their analogues and derivatives. *Prog. Lipid Res.* **2002**, *41*, 315–367. [CrossRef]

25. Andreu, C.; Marcel, Æ.; Varea, T.; Diaz, D.; Asensio, G. The introduction of fluorine atoms or trifluoromethyl groups in short cationic peptides enhances their antimicrobial activity. *Bioorgan. Med. Chem.* **2006**, *14*, 6971–6978.
26. Hiyama, T.; Yamamoto, H. Biologically active organofluorine compounds. In *Organofluorine Compounds*; Springer: Berlin/Heidelberg, Germany, 2012; pp. 137–182.
27. Isanbor, C.; Hagan, D.O. Fluorine in medicinal chemistry: A review of anti-cancer agents §. *J. Fluor. Chem.* **2006**, *127*, 303–319. [CrossRef]
28. Cheeseman, K.H.; Albano, E.F.; Tomasi, A.; Slater, T.F. Biochemical studies on the metabolic activation of halogenated alkanes. *Environ. Health Perspect.* **1985**, *64*, 85–101. [CrossRef]
29. Belli, W.A.; Buckley, D.H.; Marquis, R.E. Weak acid effects and fluoride inhibition of glycolysis by streptococcus mutans GS-5. *Can. J. Microbiol.* **1992**, *41*, 785–791. [CrossRef]
30. Suriyamongkol, P.; Weselake, R.; Narine, S.; Moloney, M.; Shah, S. Biotechnological approaches for the production of polyhydroxyalkanoates in microorganisms and plants—A review. *Biotechnol. Adv.* **2007**, *25*, 148–175. [CrossRef]
31. Abe, H.; Doi, Y. Side-Chain effect of second monomer units on crystalline morphology thermal properties and enzymatic degradability for random copolyesters of (R) -3-hydroxybutyric acid with (R) -3-hydroxyalkanoic acids. *Biomacromolecules* **2002**, *3*, 133–138. [CrossRef]
32. Madison, L.; Huisman, G. Metabolic engineering of poly(3-hydroxyalkanoates): From DNA to plastic. *Microbiol. Mol. Biol. Rev.* **1999**, *63*, 21–53. [PubMed]
33. O'Connor, S.; Szwej, E.; Nikodinovic-Runic, J.; O'Connor, A.; Byrne, A.T.; Devocelle, M.; O'Donovan, N.; Gallagher, W.M.; Babu, R.; Kenny, S.T.; et al. The anti-cancer activity of a cationic anti-microbial peptide derived from monomers of polyhydroxyalkanoate. *Biomaterials* **2013**, *34*, 2710–2718. [CrossRef] [PubMed]
34. Radivojevic, J.; Skaro, S.; Senerovic, L.; Vasiljevic, B.; Guzik, M.; Kenny, S.T.; Maslak, V.; Nikodinovic-Runic, J.; O'Connor, K.E.; O'Connor, K. Polyhydroxyalkanoate-based 3-hydroxyoctanoic acid and its derivatives as a platform of bioactive compounds. *Appl. Microbiol. Biotechnol.* **2015**, *100*, 161–172. [CrossRef] [PubMed]
35. Constantin, M.; Simionescu, C.I.; Carpov, A.; Samain, E.; Driguez, H. Chemical modification of poly (hydroxyalkanoates). Copolymers bearing pendant sugars. *Macromol. Rapid Commun.* **1999**, *94*, 91–94. [CrossRef]
36. Walsh, M.K.; Bombyk, R.A.; Wagh, A.; Bingham, A.; Berreau, L.M. Synthesis of lactose monolaurate as influenced by various lipases and solvents. *J. Mol. Catal. B Enzym.* **2009**, *60*, 171–177. [CrossRef]
37. Plou, F.J.; Cruces, M.A.; Ferrer, M.; Fuentes, G.; Pastor, E.; Bernabé, M.; Christensen, M.; Comelles, F.; Parra, J.L.; Ballesteros, A. Enzymatic acylation of di- and trisaccharides with fatty acids: Choosing the appropriate enzyme, support and solvent. *J. Biotechnol.* **2002**, *96*, 55–66. [CrossRef]
38. Clinical and Laboratory Standards Institute (CLSI); Weinstein, M.P. *Methods for Dilution Antimicrobial Susceptibility Tests for Bacteria That Grow Aerobically*, 9th ed.; Clinical and Laboratory Standards Institute: Wayne, NY, USA, 2012.
39. Kümmerer, K. Antibiotics in the aquatic environment—A. review—Part I. *Chemosphere* **2009**, *75*, 417–434. [CrossRef]
40. Wagh, A.; Walsh, M.K.; Martini, S. Effect of lactose monolaurate and high intensity ultrasound on crystallization behavior of anhydrous milk fat. *J. Am. Oil Chem. Soc.* **2012**, *90*, 977–987. [CrossRef]
41. Lucarini, S.; Fagioli, L.; Campana, R.; Cole, H.; Duranti, A.; Baffone, W.; Vllasaliu, D.; Casettari, L. Unsaturated fatty acids lactose esters: cytotoxicity, permeability enhancement and antimicrobial activity. *Eur. J. Pharm. Biopharm.* **2016**, *107*, 88–96. [CrossRef]
42. Bills, G.; Cueva, C.; Moreno-arribas, M.V.; Martı, P.J.; Vicente, M.F.; Basilio, A.; Rodrı, J.M. Antimicrobial activity of phenolic acids against commensal, probiotic and pathogenic bacteria. *Res. Microbiol.* **2010**, *161*, 372–382.
43. Pohl, C.H.; Kock, J.L.F.; Thibane, V.S. Antifungal free fatty acids: A review antifungal free fatty acids: A review. *Sci. Microb. Pathog. Curr. Res. Technol. Adv.* **2011**, *1*, 61–71.
44. Sandoval, Á.; Arias-Barrau, E.; Bermejo, F.; Cañedo, L.; Naharro, G.; Olivera, E.R.; Luengo, J.M. Production of 3-hydroxy-n-phenylalkanoic acids by a genetically engineered strain of Pseudomonas putida. *Appl. Microbiol. Biotechnol.* **2005**, *67*, 97–105. [CrossRef] [PubMed]

45. Ferrer, M.; Soliveri, J.; Plou, F.J.; López-Cortés, N.; Reyes-Duarte, D.; Christensen, M.; Copa-Patiño, J.L.; Ballesteros, A. Synthesis of sugar esters in solvent mixtures by lipases from Thermomyces lanuginosus and Candida antarctica B, and their antimicrobial properties. *Enzyme Microb. Technol.* **2005**, *36*, 391–398. [CrossRef]
46. Sofińska, K.; Barbasz, J.; Witko, T.; Dryzek, J.; Haraźna, K.; Witko, M.; Kryściak-Czerwenka, J.; Guzik, M. Structural, Topographical, and Mechanical characteristics of purified polyhydroxyoctanoate polymer. *J. Appl. Polym. Sci.* **2019**, *136*, 47192. [CrossRef]
47. Siebenhaller, S.; Gentes, J.; Infantes, A.; Muhle-Goll, C.; Kirschhöfer, F.; Brenner-Weiß, G.; Ochsenreither, K.; Syldatk, C. Lipase-Catalyzed Synthesis of Sugar Esters in Honey and Agave Syrup. *Front. Chem.* **2018**, *6*, 1–9. [CrossRef]
48. Arendrup, M.C.; Meletiadis, J.; Mouton, J.W.; Lagrou, K.; Hamal, P.; Guinea, J. Subcommittee on Antifungal Susceptibility Testing of the ESCMID European Committee for Antimicrobial Susceptibility Testing. 2017 EUCAST Definitive Document E.DEF 9.3.1: Method for the Determination of Broth Dilution Minimum Inhibitory Concentrations of Antifungal Agents for Conidia Forming Moulds. Available online: http://www.eucast.org/fileadmin/src/media/PDFs/EUCAST_files/AFST/Files/EUCAST_E_Def_9_3_1_Mould_testing__definitive.pdf (accessed on 25 April 2019).

Supplementary information

Title: *"Influence of chemical modifications of sugar fatty acid esters on their antimicrobial properties"*

Authors: *Wojciech Snoch[1], Karolina Stępień[2], Justyna Prajsnar[1], Jakub Staroń[3], Maciej Szaleniec[1], Maciej Guzik[1]*

[1]Jerzy Haber Institute of Catalysis and Surface Chemistry, Polish Academy of Sciences, Niezapominajek 8, 30 239 Kraków, Poland
[2]Medical University of Warsaw, Department of Pharmaceutical Microbiology, 3 Oczki Str. 02-007 Warsaw, Poland
[3]Institute of Pharmacology, Polish Academy of Sciences, Smętna 12, 31-343 Kraków, Poland
* Correspondence: ncguzik@cyfronet.pl, Tel.: +48 12 6395 155

Figure S1. Nonanoic acid (**1**)

Scan mode: m/z = 157 [M-H]$^-$

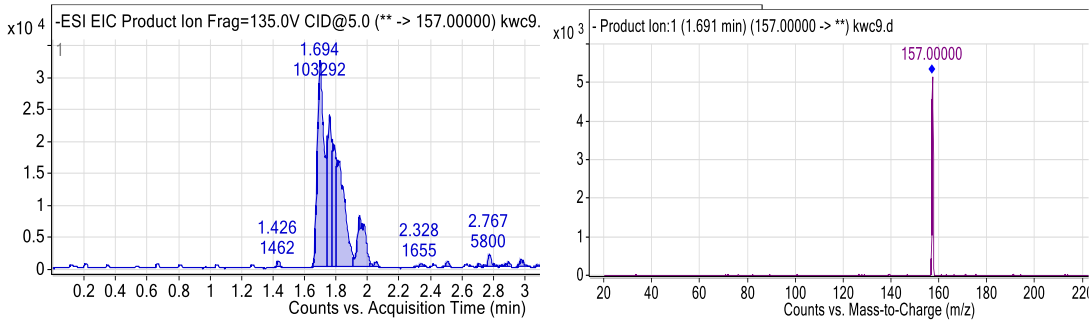

Product ion scan mode: m/z = 157 [M-H]$^-$

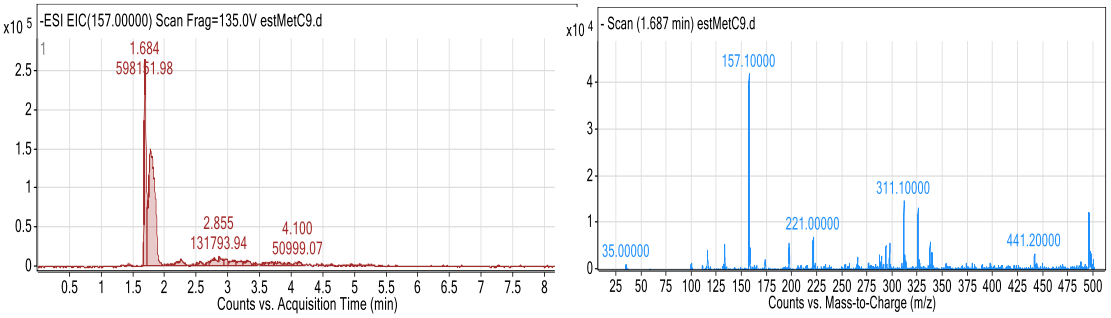

Figure S2. Methyl (3*R*)-3-hydroxynonanoate (**3**):

Scan mode: m/z = 173 [M-H]$^-$

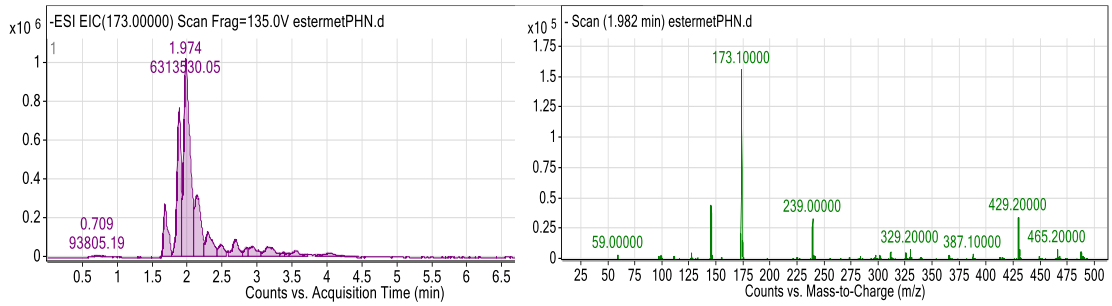

Product ion scan mode: m/z = 173 $[M-H]^-$

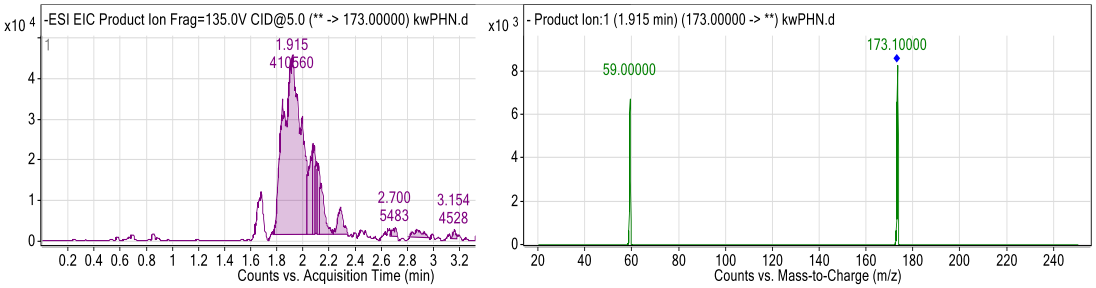

^{1}HNMR of PHN methyl ester spectrum:

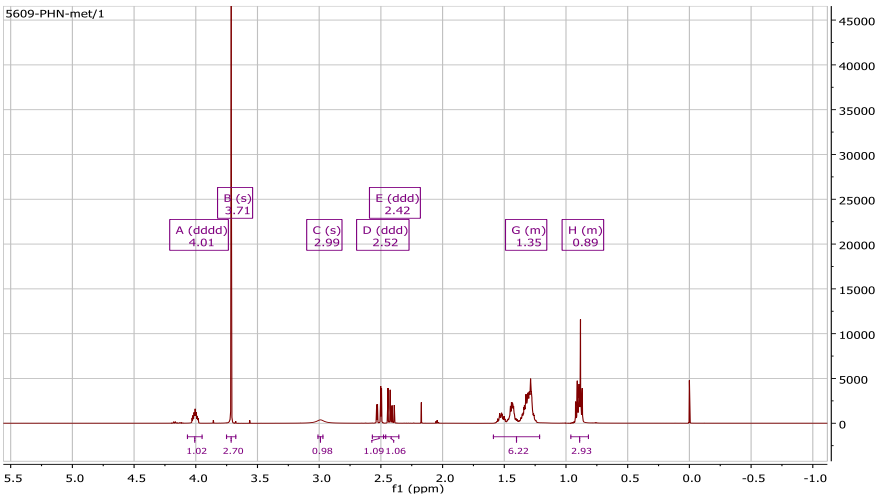

Predicted ^{1}HNMR of PHN methyl ester spectrum:

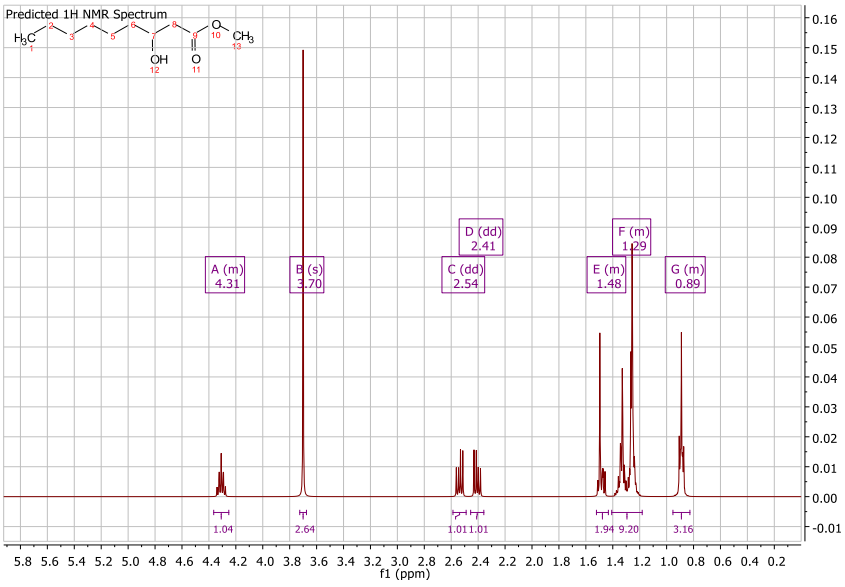

Zoom in spectra of proton localized at C7 (experiment):

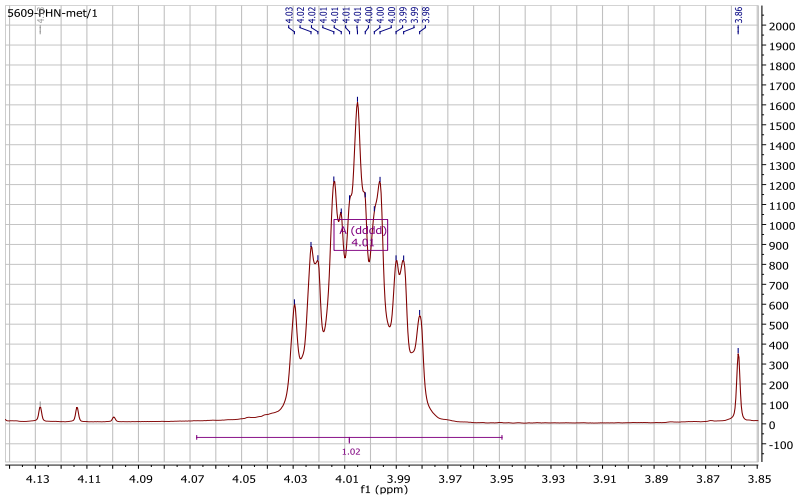

Zoom in spectra of proton localized at C7 (prediction):

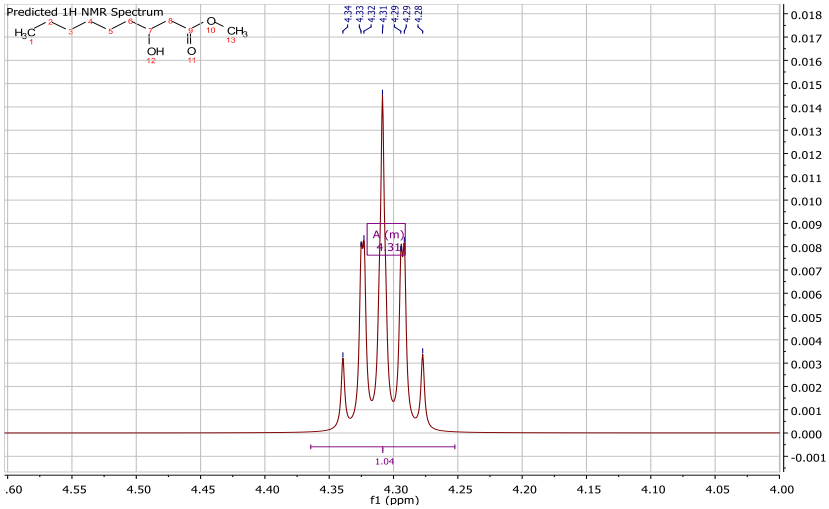

Figure S3. Methyl (3*R*)-3-hydroxyheptanoate (**4**)

Scan mode: m/z = 145 [M-H]$^-$

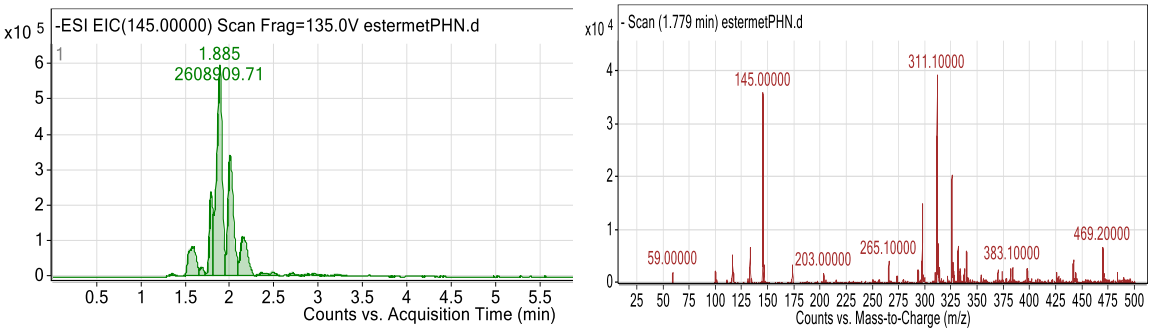

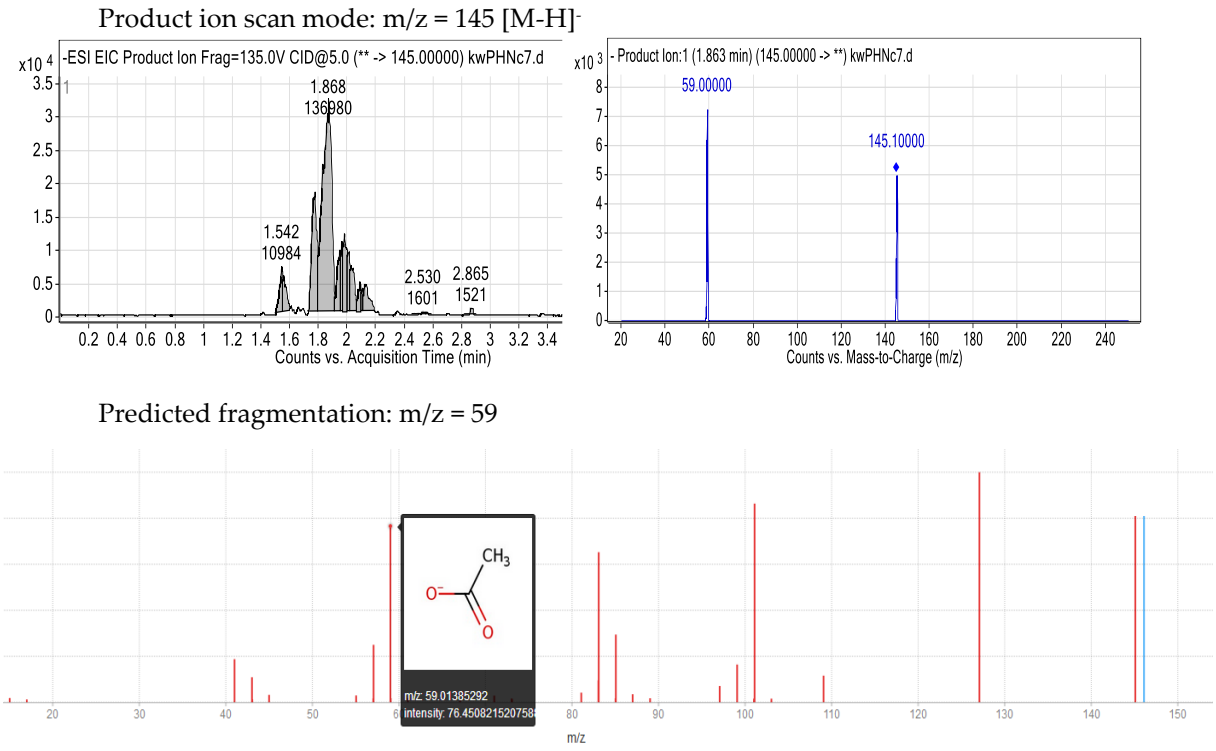

Figure S4. Methyl (3*R*)-3-(2,2,2-trifluoroethoxy)nonanoate (**10**)

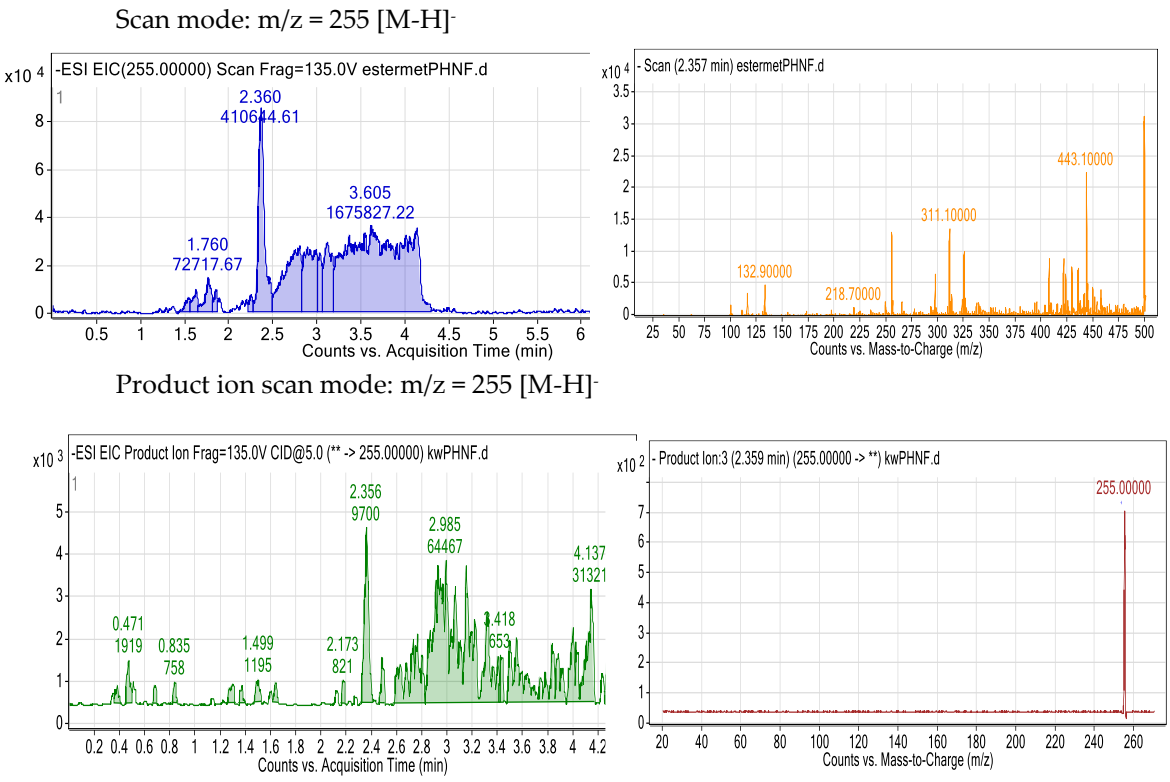

[1]HNMR spectrum of PHN-O-CH2-CF3;

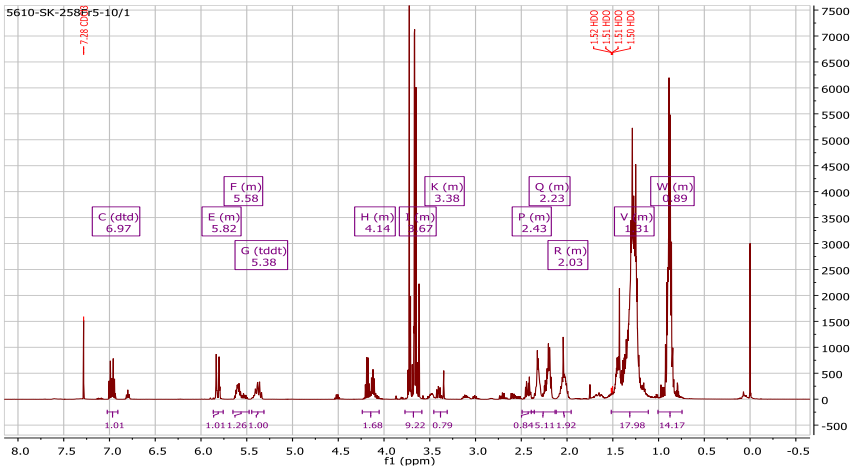

Prediction of [1]HNMR spectrum of PHN-O-CH2-CF3:

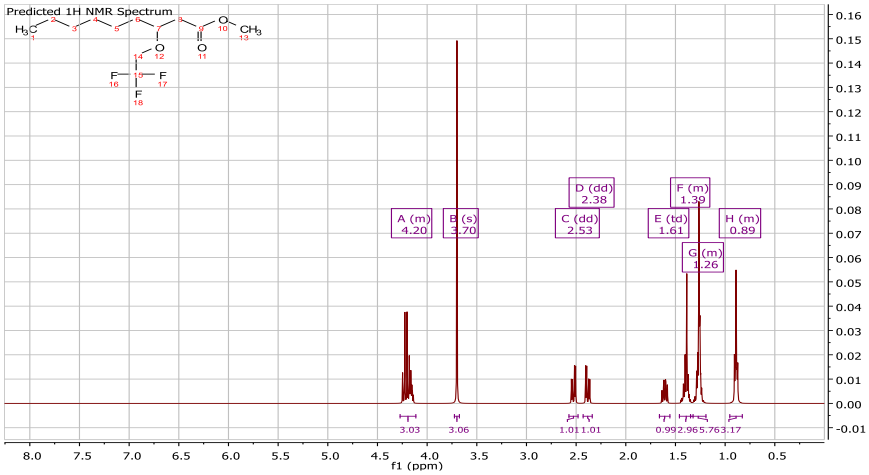

Zoom in protons localized at C7 and protons from –O- Ch2-CF3 (prediction):

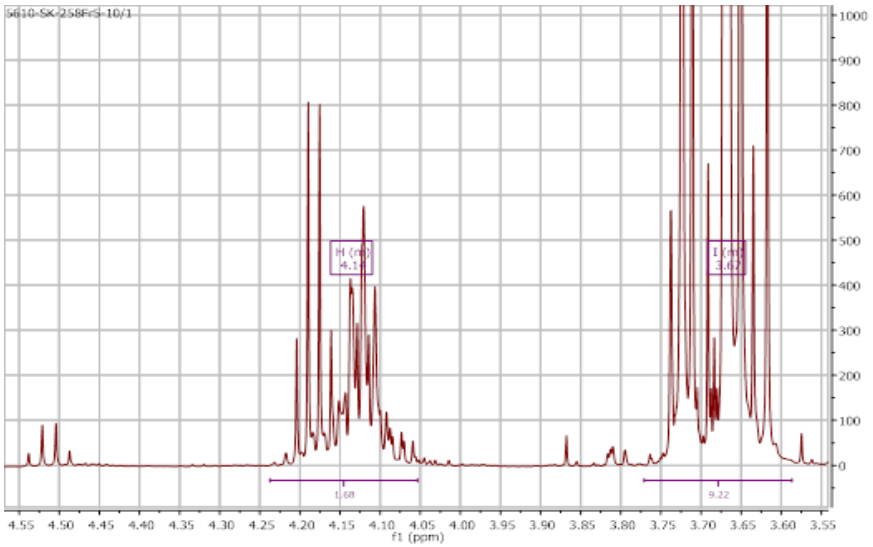

Zoom in protons localized at C7 and protons from –O-Ch2-CF3 (experiment):

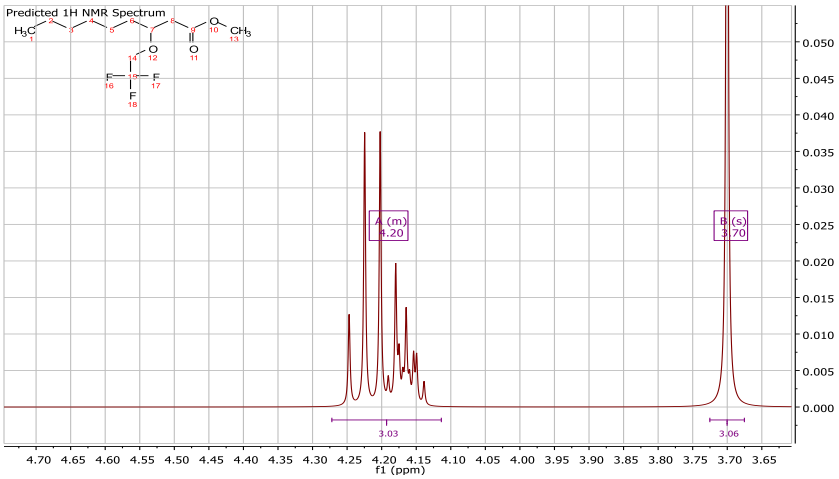

Figure S5. Methyl (3*R*)-3-(2,2,2-trifluoroethoxy)heptanoate (**11**)

Scan mode: m/z = 227 [M-H]$^-$

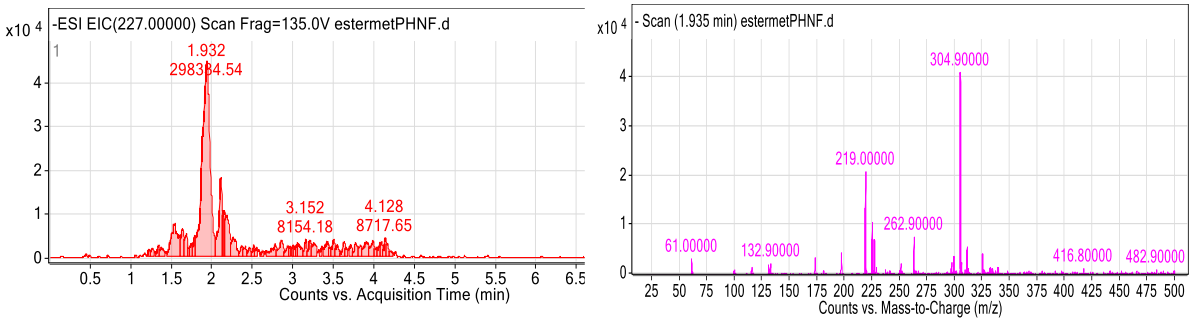

Product ion scan mode: m/z = 227 [M-H]$^-$

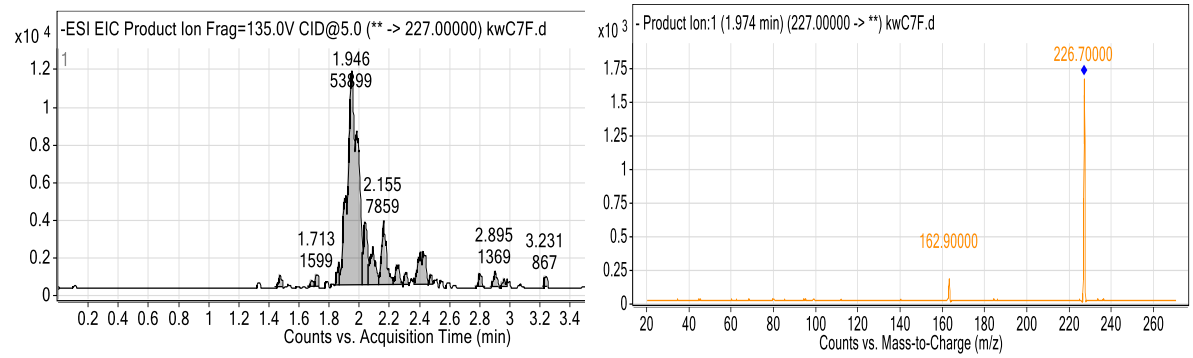

Predicted fragmentation: m/z = 163

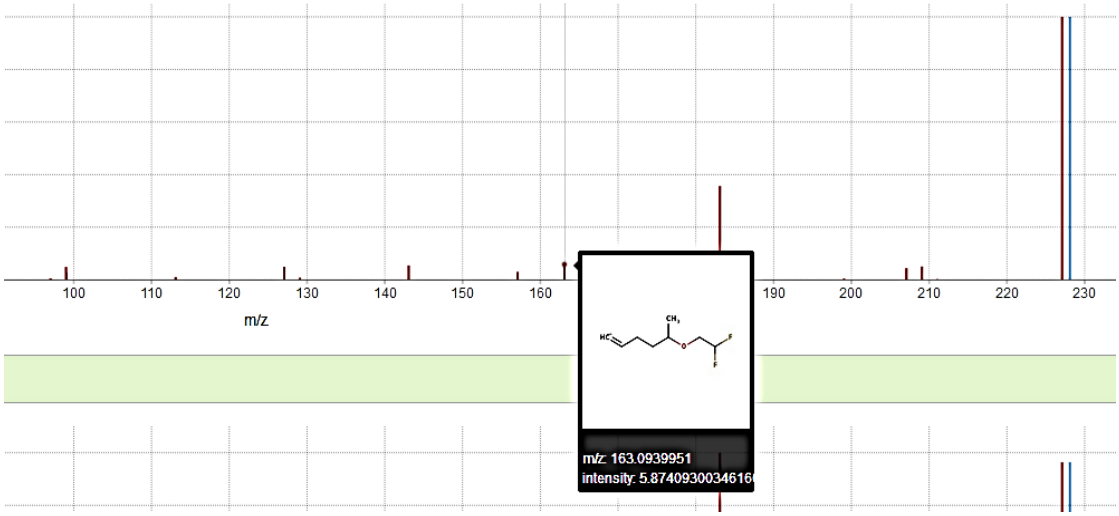

Figure S6. [(3*S*,6*S*)-3,4,5,6-tetrahydroxyoxan-2-yl]methyl nonanoate (**26**)

Scan mode: m/z = 355 [M+Cl$^-$]$^-$

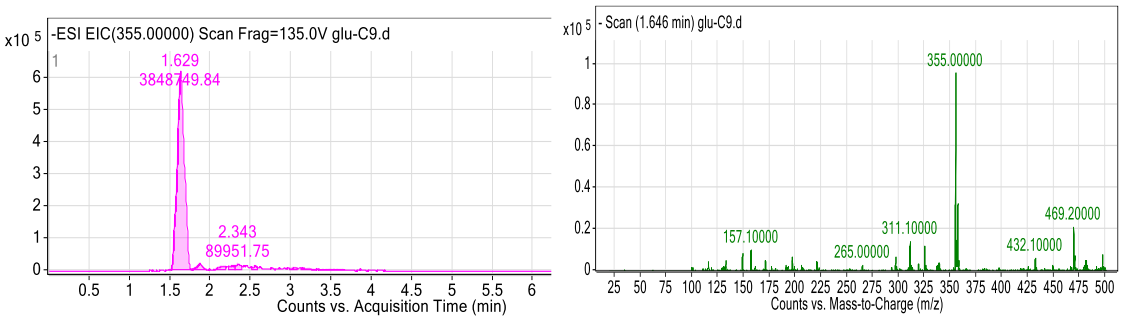

Product ion scan mode: m/z =319 [M-H]$^-$

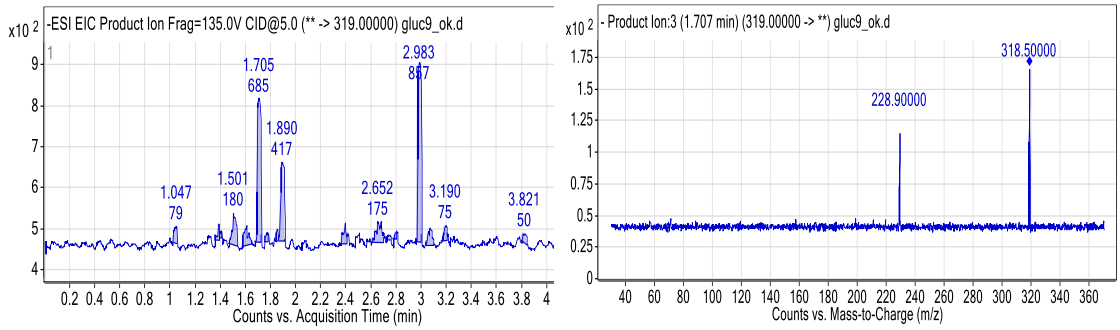

Predicted fragmentation: m/z= 229

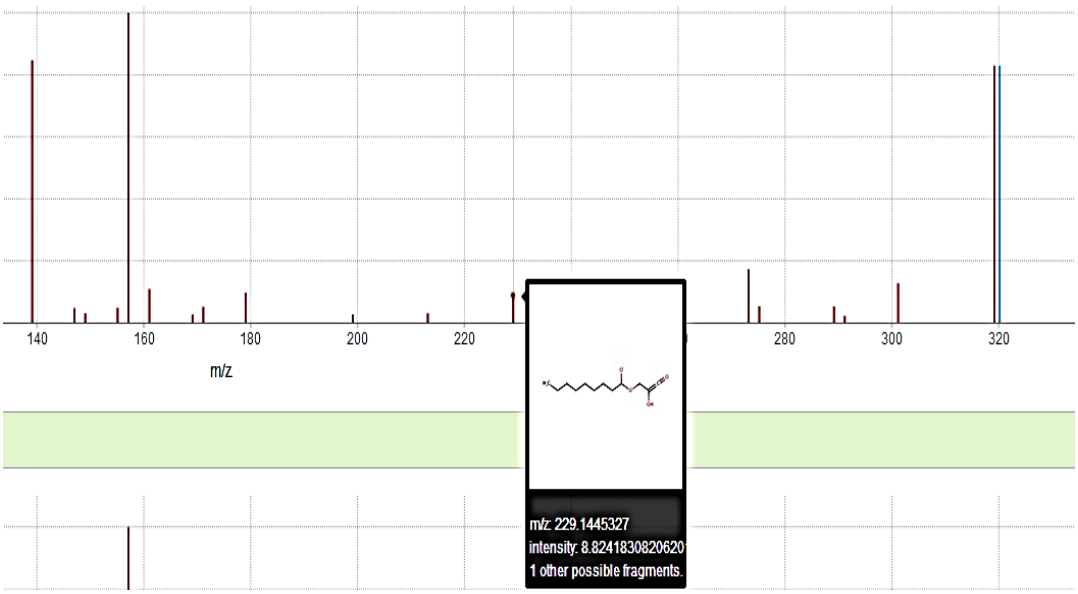

[1]HNMR spectrum of C9-Gluc ester:

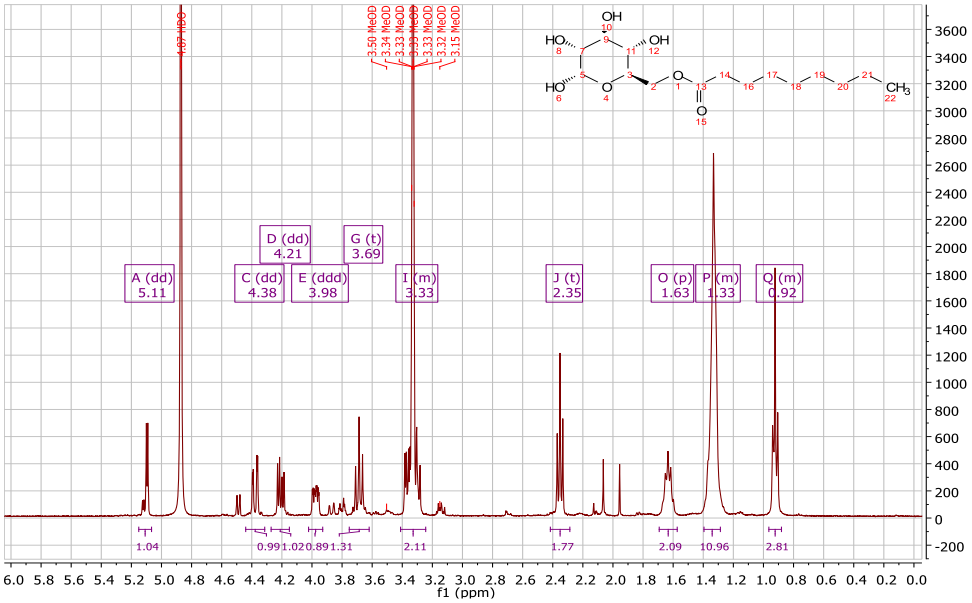

[1]H NMR (400 MHz, Methanol-d4) δ 5.11 (dd, *J* = 10.3, 3.7 Hz, 1H), 4.38 (dd, *J* = 11.8, 2.2 Hz, 1H), 4.21 (dd, *J* = 11.8, 5.4 Hz, 1H), 3.98 (ddd, *J* = 10.1, 5.4, 2.2 Hz, 1H), 3.69 (t, *J* = 9.3 Hz, 1H), 3.41 – 3.24 (m, 2H), 2.35 (t, *J* = 7.4 Hz, 2H), 1.63 (p, *J* = 7.3, 6.8 Hz, 2H), 1.40 – 1.29 (m, 11H), 0.96 – 0.88 (m, 3H).

Prediction of ^{1}HNMR spectrum of C9-Gluc ester:

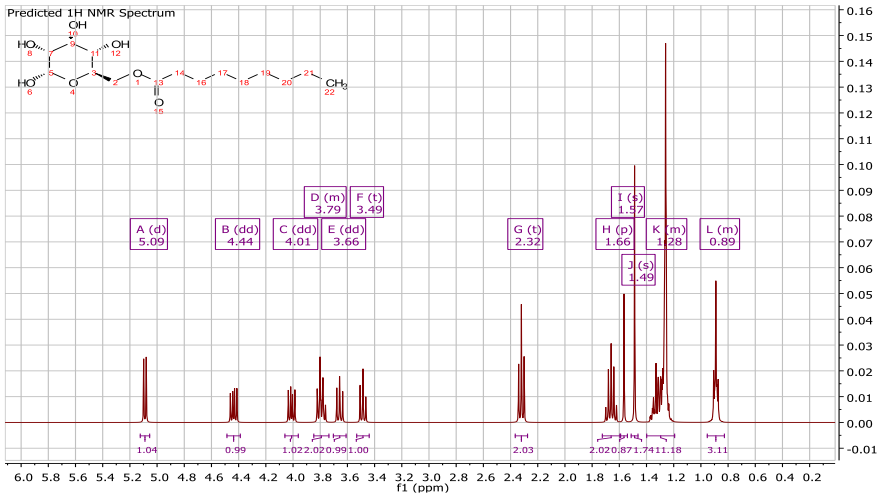

Figure S7. [(3*S*,6*S*)-3,4,5,6-tetrahydroxyoxan-2-yl]methyl (3*R*)-3-hydroxynanonoate (**27**)

Scan mode: m/z = 371 [M+Cl^{-}]$^{-}$

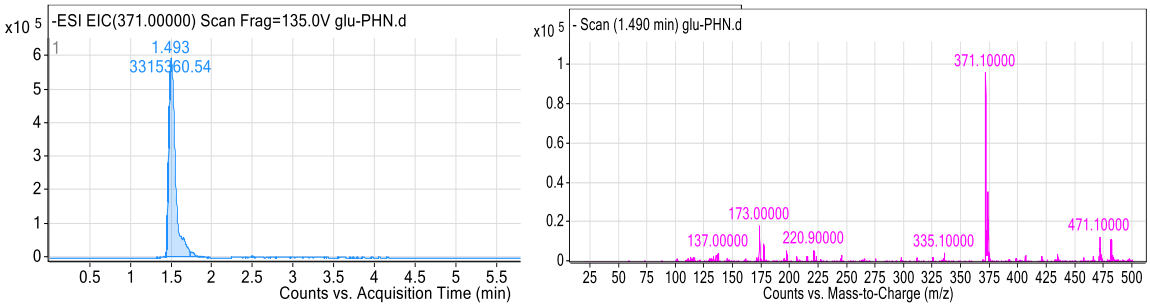

Product ion scan mode: m/z = 335 [M-H]$^{-}$

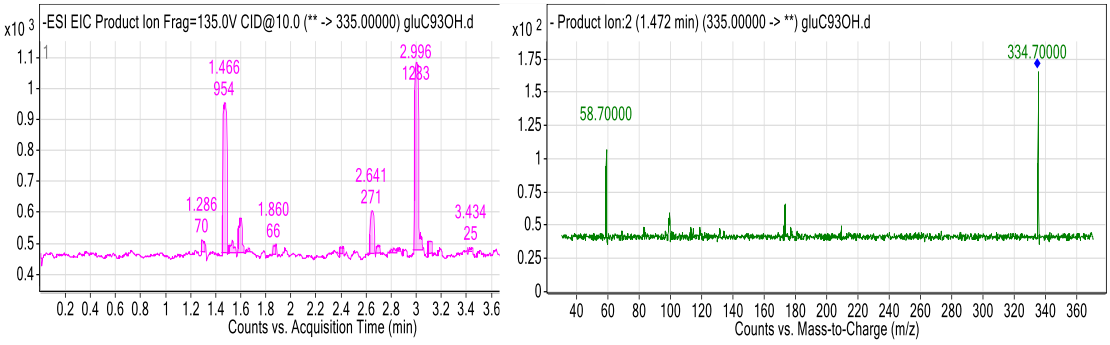

Predicted fragmentation: m/z= 59

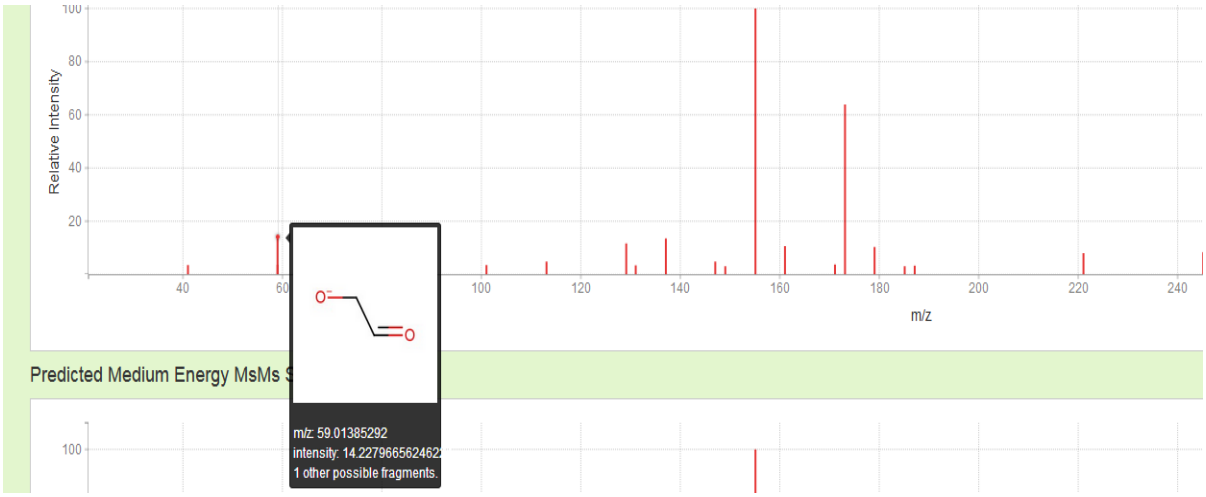

m/z=173

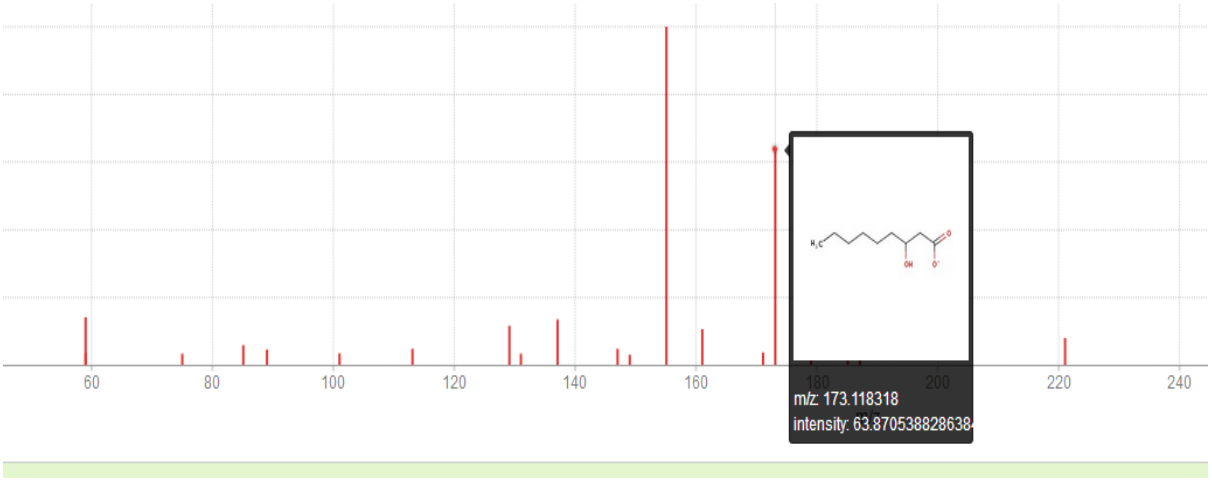

Figure S8. [(3*S*,6*S*)-3,4,5,6-tetrahydroxyoxan-2-yl]methyl (3*R*)-3-hydroxyheptanoate (**28**)

Scan mode: m/z = 343 [M+Cl$^-$]

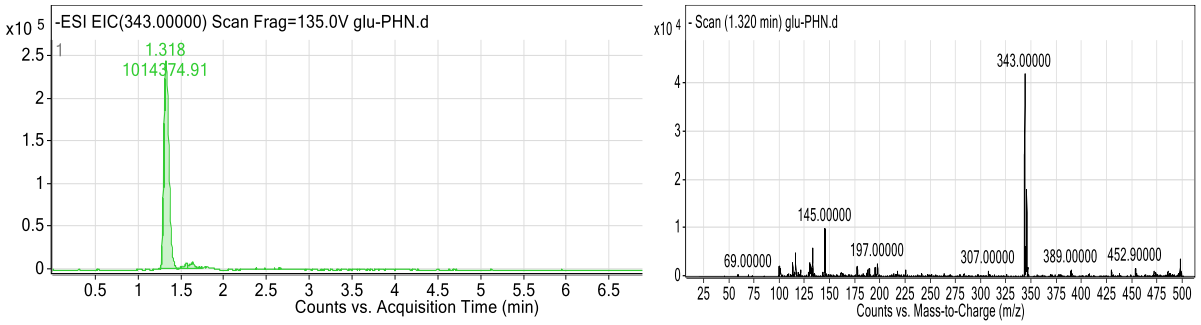

Figure S9. [(3*S*,6*S*)-3,4,5,6-tetrahydroxyoxan-2-yl]methyl (3*R*)- 3-(2,2,2-trifluoroethoxy)nonanoate (**29**)

Scan mode: m/z = 453 [M+Cl$^-$]$^-$

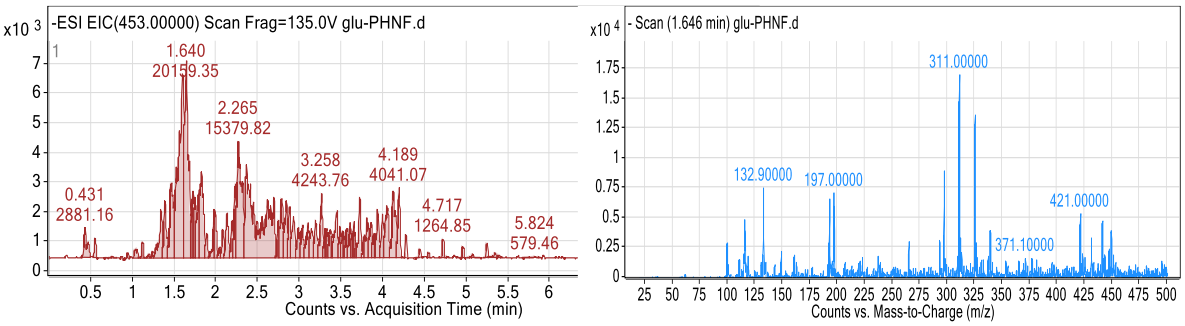

Product ion scan mode: m/z = 417 [M-H]$^-$

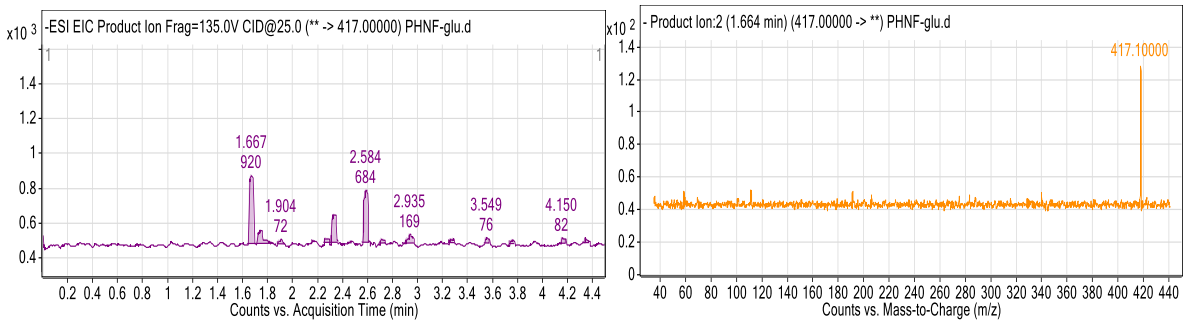

Figure S10. 5-phenylpentanoic acid (**5**)

Scan mode m/z = 191 [M-H]$^-$

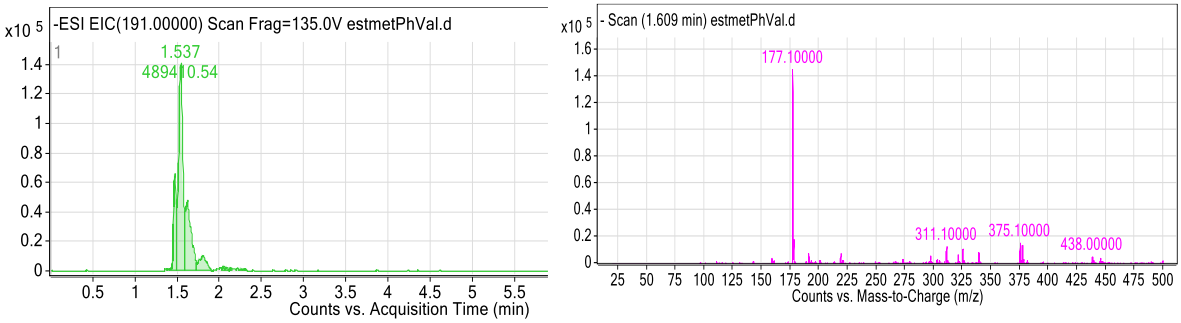

Product ion scan mode: m/z =191 [M-H]$^-$

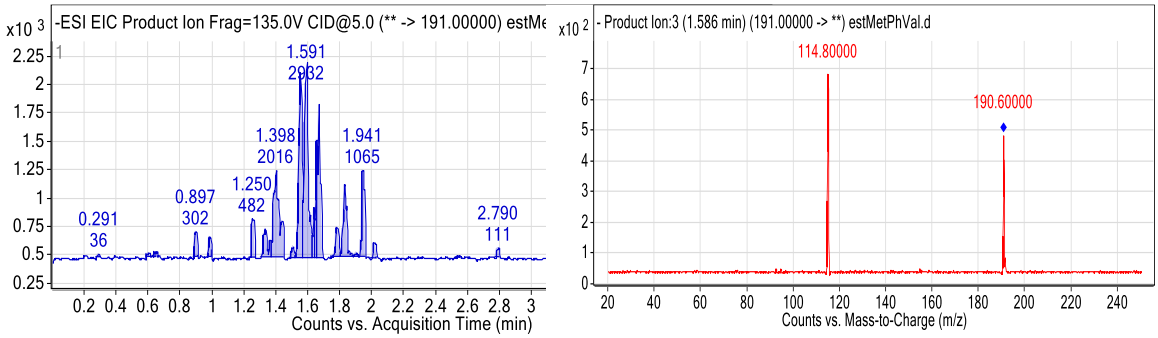

Predicted fragmentation: m/z = 115

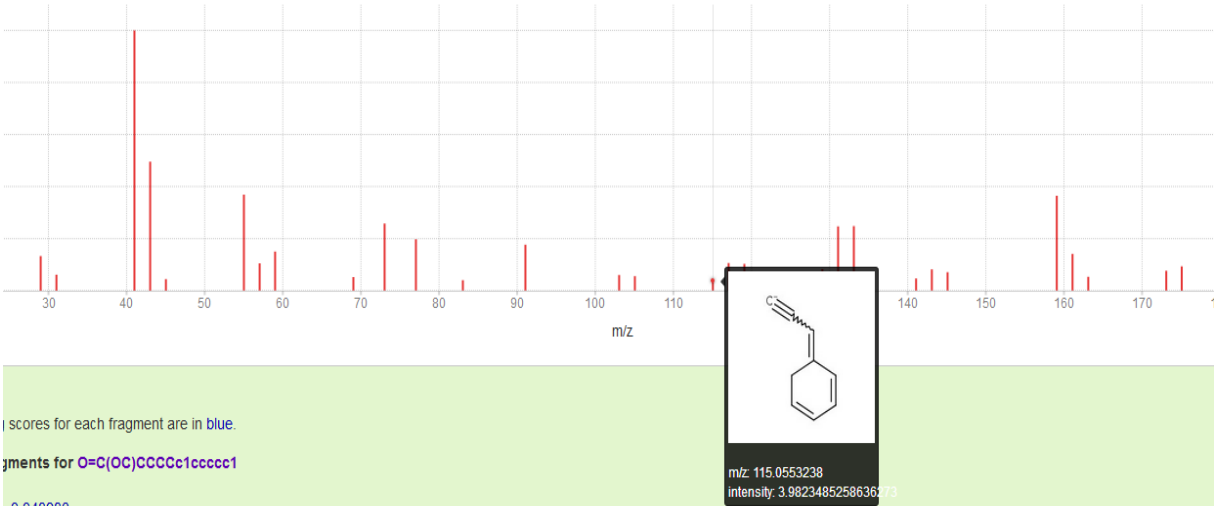

Figure S11. methyl (3*R*)-3-hydroxy-5-phenylpentanoate (**7**)

Scan mode: m/z =193 $[M-H]^-$ for (3*R*)-3-hydroxy-5-phenylpentanoic acid

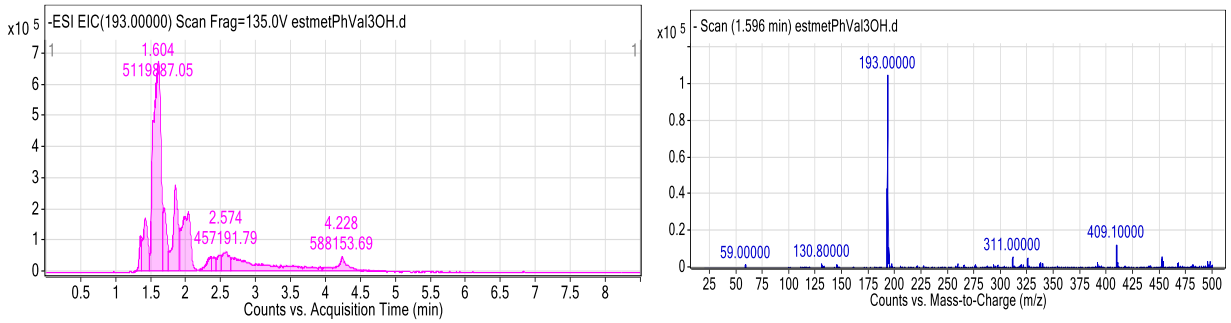

Product ion scan mode: m/z =207 $[M-H]^-$

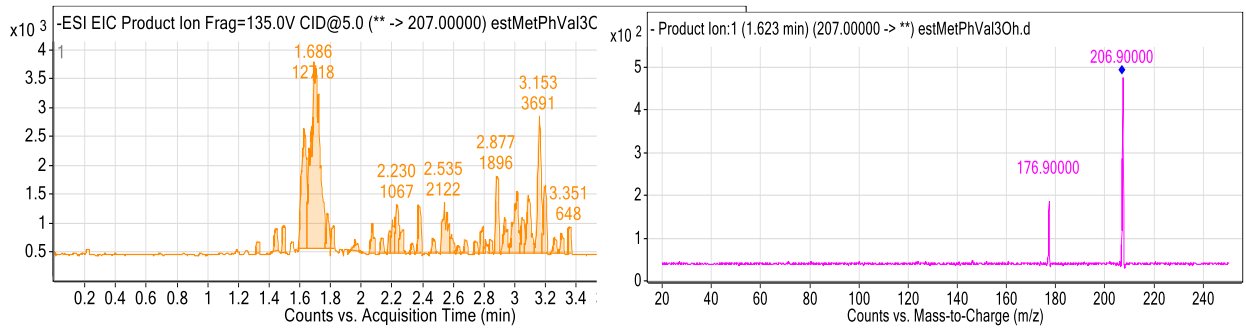

Predicted fragmentation: m/z = 177

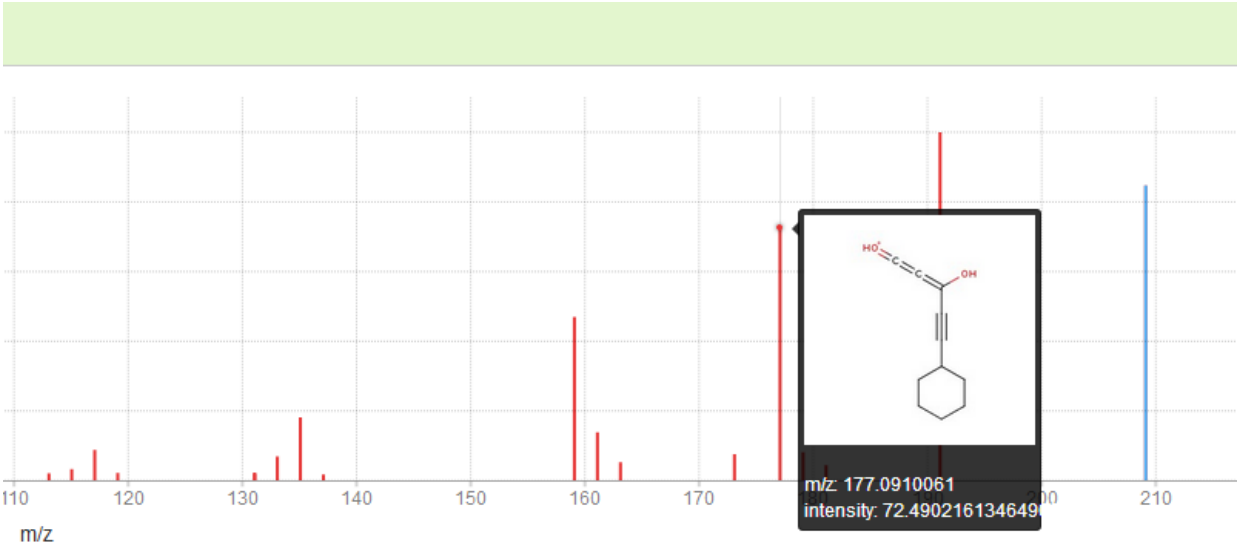

Figure S12. [(3*S*,6*S*)-3,4,5,6-tetrahydroxyoxan-2-yl]methyl 5-phenylpentanoate (**31**)

Scan mode: m/z =339 [M-H]$^-$

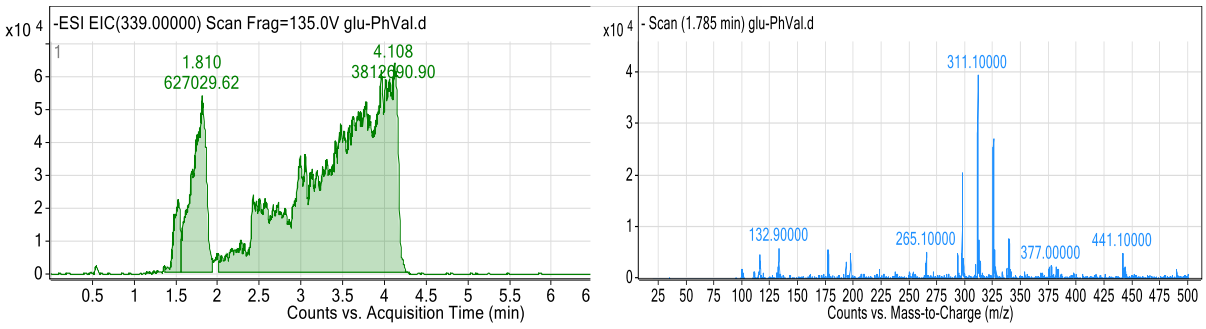

Product ion scan mode: m/z =339 [M-H]$^-$

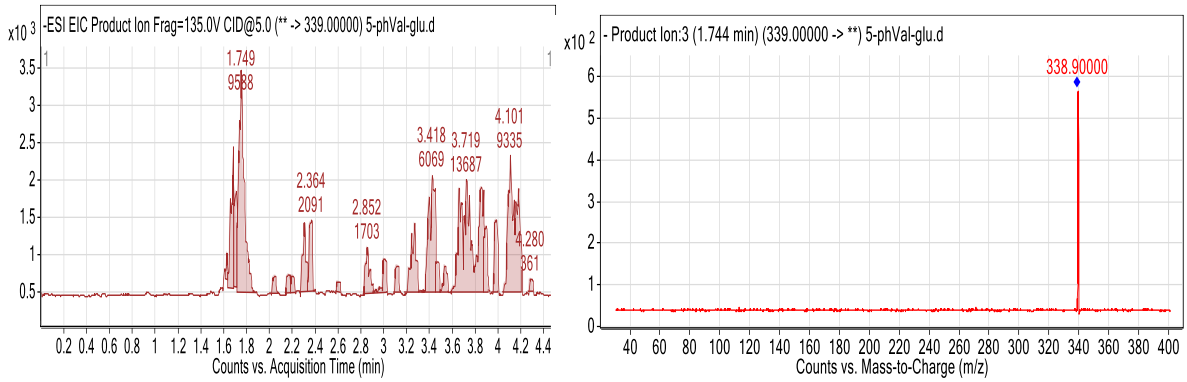

Figure S13. [(3*S*,6*S*)-3,4,5,6-tetrahydroxyoxan-2-yl]methyl (3*R*)-3-hydroxy-5-phenylpentanoate (**33**)

Scan mode: m/z = 391 $[M+Cl^-]^-$

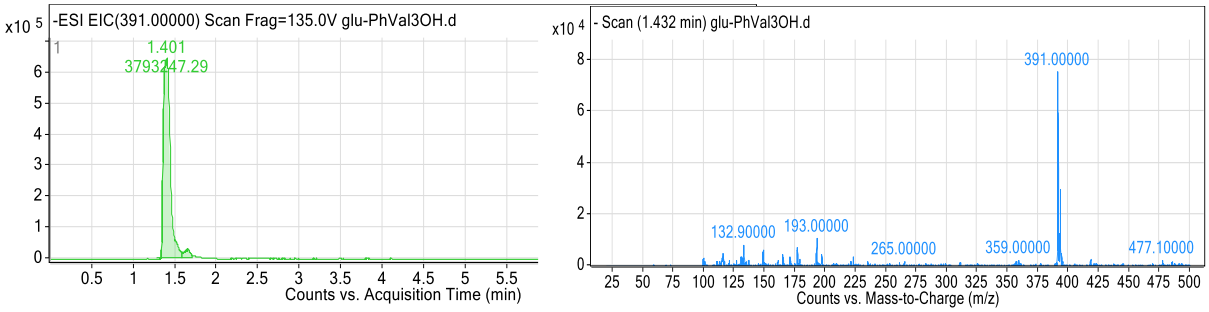

Product ion scan mode: m/z = 355 $[M-H]^-$

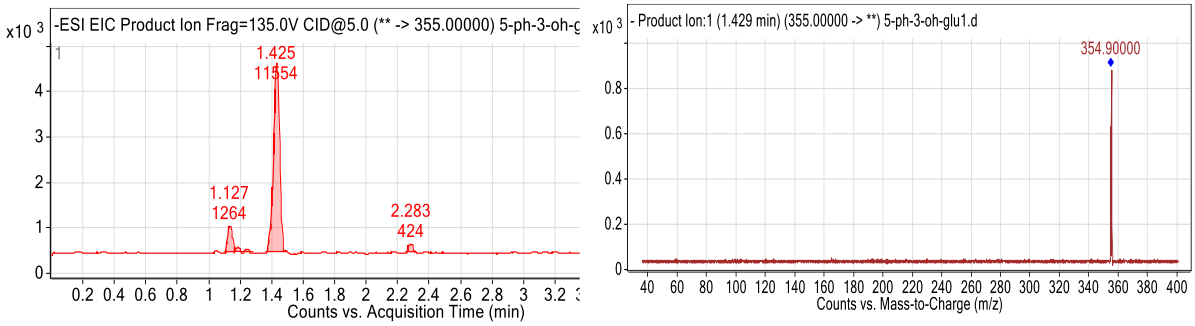

International Journal of
Molecular Sciences

MDPI

Article

In Search of Effective Anticancer Agents—Novel Sugar Esters Based on Polyhydroxyalkanoate Monomers

Wojciech Snoch [1], Dawid Wnuk [2], Tomasz Witko [1], Jakub Staroń [3], Andrzej J. Bojarski [3], Ewelina Jarek [1], Francisco J. Plou [4] and Maciej Guzik [1,*]

[1] Jerzy Haber Institute of Catalysis and Surface Chemistry, Polish Academy of Sciences, Niezapominajek 8, 30-239 Kraków, Poland; wojciech.snoch@ikifp.edu.pl (W.S.); tomasz.witko@ikifp.edu.pl (T.W.); ewelina.jarek@ikifp.edu.pl (E.J.)
[2] Department of Cell Biology, Faculty of Biochemistry, Biophysics and Biotechnology, Jagiellonian University, Gronostajowa 7, 30-387 Kraków, Poland; dawid.wnuk@uj.edu.pl
[3] Maj Institute of Pharmacology, Polish Academy of Sciences, Smętna 12, 31-343 Kraków, Poland; staron@if-pan.krakow.pl (J.S.); bojarski@if-pan.krakow.pl (A.J.B.)
[4] Instituto de Catalisis y Petroleoquimica, CSIC (Spanish National Research Council), Calle de Marie Curie 2, 28049 Madrid, Spain; fplou@icp.csic.es
* Correspondence: maciej.guzik@ikifp.edu.pl; Tel.: +48-12-6395-159

Abstract: Cancer is one of the deadliest illness globally. Searching for new solutions in cancer treatments is essential because commonly used mixed, targeted and personalized therapies are sometimes not sufficient or are too expensive for common patients. Sugar fatty acid esters (SFAEs) are already well-known as promising candidates for an alternative medical tool. The manuscript brings the reader closer to methods of obtaining various SFAEs using combined biological, chemical and enzymatic methods. It presents how modification of SFAE's hydrophobic chains can influence their cytotoxicity against human skin melanoma and prostate cancer cell lines. The compound's cytotoxicity was determined by an MTT assay, which followed an assessment of SFAEs' potential metastatic properties in concentrations below IC_{50} values. Despite relatively high IC_{50} values (63.3–1737.6 μM) of the newly synthesized SFAE, they can compete with other sugar esters already described in the literature. The chosen bioactives caused low polymerization of microtubules and the depolymerization of actin filaments in nontoxic levels, which suggest an apoptotic rather than metastatic process. Altogether, cancer cells showed no propensity for metastasis after treating them with SFAE. They confirmed that lactose-based compounds seem the most promising surfactants among tested sugar esters. This manuscript creates a benchmark for creation of novel anticancer agents based on 3-hydroxylated fatty acids of bacterial origin.

Keywords: anticancer agents; sugar esters; polyhydroxyalkanoates; fluorination; chemical modifications; melanoma; prostate cancer

Citation: Snoch, W.; Wnuk, D.; Witko, T.; Staroń, J.; Bojarski, A.J.; Jarek, E.; Plou, F.J.; Guzik, M. In Search of Effective Anticancer Agents—Novel Sugar Esters Based on Polyhydroxyalkanoate Monomers. *Int. J. Mol. Sci.* **2021**, *22*, 7238. https://doi.org/10.3390/ijms22137238

Academic Editor: Hidayat Hussain

Received: 28 May 2021
Accepted: 29 June 2021
Published: 5 July 2021

1. Introduction

According to statistics provided by the World Human Organization, cancer is one of the deadliest illness globally. It is estimated that it caused 9.6 million deaths, or one in six deaths, in 2018. Lung, prostate, colorectal, stomach and liver cancers are the most common types of cancer in men, while breast, colorectal, lung, cervical and thyroid cancers are the most common among women [1]. Based on 'Cancer Treatment and Survivorship Statistics, 2019', the most prevalent cancers in 2019 in the USA were prostate (3,650,030), colon and rectum (776,120), skin melanoma (684,470) among males and breast (3,861,520), uterine corpus (807,860), and colon and rectum (768,650) among females [2]. Moreover, prostate cancer was the fifth most common cancer in Europe in 2018 (450,000) [3]. These

statistics bring us to conclusions that searching for new solutions in melanoma and prostate cancer treatment is still essential.

Nowadays, mixed, targeted and personalized therapies are becoming more commonly used to treat cancer [2]. Many of them are combinations of surgery and radio-, chemo-, immune-, photo-, thermo- and cryotherapies. Some medicines disrupt cell division by interfering with the cell's cytoskeleton (tubulin, mitotic spindle). Others interact with the DNA (e.g., cis-Pt, doxorubicin, fluorouracil)[4,5] of the cells or even disturb signalization by interacting with transmembrane hub proteins to drive the cell to apoptosis [6]. On the other hand, the most prospective therapies are inspired by nature itself: these are either based on monoclonal antibodies or programmed bacterial pathogens specifically targeting tumor cells within a host body [7]. In spite of the wide range and high effectiveness of the mentioned therapies, sometimes even they are not sufficient. Moreover, very often they are too expensive for common patients. Therefore, our attention was drawn to other tools that could both reduce the doses of drugs and the amount of drugs used in a given mixed, targeted therapy. The properties of sugar fatty acids esters (SFAE) make them promising candidates to be another valuable tool [8,9].

SFAEs are compounds widely used in the cosmetics and food industries because their antifungal and antibacterial properties. The physiochemistry of these surfactants allows for the formation of micelles or emulsions, which extends their applicability also to the pharmaceutical industry [10–12]. It has been shown that SFAE molecules are able to block glycolysis [13]. On the other hand, fatty acid chains of SFAE may cause their non-specific anchorage in cell membranes, consequently leading to the damage of transmembrane proteins, leakage of valuable substances outside of the cell and penetration of the unfavorable ones [14]. This aspect is widely discussed in the literature on the example of the influence of SFAE on microorganisms: *Bacillus* sp., *Staphylococcus* sp., *Escherichia* sp., *Salmonella* sp. or *Listeria* sp. [12–14]. However, activity of these surfactants may be different while investigated on mammalian cells biology [15].

In 1970s scientists began research on anti-cancer properties of SFAE [16]. The experiments carried out on both in vitro and in vivo cell models confirm that SFAE may inhibit the secretion of TNF-α and some proinflammatory cytokines such as IL-1B, IL-6 and IL-8 [17]. Moreover, their ability to inhibit in vitro excessive proliferation of bone marrow cells in the acute myelogenous leukemia model was also described [18]. It has also been shown that biological activity of SFAE may depend on the length of an aliphatic chain and their number in the whole ester molecule (mono- vs. di- vs. tri-/poly-esters). Furthermore, the type of sugar that builds SFAE plays a significant impact on their properties, affecting the hydrophilic–lipophilic balance (HLB) and thus the physical properties of the whole ester (solubility, micelles formation, stabilization of emulsion systems) [15].

The biological activity of SFAEs can also be altered by their structural modifications [19]. The literature reports that the biological activity of commonly used anti-cancer drugs can be improved through the introduction of halides, and a similar strategy can also be applied to sugar esters [20]. The most commonly used in pharmacology, and simultaneously, the most promising modifications of moieties in terms of their antiproliferative properties are perfluorination [21], chlorination [22], bromination [23] and the introduction of halogenated alkyl (trifluoromethyl, pentafluoroethyl) [24] and fluorophenyl [25] or trimethoxyphenyl [26] groups. They can be obtained by the substitution of hydrogen atoms in the carbon chain or hydroxyl groups of a sugar for halide atoms into the molecular structure. As the literature reports, the cytotoxicity of the modified molecules may be changed significantly both by the number and the location of the introduced halides. For example, substitution of all carbon atoms with 6–19 fluorine atoms in the hydrophobic part of SFAE showed promising anticancer potential. However, these compounds were also highly toxic to normal cells [27]. Therefore, it is essential to pay attention to increasing selectivity towards cancer cells without harming the native ones during the drug designing process.

Here, we propose the use of bacterially derived natural monomers, namely (*R*)-3-hydroxyacids originating from polyhydroxyalkanoates polymers (PHA), as a basis for the synthesis of modified SFAE (Figure 1). PHAs can serve as material for manufacturing of nontoxic implants and other medical devices. They also are often used as media for drug delivery upon implantation [28–30]. To date, more than 150 different (*R*)-3-hydroxyacids have been reported, thus creating endless possibilities for further modifications [31]. Despite the differences, all of them share two unchanging features—a presence of carboxylic and a β-carbon-located hydroxyl groups. The first one enables the synthesis of a wide range of SFAEs, the latter, on the other hand, enables the introduction of various moieties into the SFAE molecule. Recently, we have reported routes towards synthesis of (*R*)-3-hydroxyacid- based glucose esters with fluorine modified analogues [29]. Here, we expanded the glucose esters library with galactose and lactose SFAE versions and tested the whole collection of compounds against human melanoma and prostate cancer cells in vitro. In this paper, we present the description on biocatalytic synthesis of novel SFAEs and their structural characterization by infrared and NMR spectroscopies combined with mass spectrometry analysis. Furthermore, we demonstrate a set of biological studies elucidating sugar esters' biological potential. Firstly, the cytotoxicity of these novel compounds was examined, together with their metastatic properties, in concentrations below IC_{50}. The results were compared to sugar esters from literature and some compounds commonly used in clinical oncology.

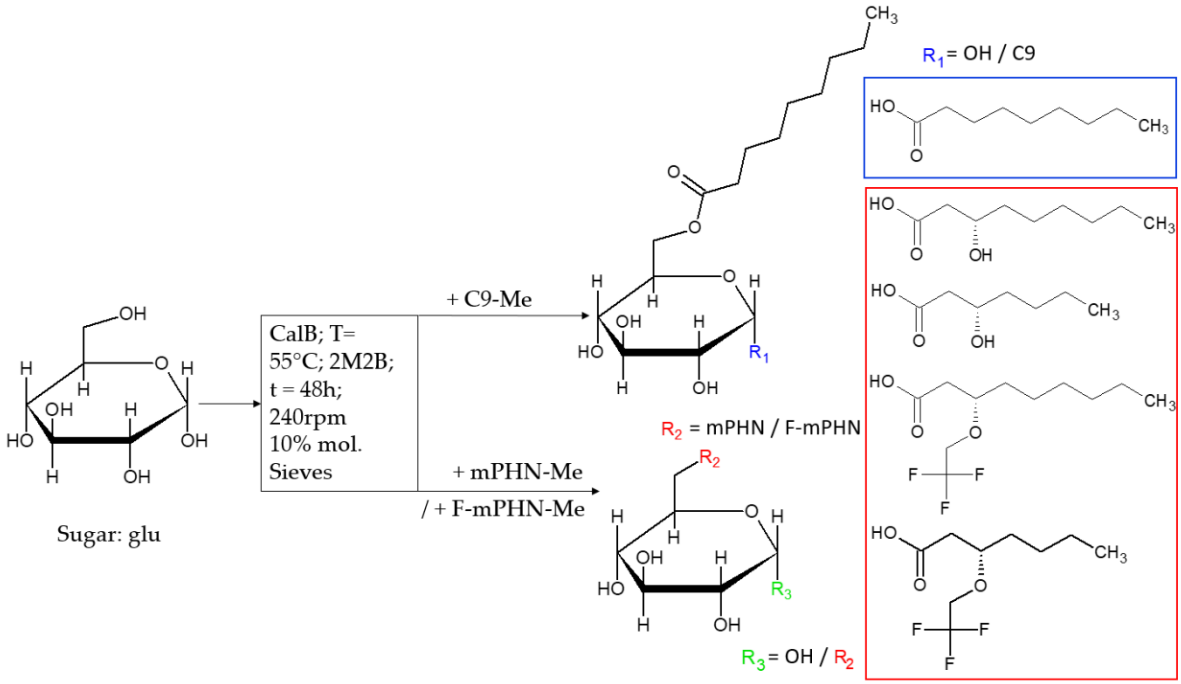

Figure 1. Scheme of sugar fatty acid esters enzymatic synthesis with glucose as an example. The remaining sugar-based SFAEs (galactose and lactose) and all structures of the obtained compounds are presented in Supplementary Figure S1. Where: R_1: -OH group or nonanoic acid—structure shown in blue rectangle; R_2: modified or not modified (mPHN or F-mPHN) PHN monomeric residues—their structures are shown in red rectangle; R_3: -OH group or one of residues which structures are shown in red rectangle.

2. Materials and Methods

2.1. Preparation of Unmodified and Modified Polyhydroxynonanoate Monomers

Polyhydroxynonanoate (PHN) was produced using *Pseudomonas putida* KT2440 in a controlled continuous fermentation process as described previously [30]. Briefly, nonanoic acid was used as a source of carbon and energy for bacteria. The polymer was extracted with ethyl acetate and characterized as described in Sofinska et al. [30]. Next, it was decomposed to monomers through acidic methanolysis. The hydroxylated acid

methyl esters were analyzed by gas chromatography. Modification of the resultant methyl esters of monomers was conducted as described previously [29]. The obtained monomers were converted into their acidic forms using *Candida antarctica* lipase B under aqueous conditions to obtain sodium salts.

2.2. Synthesis of Sugar Fatty Acid Esters (SFAE)

Enzymatic reactions were performed in 2-methyl-2-butanol (2M2B). Sugar substrates: lactose, glucose and galactose were supplemented with solvent and the remaining reagents, giving 20 mg mL^{-1} (2 molar equivalents) of final concentration in a reactor. The remaining substrates were: nonanoic acid methyl esters (C9) 6.04 mg mL^{-1} PHN monomer methyl esters 9.48 mg mL^{-1} and fluorinated PHN methyl esters 9.48 mg mL^{-1} (up to 1 molar equivalent), respectively. Additionally, 100 mg mL^{-1} of activated molecular sieves (4 Å) were added to maintain anhydrous conditions. The reactions were initiated by the addition of 40 mg mL^{-1} catalyst: enzyme Novozym *Candida antarctica* lipase B (CalB) and conducted at 55 °C for 48 h with shaking (240 rpm; New Brunswick™ Scientific Exella E 24 Incubator Shaker Series, Eppendorf, Hamburg, Germany).

2.3. HPLC Analysis

Analyses were performed using UHPLC measurements in Agilent 1290 Infinity system with automatic autosampler (Santa Clara, CA, USA) and MS Agilent 6460 Triple Quad Detector (Agilent, Singapore) equipped with Zorbax Eclipse Plus 300SB-C18 Agilent column (2.1 mm × 50 mm, 1.8 µm, Santa Clara, CA, USA). To separate the components of the reaction mixture, the column was eluted at 30 °C at a flow rate of 0.4 mL min^{-1} and developed with a gradient of elution of solvent A (water) and solvent B (methanol) as follows: 0.00 min (95% A/5% B) to 1.00 min (100% B) to 4.50 min (95% A/5% B) to 5.00 min (95% A/5% B). The interval between injections was 4.5 min. MS Agilent 6460 Triple Quad tandem mass spectrometer with Agilent Jet Stream Electrospray (ESI) interface was used in negative ion mode. Nitrogen with a flow rate of 10 L min^{-1} was used as a drying and collision gas. The drying gas temperature was set to 350 °C and the shielding gas temperature to 200 °C. The capillary voltage was set to 4000 V and the nozzle voltage to 2000 V. All compounds were monitored in scanning mode and product ions with different collision energies (5–30 eV) (m/z products in Table S1 in Supplementary Section).Workstation MassHunter Data Acquisition 1.1 version was used to control the HPLC-MS data collection and processing.

2.4. Preparative HPLC

Preparative scale liquid chromatography was used to purify SFAE products. The crude reaction mixture was purified on VersaPack™ C18 (SUPELCO Analytical, Bellefonte, PA, USA) preparative column in the MeOH/H_2O system with an increasing MeOH gradient of 50 to 100%. The elution of the reagents was monitored with TLC chromatography performed on C18 Merck silica gel plates (with the same elution system as in preparative separation) and high performance liquid chromatography coupled to mass spectrometer: Waters TQD instrument in scan mode ESI: +100–1000 m/z.

2.5.1. H NMR and ^{19}F NMR Spectroscopy

Twenty mg samples of each compound were dried under vacuum. Samples were analyzed on Bruker (BioSpin GmBH, Rheinstetten, Germany) in $CDCl_3$.

2.6. IR Spectroscopy

The compounds tested were dissolved in methanol. All spectra were collected by using IR microscope Nicolet iN10 (Thermo Scientific™ part of Thermo Fisher Scientific, Madison, USA). All reflection measurements were performed on gold layer by using high-sensitivity MCT-A detector within spectral range from 4000 cm^{-1} to 675 cm^{-1}, 128 scans

during 25 s with normal resolution just after the solvent evaporation or immediately after application in case of volatile substances. Fully automated adjustable aperture for measuring field extraction was 150 μm × 150 μm.

2.7. Cell Cultures

The following cell lines were used: human prostate cancer cells from metastases to the brain DU145 (ATCC® HTB-81™, Manassas, Virginia); healthy human prostate epithelial cell line as a control (PNT2; Sigma-Aldrich, Darmstadt, Germany); human melanoma Hs 294T (ATCC® HTB-140™, Manassas, Virginia); human epidermal keratinocytes (HaCaT) HEK001 (ATCC® CRL-2404™, Manassas, Virginia); and normal human skin fibroblasts BJ (ATCC® CRL2522™) as controls. The cells were cultured in 37 °C with humidified atmosphere enriched with 5% CO_2 in appropriate cell culture media: DMEM F12Ham (Sigma-Aldrich, Darmstadt, Germany) + 5% FBS (Thermo Fisher Scientific; Gibco; Waltham, MA, USA); RPMI-1640 (Sigma-Aldrich, Darmstadt, Germany) + 10% FBS (Thermo Fisher Scientific; Gibco; Waltham, MA, USA); DMEM high glucose (Sigma-Aldrich) + 10% FBS (Thermo Fisher Scientific; Gibco; Waltham, MA, USA); DMEM low glucose (Sigma-Aldrich, Darmstadt, Germany) + 10% FBS (Thermo Fisher Scientific; Gibco; Waltham, MA, USA). All media contained a penicillin/streptomycin (Sigma-Aldrich, Darmstadt, Germany) cocktail.

2.8. MTT Cytotoxicity Assay

For the determination of the cytotoxic effect of tested compounds, normal (control) and cancer cell lines cells were tested at a concentration of 2.5×10^4 cells cm^{-2} in appropriate culture medium into 96 well microplates (VWR, Radnor, PA, USA). Cells were preincubated with four different concentrations of tested compounds: 0.5, 0.25, 0.125 and 0.0625 mg mL^{-1} for 24 h, 72 h and 120 h in cell incubator. After the incubation, MTT labelling reagent (final concentration 0.5 mg mL^{-1}) and solubilizing solution were added according to the protocol. The samples absorbance was measured using a microplate reader (Multiscan FC; Thermo Fisher Scientific, Waltham, MA, USA) by 570 nm wavelength, 620 nm for reference.

2.9. Fluorescent Staining

Cellular studies 12-well plates were used, cell density 3×10^5 per well. After 24 h and 48 h of incubation with tested compounds (0.0625 mg mL^{-1}), the samples were fixed according to standard protocol. Tubulin (green; AlexaFluor-488 mouse anti-β-tubulin IgG; BD Biosciences, San Jose, CA, USA, Pharminogen; cat. 558605), vimentin (infra-red; I: rabbit-anti-vimentin IgG; GeneTex, Irvine, CA, USA; GTX100619; II: chicken-anti-rabbit-AlexaFluor647 IgG; ThermoFisher, Waltham, MA, USA) and counterstained nuclei (blue; Hoechst 33258; Sigma-Aldrich, Darmstadt, Germany) and F-actin (red; AlexaFluor546-phalloidin; ThermoFisher, Waltham, MA, USA). Next, the samples were washed 5 times with deionized water and prepared for imaging with Fluorescent Mounting Medium (Dako Omnis, Agilent, Santa Clara, CA, USA).

2.10. Transmigration Assay

Transmigration assay was performed using 24-well glass-bottom plate (Eppendorf) containing microporous membranes in Boyden's chamber (Corning; pore diameter: 8 μm; membrane diameter: 6.5 mm). Native DU145 and HTB140 cells were seeded at density of 3×10^5 cells per membrane with tested compounds (0.0625 mg mL^{-1}) and left for 48 and 96 h for transmigration. The transmigrating cells were fixed with 3.7% formaldehyde and counted. The result is presented as a reference to the rate of cell proliferation in the corresponding compound.

2.11. Cell Structures Imaging

Microscopic measurements and observations were carried out with the use of fluorescent techniques performed on Zeiss Axio Observer Z.1 microscope with LSM 710 module (Carl Zeiss Microscopy GmbH Carl-Zeiss-Promenade 10, 07745 Jena, Germany). Image acquisition, processing, deconvolution and analysis were performed using Zeiss ZEN Black software ver. 8.1.0.484 and FluoRender 2.21.0. An oil immersion 40×/NA:1.4 lens was used for observations. Parameters used for acquisition of cell morphology were: nucleus—blue channel (405 nm); microtubular network—green channel (488 nm); Actin—red channel (546 nm); vimentin—far red channel (647 nm).

3. Results

3.1. Synthesis and Modification of Polyhydroxynonanoate Monomers (mPHN)

The process of bacterial polyhydroxynonanoate (PHN**)** synthesis provided 130 g L^{-1} of dry biomass, which after extraction, purification and filtration, gave the desired polymer with 71% efficiency. Its composition was analyzed using gas chromatography and revealed that the PHN polymer consisted of 77.7% (*R*)-3-hydroxynonatec (R3OH-C9) and 22.3% (*R*)-3-hydroxyheptane (R3OH-C7) monomeric units. A portion of that mixture was subjected to further chemical modification. The weighed, purified and dried post-reaction mixture contained fluorinated methyl esters of mPHN monomers (mPHN-Me) (C7 and C9 chains). The actual conversion of 48.5% was determined from the average expected mass for the reaction, whose theoretical efficiency is 100%. Samples were submitted to ^{1}H and ^{19}F NMR analyses, which confirmed the structural modification of the PHN (*R*)-3-hydroxyacids and the synthesis of the (*R*)-3-(2,2,2-trifluoroethoxy) nonanoic a (*R*)-3-(2,2,2-trifluoroethoxy)heptanoic acids (together called F-mPHN-Me, Figure S1 in Supplementary Section). The infrared spectroscopic observation further confirmed the successful synthesis of the fluorinated compounds. The spectra of purified samples after reacting mPHN-Me with trifluoroethyl trifluoromethanosulphonate revealed the disappearance of stretching vibrations in the range 3000–3500 cm^{-1} characteristic for free hydroxylic group. Moreover, the appearance of new peaks was observed (1465.1 cm^{-1}, 1377 cm^{-1}, 1261 cm^{-1}), which correspond to -CF_3 groups connected to the alkyl chain of the monomers. A similar pattern was observed by Li et al., who analyzed the infrared substrate spectrum of CF_3–CH_2–O–CH_3 molecules (described and discussed in detail in the supplementary section).

3.2. Structural Analysis of Synthesized Sugar Esters

A library of sugar esters of both nonanoic acid and (*R*)-3-hydroxyacids derivatives was created by a biocatalytic approach employing immobilized *Candida antarctica* lipase B (CalB). In addition, a series of SFAEs with aliphatic, nonanoic and heptanoic hydrophobic tails were generated as controls to all further performed experiments. The structures of the sugar esters were confirmed by ^{1}H NMR and IR analyses (Figures S4–S12 in Supplementary Section). In general, it was observed that signals between 5.25 and 0.75 ppm, originated from newly synthesized fatty acid-sugar ester, consisted of several multiplets. Signals between 1.5 and 0.75 correspond to fatty acid chains, shifts between 2.25 and 5.25 came from sugar ^{1}H signals, and multiplets around 4.5 and 4.0 came from ^{1}H localized on a nearby ester bond. The differences between the fatty acids, fatty acid sugar diesters and monoester spectra are subtle and can be explained more by analyzing intensity and ratio of particular signals than appearance of additional ones. All the tested SFAE specimens showed the presence of stretching vibrations at 1725–1735 cm^{-1} (ester bonds), stretching vibrations in the range of 3000–3500 cm^{-1} (sugar ring -OH groups) and stretching vibrations in the range of 2800 to 3000 cm^{-1} (-CH_2 aliphatic chain). All these spectra showed great similarity to the spectrum of the reference sample, which was a commercially available standard of sucrose monolaurate.

Furthermore, an in-depth analysis performed by MS/MS measurements supports the obtained results from spectroscopic studies and allow for quantification of reaction yields.

The SFAEs were analyzed in positive and negative modes after ionization in electrospray (ESI) where they formed different adducts (ESI+: $[M + H]^+$; $[M + Na]^+$; $[M + K]^+$ and ESI-: $[M - H]^-$; $[M - Cl]^-$; $[M - H_2O]^-$). These specimens were fragmented to obtain structural fragments of SFAE molecules (Table S1 in Supplementary Section). It was noticed that the obtained sugar esters after biocatalytic synthesis were mixtures of different mono and diesters (Table 1). For example, the lipase produced, on average, a 6:4 ratio of mono- to diesters when methyl esters of nonanoic or (*R*)-3-hydroxynonanoic acids were used. Interestingly, when a fluorinated version of C9 PHN monomer was used, this proportion had changed—we observed that CalB produced 86.6% monoester with C9 PHN monomer, virtually no C9-C9 PHN diester and 12.7% of C7-C7 PHN diester. Monosaccharides, when reacted with nonmodified PHN monomers and aliphatic fatty acid esters predominantly, produced SFAE monoesters in the presence of CalB. When bulkier, fluorinated PHN monomers were used, the lipase synthesized diesters. Subsequently, the product ions with the highest intensities obtained from SFAE fragmentation in MS/MS experiments were used for quantification of the reaction yields. In general, the conversion yields obtained varied between 10.25 and 42.49% (Table 1). As a rule of thumb, glucose appeared to be the most reactive sugar in our experimental setup. We have observed that the introduction of a fluorinated moiety on a PHN monomer resulted in an averaged 2.3-fold drop in the reaction yield for monosaccharides but did not affect synthesis of lactose esters as much (1.1-fold decrease). All of these characterized SFEA mixtures were submitted for biological studies.

Table 1. Molar composition of sugar fatty acid ester based on LC-MS QQQ analysis and conversions of reactions.

Ester	Monoester with C9 Chains [%]	Monoester with C7 Chains [%]	Diester C9 Chains [%]	Diester C7 Chains [%]	Diester C9C7 Chains [%]	Conversion after 48 h [%]
C9-glu	57.8	-	42.2	-	-	17.8
C9-gal	99.9	-	-	-	-	17.8
C9-lac	56.2	-	43.8	-	-	10.4
mPHN-glu	88.1	0.7	-	-	11.2	42.5
mPHN-gal	38.6	-	18.8	42.7	-	24.3
mPHN-lac	59.4	-	40.6	-	-	12.6
F-mPHN-glu	0.4	8.5	76.0	10.3	4.6	18.9
F-mPHN-gal	-	-	-	90.9	9.1	10.3
F-mPHN-lac	86.6	0.2	0.5	12.7	-	11.0

Where '-'—not present.

3.3. MTT Assay Indicating Anti-Proliferative Properties of C9, mPHN and F-mPHN Based SFAE

To understand anti-cancer effect of the sugar fatty esters, in vitro inhibitory concentrations (IC_{50}) of each ester in the MTT test were determined. The experiments indicated a low cytotoxicity of the referring compounds which the hydrophilic SFAE groups are made of, namely, glu, gal and lac (data not shown). Similarly, the toxicity of the SFAE's hydrophobic molecules (i.e., nonanoic acid and its sodium salt and modified and unmodified PHN monomers (either in acidic or salt forms)) oscillated in the range of 0.23 to over 4.09×10^{-3} mol L^{-1}, respectively. They were two- to fourfold higher than the IC_{50} of the tested mPHN-based sugar esters. The most promising group of the potential therapeutic compounds turned out to be the esters of the PHN monomers armed with trifluoroethyl groups and also mPHN lactose ester (Table 2 and Supplementary Figure S15). In the case of F-mPHN-glu and F-mPHN-gal, the toxicity against DU145 prostate cancer cells was around 0.1×10^{-3} mol L^{-1} (after 72 h and 120 h) and $0.08–0.33 \times 10^{-3}$ mol L^{-1} of F-mPHN-lac, respectively. For comparison, the IC_{50} values for sodium salts of the fluorinated monomers PHN alone were 0.23×10^{-3} mol L^{-1} after 24 h and $>1.84 \times 10^{-3}$ mol

L^{-1} after 120 h. The IC_{50} values of the esters for PNT2 (control) cells were respectively: 0.93 × 10^{-3} mol L^{-1} for fluorinated glucose esters, 1.18 × 10^{-3} mol L^{-1} for galactose esters and 1.16 × 10^{-3} mol L^{-1} for lactose esters. Fluorinated PHN monomers alone gave this effect at more than 4.09 × 10^{-3} mol L^{-1} at 72 h and 1.84 × 10^{-3} mol L^{-1} at 120 h.

Table 2. Cytotoxicity IC_{50} of SFAE determined by MTT assay.

		IC_{50} [10^{-3} mol L^{-1}]								
	Time [h]	C9-glu	C9-gal	C9-lac	PHN-glu	PHN-gal	PHN-lac	F-mPHN-glu	F-mPHN-gal	F-mPHN-lac
DU145	24	1.32	1.56	0.92	0.93	0.75	0.16	-	-	-
	72	0.66	0.78	0.84	0.54	0.50	0.13	0.10	0.10	0.08
	120	1.32	1.56	0.46	0.32	0.30	0.09	0.10	0.10	0.34
PNT2	24	2.49	2.39	1.71	1.51	1.26	0.42	-	-	-
	72	1.11	1.23	0.92	1.31	0.61	0.20	0.93	1.18	1.16
	120	2.05	2.36	1.74	1.18	1.84	0.17	1.08	0.70	0.66
HTB140	24	1.47	1.66	0.62	1.77	0.97	0.64	0.06	0.16	0.19
	72	1.32	1.56	0.92	1.20	1.22	0.28	0.09	0.16	0.22
	120	1.13	1.56	0.81	1.69	1.50	0.44	0.37	0.25	0.39
HaCAT	72	1.32	1.56	0.92	1.43	1.20	0.38	0.73	0.58	0.64
	120	-	-	-	-	-	-	0.80	0.95	0.67
HSF	72	1.32	1.56	0.92	0.61	0.62	0.45	-	-	-
	120	-	-	-	0.76	0.50	0.63	0.76	0.50	0.63

DU145—prostate cancer; PNT2—prostate epithelium—control; HTB140—human skin melanoma; HaCAT—human skin keratynocytes; HSF—human skin fibroblasts; -—not determined. Red fillings mark the lowest concentrations needed to reduce a cell population to 50% and green—the highest. Standard deviations of IC50 values are available in Supplementary Table S2 and graphical representation contains Supplementary Figure S15.

Analyzing the effect of sugar esters based on F-mPHN against the melanoma HTB140 line after 24 and 72 h incubation, a higher effectiveness of F-mPHN-glu in antiproliferative activity (IC_{50} values 0.06 and 0.09 × 10^{-3} mol L^{-1}, respectively) than F-mPHN-gal (0.156 × 10^{-3} mol L^{-1}) could be observed. Extending the times of incubation up to 120 h did not affect the cancer cells negatively. It caused increase of IC_{50} concentrations up to 0.37 × 10^{-3} mol L^{-1} for F-mPHN-glu, up to 0.25 × 10^{-3} mol L^{-1} for F-mPHN-gal and 0.39 × 10^{-3} mol L^{-1} for F-mPHN-lac, respectively. In relation to the HaCaT and HSF control cells it was necessary to use about two- to eightfold fold greater concentrations of the discussed compounds, respectively. mPHN-lac showed much higher toxicity against DU145 line than their mPHN-glu and mPHN-gal counterparts and less than those having trifluoroethyl groups. The IC_{50} value of mPHN-lac dropped from 0.16 × 10^{-3} mol L^{-1} at 24 h to 0.13 × 10^{-3} mol L^{-1} at 72 h to less than 0.09 × 10^{-3} mol L^{-1} at 120 h. mPHN-lac turned out to be less harmful to PNT2 cells because their IC_{50} values decreased from at least 0.42 × 10^{-3} mol L^{-1} after 24 h to 0.16 × 10^{-3} mol L^{-1} after 120 h. Additionally, a more promising situation was not the case of melanoma cells. The IC_{50} of these compounds were 0.69 × 10^{-3} mol L^{-1} after 24 h; 0.28 × 10^{-3} mol L^{-1} after 72 h and 0.43 × 10^{-3} mol L^{-1} after 120 h for HTB140 cells, whereas IC_{50} after 72 h for control cells: HaCaT was 0.38 × 10^{-3} mol L^{-1} and 0.50 × 10^{-3} mol L^{-1} for HSF.

3.4. Cell Structures Imaging Indicate Reorganization of Intermediate Filaments in the Presence of a Selected SFAE

Three cytoskeletal elements were analyzed: actin filaments (red ladder), microtubules (green ladder) and intermediate filaments (vimentin—white; Figure 2). These fibers showed morphology characteristic for normal cells grown on glass [32]. The actin filaments were thick and rarely distributed and the microtubules were seen as thick

and distinctly separated beams. It was also noticed (Figure 2b) that the presence of the investigated SFAE caused some changes in the other components of the cytoskeleton: actin and microtubules. In the case of microscopic images showing the cytoskeleton, an increased presence of biodiverse pickling inside the cytoplasm can be seen, which may suggest an elevated content of depolymerized actin. On the other hand, the microtubules in cells in the presence of sugar esters show a greater density of fibers and their lower diameter. Similar changes in the cytoskeleton are often associated with the apoptosis process [33,34]. The literature shows the direct influence of the cell's environment on the shape, dynamics and architecture of both actinic and microtubule fibers [32]. However, these differences are not big enough to specify and propose any certain intracellular mechanism of interaction with the SFAE.

Analysis of cell nuclei shape provided information about their condition. Using image analysis algorithms their roundness was determined for each cell individually (Figure 3). For DU145 cells (Figure 3a) after the first 24 h, the roundness of nuclei was in the range of 0.6–0.9, which is characteristic for normal cells in standard culture on glass medium [35]. After 48 h no significant changes in nuclei shapes of tested cells did not appear. Only in case of mPHN-lac was an increase in roundness was observed. For the cells cultured in C9-lac and mPHN acid, a decrease in nucleus roundness index was observed.

In the case of the HTB140 cell line, the situation was different (Figure 3b). It was clearly visible that for these cells the general circularity index of the organelle was lower and in the range 0.5–0.75, which is normal for elongated melanoma nuclei and usually associated with changes in cytoskeleton architecture and focal adhesion appearance [36]. These changes correlated with subtle alterations of in microtubules and intermediate filaments observed in microscope (Figure 2). After the first 24 h from the start of cultivation the highest circularity index was presented by cells with C9-lac and mPHN-lac. The smallest round nuclei were found in cells cultured with glucose, galactose, mPHN and F-mPHN sodium salts. The changes of the nuclei shape caused by the compounds were more significant after the next 24 h. The changes occurred in almost all cell groups and a decrease in roundness index was observed in each case. The biggest change occurred in a presence of C9-lac esters, mPHN-lac and F-mPHN-lac.

Subcellular structures imaging brought our attention to changes of intermediate filaments. Our study focused on the analysis of adhesion points. They were observed as dot forms placed in the focal plane located between the cell body and glass surface. After 24 h, DU145 cells formed the smallest number of adhesion points in medium supplemented with mPHN-gal and mPHN sodium salt. All cells grown in F-mPHN mediums were characterized with a high number of adhesion points similar to pure glucose. After 48 h in all samples, except those containing glucose, a significant increase in the number of adhesion points was observed. The highest increase occurred in cells grown in media containing mPHN-gal and F-mPHN-glu solutions. The cells grown in medium with F-mPHN-gal showed a similar growth. This growth did not exceed the statistical significance in the rest of experimental samples. In case of HTB140 cells, no vimentin analysis was performed due to its almost complete depolymerization and lack of possibility of correct imaging. Metastases is a process associated with the migration of cancer cells in the body. Its reduction may minimize this harmful phenomenon. An increase in the number of adhesion points (Figure 4) may indicate that selected compounds cause cancer cells to bond more strongly to the substrate or to the glass surface and thus their migration may be limited [37]. On the other hand, these observations may indicate an increasing the intensity of the attachment points production allowing the cells to migrate [38]. In order to verify which of these processes was more likely in our case, transmigration tests were carried out and proliferated cells were counted.

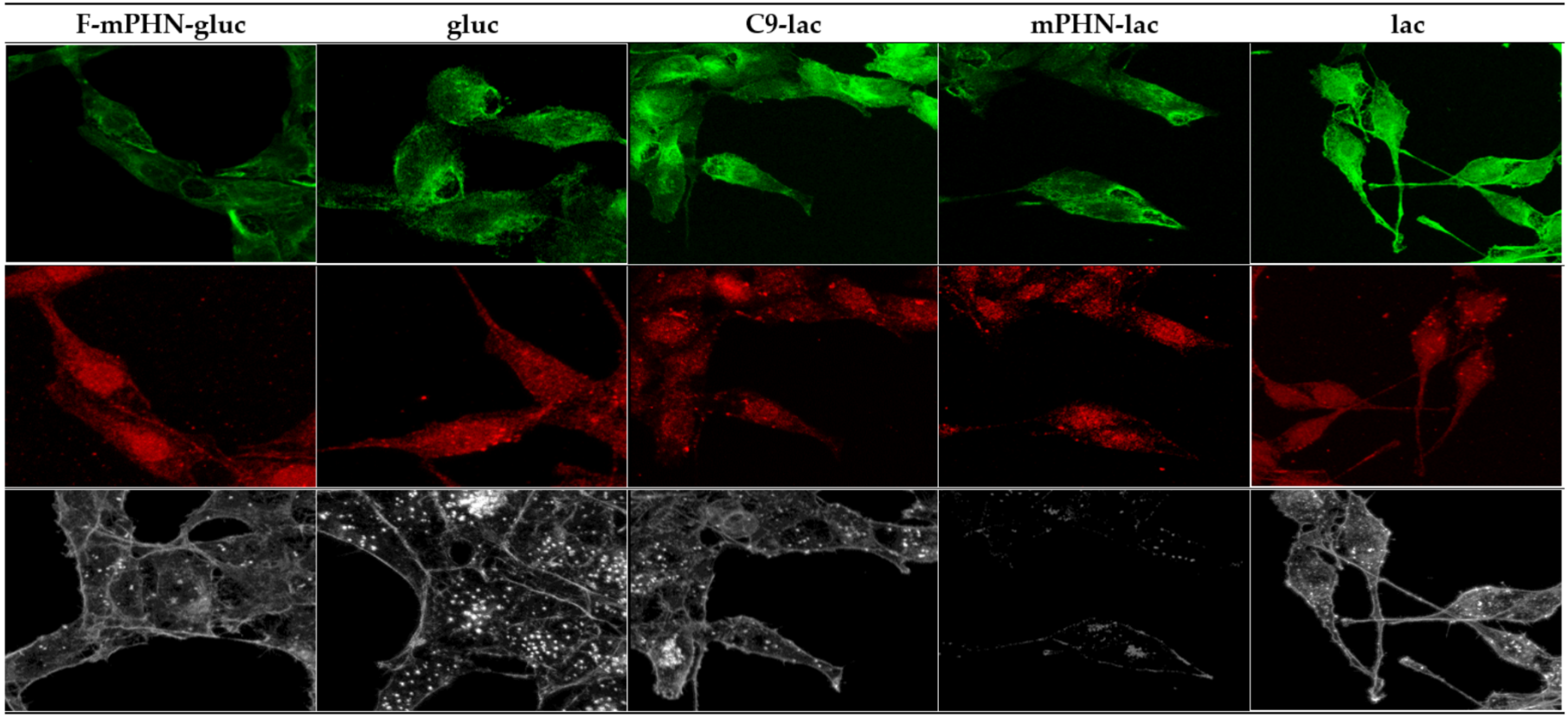

(**a**)

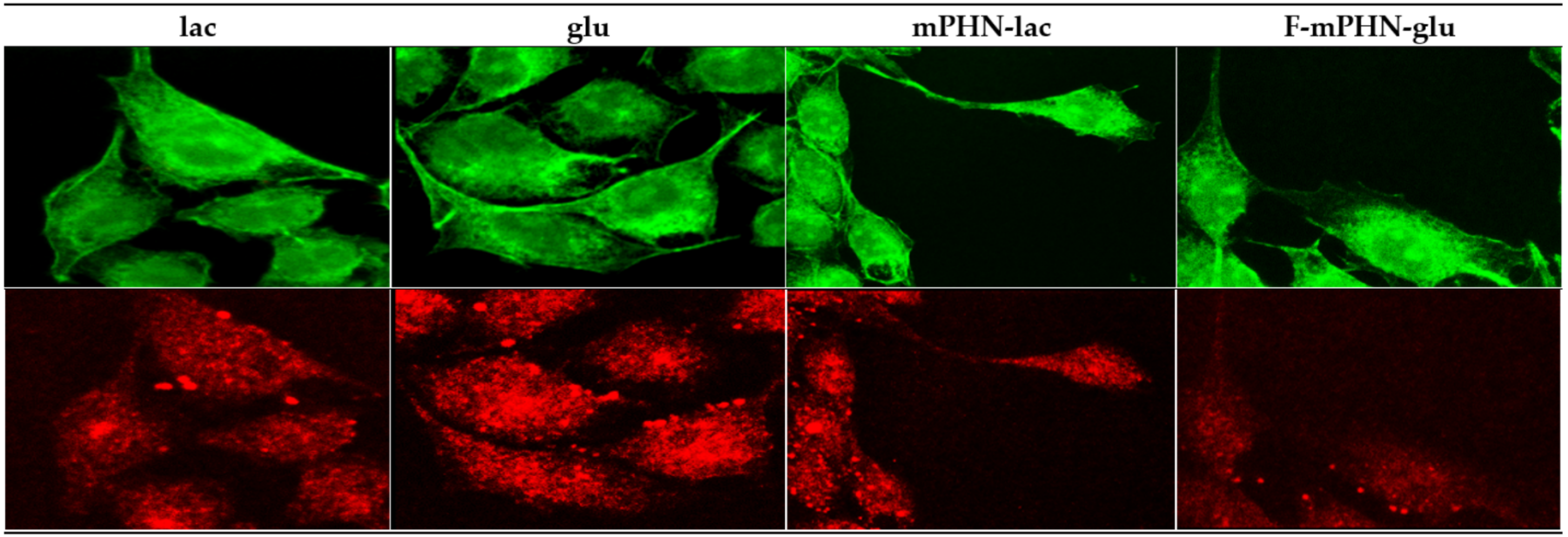

(**b**)

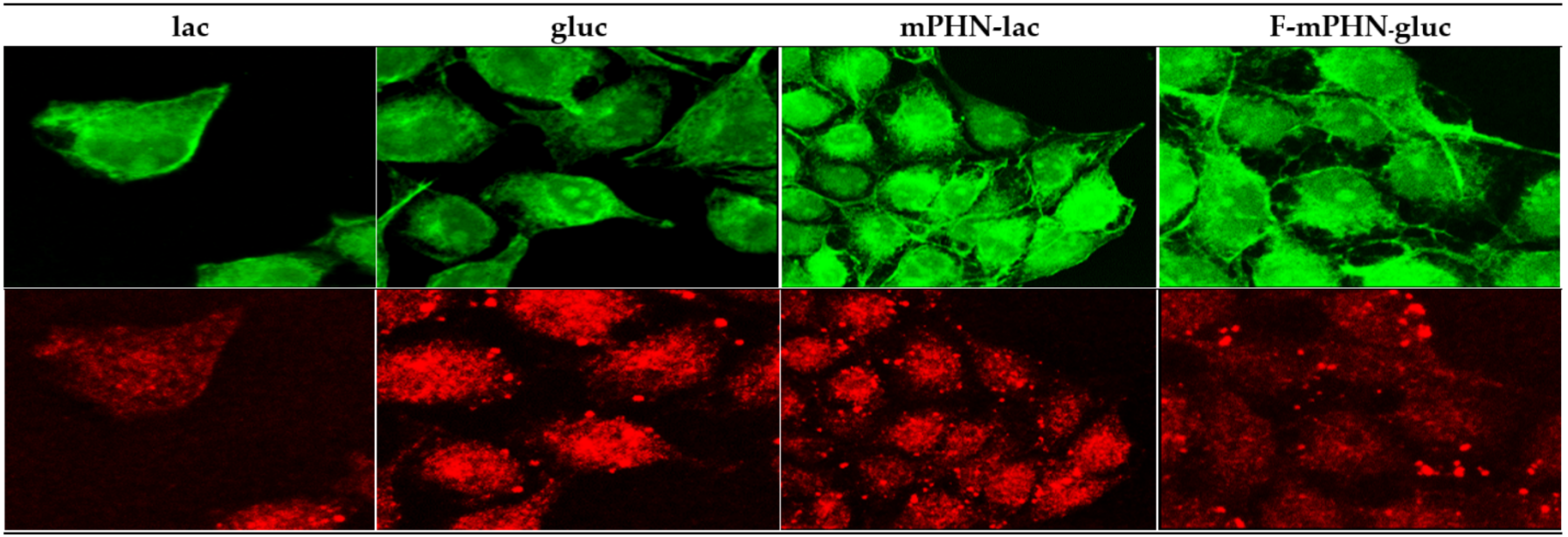

Figure 2. Changes in cytoskeleton of cancer cells visualized with confocal microscopy. Microtubular network—green channel (488 nm); Actin-cytokinoskeleton—red channel (546 nm); intermediate filaments (vimentin)—white channel (excitation—far red 647 nm). Brighter areas (greater density) that can be observed in green channels indicate greater polymerization of microtubules. An increased presence of biodiverse pickling inside the cytoplasm can be seen in red channels suggests an elevated content of depolymerized actin: (**a**) DU145 after 48 h of incubation; (**b**) High resolution images of DU145 after 48 h of incubation; (**c**) High resolution images of HTB140 after 48 h of incubation.

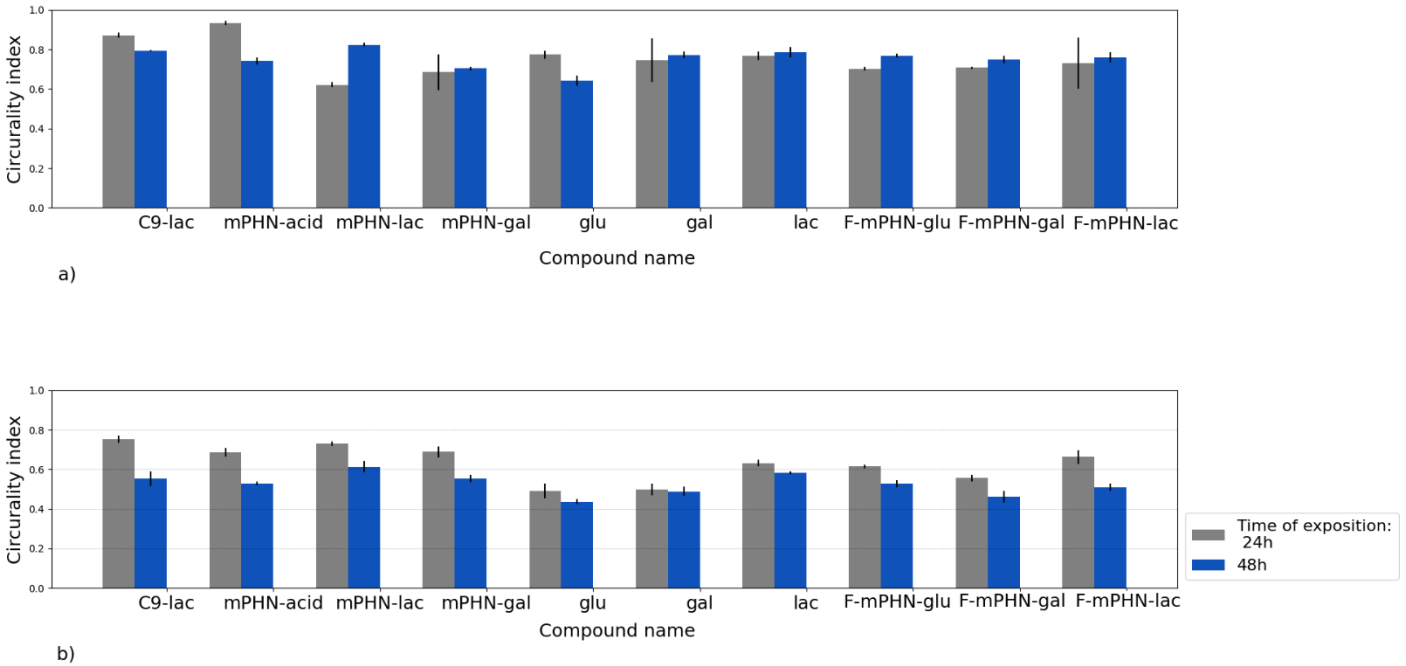

Figure 3. Changes of nuclei roundness based on image analysis algorithms. These small changes may indicate some reorganizations of cytoskeleton but are not typical for metastatic transition: (**a**) DU145; (**b**) HTB140.

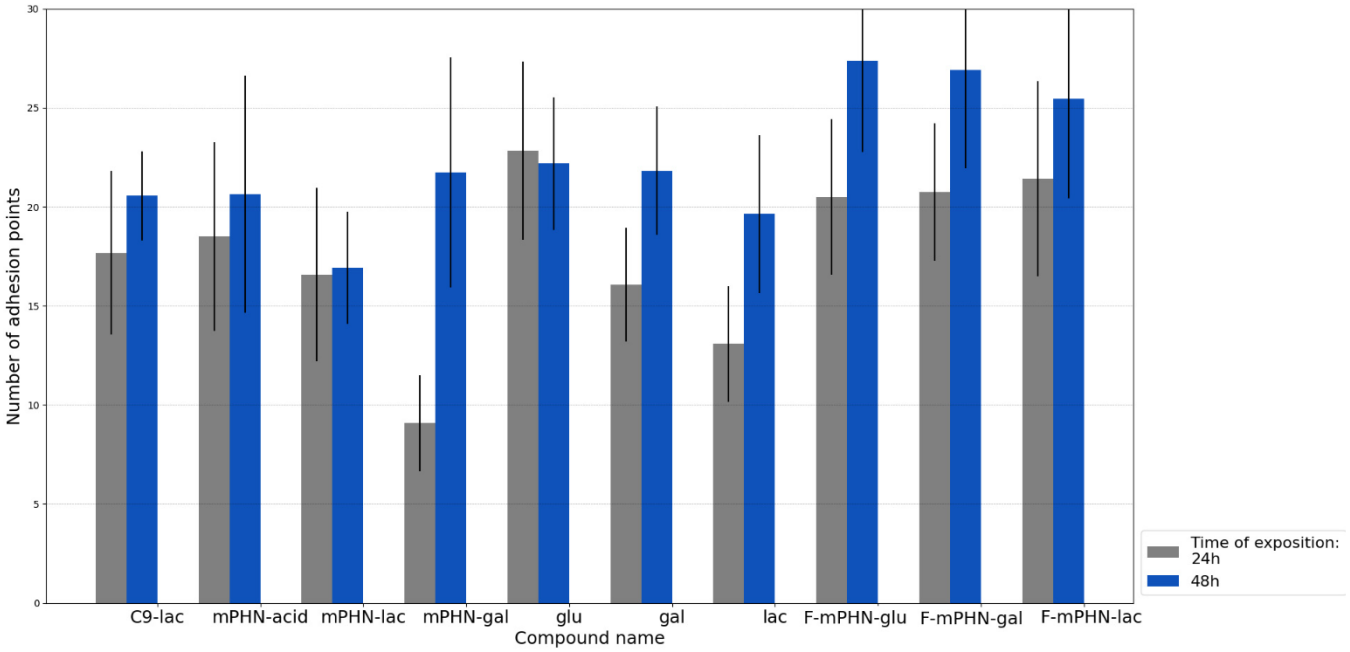

Figure 4. Number of adhesion points formed by DU145 cells during incubation with the investigated compounds (with concentrations below IC_{50}). Adhesion points defined as dot forms placed in the focal plane located between the cell body and glass surface. Their greater number may suggest intensification of migration process caused by investigated compounds. In case of HTB140 cells, no vimentin analysis was performed due to its almost complete depolymerization which indicates strong impact of SFAE on cytoskeleton.

3.5. Inhibition of Transmigration Caused by C9, mPHN-lac and mPHN-glu

The transmigration test was a model experiment that was performed to illustrate the ability of cells to transmigration through a microporous membrane, where the pores mimic chinks between epithelial cells. Cancer cells are able to penetrate the tissues and migrate through the walls of blood vessels into the vascular system, which is referred to as epithelial to mesenchymal transition [39]. This process allows cells to populate new niches in other tissues, creating metastases. The key issue was to learn whether the cancer cells migrate in a medium supplemented with the investigated SFAE below the IC_{50} values, and if yes, whether they are able to proliferate actively after the transition process. Therefore, transmigration values obtained after 96 h for the cancer cells treated with tested compounds were checked. In parallel, the proliferation of cells with the tested compounds was examined.

The results presented in Figure 5 are the ratios of transmigration to proliferation from the experimental conditions (from tested SFAE compounds at 0.0625 mg mL^{-1} concentration) in relation to the same ratios of the controls (glu, gal and lac, respectively at the same concentrations). Transmigration rates above 1.0 (100%) mean that the transmigration is enhanced, while rates below 1.0 mean that the total transmigration is inhibited by the tested compounds.

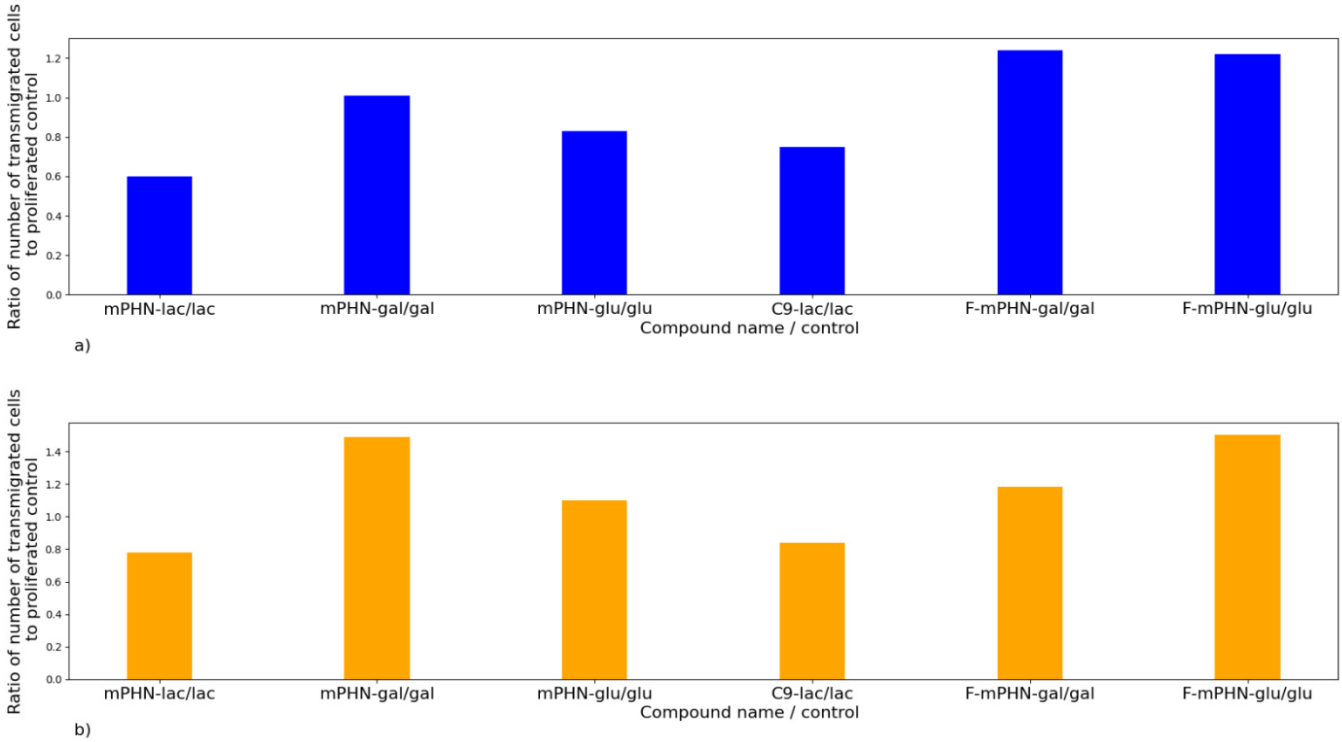

Figure 5. Transmigration assay of cancer cells in a presence of the investigated SFAE measured after 96 h. An increase in the ratio of proliferated cells after passing through the inserts, caused by the SFAE, may indicate that tested compounds could promote metastasis (at concentrations below the IC_{50}). A decrease in this ratio may indicate lack of such effect. (**a**) DU145; (**b**) HTB140.

Figure 5 shows that the concentration of 0.0625 mg mL^{-1} of mPHN-lac present in the culture medium reduced transmigration of DU145 cells in 96 h by 40%, mPHN-glu ester reduced this ability by 17%, whereas C9-lac by 25% and F-mPHN-glu by 7%. The rest of compounds had no significant effect or in case of mPHN-gal and fluorinated esters even increased the cell's ability of transmigration up to 22 to 24%. All compounds except mPHN-lac and c9-lac enhanced the transmigration of HTB140 cells from 6% (F-mPHN salt) even to 55% (F-mPHN-glu), respectively (Figure 5b). The mPHN-lac ester and the C9-lac ester decreased this factor by 22% and 16%, respectively. These data suggest that lactose esters inhibit transmigration of either prostate cancer and melanoma cells below IC_{50} concentrations. Moreover, presence of either not modified and modified mPHN component in the sugar esters affected positively on transmigration process below IC_{50} values.

4. Discussion

Analysis of SFAE composition basing on MS/MS detections (Table 1) confirmed the number of monomers attached to the sugar molecule impacts the quantity of alkyl halides introduced into the ester structure. The amount of hydrophobic chains attached to a sugar is determined by the lipase specificity and the conditions of the enzymatic reaction. As shown by the MTT results and reported by others, each of these modifications can have a significant effect on the cytotoxicity of the final SFAE. Synthesized sugar esters based on nonanoic acid, unmodified and modified mPHN turned out to affect DU145 and HTB140 cancer cells. The IC_{50} values determined by MTT tests were two to four times lower than in cells threated by the control compounds (C9, mPHN, F-mPHN, glu, gal and lac ranged from 0.23 to over 0.41 × 10^{-3} mol L^{-1}). At the same time, our SFAEs were less toxic towards the healthy cell lines (PNT2, HaCAT, HSF) with the cytotoxic concentrations being eightfold higher than these used to eliminate the cancer lines (from 0.17 to 2.4 × 10^{-3} mol L^{-1}, respectively). The range of these concentrations corresponds with the available

literature data on the antiproliferative properties of other sugar esters, especially those having the same number of carbon atoms in hydrophobic part of the molecule [15].

From the experimental data gathered it was evidenced that type and quantity of the monomers attached to the sugar molecule by the lipase, and also the type of sugar used, both have impact on the biological behavior of SFAE. Based on the UHPLC-MS/MS analysis of the compositions of each synthesized SFAE, together with the corresponding IC_{50} values, the structure–toxicity relations can be discussed. For example, C9-glu and C9-lac were composed of similar ratios of monoesters to diesters but exhibited different cytotoxicity levels towards tested cancer lines. That observation may suggest that the kind of sugar used (mono- vs. disaccharide) has a greater influence on the anticancer properties of SFAE when the same hydrophobic chain is considered. A similar pattern was observed when mPHN-based SFAE were tested, however the presence of the hydroxyl group on the aliphatic chain of SFAE resulted in the increased antiproliferative character of these sugar esters. Other studies report an important correlation in the level of cytotoxicity and the chain length of the hydrophobic component [30,35]. For example, the IC_{50} of an octanoic acid glucose ester against Jurkat (Human T-cell leukemia) was 0.12×10^{-3} mol L^{-1}, whereas the 16 carbon atoms counterpart was as low as 0.02×10^{-3} mol L^{-1}. This suggest that in future research it will be beneficial to screen longer fatty acid mixtures originating from polyhydroxyalkanoates for their potential in modulating the cytotoxicity of synthesized SFAEs.

The introduction of trifluoroethyl groups into mPHN further increased the cytotoxicity of the glucose and galactose esters. Interestingly, this modification did not have such a great effect on the lactose-based SFAE when compared to C9-lac or mPHN-lac compounds. It is known form the literature that nonspecific modifications of the aliphatic chain of SFAE by substitutions of hydrogen atoms by halides may further reduce the biological activity of the molecule (e.g., decrease of the glucose ester's cytotoxicity to over 0.20×10^{-3} mol L^{-1}), thus suggesting that a plan for manipulation of cytotoxicity of the SFAE presented in this work is promising for potential drug designing process.

Having examined the cytotoxicity of SFAE, we looked at the subcellular structures of the assayed cell lines after their exposition to the tested compounds below their IC_{50} concentrations. Esters (especially these based on lactose) interacted to some extend with intermediate pillars, in particular with vimentin (Figure 2—white channel), which was manifested by a minor increase in the number of cluster points after 48 h exposure to all of the tested compounds (Figure 4). In the literature, there is scarce information on SFAE interaction with the cytoskeleton. However preliminary conclusions can be drawn from observations of polyethylene glycol inhibition of polymerization/depolymerization of microtubules [40] or interactions of gallic acid-based glycoconjugates that target tubulin and its colchicine binding site [41]; that may in future help to explain antiproliferative properties of PHA-based SFAE. Nuclei shape and number of adhesion points may provide information about potential metastatic stages. Therefore, we have conducted microscopic observations of these structures. There were minimal changes in the roundness of the cell's nuclei over a period of 24–48 h that may indicate that all of the tested SFAE did not affect these organelles significantly while treating them below the IC_{50} concentrations (Figure 3). In addition, no significant differences were seen in the amounts of adhesion points between treated and untreated cells. Our survey showed decrease in transmigration of DU145 and HTB140 cells in most of the tested compounds, with the exception of these containing fluorine atoms. This phenomenon may be associated with disturbances in the cytoskeleton architecture, however it requires additional analysis of signaling pathways related to the cytoskeleton and cell movement at the molecular levels [41]. Altogether, and keeping in mind the relatively high cytotoxicity of SFAE (Table 2), we can assume that the synthesized sugar esters will not promote metastasis.

5. Conclusions

Despite relatively high IC_{50} values (0.06–0.17 × 10^{-3} mol L^{-1}) of the synthesized SFAEs in comparison to commonly used chemotherapeutics, the studied compounds can compete with other SFAEs already described in the literature. Their contribution in drug designing process may rely on either using the SFAE as potentially active substances or as supporting therapeutics. These PHA-based surfactants may form microemulsions or self-microemulsifying drug delivery system (SMEDDS), which may help to stabilize and distribute commercially used medicines for cancer treatment or gene therapy; thus, SFAE-based carriers could co-work with chemotherapeutics by their own cytotoxic properties [42–44]. However, antimetastatic properties of our SFAE require further investigations due to their visible influence on cytoskeleton and cell intermediate filaments [41]. Finally, the panel of tested cell lines in the cytotoxicity experiments should be extended to include other lines that may be more sensitive to the synthesized compounds. In summary, the data contained within this manuscript are benchmarks for future studies related to the creation of SMEDDS based on synthetized SFAE for targeted anticancer therapies.

6. Patents

The work presented in this manuscript is a part of a Polish patent application number P.437233 "Use of sugar esters of fatty acids, with an acid component as a mixture of monomers derived from bacterial polyhydroxynonanoate-co-heptanoate, to inhibit tumour cell proliferation in the treatment and prevention of diseases" submitted on 8 March 2021.

Supplementary Materials: Supplementary Materials can be found at www.mdpi.com/1422-0067/22/13/7238/s1.

Author Contributions: Conceptualization. M.G.; methodology. W.S., D.W., T.W. and J.S.; validation. W.S., D.W., T.W. and J.S.; formal analysis. W.S. and D.W.; investigation. W.S., D.W., T.W. and E.J.; resources. M.G., A.J.B. and F.J.P.; data curation. W.S.; writing—original draft preparation. W.S., T.W. and D.W.; writing—review and editing. M.G., A.J.B., J.S. and F.J.P.; visualization. W.S. and T.W.; supervision. M.G. and J.S.; project administration. M.G.; funding acquisition. M.G. All authors have read and agreed to the published version of the manuscript.

Funding: This work was supported by the National Science Centre, Poland [SONATA no. 2015/17/D/ST4/00514].

Institutional Review Board Statement: Not applicable.

Informed Consent Statement: Not applicable.

Data Availability Statement: Data is contained within the article or supplementary material.

Acknowledgments: We thank Zbigniew Madeja and Justyna Drukała from the Department of Cell Biology of the Jagiellonian University for providing the equipment for conducting cell tests in this publication. Wojciech Snoch acknowledges the support of InterDokMed project no. POWR.03.02.00-00-I013/16. We greatly acknowledge the joint consortium "Interdisciplinary Centre of Physical, Chemical and Biological Sciences" of ICSC PAS and INP PAS for providing access to the Agilent 1290 Infinity System with an automatic autosampler and an MS Agilent 6460 Triple Quad Detector.

Conflicts of Interest: The authors declare no conflict of interest. The funders had no role in the design of the study, in the collection, analyses, interpretation of data, in the writing of the manuscript.

Abbreviations

C9	nonanoic acid
C9-Me	nonanoic methyl ester
PHN	poly-(3R)-hydroxynonanoate-co-(3R)-hydroxyheptanoate
R3OH-C9	(3R)-hydroxynonanoate
R3OH-C7	(3R)-hydroxyheptanoate

mPHN	mixture of PHN monomers hydroxyacids: (3R)-hydroxynonanoate and (3R)-hydroxyheptanoate
mPHN-Me	mixture of PHN monomemers methyl esters: (3R)-hydroxynonanoate methyl esters
R3OH-C9-Me	(3R)-hydroxynonanoate methyl esters
R3OH-C7-Me	(3R)-hydroxyheptanoate methyl esters
F-mPHN-Me	mixture of fluorinated PHN monomers: (3R)-3-(2,2,2-trifluoroethoxy)nonanoate methyl esters and (3R)-3-(2,2,2-trifluoroethoxy)heptanoate methyl esters
glu	α-D-glucopiranose
gal	β-d-galactopyranose
lac	β-D-Galactopyranosyl-(1→4)-D-glucopiranose
C9-glu	glucose nonanoic ester
C9-gal	galactose nonanoic ester
C9-lac	lactose nonanoic ester
mPHN-glu	mixture of (3R)-hydroxynonanoate glucose esters and (3R)-hydroxyheptanoate glucose esters
mPHN-gal	mixture of (3R)-hydroxynonanoate galactose esters and (3R)-hydroxyheptanoate galactose esters
mPHN-lac	mixture of (3R)-hydroxynonanoate lactose esters and (3R)-hydroxyheptanoate lactose esters
F-mPHN-glu	mixture of (3R)-3-(2,2,2-trifluoroethoxy)nonanoate glucose esters and (3R)-3-(2,2,2-trifluoroethoxy)heptanoate glucose esters
F-mPHN-gal	mixture of (3R)-3-(2,2,2-trifluoroethoxy)nonanoate galactose esters and (3R)-3-(2,2,2-trifluoroethoxy)heptanoate galactose esters
F-mPHN-lac	mixture of (3R)-3-(2,2,2-trifluoroethoxy)nonanoate lactose esters and (3R)-3-(2,2,2-trifluoroethoxy)heptanoate lactose esters

References

1. WHO Cancer. 2021. Available online: https://www.who.int/health-topics/cancer (accessed on 15 March 2021).
2. Miller, K.D.; Nogueira, L.; Mariotto, A.B.; Rowland, J.H.; Yabroff, K.R.; Alfano, C.M.; Jemal, A.; Kramer, J.L.; Siegel, R.L. Cancer treatment and survivorship statistics, 2019. *CA Cancer J. Clin.* **2019**, *69*, 363–385, doi:10.3322/caac.21565.
3. Ferlay, J.; Colombet, M.; Soerjomataram, I.; Dyba, T.; Randi, G.; Bettio, M.; Gavin, A.; Visser, O.; Bray, F. Cancer incidence and mortality patterns in Europe: Estimates for 40 countries and 25 major cancers in 2018. *Eur. J. Cancer* **2018**, *103*, 356–387, doi:10.1016/j.ejca.2018.07.005.
4. Babaei, N.; Salamci, M.U. Mixed therapy in cancer treatment for personalized drug administration using model reference adaptive control. *Eur. J. Control* **2019**, *50*, 117–137, doi:10.1016/j.ejcon.2019.03.001.
5. Rao, S.; Sclafani, F.; Eng, C.; Adams, R.A.; Guren, M.G.; Sebag-Montefiore, D.; Benson, A.; Bryant, A.; Peckitt, C.; Segelov, E.; et al. International rare cancers initiative multicenter randomized phase II trial of cisplatin and fluorouracil versus carboplatin and paclitaxel in advanced anal cancer: InterAAct. *J. Clin. Oncol.* **2020**, *38*, 2510–2518, doi:10.1200/JCO.19.03266.
6. Meric-Bernstam, F.; Gonzalez-Angulo, A.M. Targeting the mTOR signaling network for cancer therapy. *J. Clin. Oncol.* **2009**, *27*, 2278–2287, doi:10.1200/JCO.2008.20.0766.
7. Kalia, V.C.; Patel, S.K.S.; Cho, B.-K.; Wood, T.K.; Lee, J.-K. Emerging applications of bacteria as antitumor agents. *Semin. Cancer Biol.* **2021**, doi:10.1016/j.semcancer.2021.05.012.
8. Kovvasu, S.P.; Kunamaneni, P.; Joshi, R. Self-emulsifying Drug Delivery Systems and their Marketed Products: A Review. *Asian J. Pharm.* **2019**, *13*, 73–84.
9. Staroń, J.; Dąbrowski, J.M.; Cichoń, E.; Guzik, M. Lactose esters: Synthesis and biotechnological applications. *Crit. Rev. Biotechnol.* **2018**, *38*, 245–258, doi:10.1080/07388551.2017.1332571.
10. El-Laithy, H.M.; Shoukry, O.; Mahran, L.G. Novel sugar esters proniosomes for transdermal delivery of vinpocetine: Preclinical and clinical studies. *Eur. J. Pharm. Biopharm.* **2011**, *77*, 43–55, doi:10.1016/j.ejpb.2010.10.011.
11. Liang, M.Y.; Banwell, M.G.; Wang, Y.; Lan, P. Effect of Variations in the Fatty Acid Residue of Lactose Monoesters on Their Emulsifying Properties and Biological Activities. *J. Agric. Food Chem.* **2018**, *66*, 12594–12603, doi:10.1021/acs.jafc.8b05794.
12. Enayati, M.; Gong, Y.; Goddard, J.M.; Abbaspourrad, A. Synthesis and characterization of lactose fatty acid ester biosurfactants using free and immobilized lipases in organic solvents. *Food Chem.* **2018**, *266*, 508–513, doi:10.1016/j.foodchem.2018.06.051.
13. Marquis, R.E.; Clock, S.A.; Mota-Meira, M. Fluoride and organic weak acids as modulators of microbial physiology. **2003**, *26*, 493–510.
14. Lucarini, S.; Fagioli, L.; Campana, R.; Cole, H.; Duranti, A.; Baffone, W.; Vllasaliu, D.; Casettari, L. Unsaturated fatty acids lactose esters: Cytotoxicity, permeability enhancement and antimicrobial activity. *Eur. J. Pharm. Biopharm.* **2016**, *107*, 88–96, doi:10.1016/j.ejpb.2016.06.022.

15. Lucarini, S.; Fagioli, L.; Cavanagh, R.; Liang, W.; Perinelli, D.R.; Campana, M.; Stolnik, S.; Lam, J.K.W.; Casettari, L.; Duranti, A. Synthesis, structure–activity relationships and in vitro toxicity profile of lactose-based fatty acid monoesters as possible drug permeability enhancers. *Pharmaceutics* **2018**, *10*, 81, doi:10.3390/pharmaceutics10030081.
16. Ferrer, M.; Perez, G.; Plou, F.J.; Castell, J.V.; Ballesteros, A. Antitumour activity of fatty acid maltotriose esters obtained by enzymatic synthesis. *Biotechnol. Appl. Biochem.* **2005**, *42 Pt 1*, 35–39, doi:10.1042/BA20040122.
17. Okabe, S.; Suganuma, M.; Tada, Y.; Ochiai, Y.; Sueoka, E.; Kohya, H.; Shibata, A.; Takahashi, M.; Mizutani, M.; Matsuzaki, T.; et al. Disaccharide esters screened for inhibition of tumor necrosis factor-α release are new anti-cancer agents. *Jpn. J. Cancer Res.* **1999**, *90*, 669–676, doi:10.1111/j.1349-7006.1999.tb00799.x.
18. Yanagita, R.C.; Kobashi, K.; Ogawa, C.; Ashida, Y.; Yamaashi,H.; Kawanami, Y. Anti-proliferative activity of 6-O-acyl-D-allose against the human leukemia MOLT-4F cell line. *Biosci. Biotechnol. Biochem.* **2014**, *78*, 190–194, doi:10.1080/09168451.2014.882747.
19. Kasuya, M.C.Z.; Ito, A.; Cusi, R.; Sato, T.; Hatanaka, K. Cellular uptake and saccharide chain elongation of "fluoro- amphiphilic" glycosides. *Chem. Lett.* **2005**, *34*, 856–857, doi:10.1246/cl.2005.856.
20. Yerien, D.E.; Bonesi, S.; Postigo, A. Fluorination methods in drug discovery. *Org. Biomol. Chem.* **2016**, *14*, 8398–8427, doi:10.1039/c6ob00764c.
21. Murphy, C.D.; Sandford, G. Recent advances in fluorination techniques and their anticipated impact on drug metabolism and toxicity. *Expert Opin. Drug Metab. Toxicol.* **2015**, *11*, 589–599, doi:10.1517/17425255.2015.1020295.
22. Gál, B.; Bucher, C.; Burns, N.Z. Chiral alkyl halides: Underexplored motifs in medicine. *Mar. Drugs* **2016**, *14*, 206, doi:10.3390/md14110206.
23. Zhou, J.; Gupta, K.; Aggarwal, S.; Aneja, R.; Chandra, R.; Panda, D.; Joshi, H.C. Brominated derivatives of noscapine are potent microtubule-interfering agents that perturb mitosis and inhibit cell proliferation. *Mol. Pharmacol.* **2003**, *63*, 799–807, doi:10.1124/mol.63.4.799.
24. Isanbor, C.; Hagan, D.O. Fluorine in medicinal chemistry : A review of anti-cancer agents. *J. Fluor. Chem.* **2006**, *127*, 303–319, doi:10.1016/j.jfluchem.2006.01.011.
25. Kirk, K.L. Fluorine in medicinal chemistry : Recent therapeutic applications of fluorinated small molecules. *J. Fluor. Chem.* **2006**, *127*, 1013–1029, doi:10.1016/j.jfluchem.2006.06.007.
26. Ducki, S.; Forrest, R.; Hadfield, J.A.; Kendall, A.; Lawrence, N.J.; McGown, A.T.; Rennison, D. Potent antimitotic and cell growth inhibitory properties of substituted chalcones. *Bioorganic Med. Chem. Lett.* **1998**, *8*, 1051–1056, doi:10.1016/S0960-894X(98)00162-0.
27. Li, X.; Turánek, J.; Knötigová, P.; Kudláčková, H.; Mašek, J.; Parkin, S.; Rankin, S.E.; Knutson, B.L.; Lehmler, H.J. Hydrophobic tail length, degree of fluorination and headgroup stereochemistry are determinants of the biocompatibility of (fluorinated) carbohydrate surfactants. *Colloids Surf. B Biointerfaces* **2009**, *73*, 65–74, doi:10.1016/j.colsurfb.2009.04.023.
28. Kalia, V.C.; Singh Patel, S.K.; Shanmugam, R.; Lee, J.K. Polyhydroxyalkanoates: Trends and advances toward biotechnological applications. *Bioresour. Technol.* **2021**, *326*, 124737, doi:10.1016/j.biortech.2021.124737.
29. Snoch, W.; Stępień, K.; Prajsnar, J.; Staroń, J.; Szaleniec, M.; Guzik, M. Influence of chemical modifications of polyhydroxyalkanoate-derived fatty acids on their antimicrobial properties. *Catalysts* **2019**, *9*, 510, doi:10.3390/catal9060510.
30. Sofińska, K.; Barbasz, J.; Witko, T.; Dryzek, J.; Haraźna, K.; Witko, M.; Kryściak-Czerwenka, J.; Guzik, M. Structural, topographical, and mechanical characteristics of purified polyhydroxyoctanoate polymer. *J. Appl. Polym. Sci.* **2019**, *136*, 136, doi:10.1002/app.47192.
31. Guzik, M.; Witko, T.; Steinbüchel, A.; Wojnarowska, M.; Sołtysik, M.; Wawak, S. What Has Been Trending in the Research of Polyhydroxyalkanoates? A Systematic Review. *Front. Bioeng. Biotechnol.* **2020**, *8*, 35–39, doi:10.3389/fbioe.2020.00959.
32. Witko, T.; Solarz, D.; Feliksiak, K.; Rajfur, Z.; Guzik, M. Cellular architecture and migration behavior of fibroblast cells on polyhydroxyoctanoate (PHO): A natural polymer of bacterial origin. *Biopolymers* **2019**, *110*, e23324, doi:10.1002/bip.23324.
33. Povea-Cabello, S.; Oropesa-Ávila, M.; de la Cruz-Ojeda, P.; Villanueva-Paz, M.; de la Mata, M.; Suárez-Rivero, J.M.; Álvarez-Córdoba, M.; Villalón-García, I.; Cotán, D.; Ybot-González, P.; et al. Dynamic reorganization of the cytoskeleton during apoptosis: The two coffins hypothesis. *Int. J. Mol. Sci.* **2017**, *18*, 2393, doi:10.3390/ijms18112393.
34. Gourlay, C.; Ayscough, K. The actin cytoskeleton in ageing and apoptosis. *FEMS Yeast Res.* **2005**, *5*, 1193–1198.
35. Ankam, S.; Teo, B.K.K.; Pohan, G.; Ho, S.W.L.; Lim, C.K.; Yim, E.K.F. Temporal Changes in Nucleus Morphology, Lamin A/C and Histone Methylation During Nanotopography-Induced Neuronal Differentiation of Stem Cells. *Front. Bioeng. Biotechnol.* **2018**, *6*, 6, doi:10.3389/fbioe.2018.00069.
36. Lennerz, J.; Schöchlin, M.; Weissinger, S.; Brandes, A.; Herrmann, M.; Möller, P. A nuclear circularity-based classifier for diagnostic distinction of desmoplastic from spindle cell melanoma in digitized histological images. *J. Pathol. Inform.* **2014**, *5*, 40, doi:10.4103/2153-3539.143335.
37. Wang, B.; Hu, Q.; Wan, T.; Yang, F.; Cui, L.; Hu, S.; Gong, B.; Li, M.; Zheng, Q.C. Porous Lactose-Modified Chitosan Scaffold for Liver Tissue Engineering: Influence of Galactose Moieties on Cell Attachment and Mechanical Stability. *Int. J. Polym. Sci.* **2016**, *2016*, 2862738, doi:10.1155/2016/2862738.
38. Carolina, N.; Carolina, N.; Hill, C.; Carolina, N. Cell Migration. *Compr Physiol.* **2015**, *2*, 2369–2392, doi:10.1002/cphy.c110012.Cell.
39. Liu, C.Y.; Lin, H.H.; Tang, M.J.; Wang, Y.K. Vimentin contributes to epithelial-mesenchymal transition ancer cell mechanics by mediating cytoskeletal organization and focal adhesion maturation. *Oncotarget* **2015**, *6*, 15966–15983, doi:10.18632/oncotarget.3862.

40. Bachand, G.D.; Jain, R.; Ko, R.; Bouxsein, N.F.; Vandelinder, V. Inhibition of Microtubule Depolymerization by Osmolytes. *Biomacromolecules* **2018**, *19*, 2401–2408, doi:10.1021/acs.biomac.7b01799.
41. Upadhyaya, K.; Hamidullah; Singh, K.; Arun, A.; Shukla, M.; Srivastava, N.; Ashraf, R.; Sharma, A.; Mahar, R.; Shukla, S.K.; et al. Identification of gallic acid based glycoconjugates as a novel tubulin polymerization inhibitors. *Org. Biomol. Chem.* **2016**, *14*, 1338–1358, doi:10.1039/c5ob02113h.
42. Zhao, Y.; Liu, A.; Du, Y.; Cao, Y.; Zhang, E.; Zhou, Q.; Hai, H.; Zhen, Y.; Zhang, S. Effects of sucrose ester structures on liposome-mediated gene delivery. *Acta Biomater.* **2018**, *72*, 278–286, doi:10.1016/j.actbio.2018.03.031.
43. Guan, Y.; Chen, H.; Zhong, Q. Nanoencapsulation of caffeic acid phenethyl ester in sucrose fatty acid esters to improve activities against cancer cells. *J. Food Eng.* **2019**, *246*, 125–133, doi:10.1016/j.jfoodeng.2018.11.008.
44. Richard, J. Challenges and opportunities in the delivery of cancer therapeutics. *Ther. Deliv.* **2011**, *2*, 107–121, doi:10.4155/tde.10.89.

In search for effective anticancer agents – novel sugar esters based on polyhydroxyalkanoate monomers

Wojciech Snoch[1], Dawid Wnuk[2], Tomasz Witko[1], Jakub Staroń[3], Andrzej J. Bojarski[3], Ewelina Jarek[1], Francisco J. Plou[4], Maciej Guzik[1]

[1] Jerzy Haber Institute of Catalysis and Surface Chemistry, Polish Academy of Sciences, Niezapominajek 8, 30-239 Kraków, Poland

[2] Department of Cell Biology, Faculty of Biochemistry, Biophysics and Biotechnology, Jagiellonian University, Gronostajowa 7, 30-387 Kraków, Poland

[3] Institute of Pharmacology, Polish Academy of Sciences, Smętna 12, 31-343 Kraków, Poland

[4] Instituto de Catalisis y Petroleoquimica, CSIC (Spanish National Research Council), Calle de Marie Curie, 2, 28049 Madrid, Spain

* Correspondence: maciej.guzik@ikifp.edu.pl; Tel.: +48 12 6395 159

SUPPLEMENTARY

Index of figures and tables:

- Fig 13. IR spectra of lactose mono and diesters esters originated from mixture of fluorinated PHN monomers (F-mPHN-lac)
- Fig 14. IR spectra of fluorinated esters set together

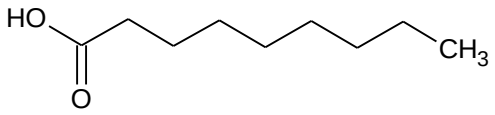

a) **C9**: nonanoic acid

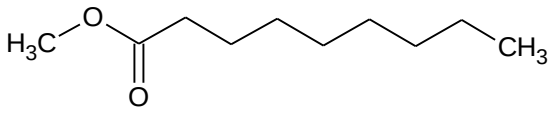

b) **C9-Me**: nonanoic methyl ester

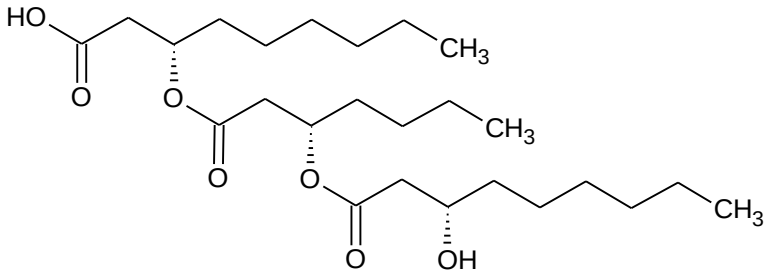

c) **PHN**: poly -(3*R*)-hydroxynonanoate- co- (3*R*)-hydroxyheptanoate

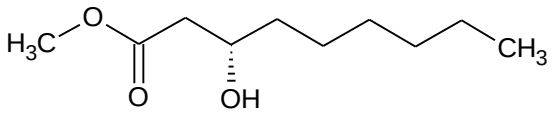

d) **R3OH-C9-Me**: mixture of (3*R*)-hydroxynonanoate methyl esters

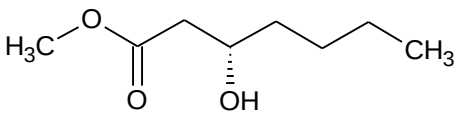

e) **R3OH-C7-Me**: mixture of (3*R*)-hydroxyheptanoate methyl esters

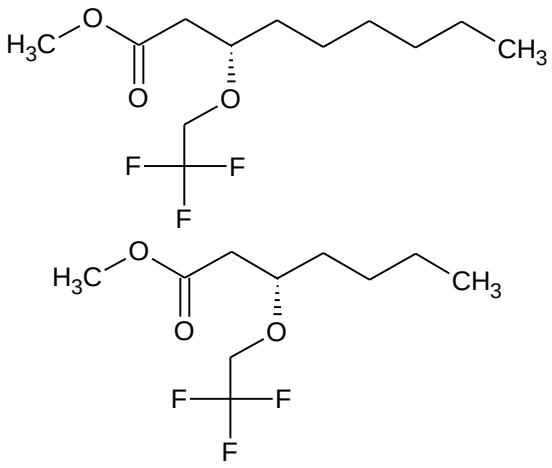

f) **F-mPHN-Me**: mixture of fluorinated PHN monomers: (3*R*)-3-(2,2,2-trifluoroethoxy)nonanoate methyl esters and (3*R*)-3-(2,2,2-trifluoroethoxy)heptanoate methyl esters

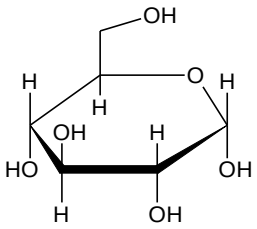

g) **glu**: α-D-glucopiranose

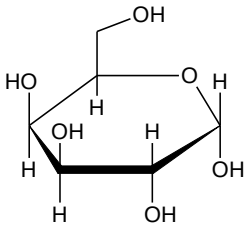

h) **gal**: β-D-galactopyranose

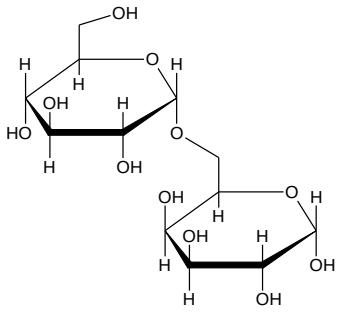

i) **lac**: β-D-Galactopyranosyl-(1→4)-D-glucopiranose

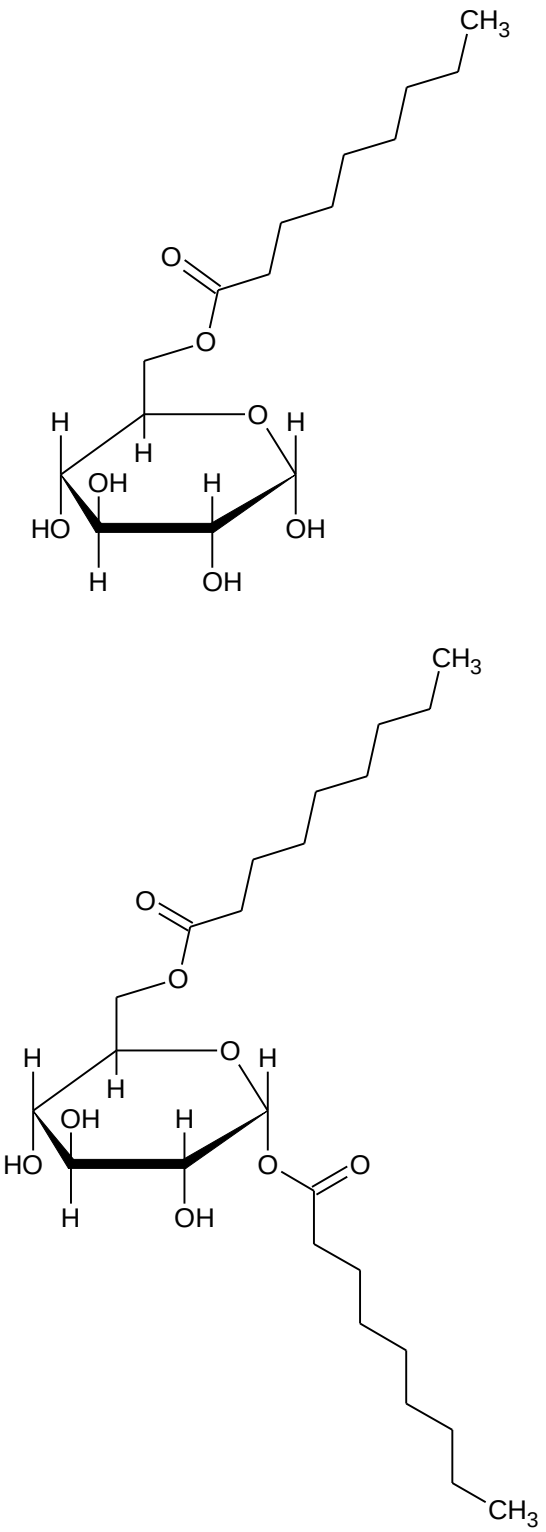

j) **C9-glu**: mixture of glucose nonanoic mono and diesters

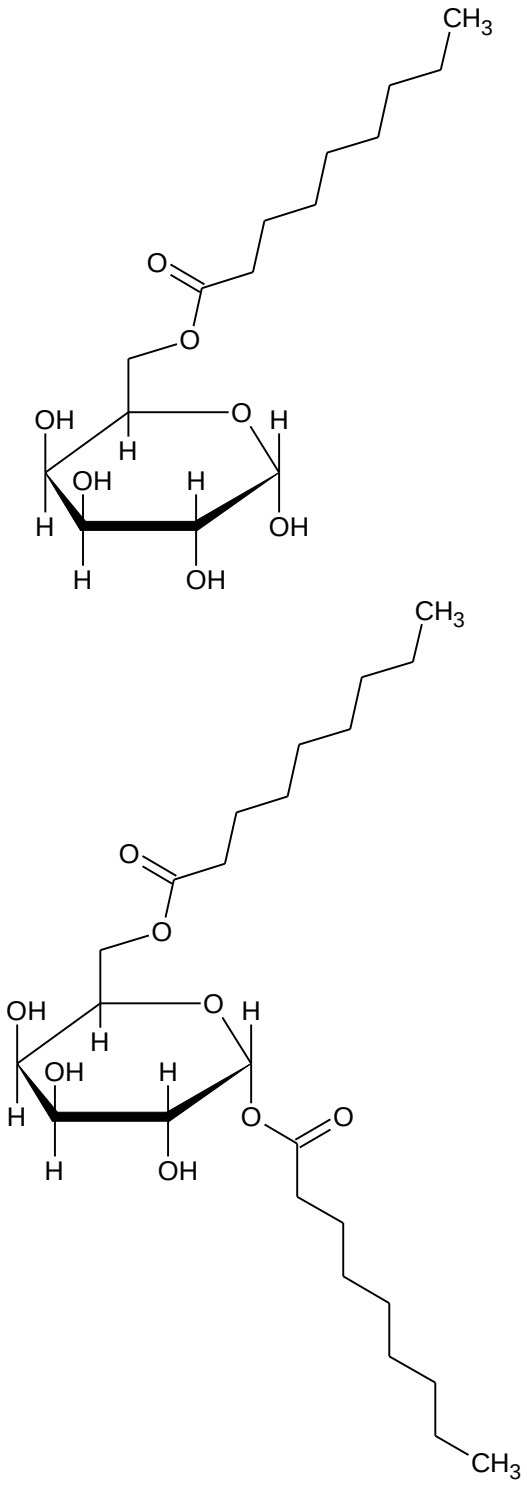

k) **C9-gal**: mixture of galactose nonanoic mono and diesters

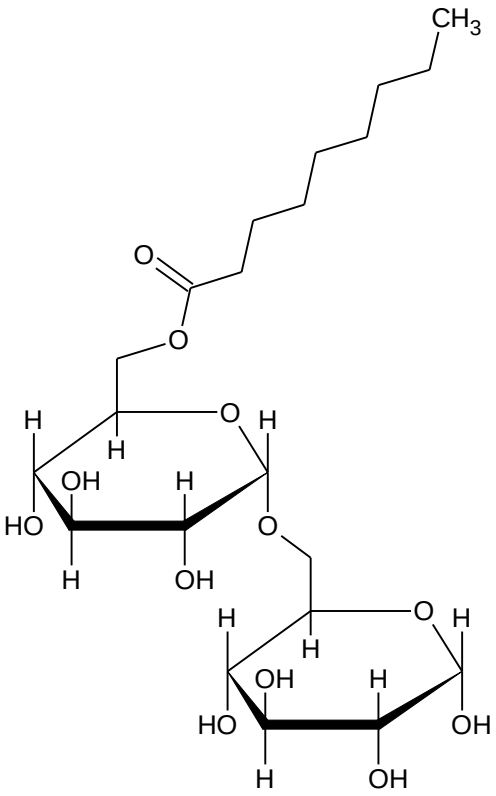
CH3
O
O
H
O
H
H
OH
H
HO
O
H
OH
H
O
H
H
OH
H
HO
OH
H
OH

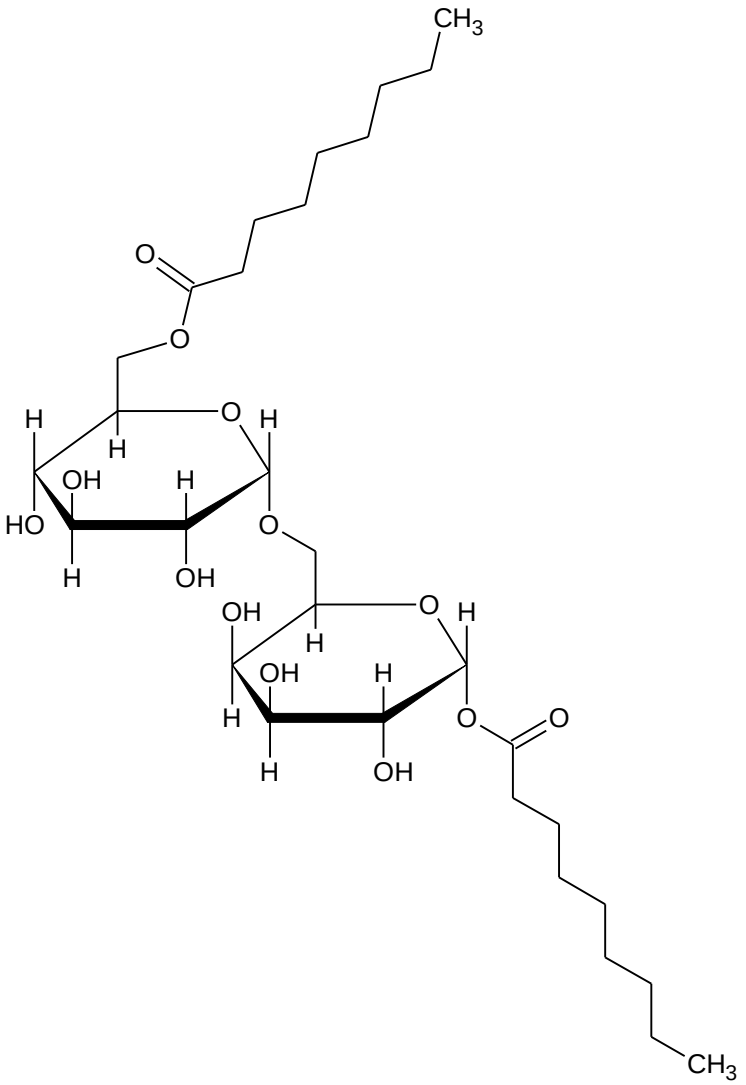

l) **C9-lac**: mixture of lactose nonanoic mono and diesters

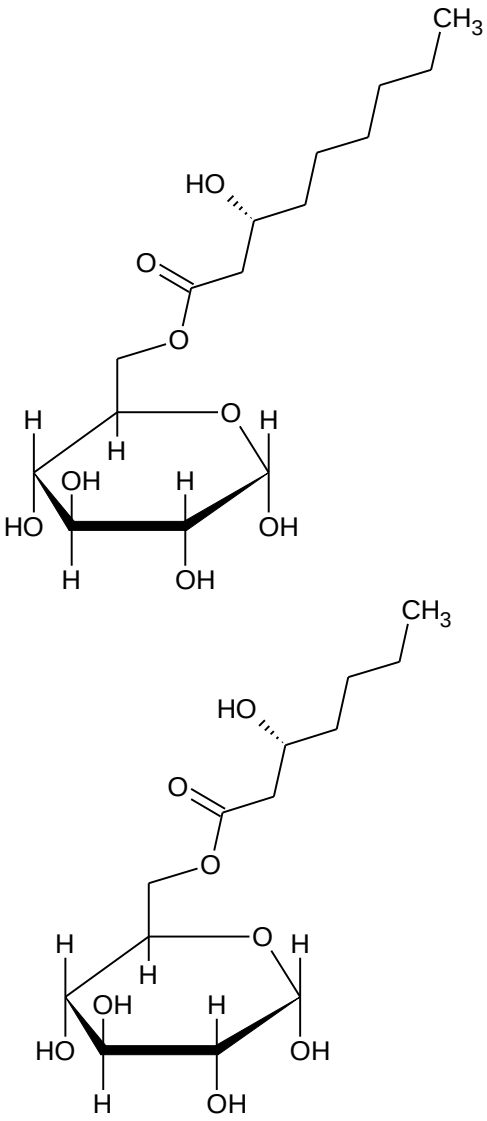
CH3
HO
O
O
H
O
H
H
H
OH
H
HO
OH
H
OH
CH3
HO
O
O
H
O
H
H
H
OH
H
HO
OH
H
OH

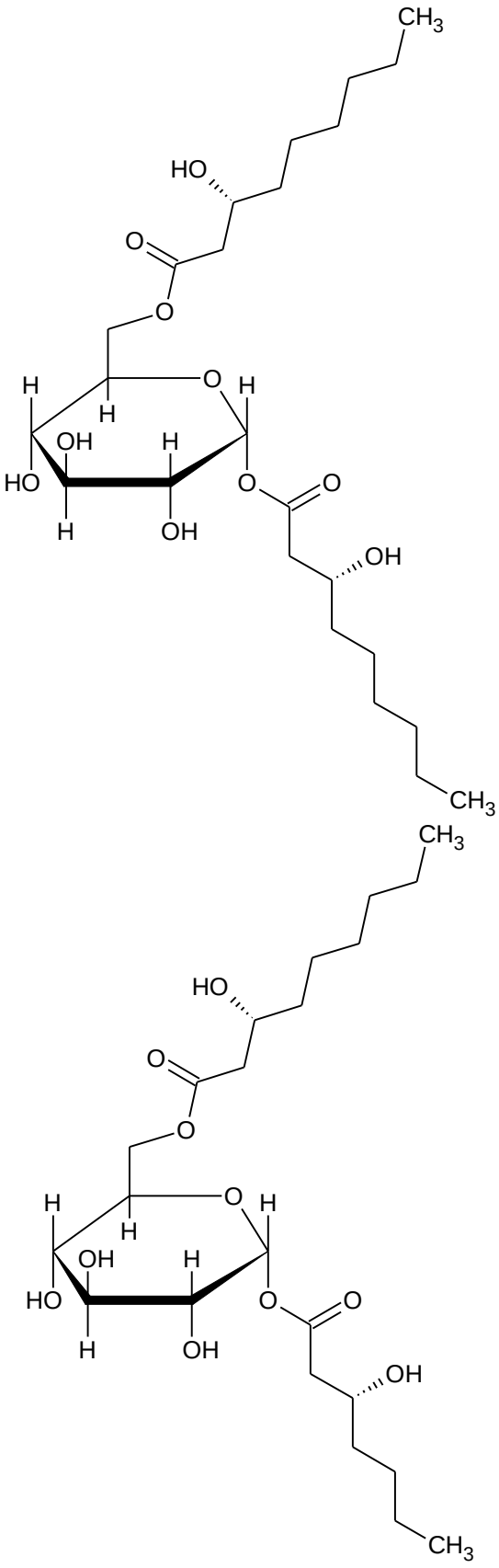
CH3
HO
O
O
H
H
O
H
OH
H
HO
O
O
H
OH
OH
CH3
CH3
HO
O
O
H
H
O
H
OH
H
HO
O
O
H
OH
OH
CH3

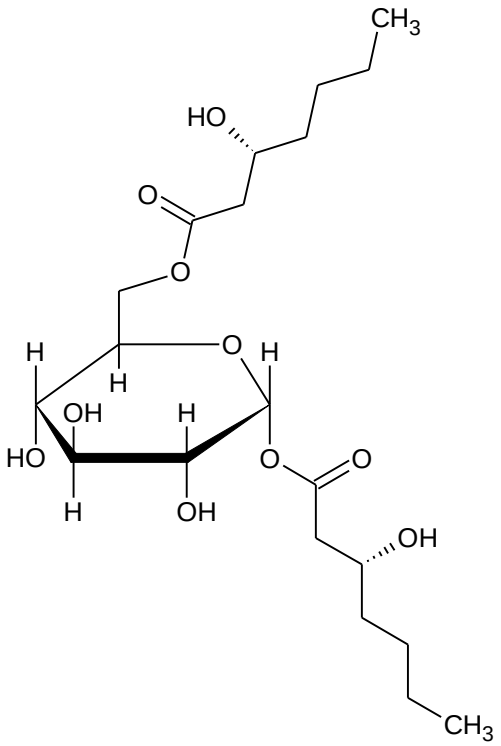

m) **mPHN-glu**: mixture of (3*R*)-hydroxynonanoate glucose esters and (3*R*)-hydroxyheptanoate glucose mono and diesters

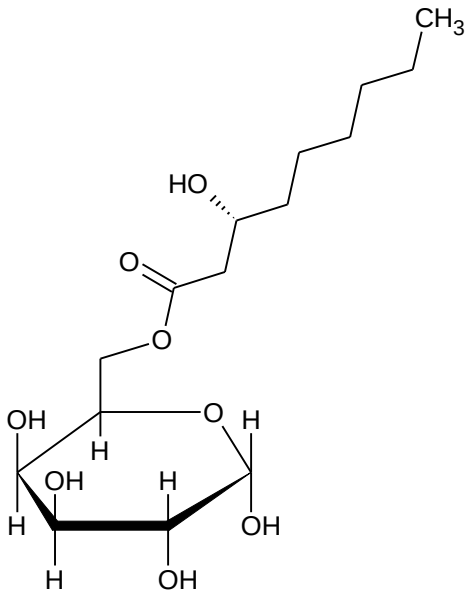

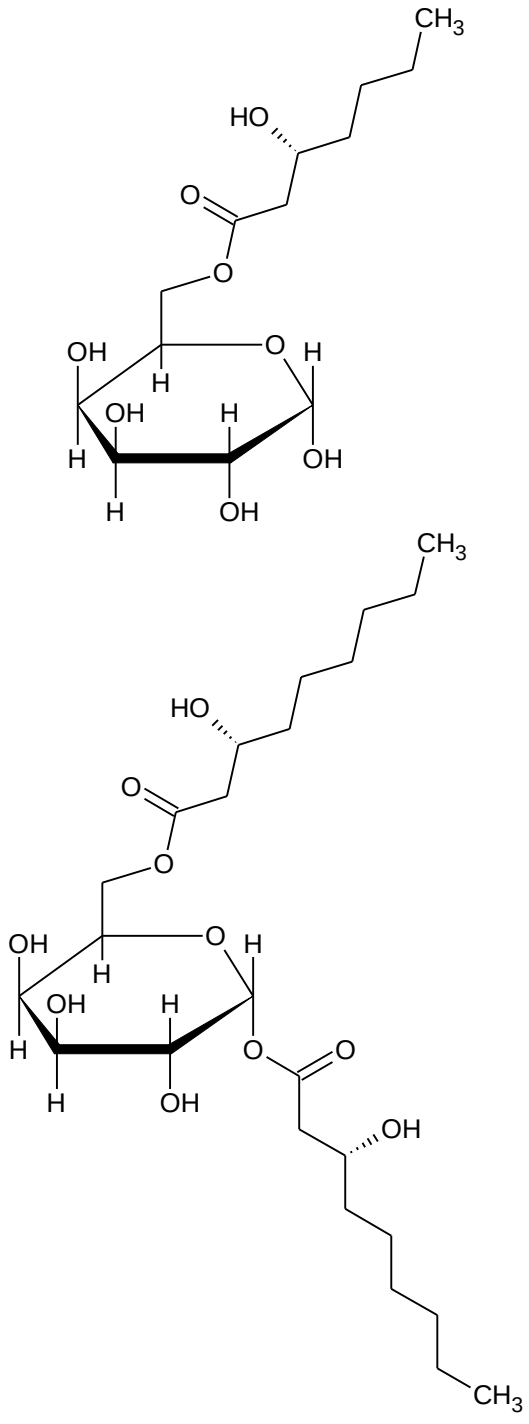
CH3
HO
O
O
OH
O
H
H
OH
H
H
OH
H
H
OH
CH3
HO
O
O
OH
O
H
H
OH
H
H
O
O
OH
H
H
OH
CH3

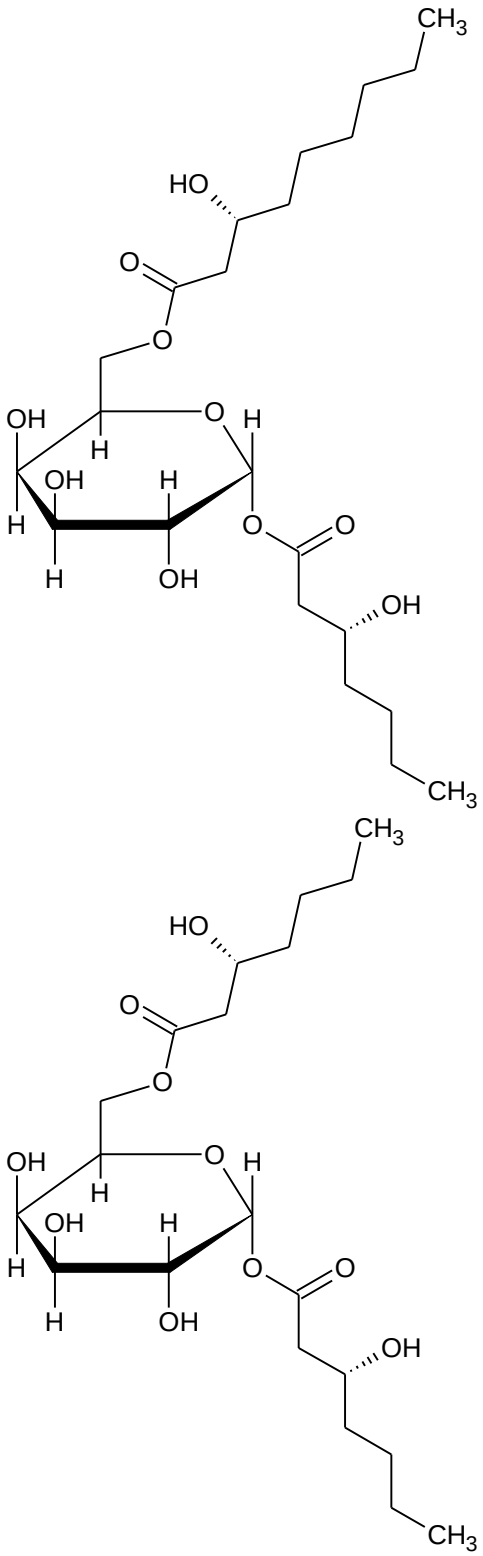

n) **mPHN-gal**: mixture of (3*R*)-hydroxynonanoate galactose esters and (3*R*)-hydroxyheptanoate galactose mono and diesters

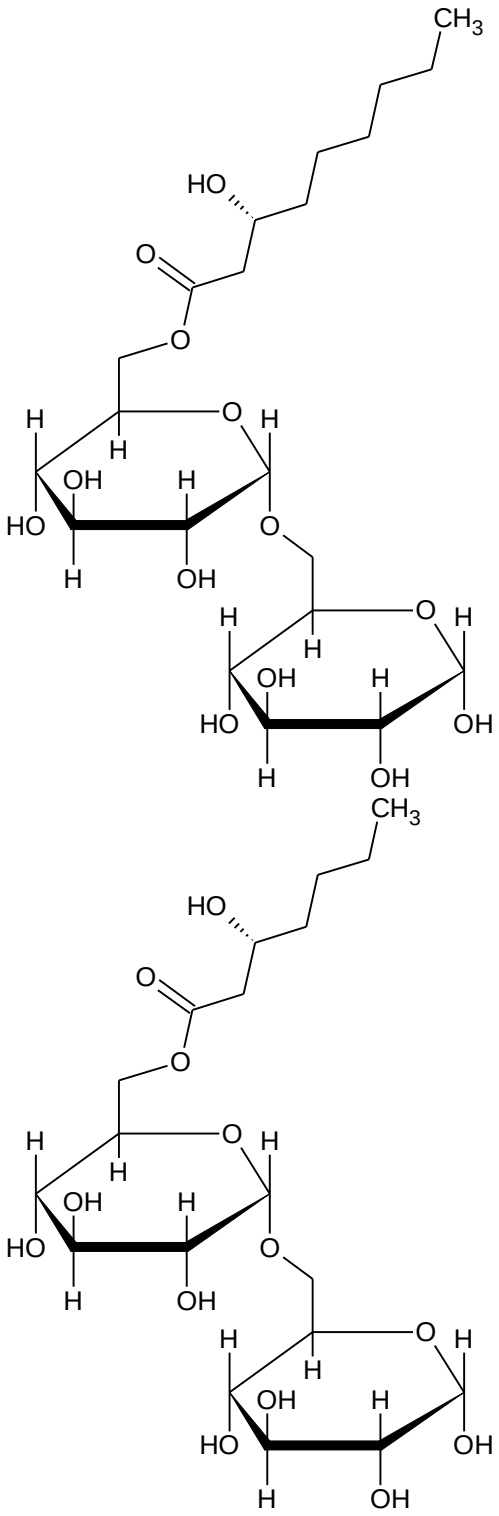
CH3
HO
O
O
H
O
H
H
OH
H
HO
O
H
OH
O
H
H
OH
H
HO
OH
H
OH
CH3
HO
O
O
H
O
H
H
OH
H
HO
O
H
OH
O
H
H
OH
H
HO
OH
H
OH

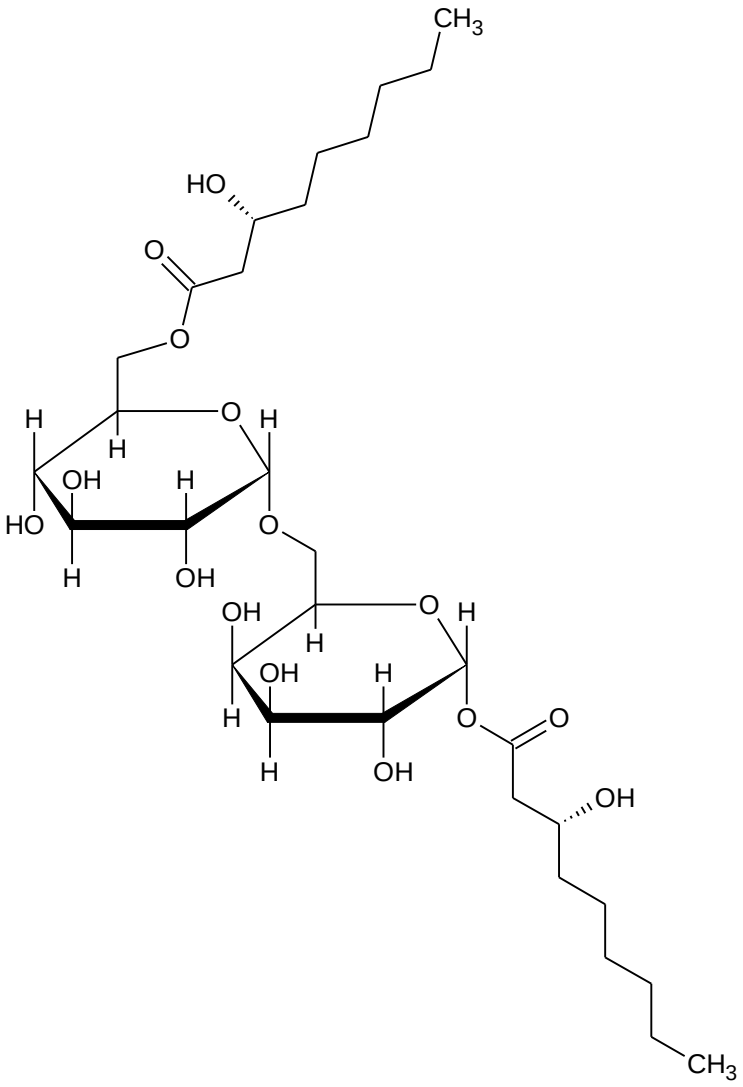
CH3
HO
O
O
H
O
H
H
OH
H
HO
O
H
OH
OH
O
H
H
OH
H
O
O
H
OH
OH

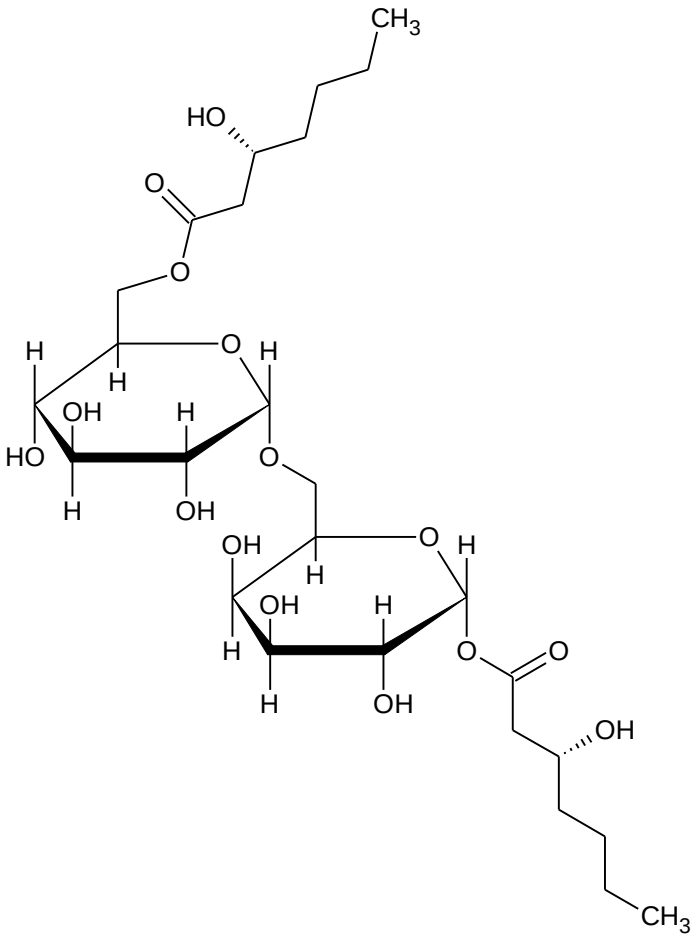
CH3
HO
O
O
H
O
H
H
OH
H
HO
O
H
OH
OH
O
H
OH
H
H
O
O
H
OH
OH
CH3

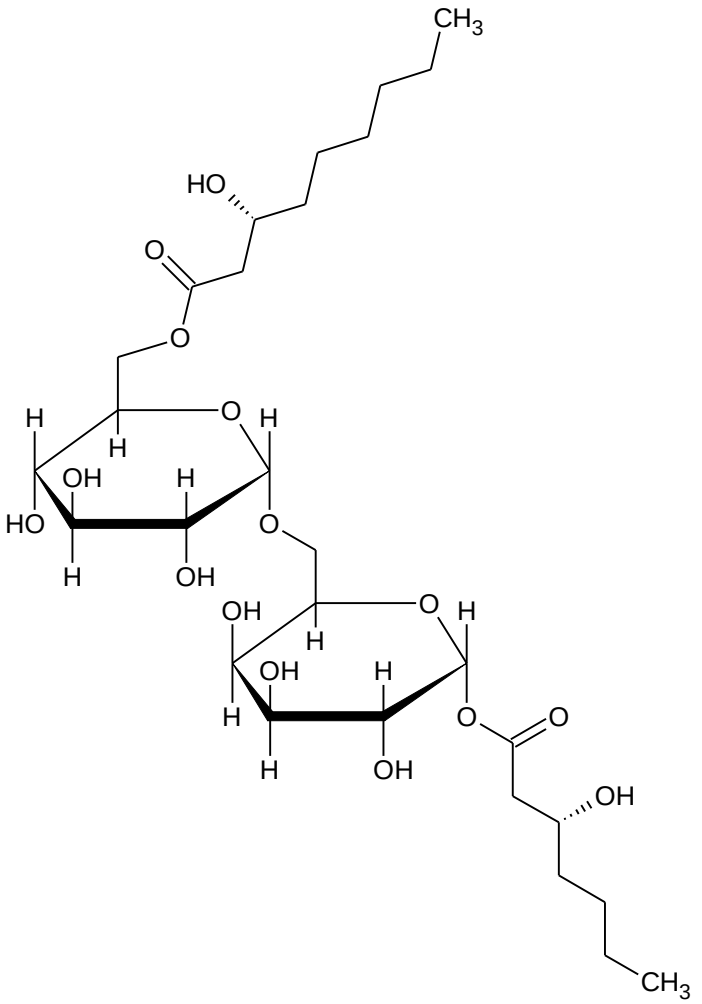

o) **mPHN-lac**: mixture of (3*R*)-hydroxynonanoate lactose and (3*R*)-hydroxyheptanoate lactose mono and diesters

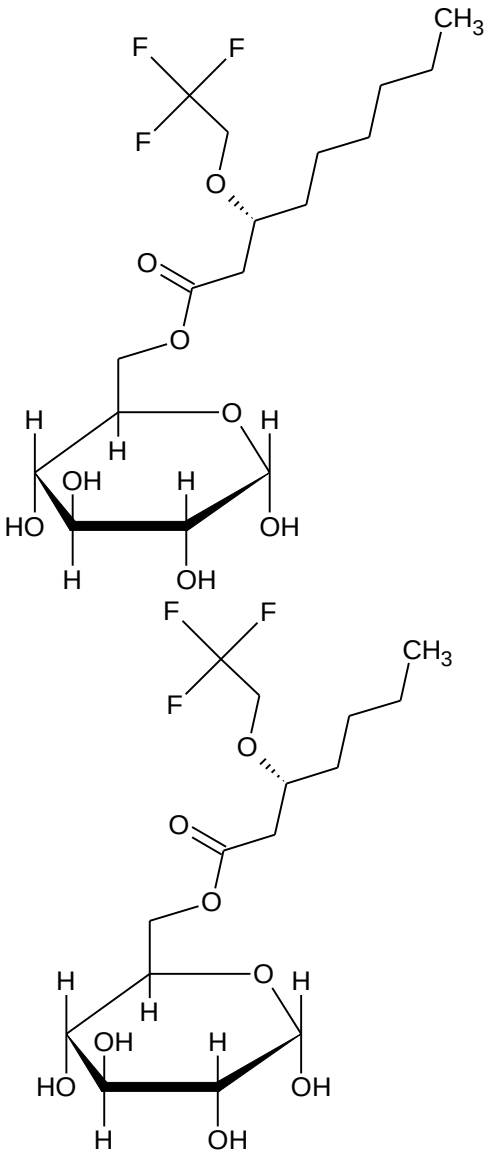
CH3
F
F
F
O
O
O
H
O
H
H
OH
H
HO
OH
H
OH
F
F
F
CH3
O
O
O
H
O
H
H
OH
H
HO
OH
H
OH

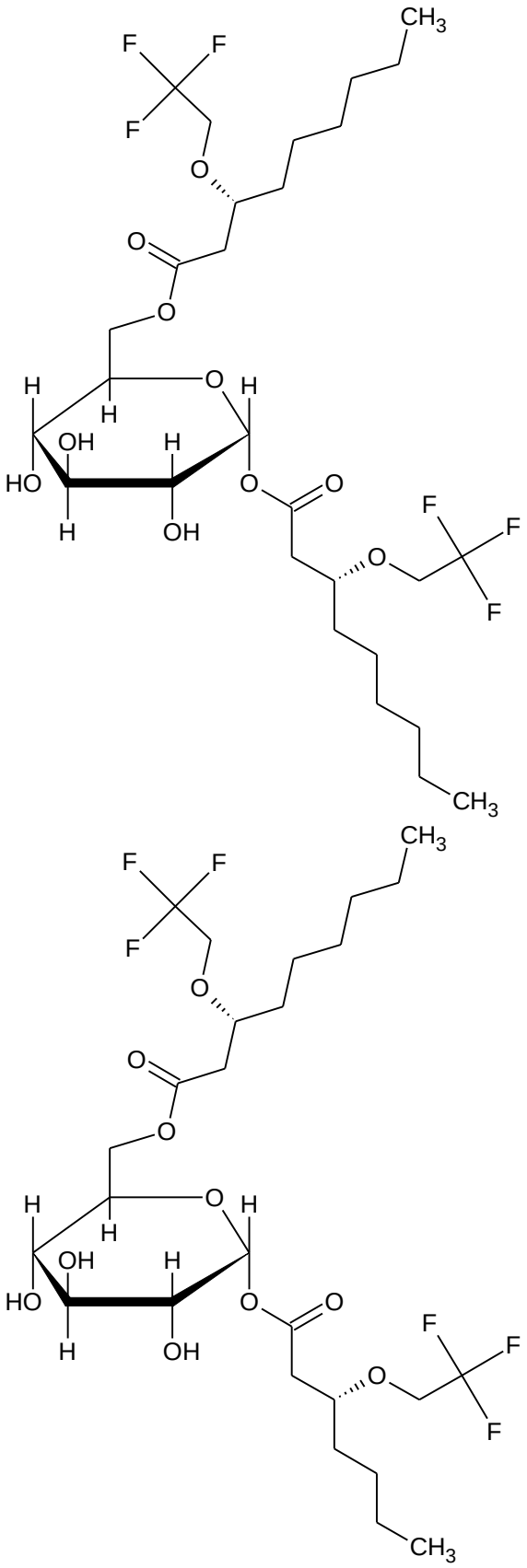

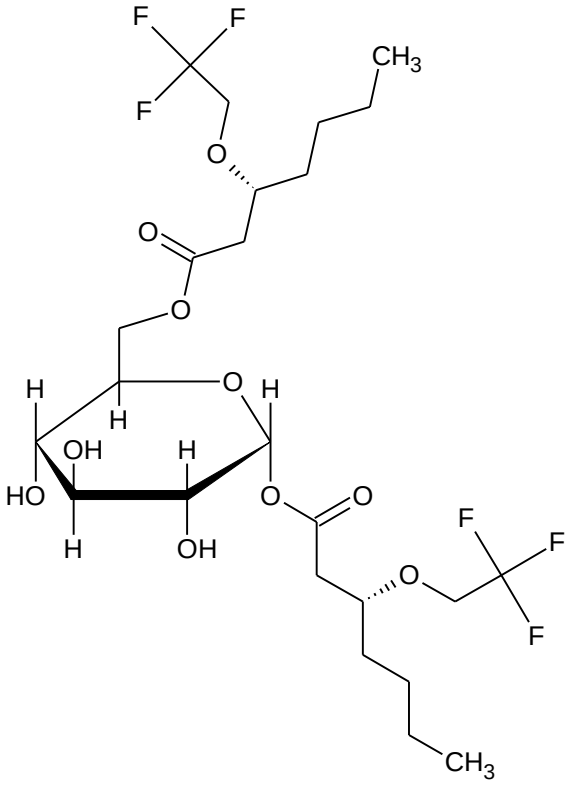

p) **F-mPHN-glu**: mixture of (3*R*)-3-(2,2,2-trifluoroethoxy)nonanoate glucose and (3*R*)-3-(2,2,2-trifluoroethoxy)heptanoate glucose mono andesters

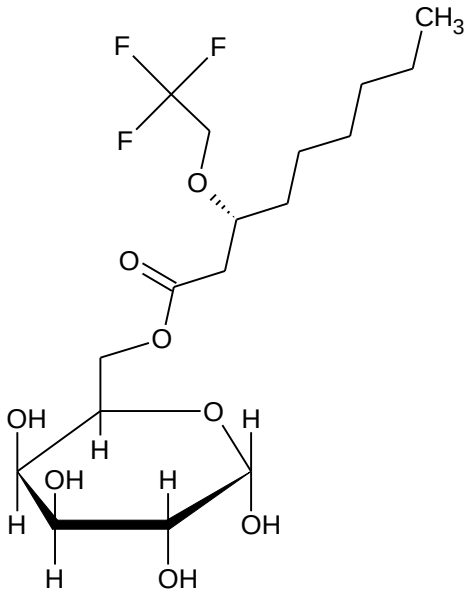

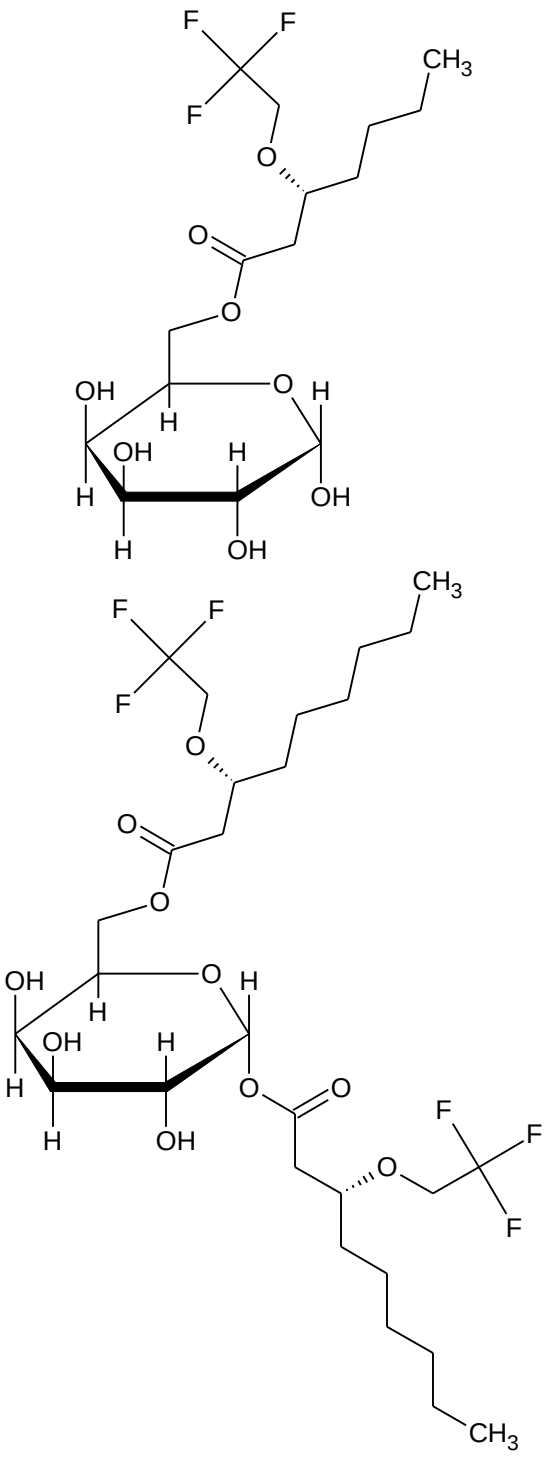
F
F
F
CH3
O
O
O
OH
O
H
H
OH
H
H
OH
H
OH
CH3
F
F
F
O
O
O
OH
O
H
H
OH
H
H
O
O
H
OH
F
F
O
F
CH3

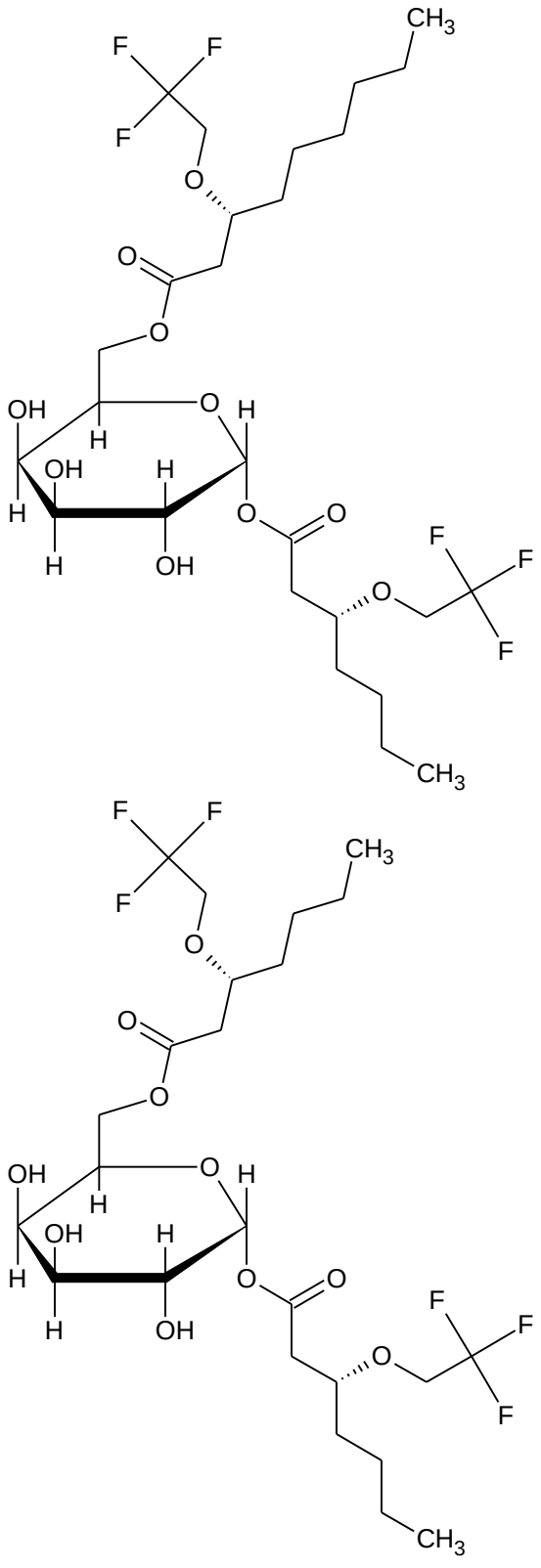

r) **F-mPHN-gal**: mixture of (3*R*)-3-(2,2,2-trifluoroethoxy)nonanoate galactose and (3*R*)-3-(2,2,2-trifluoroethoxy)heptanoate galactose mono and diesters

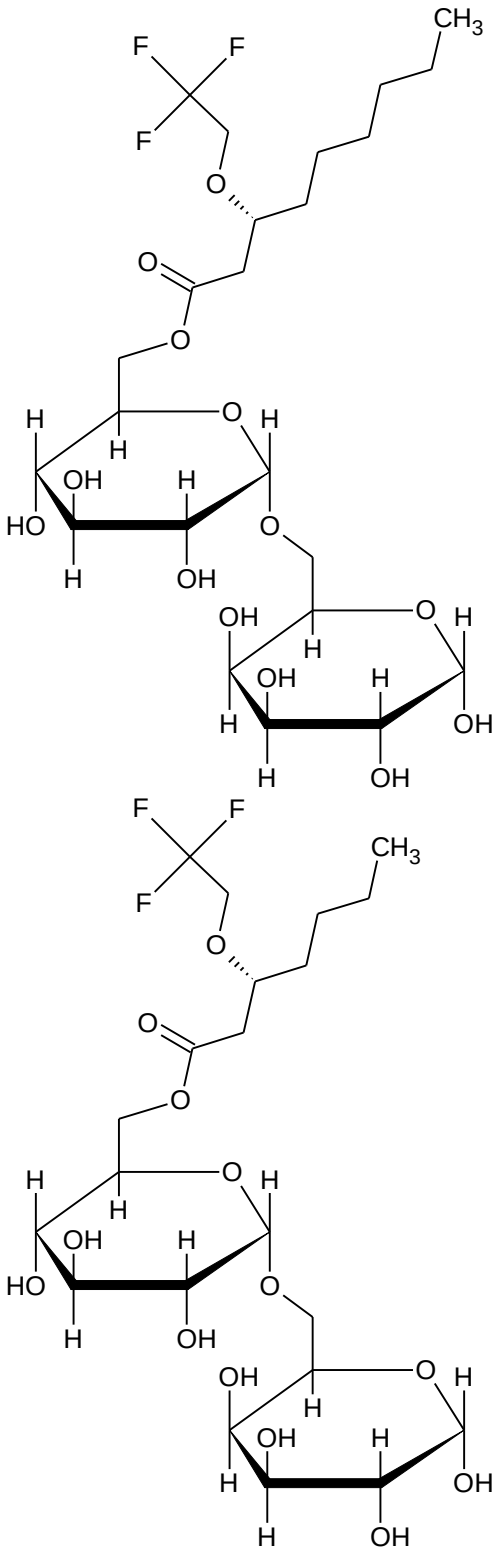
CH3
F
F
F
O
O
O
H
H
H
O
H
OH
H
HO
O
H
OH
OH
O
H
H
OH
H
H
OH
H
OH
F
F
F
CH3
O
O
O
H
H
H
O
H
OH
H
HO
O
H
OH
OH
O
H
H
OH
H
H
OH
H
OH

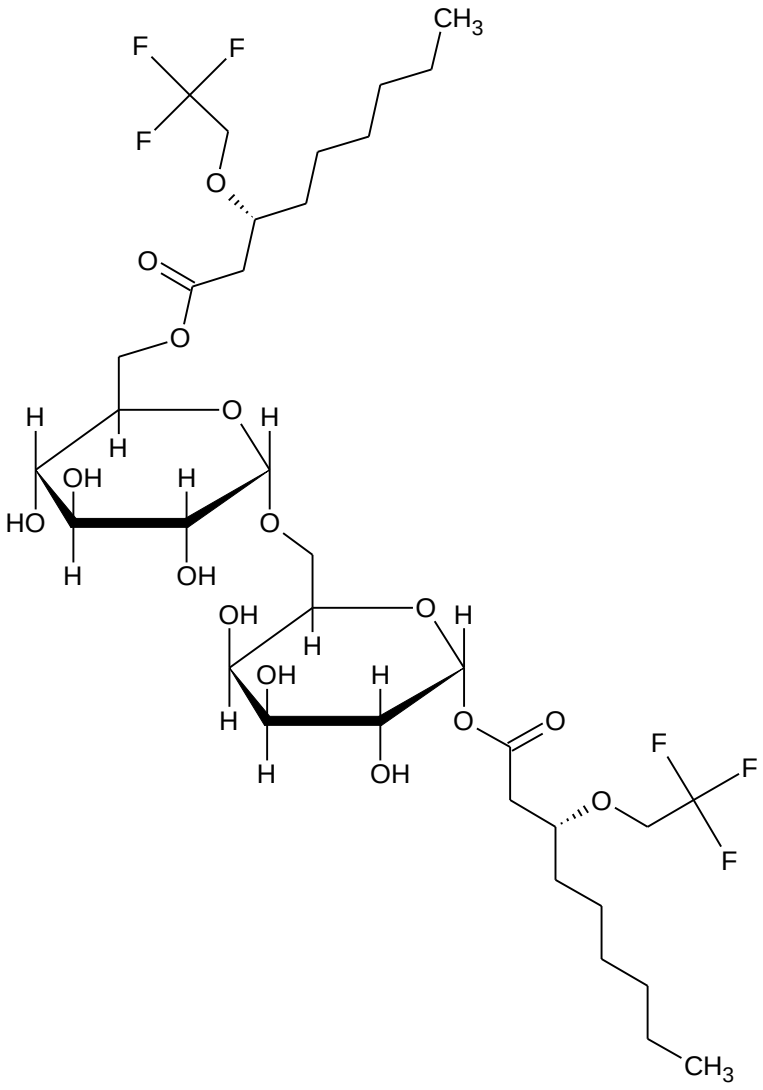
CH3
F
F
F
O
O
O
H
O
H
H
OH
H
HO
O
H
OH
OH
H
O
H
OH
H
H
O
O
H
OH
O
F
F
F
CH3

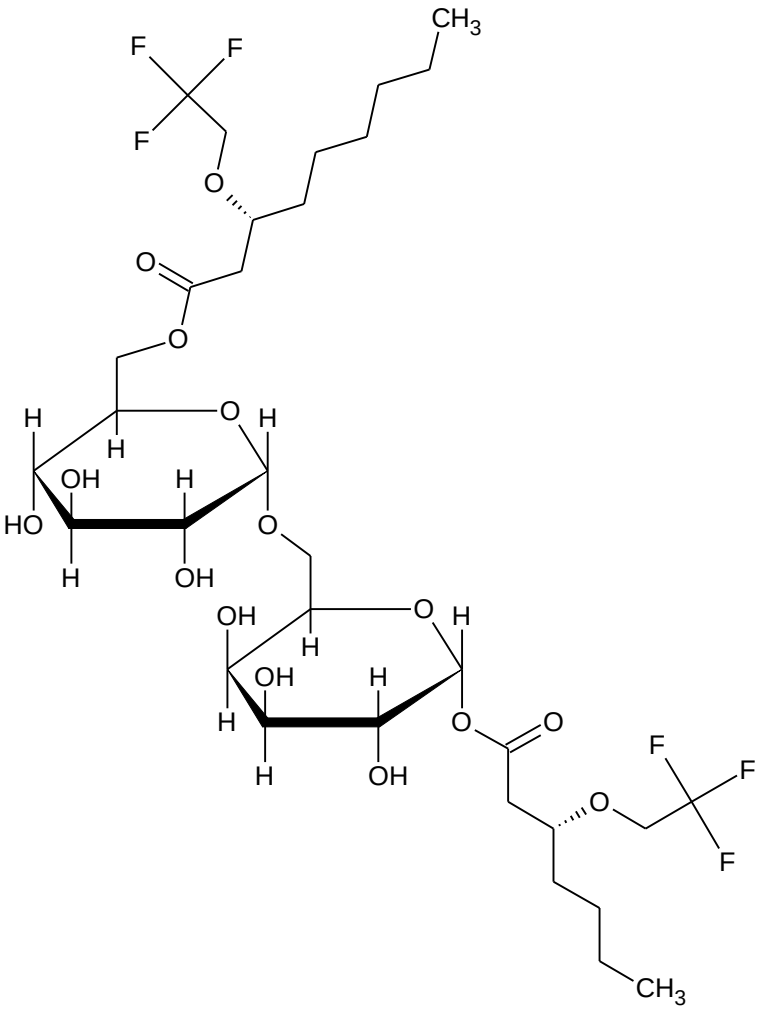
CH3
F
F
F
O
O
O
H
O
H
H
OH
H
HO
O
H
OH
OH
O
H
H
OH
H
H
O
O
F
F
O
F
CH3

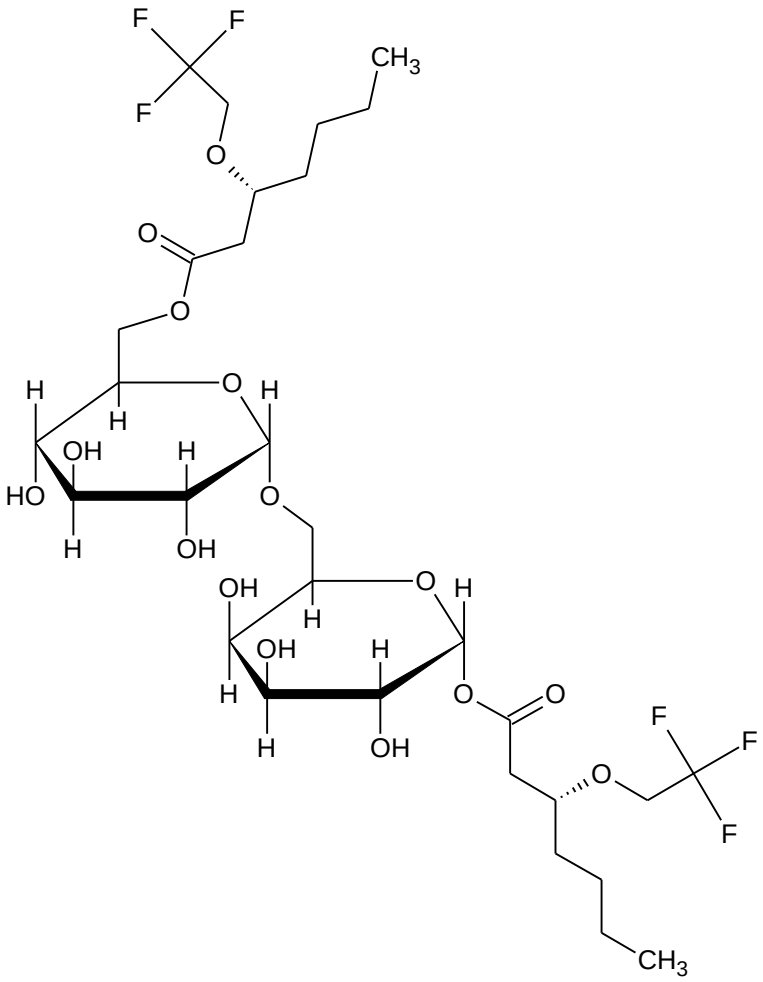

s) **F-mPHN-lac**: mixture of (3*R*)-3-(2,2,2-trifluoroethoxy)nonanoate lactose and (3*R*)-3-(2,2,2-trifluoroethoxy)heptanoate lactose mono and diesters

Fig 1. **List of compound names, shortcuts and structures generated in ChemSketch**

Table 1. Precursor and product ions of sugar esters obtained in MRM LC-MS QQQ analysis:

Compound:		MRM: Precursor ion -> product ion	Fragmentor:	Collision energy:
C9-gluc	C9 monoester	[M+K]-: 359.14 -> 341.3	93	6
		[M+K]-: 359.14 ->193.3		18
		[M+K]-: 359.14 -> 41.1		74
		[M+K]-: 359.14 -> 202.5		26
	C9 C9 diester	[M+Na]+: 483.69 -> 69	142	22
C9-gal:	C9 monoester	[M+K]-: 359.14 -> 341.3	98	6
		[M+K]-: 359.14 -> 43.1		54
		[M+K]-: 359.14 -> 202.4		18
	C9 C9 diester	[M+Na]+: 483.69 -> 69	142	22
C9-lac:	C9 monoester	[M+H_2O+H]-: 517.2 -> 157.1	136	22
		[M+H_2O+H]-: 517.2 -> 282.1		46
	C9 C9 diester	[M+Na]+: 657.3 -> 157.1	131	30
mPHN- glu:	C9 monoester	[M+Cl]-: 371,15 -> 35	98	14
	C7 monoester	[M+K]+: 429.11 -> 73.1		
		[M+MeOH]+: 340.15 -> 295.7	132	6
		[M+MeOH]+: 340.15 -> 180.4		26
	C9 C9 diester	[M+Cl]-: 527,26 -> 35	137	30
	C7 C7 diester	-	-	-
	C9 C7 diester	[M+Cl]-: 499.23 -> 35	137	18
mPHN- gal:	C9 monoester	[M+Cl]-: 371.15 -> 35	98	14
	C7 monoester	[M+K]+: 429.11 -> 73.1		
	C9 C9 diester	[M+H]+: 493.3 -> 59.1	113	18
		[M+H]+: 493.3 -> 42.1		126
	C7 C7 diester	[M+H]+: 437.24 -> 23.1	181	30
mPHN -lac:	C9 monoester	[M+H2O+H]-: 517.2 -> 157.1	116	26
		517.2 -> 282.1	116	38
	C9 C9 diester	[M+Na]+: 657.3 -> 157.1	111	26
F-mPHN-gluc:	C9 monoester	[M+K]+: 457.14 -> 23	172	34
	C7 monoester	[M+K]:+429.11 -> 73.1	245	46
		[M+K]:+429.11 -> 45		94
		[M+K]:+429.11 -> 43.1		178
		[M+K]:+429.11 -> 218.7		22
	C9 C9 diester wth two –CF_3	[M+MeOH]+: 688.3 -> 73.1	147	70
		[M+MeOH]+: 688.3 -> 355.1		26
	C9 C7 diester with one –CF_3	[M+Na]+: 651.26 -> 73	235	78
		[M+Na]+: 651.26 -> 45.1		166
	C9 C7 diester with one –CF_3	[M-H]-: 627.26 -> 325	191	38
F-mPHN-gal:	C9 C7 diester with two –CF_3	[M+H]+: 629.28 -> 324.4	113	14
	C7 C7 diester with one –CF_3 group	[M+H]+: 457.14 -> 23.1	167	38
F-mPHN-lac:	C9 C9 diester with two –CF_3 groups	[M+MeOH]+: 851.36 -> 73.1	162	114
		[M+MeOH]+: 851.36 -> 436.4		50
	C9 C9 diester with one –CF_3 group	[M+Na]+: 759.34 -> 73.1	127	78
		[M+Na]+: 759.34 -> 45		190
	C7C7diester with one -CF_3	[M+Na]+: 703.28 -> 355.1	118	30
	C7C7 with two –CF_3 groups	[M+Na]+: 833.28 -> 73.1	181	122
		[M+Na]+: 833.28 -> 45		198

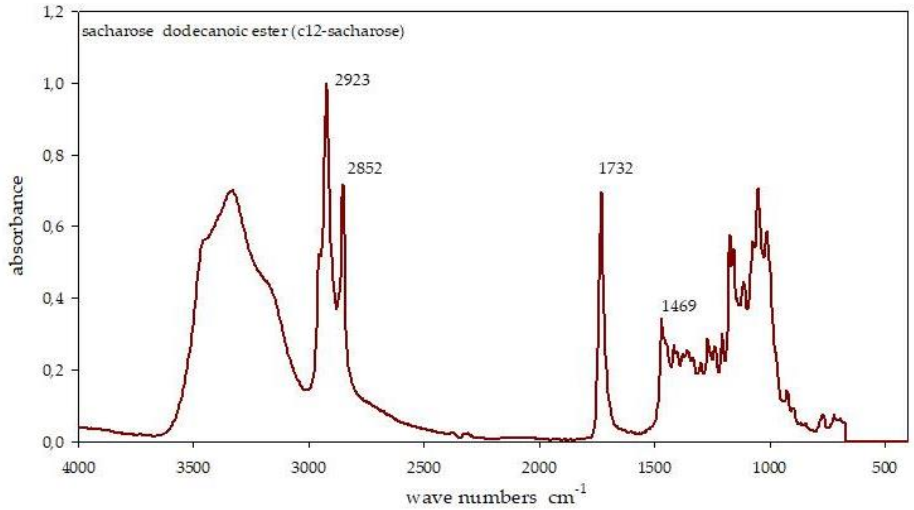

Fig 2. IR spectrum of C12- (sucrose monolaurate) as a referring compound

Following peaks inform about:

- Stretching vibrations: 3000- 3500 cm^{-1} indicate presence -OH group
- Stretching vibrations: 2900 cm^{-1} come from -CH_2 aliphatic residues
- Stretching vibrations around 1725 cm^{-1} responsible for ester bonds

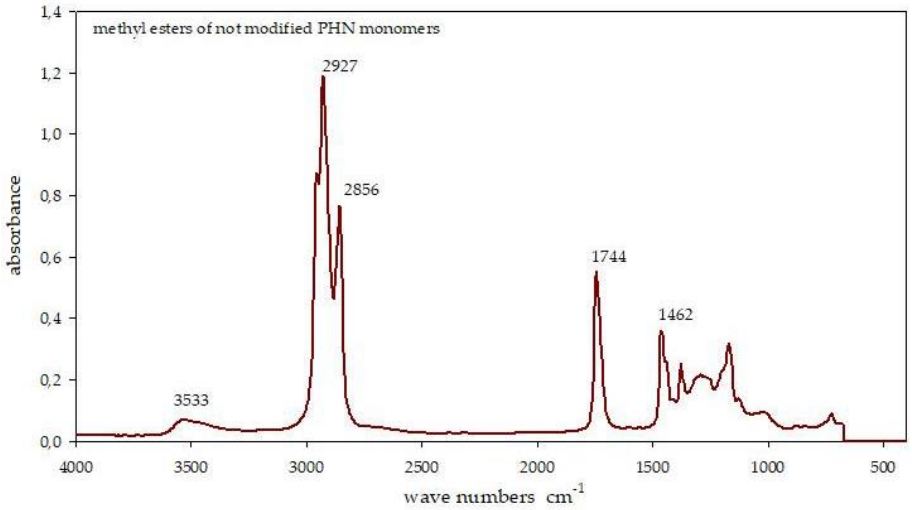

Fig 3. IR spectra of methyl esters of not modified PHN monomers (mixture of 3-(*R*)- hydroxynonanoic and 3-(*R*)- hydroxyheptanoic acids)

	Parameter	Value
1	Comment	25338-1H WS1
2	Origin	Bruker BioSpin GmbH
3	Solvent	CDCl3
4	Temperature	298.1
5	Pulse Sequence	zg30
6	Number of Scans	32
7	Receiver Gain	200
8	Relaxation Delay	0.0000
9	Pulse Width	14.5000
10	Acquisition Time	3.5001
11	Acquisition Date	2020-02-27T11:37:04
12	Modification Date	2020-02-27T11:37:04
13	G to G'	1.00000000
14	Echo Delay	0.0000
15	Gradient Duration	0.0000
16	Spectrometer Frequency	300.20
17	Spectral Width	6009.6
18	Lowest Frequency	-1158.2
19	Nucleus	1H
20	Acquired Size	21034
21	Spectral Size	65536

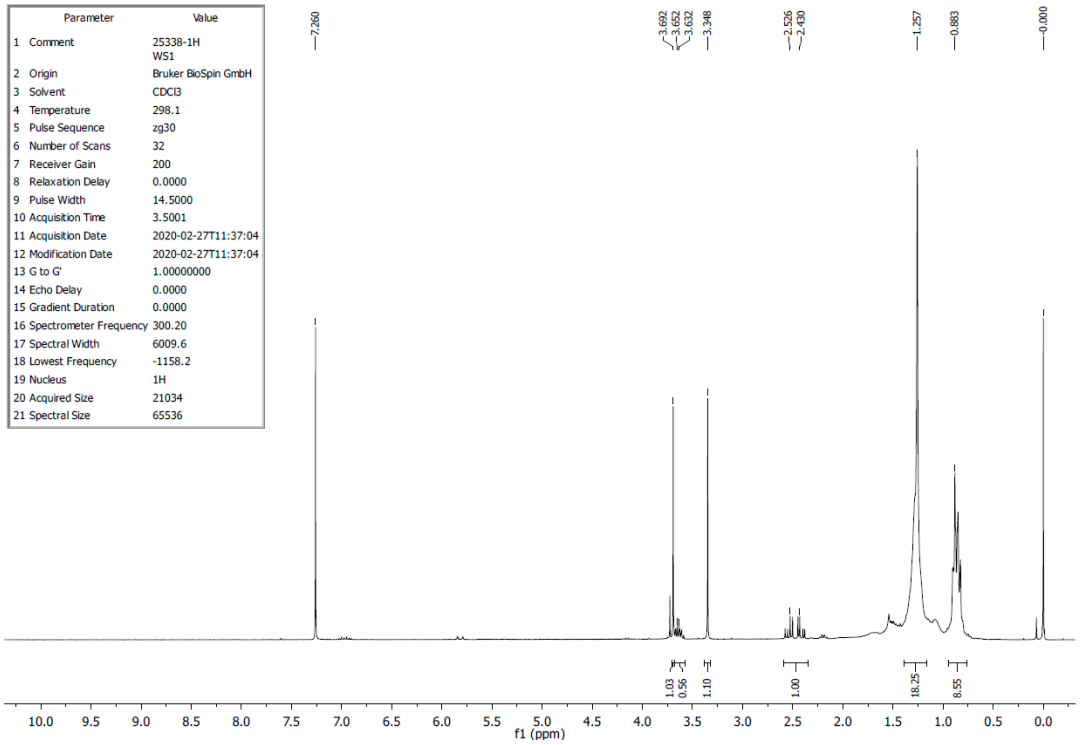

	Parameter	Value
1	Comment	25340-1H WS3
2	Origin	Bruker BioSpin GmbH
3	Solvent	CDCl3
4	Temperature	298.1
5	Pulse Sequence	zg30
6	Number of Scans	32
7	Receiver Gain	200
8	Relaxation Delay	0.0000
9	Pulse Width	14.5000
10	Acquisition Time	3.5001
11	Acquisition Date	2020-02-27T11:45:58
12	Modification Date	2020-02-27T11:45:58
13	G to G'	1.00000000
14	Echo Delay	0.0000
15	Gradient Duration	0.0000
16	Spectrometer Frequency	300.20
17	Spectral Width	6009.6
18	Lowest Frequency	-1158.2
19	Nucleus	1H
20	Acquired Size	21034
21	Spectral Size	65536

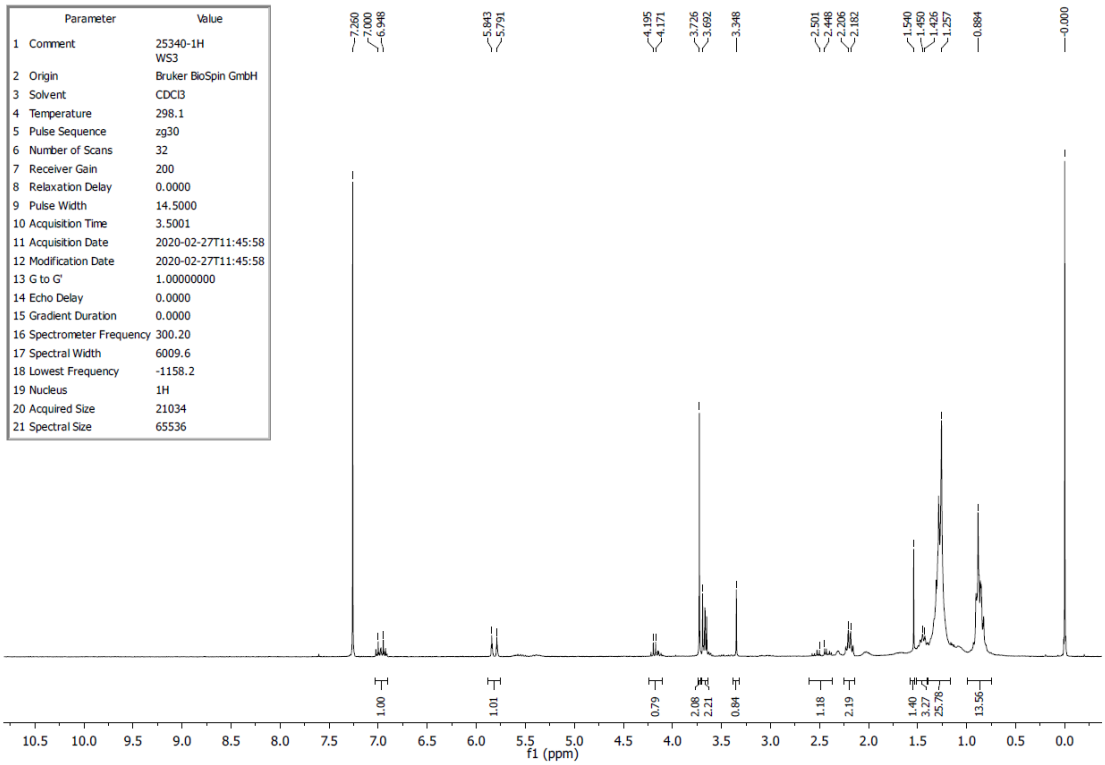

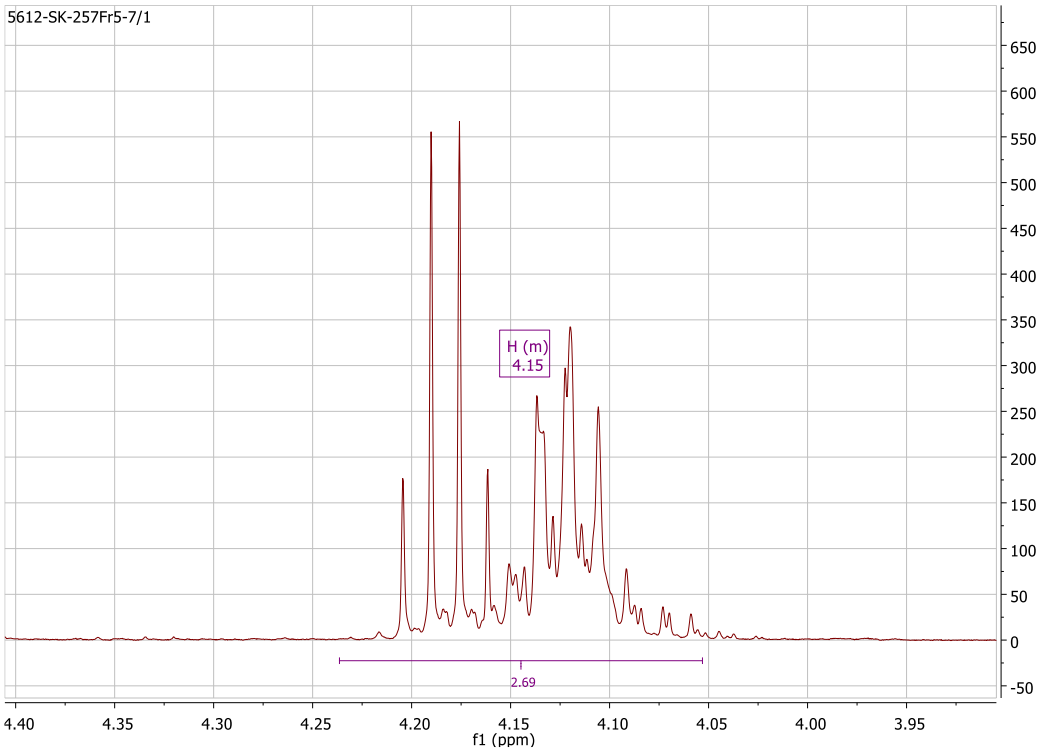

a) [1]HNMR spectra

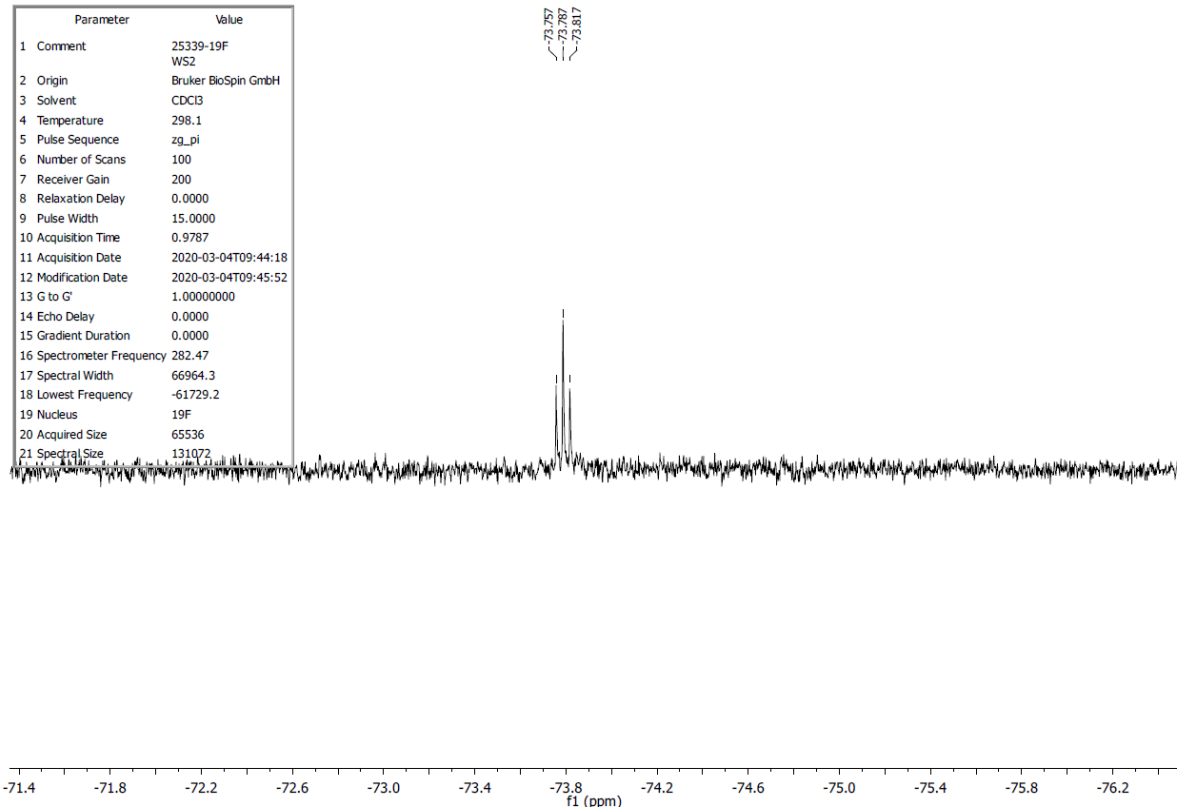

b) [19]F NMR spectra of the modified PHN monomers confirmed a presence of fluoric moieties

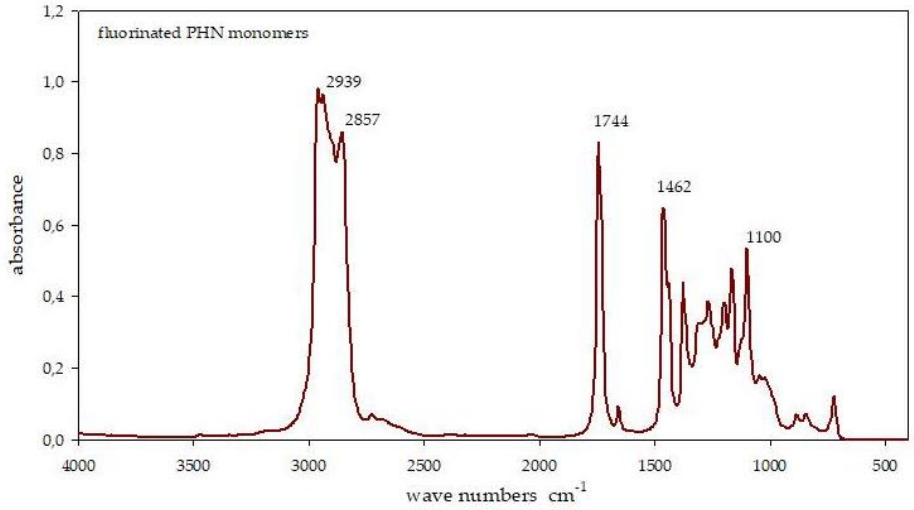

c) IR spectra of the purified PHN mixture after modification

Fig 4. Spectra analysis of methyl esters of methyl esters of 3-(*R*)- (2 -2′- 2′′- trlifluoroethyl)-nonanoic and heptanoic acids (fluorinated PHN monomers or mPHN-F)

IR Spectra description:

Stretching vibrations between ~ 1360-1090 cm^{-1} suggests presence of -CF_3 groups

Stretching vibrations between ~ 1360-1000 cm^{-1} and 1110-1000 cm^{-1} suggests presence of –CF bonds

And 2859 cm^{-1} for -C-O-C etheric bonds

1734 cm^{-1} stretching vibrations inform about presence of ester bonds between methyl groups and carboxyl groups of PHN monomers

Spectrum profile refers to inverted IR spectra of 2,2,2-Trifluoroethyl Methyl Ether taken from*:*

"Low-Resolution Microwave, Infrared, and Raman Spectra, Conformational Stability, and Vibrational Assignment of 2,2,2-Trifluoroethyl Methyl Ether"; J. Phys. Chem. 1987, 91, 1334-1344

Additionally, lack of large peak between 3000-3500 cm^{-1} suggests –OH groups are not present in a structure of the analyzed compound which confirms that reaction of protecting –OH group occurred

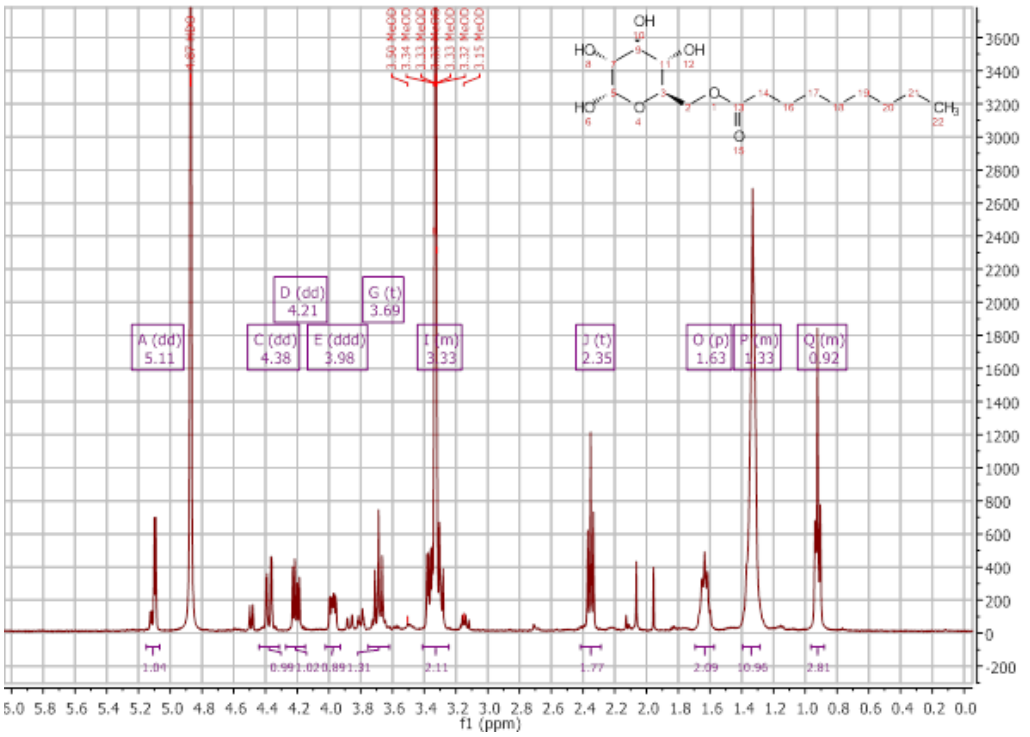

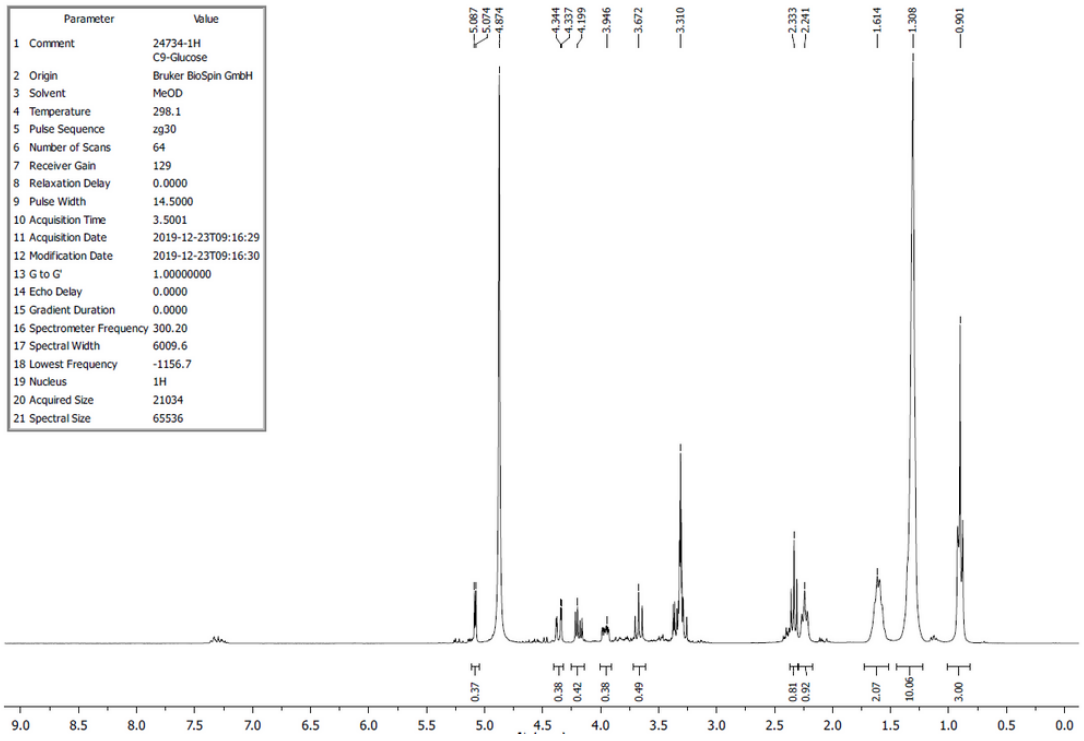

	Parameter	Value
1	Comment	24734-1H C9-Glucose
2	Origin	Bruker BioSpin GmbH
3	Solvent	MeOD
4	Temperature	298.1
5	Pulse Sequence	zg30
6	Number of Scans	64
7	Receiver Gain	129
8	Relaxation Delay	0.0000
9	Pulse Width	14.5000
10	Acquisition Time	3.5001
11	Acquisition Date	2019-12-23T09:16:29
12	Modification Date	2019-12-23T09:16:30
13	G to G'	1.00000000
14	Echo Delay	0.0000
15	Gradient Duration	0.0000
16	Spectrometer Frequency	300.20
17	Spectral Width	6009.6
18	Lowest Frequency	-1156.7
19	Nucleus	1H
20	Acquired Size	21034
21	Spectral Size	65536

a) [1]HNMR spectra

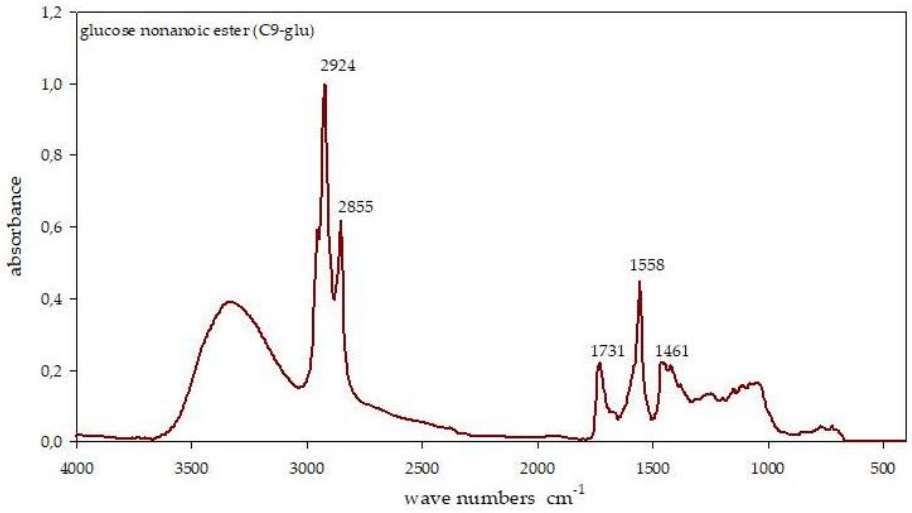

b) IR spectra

Fig 5. Spectral analysis of glucose nonanoate (C9-glu)

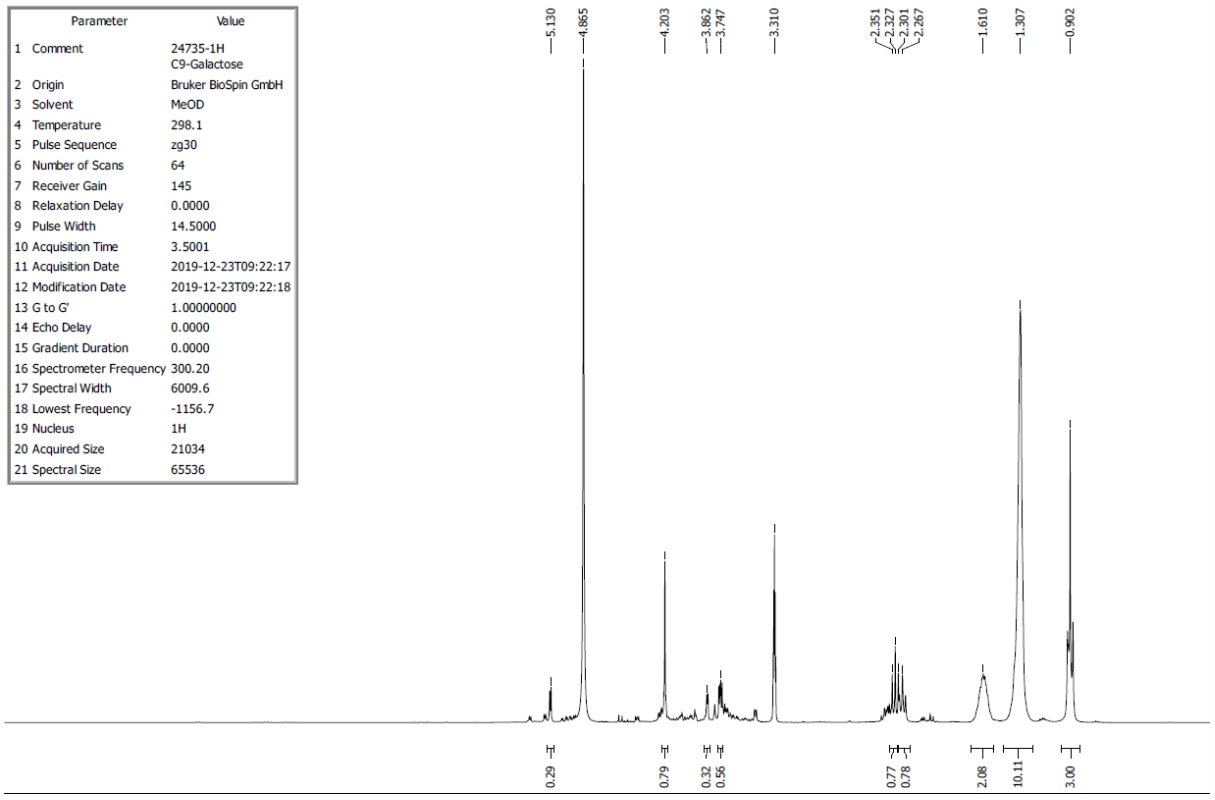

a) ^{1}HNMR spectra

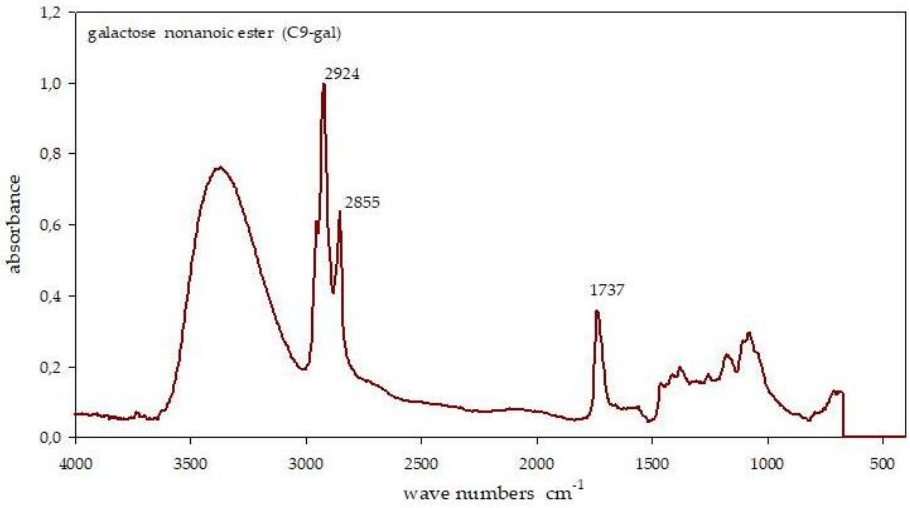

a) IR spectra

Fig 6. Spectral analysis galactose nonanoate (C9-gal)

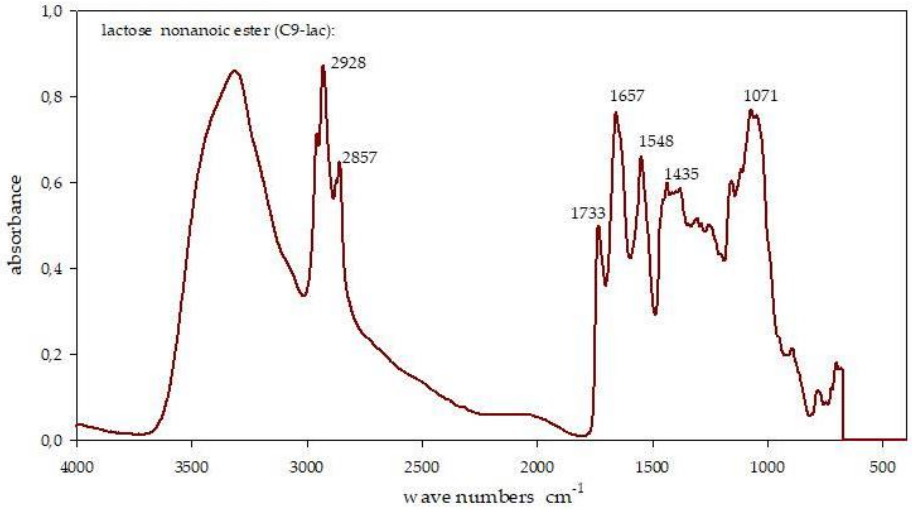

Fig 7. IR spectra of lactose nonanoate (C9-lac)

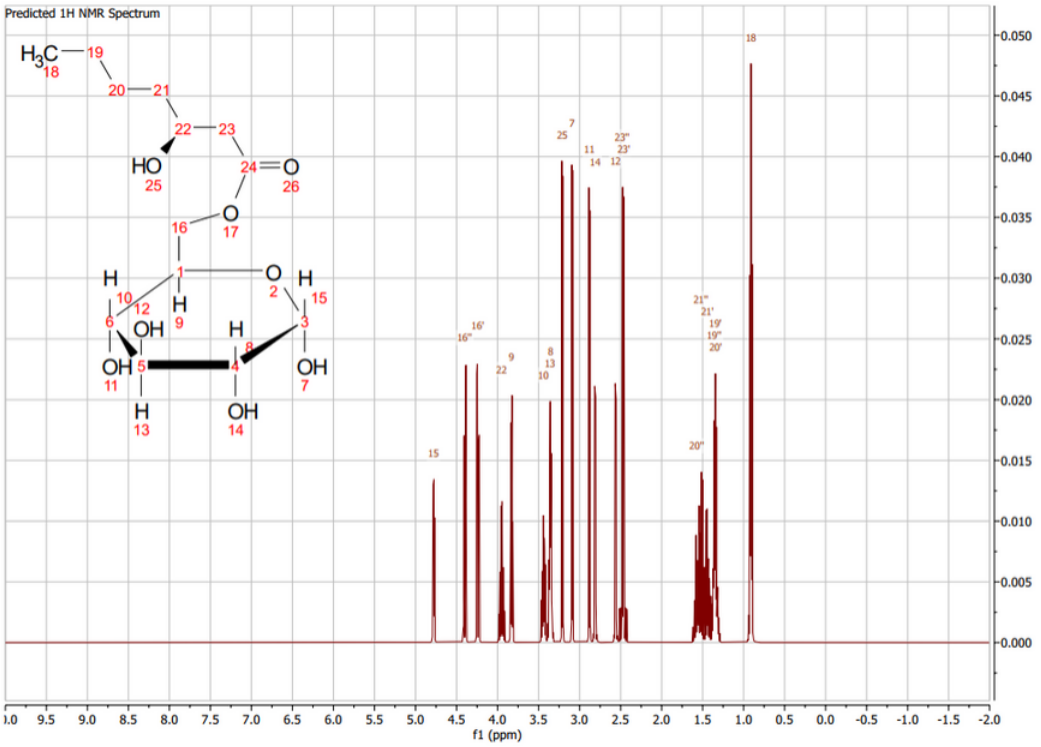

a) [1]HNMR spectra prediction

	Parameter	Value
1	Comment	25345-1H WS4
2	Origin	Bruker BioSpin GmbH
3	Solvent	MeOD
4	Temperature	298.1
5	Pulse Sequence	zg30
6	Number of Scans	28
7	Receiver Gain	145
8	Relaxation Delay	0.0000
9	Pulse Width	14.5000
10	Acquisition Time	3.5001
11	Acquisition Date	2020-02-28T09:17:37
12	Modification Date	2020-02-28T09:19:09
13	G to G'	1.00000000
14	Echo Delay	0.0000
15	Gradient Duration	0.0000
16	Spectrometer Frequency	300.20
17	Spectral Width	6009.6
18	Lowest Frequency	-1156.7
19	Nucleus	1H
20	Acquired Size	21034
21	Spectral Size	65536

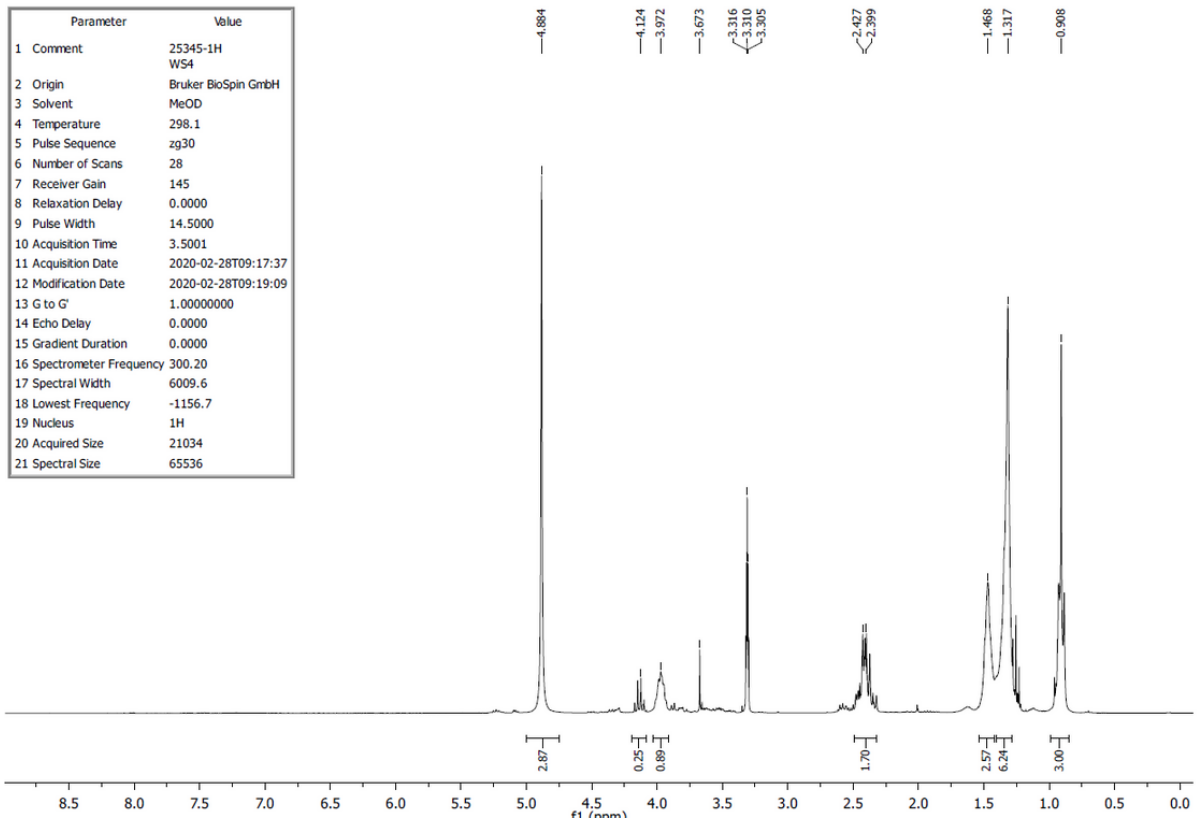

b) [1]HNMR spectra: [1]H NMR (300 MHz, Methanol-d4) δ 4.93 (s, 3H), 4.10 – 3.89 (m, 1H), 3.33 (td, *J* = 3.7, 2.1 Hz, 1H), 2.55 – 2.29 (m, 2H), 1.62 – 1.21 (m, 12H), 1.02 – 0.85 (m, 3H)

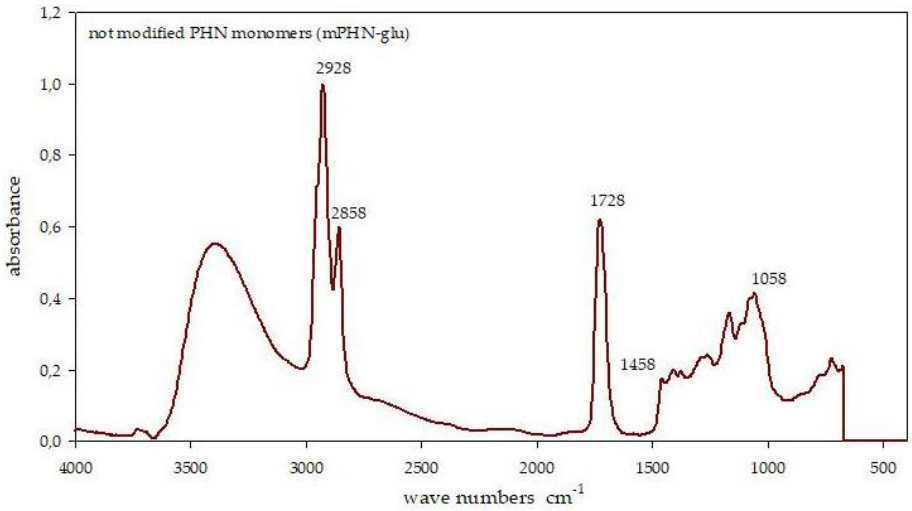

c) IR spectra

Fig 8. Spectral analysis of glucose mono and diesters esters originated from mixture of not modified PHN monomers (mPHN-glu)

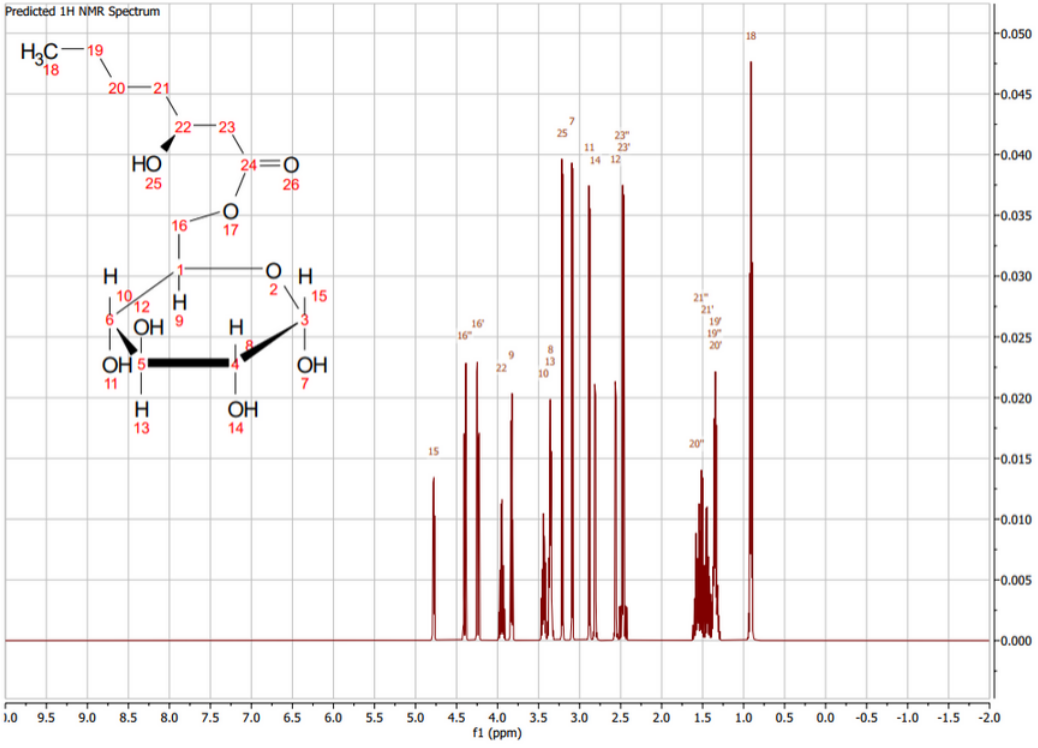

a) [1]HNMR spectra prediction

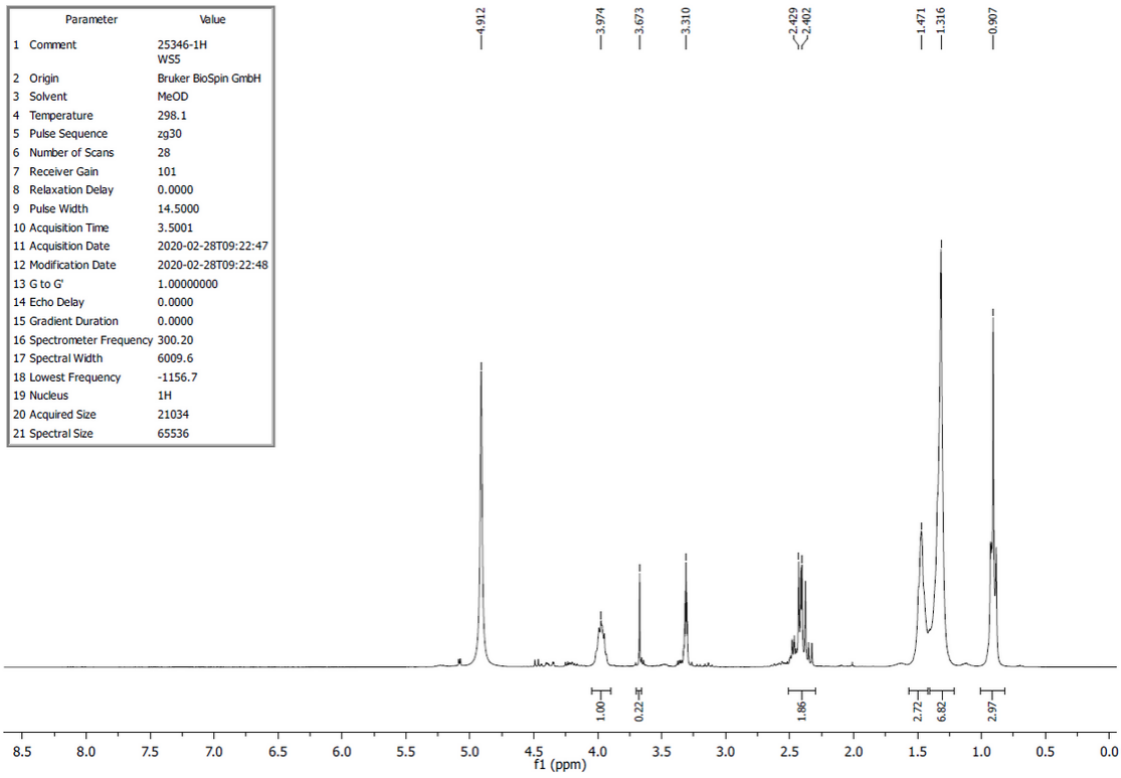

b) [1]HNMR spectra: [1]H NMR (300 MHz, Methanol-d4) δ 4.94 (s, 3H), 3.99 (dtd, *J* = 9.5, 7.0, 3.4 Hz, 1H), 3.33 (p, *J* = 1.7 Hz, 1H), 2.54 – 2.28 (m, 2H), 1.63 – 1.22 (m, 12H), 1.03 – 0.84 (m, 3H).

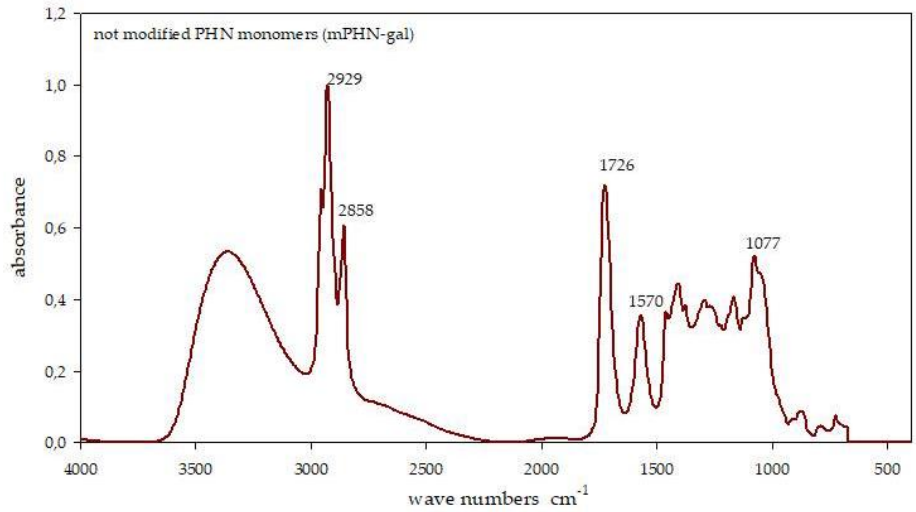

c) IR spectra

Fig 9. Spectral analysis of galactose mono and diesters esters originated from mixture of not modified PHN monomers (mPHN-gal)

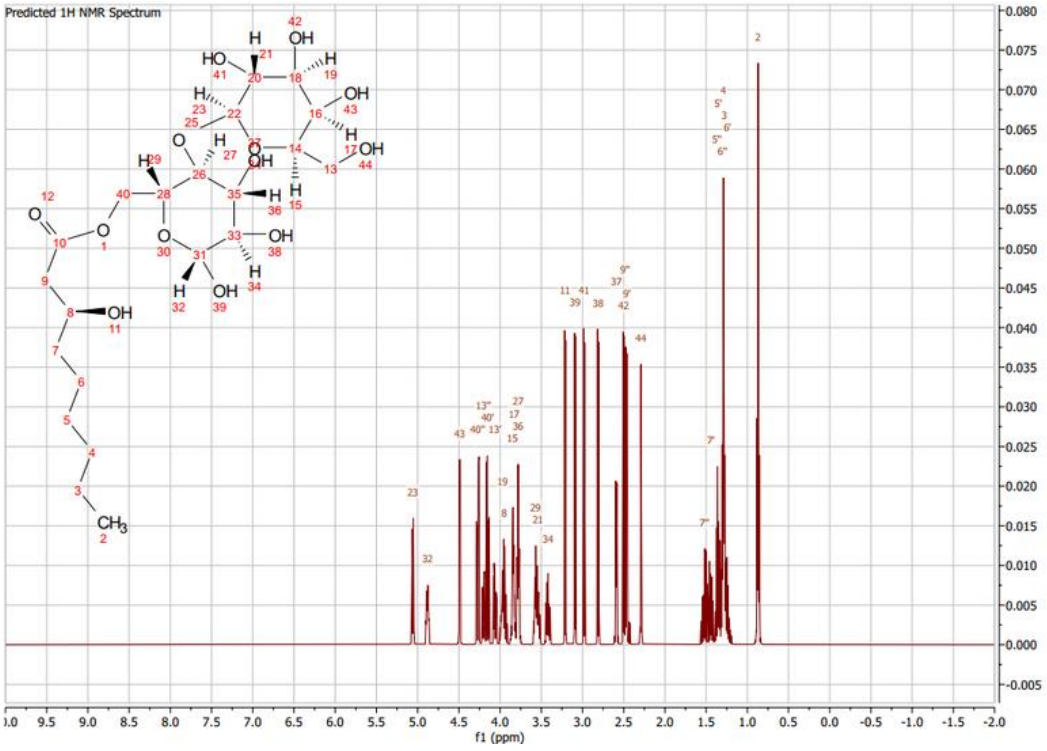

a) [1]HNMR spectra prediction

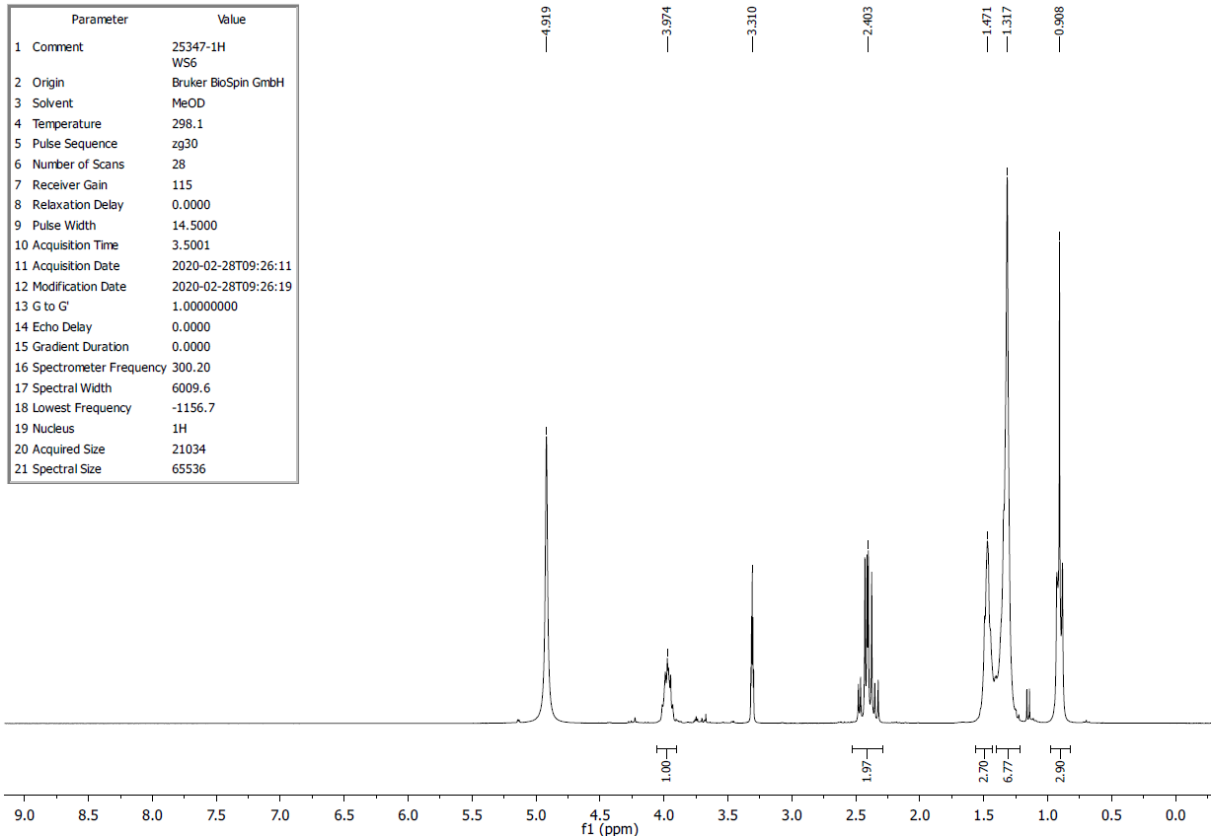

b) ^{1}HNMR spectra: (300 MHz, Methanol-d4) δ 4.90 (s, 3H), 4.16 (q, *J* = 7.1 Hz, 1H), 4.07 – 3.91 (m, 1H), 3.33 (p, *J* = 1.6 Hz, 1H), 2.55 – 2.31 (m, 2H), 1.58 – 1.23 (m, 11H), 1.03 – 0.82 (m, 3H)

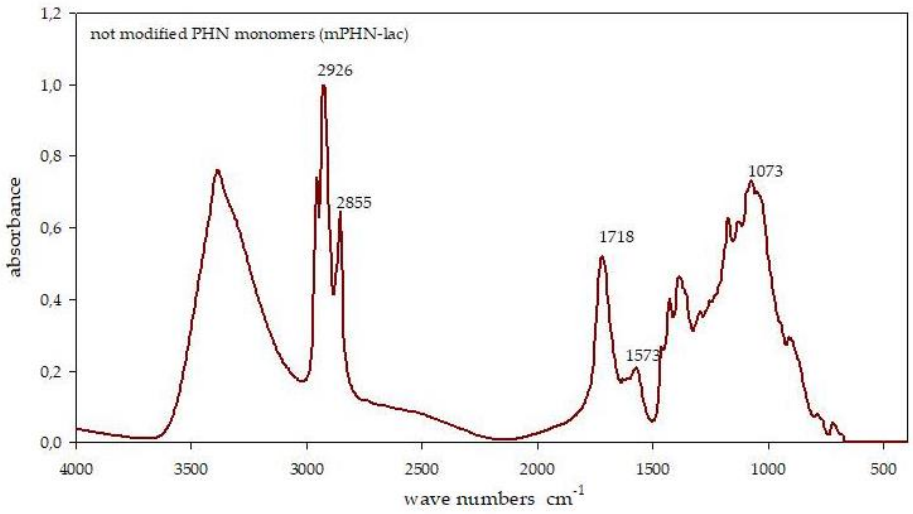

c) IR spectra

Fig 10. Spectral analysis of lactose mono and diesters esters originated from mixture of not modified PHN monomers (mPHN-lac)

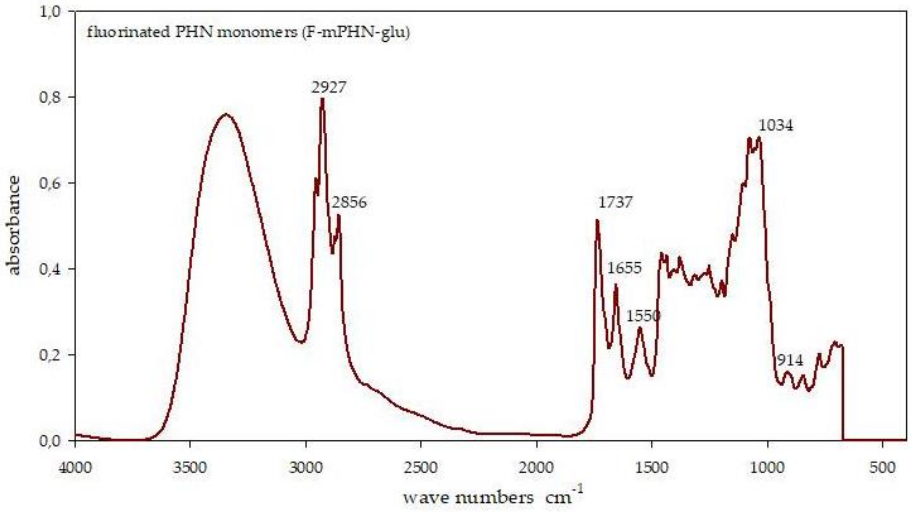

Fig 11. IR spectra of glucose mono and diesters esters originated from mixture of fluorinated PHN monomers (F-mPHN-glu)

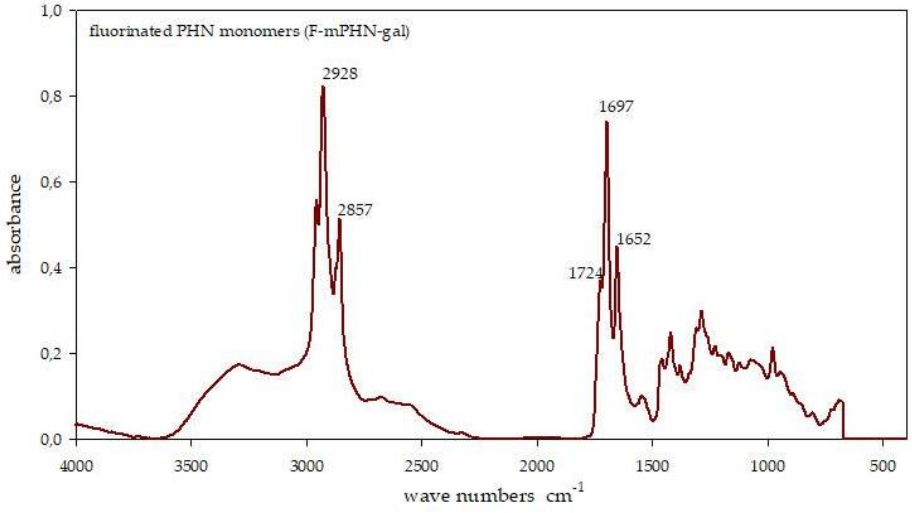

Fig 12. IR spectra of galactose mono and diesters esters originated from mixture of fluorinated PHN monomers (F-mPHN-gal)

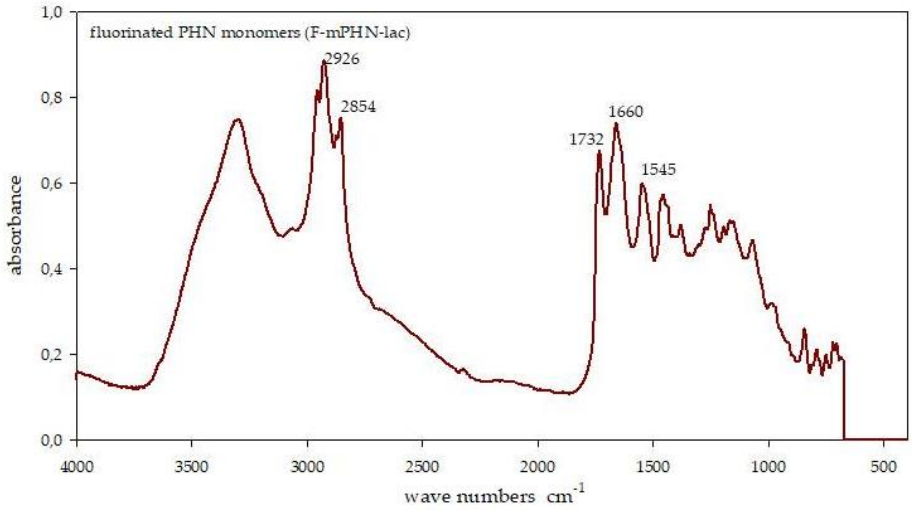

Fig 13. IR spectra of lactose mono and diesters esters originated from mixture of fluorinated PHN monomers (F-mPHN-lac)

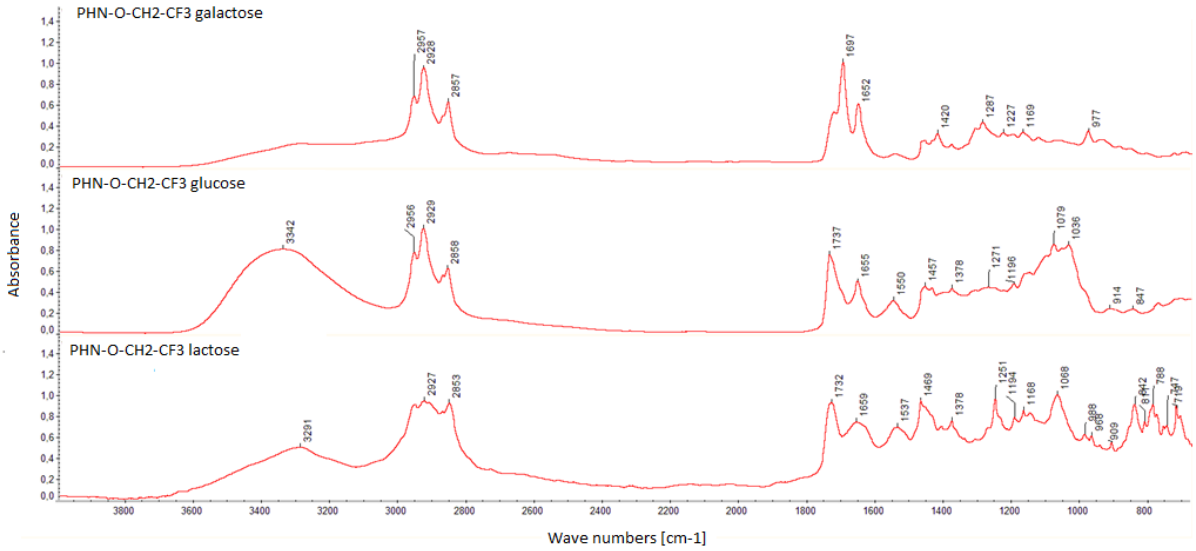

Fig 14. IR spectra of fluorinated esters set together

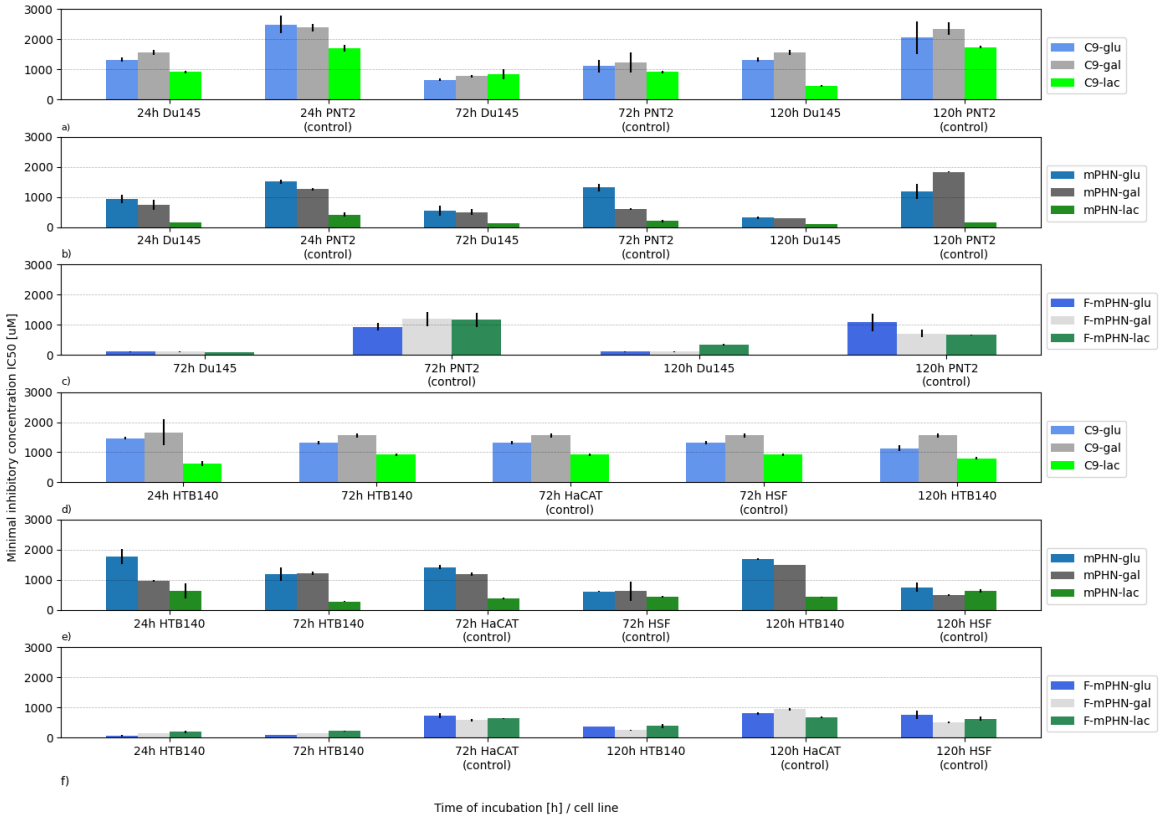

Fig 15. Cytotoxicity of SFAE determined by MTT assay, where IC_{50} is a concentration [μM] of a particular compound that causes reduction of a tested cell culture to 50% :

a) nonanoic acid originated SFAE tested on DU145 / PNT2 (control)

b) mPHN originated SFAE tested on DU145 / PNT2 (control)

c) F-mPHN originated SFAE tested on DU145 / PNT2 (control)

d) nonanoic acid originated SFAE tested on HTB40 /HaCat/ HSF (control)

e) mPHN originated SFAE tested on HTB40 /HaCat/ HSF (control)

f) F-mPHN originated SFAE tested on HTB40 /HaCat/ HSF (control)

Table 2. Cytotoxicity of SFAE determined by MTT assay: – not determined; d – standard deviation. Red fillings mark the most lowest concentrations, green- the highest.

	Time [h]	C9-glu	C9-gal	C9-lac	PHN-glu	PHN-gal	PHN-lac	F-mPHN-glu	F-mPHN-gal	F-mPHN-lac
DU145 (prostate cancer)	24	1317.1	1560.5	919.5	932.1	750.9	161.2	-	-	-
	d	66	78	46	146	169	3	-	-	-
	72	658.6	780.3	836.9	541.1	500.0	131.4	100.0	100.0	83.8
	d	33	39	169	159	100	5	5	5	4
	120	1317.1	1560.8	459.8	315.7	304.6	91.3	100.0	100.0	335.0
	d	66	78	23	41	2	3	5	5	17
PNT2 (control)	24	2491.5	2390.9	1707.2	1507.6	1256.8	421.0	-	-	-
	d	285	120	110	80	32	79	-	-	-
	72	1110.5	1233.3	919.5	1312.2	612.5	199.5	926.8	1183.5	1156.4
	d	207	327	46	115	31	42	127	238	234
	120	2053.1	2355.3	1743.7	1180.2	1838.4	165.2	1075.5	704.9	662.5
	d	538	220	33	247	20	5	296	117	8
HTB 140 (melanoma)	24	1468.8	1659.0	621.6	1767.6	967.3	640.0	63.3	155.9	189.0
	d	46	434	77	253	26	250	24	3	49
	72	1317.1	1560.5	919.5	1195.7	1224.9	283.4	89.3	155.9	216.9
	d	66	78	46	232	61	8	2	3	21
	120	1133.9	1560.5	805.3	1689.4	1496.4	435.0	372.4	247.9	394.2
	d	92	78	51	35	2	10	3	11	70
HaCAT (human keratinocytes-control)	72	1317.1	1560.5	919.5	1427.3	1200.0	383.9	733.7	580.0	644.1
	d	66	78	46	71	60	25	81	37	17
	120	-	-	-	-	-	-	800.8	945.9	670.0
	d	-	-	-	-	-	-	40	47	33
HSF (human skin fibroblasts-control	72	1317.1	1560.5	919.5	613.4	624.2	445.8	-	-	-
	d	66	78	46	12	322	24	-	-	-
	120	-	-	-	761.2	499.6	631.1	761.2	499.6	631.1
	d	-	-	-	143	25	64	143	25	64

frontiers | Frontiers in Bioengineering and Biotechnology

TYPE Original Research
PUBLISHED 09 February 2023
DOI 10.3389/fbioe.2023.1112053

OPEN ACCESS

EDITED BY
Kevin Edward O Connor,
University College Dublin, Ireland

REVIEWED BY
Anastasia Zerva,
Agricultural University of Athens, Greece
Eduardo J. Gudiña,
University of Minho, Portugal

*CORRESPONDENCE
Maciej Guzik,
maciej.guzik@ikifp.edu.pl

SPECIALTY SECTION
This article was submitted to Industrial Biotechnology, a section of the journal Frontiers in Bioengineering and Biotechnology

RECEIVED 30 November 2022
ACCEPTED 16 January 2023
PUBLISHED 09 February 2023

CITATION
Snoch W, Jarek E, Milivojevic D, Nikodinovic-Runic J and Guzik M (2023), Physicochemical studies of novel sugar fatty acid esters based on (*R*)-3-hydroxylated acids derived from bacterial polyhydroxyalkanoates and their potential environmental impact.
Front. Bioeng. Biotechnol. 11:1112053.
doi: 10.3389/fbioe.2023.1112053

Physicochemical studies of novel sugar fatty acid esters based on (*R*)-3-hydroxylated acids derived from bacterial polyhydroxyalkanoates and their potential environmental impact

Wojciech Snoch[1], Ewelina Jarek[1], Dusan Milivojevic[2], Jasmina Nikodinovic-Runic[2] and Maciej Guzik[1]*

[1]Jerzy Haber Institute of Catalysis, Surface Chemistry Polish Academy of Sciences, Kraków, Poland, [2]Institute of Molecular Genetics and Genetic Engineering, University of Belgrade, Belgrade, Serbia

Sugar fatty acids esters are popular compounds widely used in both the nutritional, cosmetic and pharmaceutical industries due to their amphiphilic structure and consequent ability to reduce the surface tension of solutions. Furthermore, an important aspect in the implementation of any additives and formulations is their environmental impact. The properties of the esters depend on the type of sugar used and the hydrophobic component. In this work, selected physicochemical properties of new sugar esters based on lactose, glucose and galactose and hydroxy acids derived from bacterial polyhydroxyalkanoates are shown for the first time. Values for critical aggregation concentration, surface activity and pH make it possible that these esters could compete with other commercially used esters of similar chemical structure. The investigated compounds showed moderate emulsion stabilization abilities presented on the example of water-oil systems containing squalene and body oil. Their potential environmental impact appears to be low, as the esters are not toxic to *Caenorhabditis elegans* even at concentrations much higher than the critical aggregation concentration.

KEYWORDS

polyhydroxyalkanoates (PHA), sugar esters, cosmetic industry, *Caenorhabditis elegans*, environmental impact, surface activity

Introduction

The demand for various emulsion systems and lubricants for skin care and protection is increasing every year (Farias et al., 2021). It became even more significant in recent years due to the fight against the COVID-19 pandemic–when the frequency of disinfection has become an inseparable part of everyone's life (Masen, 2020; Patruno et al., 2020; Dini and Laneri, 2021). Therefore, the pharmaceutical and cosmetic industries are constantly working on perfect water-oil (W/O) systems that are less irritating to skin, are more stable in temperature and time, and are even capable of delivering bioactive compounds (Fabbron-Appas et al., 2021). At the same time, the impact of these systems on the environment is not without significance. Emulsions used in the industry should have physical and chemical parameters allowing them to be easily decomposed to not harm living organisms (Dini and Laneri, 2021; Tang et al., 2022). In order to meet these requirements a perfect combination of the oil phase and the emulsion stabilizer

10.3389/fbioe.2023.1112053

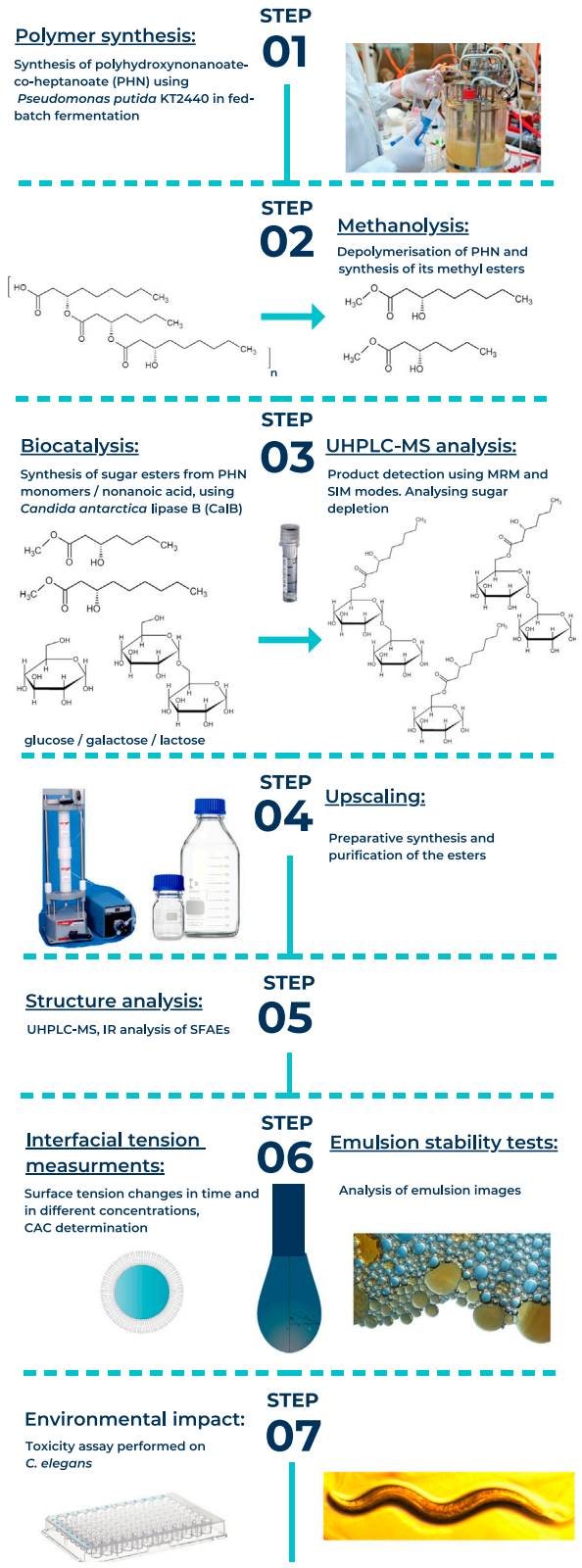

FIGURE 1
Scheme of the research and it's workflow.

needs to be sought. Sugar fatty acid esters (SFAE) seem to be fair candidates for supporting such W/O systems. Their chemical structure and physicochemical properties, provide numerous applications in the pharmaceutical, cosmetic and food industries, including dietary supplements (Kumar, 2005; Łopaciuk and Łoboda, 2013; Blanc, 2015). The foremost important feature these chemicals offer in the formulation of products (i.e. creams, gels, foams, *etc.*) are their ability to decrease interfacial tension and to stabilize emulsions. Sometimes they are even accompanied by antimicrobial characteristics (Hill and Rhode, 1999; Van Kempen et al., 2013; Lucarini et al., 2016; Shao et al., 2018). These surfactant features can be manipulated either by the number of–OH groups within a sugar component, the length or modification of an aliphatic chain, which together can be described by hydrophilic-lipophilic balance (HLB) values (Sharma and Sarangdevot, 2012; Lémery et al., 2015; Pe et al., 2017). The hydrophobic component may be branched, include unsaturated bonds, additional hydroxylic groups or other desirable functionalities (van Kempen et al., 2014; Zhou et al., 2014; Riecan et al., 2022). Worth mentioning is a fact that global surfactant market size was 39,901 million USD in 2019 and is projected to grow to 52,417 million USD by 2025 (Tortilla et al., 2019).

Having the above in mind, our attention was drawn by a family of bacterial polyesters, namely polyhydroxyalkanoates (PHAs), as a source of easily modifiable hydroxyacids, used here as the hydrophobic component of SFAEs. Polyhydroxyalkanoates are synthesized by bacteria in response to environmental stress from various carbon sources and so far around 150 different building blocks are incorporated in their structure (Steinbiichel and Steinbiichel, 1995). The PHA monomers, namely (*R*)-3-hydroxylated fatty acids, are promising components for SFAEs synthesis with intrinsic antimicrobial and anticancer potential (Snoch et al., 2019; Snoch et al., 2021). Their structure–a hydroxyl group at the 3rd position–allows for further modifications by decorating the molecule with the desired functionality (i.e. *via* an ether or an ester bond). Moreover, these sugar esters can be synthesized with an aid of biocatalysis, using enzymes such as lipases or esterases (Ansorge-Schumacher and Thum, 2013; Khan and Rathod, 2015; Pappalardo et al., 2017; Staroń et al., 2018), enabling preparation of true green additives. We have followed this path and employed biocatalysis in synthesis of our novel esters. However, little is known about their physicochemical characteristics.

This work describes surface activity of biotically synthesized sugar esters in comparison with their aliphatic counterparts (Figure 1). Their hydrophobic part was originated from bacterial poly–(*R*)–3–hydroxynonanoate–co–heptanoate (PHN). Firstly, we provide data on critical aggregation concentration (CAC), the point, conventionally chosen, where an increase of the surfactant concentration does not lead to a significant further reduction of the surface tension (Garofalakis et al., 2000) of the investigated compounds. Additionally, we performed simple tests of their emulsifying abilities with popular ingredients in cosmetic industry as skincare oil and squalene. Next, determination of emulsion stabilizing properties of these systems enabled us to verify industrial potential application of the SFAE as emulsifier. Finally, performing toxicity assay on *Caenorhabditis elegans* provided prognosis about the final key issue: potential environmental impact of the investigated stabilizers (Place, 2020; Ali and El-Ashry, 2021; Lanzerstorfer et al., 2021).

Materials and methods

Sugar esters used in this study

Sugar esters of aliphatic nonanoic acid along with a mixture of (*R*)-3-hydroxylated nonanoic acid and heptanoic acids (mPHN, derived from PHN) of glucose, galactose and lactose were obtained and characterized as

10.3389/fbioe.2023.1112053

TABLE 1 Composition of enzymatically obtained sugar esters used in this work.

Compound name[a]	Type of mono/diester	Amount of mono/diester (%)	Mean molar mass (g mol^{-1})
C9-glu	c9	75.8	370.57
	c9c9	24.2	
C9-gal	c9	91.0	352.68
	c9c9	9.0	
C9-lac	c9	89.4	497.31
	c9c9	10.6	
mPHN-glu	c9	20.0	406.98
	c9c9	09.8	
	c7	16.3	
	c7c7	32.9	
	c9c7	21.0	
mPHN-gal	c9	20.5	401.61
	c9c9	27.0	
	c7	25.6	
	c7c7	15.0	
	c9c7	11.9	
mPHN-lac	c9	24.6	584.22
	c9c9	18.9	
	c7	06.3	
	c7c7	21.5	
	c9c7	28.8	

a) C9-glu: a mixture of mono and diesters of glucose nonanoate, C9-gal: a mixture of mono and diesters of galactose nonanoate, C9-lac: a mixture of mono and diesters of lactose non-aoate, mPHN-glu: a mixture of PHN monomers originated glucose mono and diesters, mPHN-gal: a mixture of PHN monomers originated from galactose mono and diesters, mPHN-lac: a mixture of PHN monomers originated lactose mono and diesters.

- c9-monoester containing one nine carbon atom chain
- c7-monoester containing one seven carbon atom chain
- c9c9-diester containing two nine carbon atom chains
- c7c7-diester containing two seven carbon atom chains
- c9c7-diester containing one nine and one seven carbon atom chain

described in our previous works. In search of effective anticancer agents—novel sugar esters based on polyhydroxyalkanoate Monomers (Snoch et al., 2021). The composition of new synthesized compounds is presented in Table 1, the yields and their purity are presented in Supplementary Table S1.

Determination of surface activity of synthesized compounds

The surface tension has been measured for different batches of synthetized compounds by using pendant drop shape analysis method by two apparatus. First apparatus: a home-made experimental set-up described in detail in (Para et al., 2006), with experimental error equals to 2 mN/m, was used. The Young–Laplace capillary equation was fitted to the digitally recorded drop image. Measured surface tension value corresponds to the value of the best fit (note: it is as the only unknown parameter in this equation). The dynamic surface tension measurements were performed every 5 s. Measured equilibrium surface tension corresponded to the obtained steady-state time after adsorption, which was depended on surfactant concentration. The studied solutions of surfactant were mixtures of sugars mono and diesters, which can differ by number of hydrophobic hydrocarbon chains. As a consequence, the kinetic curves for different drops of the same solution did not often overlap. That is why the experimental values for one solution are the mean values from all the recorder dynamic curves. As second apparatus a commercial tensiometer (PAT–1M, Sinterface, Berlin, Germany), with experimental error of 0.2 mN/m, was used. (Kairaliyeva et al., 2017). The PAT-1M apparatus allows for an accurate control of the droplet area (or its volume) by a syringe pump, driven by a feedback loop software based on the drop imaging. The dynamic interfacial tension *versus* time on a freshly formed drop is measured during the ageing of the interface while keeping the drop volume constant (11 μL). The equilibrium interfacial

tensions are obtained from these data at long period of time. The greatest experimental error is mainly connected with small differences in composition from batch to batch so we present all experimental points and determined the critical aggregation concentration (CAC). All surface tension measurements were performed at 295 K. For all the experiments, ultrapure water—produced from the Millipore Direct-Q ® 5UV purification system (18 MΩ cm^{-1}), was used. Its surface tension measurement provides a value of 72.5 ± 0.2 mN/m, stable for at least 2 hours at 20°C meaning negligible amount of surface-active impurities.

Determination of hydrophilic- lipophilic balance

Hydrophilic-Lipophilic Balance was determined according Griffin method by using following equation (Griffin W.C., 1954)

$$HLB = 20\,x\,\frac{hydrophilic\ group\ molecular\ weight}{total\ surfactant\ molecular\ weight} \quad (1)$$

Emulsion stability

The ability of the SFAE to stabilize water–oil (W/O) systems was estimated by measuring time of phase separation in each performed emulsion. The experiment was conducted under following protocol: 5 g of each SFAE solutions were prepared as water phase and mixed with 0.5 g of oil phase: squalane or popular commercially available skincare oil- Bambino® respectively. Concentrations of the SFAE in solutions were: 0.5 × CAC, 1.0 × CAC 1.5 × CAC respectively. The skincare oil consisted of: glycine soya oil, paraffinum liquidum, parfum, ethyl linolate, ethyl oleate, tocopherol, propylene glycol, propyl galate, citric acid, BHA, according to the manufacturer label in the unknown proportions. The mixtures were mixed in shaker at 25 C for 20 min and mixed vigorously with Vortex for another 1 min to ensure the phases were mixed sufficiently (An et al., 2019; Li and Xiang, 2019).

Caenorgabditis elegans toxicity assay

Potential environmental impact of the investigated compounds was tested by treating *Caenorhabditis elegans* according to following protocol adapted from WormBook (Stiernagle, 2006) and (Djapovic et al., 2021). Briefly, synchronized worms (L4 stage) were suspended in a medium containing 95% M9 buffer (3.0 g of KH_2PO_4, 6.0 g of Na_2HPO_4, 5.0 g of NaCl, and 1 mL of 1 mol L^{-1} $MgSO_4$ × 7 H_2O in 1 L of water), 5% LB broth (10 g L^{-1} tryptone, 5 g L^{-1} yeast extract, and 10 g L^{-1}NaCl), and 10 μg mL^{-1} of cholesterol. The experiment was carried out in 96-well flat-bottomed microtiter plates (Sarstedt, Nümbrecht, Germany) in the final volume of 100 μL per well. Suspension of nematodes (25 μL containing 25–35 nematodes) was transferred to the wells of a 96-well microtiter plate, where 50 μL of the medium was previously added. Next, 25 μL of a solvent control (DMSO) or 25 μL of a concentrated solution was added to the test wells. The examined esters were dissolved in DMSO to obtain stock solutions than added to the wells with worms. The final concentrations of the compounds were 2.0, 1.5, 1.0, 0.5, 0.25 and 0.125 mg mL^{-1}. The final concentration of DMSO in each well was 1% (v/v) Subsequently, the plates were incubated at 25 C for 2 days. The fraction of dead worms was determined after 48 h by counting the number of dead worms and the total number of worms in each well, using a stereomicroscope (SMZ143-N2GG, Motic, Wetzlar, Germany). As a negative control experiment, nematodes were exposed to the medium containing 1% (v/v) DMSO.

Results

After preparative synthesis, purification and drying the obtained SFAE were analyzed using UHPLC-MS (QQQ) in both selected ionic mass (SIM) and multiple reaction monitoring (MRM) modes. The obtained peaks from ESI+, i.e. $(M + Na)^+$ adducts, were integrated so their peak areas enabled us to calculate fractions of mono and diesters. Mean molar masses of SFAE mixtures were calculated as well. The obtained results are presented below in Table 1.

Instead of the critical micelle concentration (CMC), we decided to use the more general term—critical aggregation concentration (CAC)—because the LC-MS analysis shows that the synthesised compounds are in fact mixtures of mono and diesters with different percentage compositions (See Table 1) and undefined stereochemistry of the resulting esters. As the concentration of the surfactants tested increases, the surface tension does not transition sharply to a constant value, as is the case with pure mono-component surfactant solutions, but gradually changes marginally (Supplementary Figure S1). We used as CAC values the concentration at which the slopes of the curves connecting the experimental points significantly change shape and the surface tension for subsequent concentrations does not differ significantly (dashed lines in Figure 2). Despite the large scatter in the data obtained especially for the galactose derivatives, the experimental results of the solutions of the different batches, obtained on the two apparatus, coincide, and the trend in the differences in surface activity between the simple esters and mPHN derivatives is the same (Figure 2). The lactose derivatives are the most surface active, followed by galactose and the least glucose, as evidenced by the increasing values of the critical aggregation concentration (Table 2). A comparison of the aliphatic sugar esters and the corresponding mPHN derivatives shows that the mPHN derivatives are more surface active (Figure 3). In our case the quality of the anomers (α or β) in the tested solutions was not determined. Nevertheless, literature data indicate that the stereochemistry of the sugar derivatives can affect the surface tension. For example, *ß* anomers are more effective surfactants than α anomers, and differences in surface tension can be as high as 8 mN m^{-1}. This is a result of differences in the ability to form intermolecular hydrogen bonds with other ester molecules and the surrounding water molecules (Nilsson et al., 1998). As a consequence, the sugar moieties' hydrophilicity, surface activity and solubility are altered, which can result in the presence of relatively large aggregates in solution, but too fine (below 300 nm) to cause visible turbidity in solutions (Nilsson and So, 1998; Larsson et al., 2019). Clearly, this is an issue that will require additional research in the future.

The pH of the solutions tested for simple sugar derivatives and mPHN-lac ranged from 5.2 to 6.8, which is characteristic of aqueous solutions in contact with carbon dioxide. Only in the case of mPHN-glu and mPHN-gal were the solutions slightly acidic (pH = 4.0 ± 0.2),

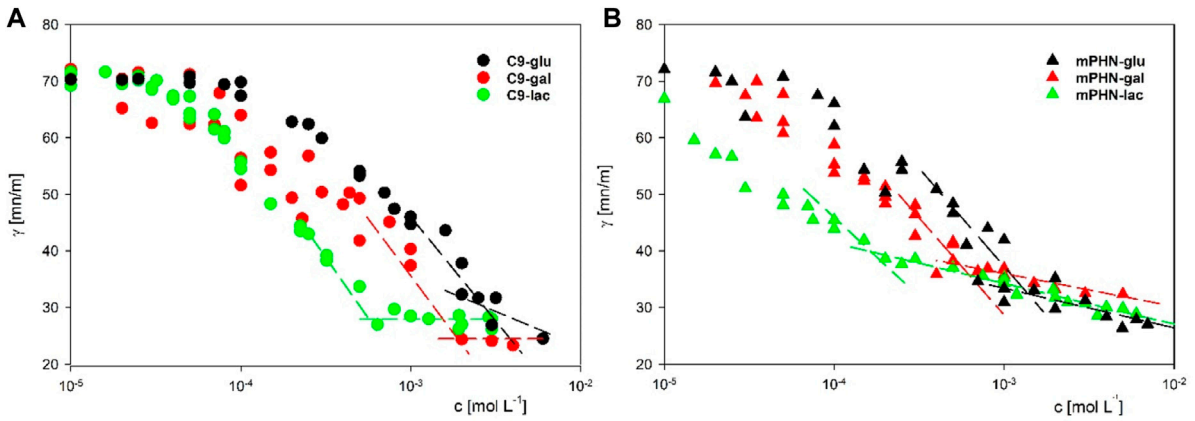

FIGURE 2
The surface tension dependency on surfactants concentration **(A)** C9-glu black circles; C9-gal red circles; C9-lac green circles **(B)** mPHN-glu black triangles; mPHN-gal red triangles; mPHN-lac green triangles. The intersection of the lines indicates the concentration at which the slope of the surface tension isotherms changes significantly, which is conventionally taken as CAC.

so surface tension measurements were carried out for these solutions (C = 1 mmol L^{-1}) in the presence of 0.1 mol L^{-1} NaCl. Increasing the ionic strength did not result in significant changes in surface tension (e.g. from 34.8 mN m^{-1} in H_20 to 33.1 mN m^{-1} in 0.1 mol L^{-1} NaCl for mPHN-gal and from 34.5 mN m^{-1} in H_20 to 32.6 in 0.1 mol L^{-1} NaCl), which are within the experimental limit of the apparatus error (2 mN m^{-1}). This may indicate that surface-active ionic compounds are absent from the solution. In contrast, measurements in 0.1 mol L^{-1} NaOH solution resulted in a significant increase in surface tension (e.g. for mPHN-gal it increased to a value of 42 mN m^{-1} and for mPHN-gal to 58.6 mN m^{-1}). This may be due to the different susceptibility to hydrolysis - the released organic acids dissociate in an alkaline environment and, as ionic surfactants, show much lower surface activity. In addition, the different degree of hydrolysis may be due to the different content of α and *ß* anomers.

Both glucose and galactose esters CAC values were much lower than the referenced CMC glucose monooctanoate (10.5 mmol L^{-1}) and higher than glucose monodecanoate (0.71–1.5 mmol L^{-1}) (Lee et al., 2018), which directly correlates with the chain length of the hydrophobic component of SFAE. Interestingly, C9-lac and mPHN-gal ester mixtures are somewhat identical to the commercial sucrose monodecanoate (SM-1000), the CMC of which was 0.56 mmol L^{-1}. In general CACs of the mPHN derived esters obtained are higher than their counterparts in the literature, giving slightly lower interfacial tension values. The difference was observed for mPHN-lac which CAC is much lower than sucrose and lactose caprate (c10), laurate (c12) and even oleate (c18). Although mPHN-lac can be compare to Tween 80 (γ = 0.01 mmol L^{-1}, 38 mN m^{-1}). (Lee et al., 2018) (Lucarini et al., 2018) (Ye et al., 2016). All the synthesized based SFAE have their measured surface tension at the similar level (varying for the lowest of γ = 25.2–23.5 mN m^{-1} for C9-gal to the highest of γ = 32–28 mN m^{-1} for mPHN-lac, without any visible trend, Table 2). The HLB indexes calculated are lower for mono carbohydrates in both groups when compared to lactose esters. However, when hydrophobic component is considered, the HLB indexes are larger by 1–3 units for the aliphatic SFAEs. All the HLB values were in range of the referenced compounds (Table 2) regardless of whether the calculations took into account the content of mono- or diesters.

On the basis of the obtained interfacial tension profiles, it was possible to draw equilibrium concentrations curves, thus to determine aggregation concentrations (Figures 2A,B). The curves for different concentrations, but with a similar profile and little difference in values, are indicative of aggregation or micelle formation. They also provide indirect information on how the presence of mono- and diesters of c7 and c9 chains affects the ability to reduce surface tension. It is noticeable that the shape of each curve is depended on the sugar component (glucose and galactose vs. lactose esters, Figures 2A,B). In both cases the slopes of lactose esters were steeper than in these of glucose and galactose esters mixtures, which may be related to the difference in the size of the hydrophilic sugar heads. (Gaudin et al., 2019). Moreover, the slope of the curve for the mPHN-lac mixture was steeper than C9-lac (containing 89.4% monoester, 10.6% diesters), which may be related to the higher ratio of diesters in the mPHN-lac mixture (containing 30.8% of the total monoesters of c9 and c7 and 69.2% of the total of c9c9, c7c7, c9c7 diesters).

Taking into account the composition of the tested mixtures and contribution of diesters, we would expect lower ranges of CAC concentrations. Similar to those presented in Table 2 e.g. sucrose oleate. As can be seen, the presence of additional c9 or c7 chains in the hydrophobic component does not translate directly into properties comparable to twice as long aliphatic chains of other esters. It can be partially explained by the catalytic action of the lipase, which decorates a sugar moiety by attaching hydrophobic components on the opposite sides of the carbohydrate. There is also uncertainty when it comes to decorating sugars with (*R*)–3–hydroxylated fatty acids by the action of lipase, whether the final structure of the resultant SFAE is as described above for the aliphatic appendixes or it reassembles this of rhamnolipids (sugar + (*R*) –3-hydroxylated fatty acid + (*R*)–3-hydroxylated fatty acid). Moreover, the mere presence of hydroxyl group of monomers can also influence the branching of the entire molecule and disrupt the hydrophobicity of a carbon chain. (Hollenbach et al., 2020). Therefore, more detailed studies are needed in order to elucidated the final structure of the produced esters and also their behaviour on the molecular scale.

10.3389/fbioe.2023.1112053

TABLE 2 Physicochemical properties of the synthetized sugar esters and reference compounds.

Compounds used in this study								
Compound name	CAC	Surface tension γ	HLB griffin for each SFAE component					pH
	(mmol L–1)	(mN m–1)	c9	c7	c9c9	c7c7	c9c7	
C9-glu	2.7	31.5–24.5	11.25	–	7.83	–	–	5.39
C9-gal	2	25.2–23.5	11.25	–	7.83	–	–	5.33
C9-lac	0.56	29.2–25.8	14.2	–	11	–	–	6.29
mPHN-glu	1.4	35–26	11.72	12.79	8.7	9.81	9.22	3.92
mPHN-gal	0.56	37–32	11.72	12.79	8.7	9.81	9.22	4.12
mPHN-lac	0.016	39–28.5	14.41	15.27	11.49	12.57	12.01	6.8

Referenced compounds				
Compound name	CMC/CAC	Surface tension γ	HLB Griffin	References
	(mmol L-1)	(mN m-1)		
octyl- B-D- glucoside	21.2	31	12.32	Gaudin et al. (2019)
nonyl- B-D- glucoside	6.9	29.6	11.7	
Glucose monooctanoate (c8)	10.15	26.37	11.76	Zhang et al. (2015)
Glucose monodecanoate (c10)	0.71	30.49	10.77	
Glucose monodecanoate (c10)	1.5	25.5	10.77	Hollenbach et al. (2020)
Lactose caprate (c10)	2.5	40.6	14.8	Lee et al. (2018); Lucarini et al. (2018)
Lactose laurate (c12)	0.55	40.4	14.1	
Sucrose Laurate (c12)	1.2	19.7	8.19	Ye et al. (2016)
Sucrose oleate (c18)	0.0345	29.6	10.1	
Tween 80	0.01	38	15	
α-D-Glucose laurate (c12)	0.13	41.2	3.8	Garofalakis et al. (2000)
α-D-Maltose laurate (c12)	0.12	35.9	4.5	
Lactose tetradecanoate (c14)	0.041	38.6	4.3	
Sucrose monooctanoate (c8) SM- 800 ®	6	28.7	15.8	
Sucrose monooctanoate (c10) SM- 1000 ®	0.57	32.9	–	
Sucrose monooctanoate (c12) SM- 1200 ®	0.29	33.5	–	

Emulsion stability

Basing on a series of 5-min films and images taken up to 48 h of water/oil systems containing different concentrations of the tested SFAEs, it was not possible to measure the thickness of the emulsion layer and thus determine the stability index of the emulsion (Supplementary Figure S2). This was due to the short lifetime of the emulsion. However, depending on the type of ester, its concentration, and the composition of the oil phase, emulsion systems formed and maintained from several minutes to 1 hour (Table 3.). Emulsions containing squalene were less stable. W/O control systems containing no esters blurred after only a few minutes. On the other hand, systems containing SFAEs based on body care oil turned out to be more durable, as they had a diverse composition and contained co-surfactants such as alcohols. Furthermore, in most cases, differences in the durability and consistency of emulsions can be observed. They depend on the concentration of SFAEs in aqueous solutions. The higher the SFAE concentration, the more stable and homogeneous the system was. Systems containing C9-glu and C9-gal proved to be the most stable. The least stable system contained C9-lac. Emulsions based on mPHN-glu and mPHN-gal esters proved to be less stable than those originated from nonanoic acid. In contrast, the emulsions containing mPHN-lac exhibited a higher persistence than mPHN-glu, mPHN-gal and C9-lac. The maximum lifetime of the investigated homogeneous emulsion systems (Table 3 emulsion quality assessment 3, Supplementary Figure S2) was 60 min. These were systems containing a commercial baby care oil. However, some remaining emulsions were visible and even more stable: 180 min for mPHN-glu, mPHN-gal and mPHN-lac to 1440 min for C9-glu, C9-gal, C9-lac. In W/O systems that contained squalane, after 60 min, the quality rating were 2 or 1, respectively. These lifetimes are definitely too short to make them competitive against other surfactants used in the industry, such

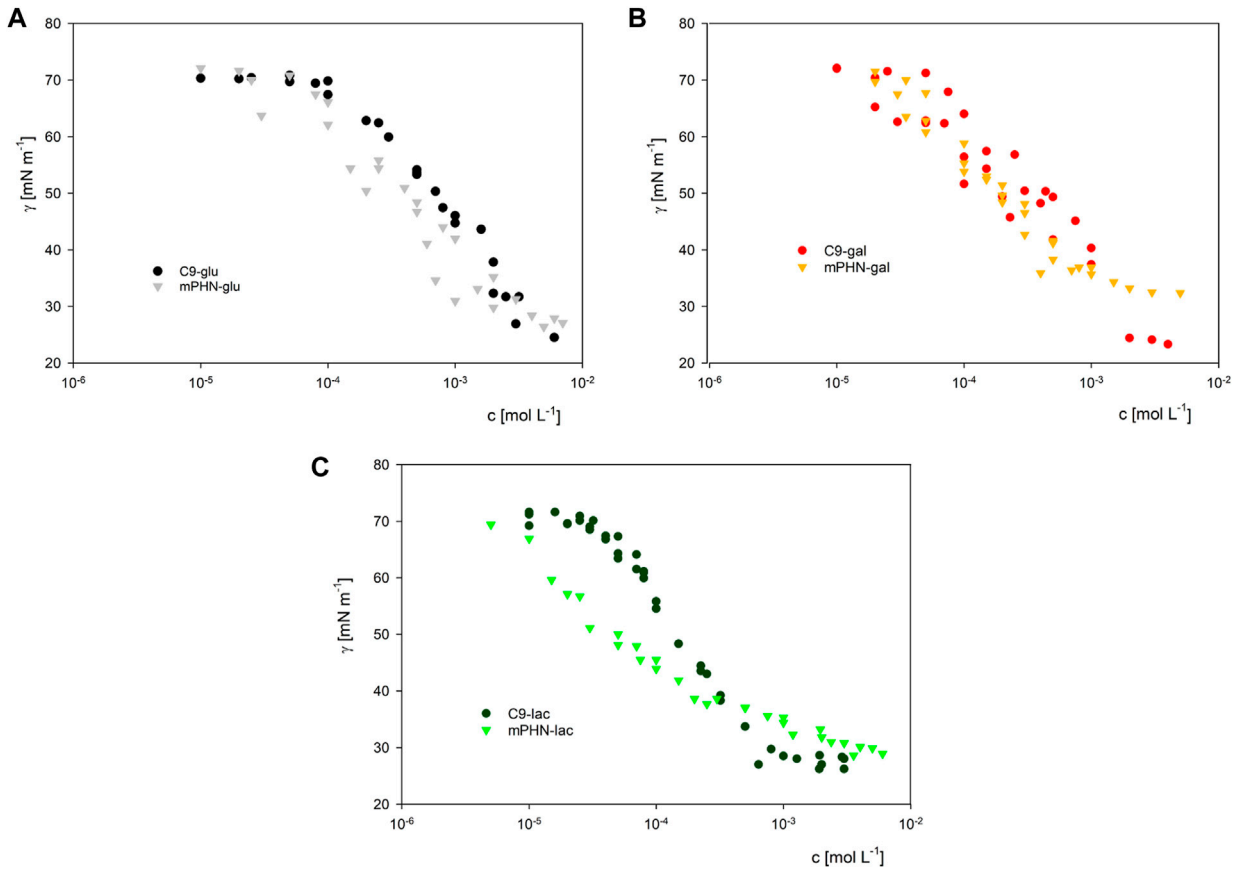

FIGURE 3
The comparison of surface activity of biocatalytically synthesized mPHN sugar esters with their aliphatic counterparts. Respectively for glucose (Panel A), galactose (Panel B) and lactose (Panel C) derivatives.

as Tween 80, Triton-X, Span 20, Span 60, polyethylene glycol (PEG). However, noteworthy is that commercially available products very often contain combinations of various surfactants e.g. Tween 80- polyoxoethylene sorbitan monooleate or Triton X-100-consisted of PEG and p-tert-octylphenol. Usually investigated W/O systems are based on combinations of two or more different ionic and/or nonionic surfactants and other co-surfactants i.e. alcohols and fatty acids, that make together the emulsions even more stable and extend their lifetime. (Watanabe et al., 2018). (Li and Friberg, 1982; McClements and Jafari, 2018). This approach should be investigated with our biocatalytically synthetized SFAE.

Although the expected lifetime of a commercially acceptable emulsion should be counted in days up to 1 month, the prepared here W/O systems did not perform well more than 24 h. We can explain this either by poor stabilizing properties of the SFAEs or their too-low concentrations used in preparation W/O systems, as well as lack of other co-surfactants. The calculated concentrations of the investigated surfactants present in the emulsions were between 0.001% and 1.0% m/v respectively (from 0.5 to 1.5 x CAC) while usually used concentrations of surfactants from the literature are between 0.1% and 5.0% m/v (Feng et al., 2022) but rarely calculated on their CAC or CMC values. That makes our system difficult to compare. Moreover, literature mentions several different techniques used for emulsion preparation i.e. shaking, ultrasound mixing, microwave pulsing, (Taha et al., 2020; Hyde et al., 2021), magnetic mixing, high pressure homogenization (Li and Xiang, 2019), and syringe mixing (Koursari et al., 2020). In recent years, even use of solid stabilizing particles (Pickering emulsions) became more popular. Nanomaterials derived from natural sources are an interesting alternative or supplementary for this application. (Velásquez-Cock et al., 2021). In order to compare our surfactants for their feasibility in applications other than described below (drug delivery purposes), studies should be conducted in greater concentrations and with other additives.

The ideal W/O system used in the cosmetic or pharmaceutical industry should arise from natural sources, and also should be able to form stable and durable emulsions. Emulsions need to be stable enough to be stored at room temperature. Most importantly, they should be biodegradable and biocompatible. When it comes to drug delivery systems, their life time longer than 48–72 h is not advisable either. Another crucial factor is emulsion bioaccessibility. That means easy absorption by the epithelial surfaces, passing through cell membranes but not damaging them. (Production of green surfactants: Market prospects | Elsevier Enhanced Reader) The micelles protecting the structure of the drug from enzymes and/or pH changes should be able to release it gradually to the tissues. (Felzenszwalb et al., 2019). The micelle-building components ought to be easily degraded or removed from the body and easily decomposed in the environment. (Tovar-Sanchez et al., 2020) (Hunt, 2017) (Fagan and Portman, 2014). Undoubtedly, the studied SFAEs show some emulsion-stabilizing properties, but in order to give these W/O systems the desired longer lifespan, further optimization of SFAEs concentration, oil phase composition, mixing methods and addition of co-surfactants is required.

TABLE 3 Emulsion stability of two exemplary water/oil systems in time. Numbers-colors and their intensity is a scale referring to the intensity of a particular emulsion. Exemplary photos of the formed emulsions Supplementary Figure S2. a) Control- W/O systems with no SFAE addition b) squalene as oil phase with SFAEs as stabilizers c) baby care oil as an oil phase with SFAEs as stabilizers.

A

time [min]	Squalane	Olive
0	3	3
1	1	3
5	0	2
30	0	1
60	0	0
180	0	0
1440	0	0

B

		C9-glu			C9-gal			C9-lac			mPHN-glu			mPHN-gal			mPHN-lac		
N x CMC	Control	0.5 × CAC	1.0 × CAC	1.5 × CAC	0.5 × CAC	1.0 × CAC	1.5 × CAC	0.5 × CAC	1.0 × CAC	1.5 × CAC	0.5 × CAC	1.0 × CAC	1.5 × CAC	0.5 × CAC	1.0 × CAC	1.5 × CAC	0.5 × CAC	1.0 × CAC	1.5 × CAC
time [min]																			
0	3	3	3	3	3	3	3	1	1	1	3	3	3	3	3	3	3	3	3
1	1	3	3	3	3	3	3	1	1	1	2	3	3	3	3	3	3	3	3
5	0	1	2	2	2	3	2	1	1	1	2	3	3	2	3	3	2	3	3
30	0	1	2	2	2	2	2	0	0	0	1	2	2	1	2	2	1	2	2
60	0	0	1	2	2	2	2	0	0	0	0	1	1	0	1	1	0	1	1
180	0	0	1	1	1	1	1	0	0	0	0	1	1	0	1	1	0	1	1
1440	0	0	0	0	0	0	1	0	0	0	0	0	0	0	0	0	0	0	0

C

		C9-glu			C9-gal			C9-lac			mPHN-glu			mPHN-gal			mPHN-lac		
N x CMC	Control	0.5 × CAC	1.0 × CAC	1.5 × CAC	0.5 × CAC	1.0 × CAC	1.5 × CAC	0.5 × CAC	1.0 × CAC	1.5 × CAC	0.5 × CAC	1.0 × CAC	1.5 × CAC	0.5 × CAC	1.0 × CAC	1.5 × CAC	0.5 × CAC	1.0 × CAC	1.5 × CAC
time [min]																			
0	3	4	4	4	4	4	4	3	4	3	3	3	3	3	4	4	3	4	4
1	3	3	3	3	4	4	3	3	3	3	2	3	2	3	3	4	3	3	4
5	2	3	3	3	4	4	3	3	3	3	2	3	2	3	3	3	3	3	3
30	1	3	3	3	3	3	3	2	3	2	2	3	1	3	3	3	3	3	3
60	0	3	3	3	3	3	3	2	3	2	2	2	1	3	3	3	3	3	3
180	0	2	2	2	1	2	2	2	2	1	2	2	1	1	1	2	1	1	2
1440	0	1	2	2	1	2	2	2	2	1	0	0	0	0	1	1	0	1	1

(McCartney et al., 2019). The emulsion stabilizing properties of the investigated SFAE may not be spectacular, nevertheless sometimes desired if there is a need of administration of a less stable formulation to a patient prepared minutes prior injection/topical application. The used SFAE were already shown to exhibit anticancer properties, which increase their possibility to be applied in the medical industry (Tuvia et al., 2014).

Environmental impact of sugar fatty acid esters

Caenorhabditis elegans is a multicellular, non-parasitic model organism that is a valuable research object for testing the effects of various industrial chemicals such as anti-cancer drugs and antibiotics (Judy et al., 2019; Wittkowski et al., 2019). Every year, mankind supplies a huge amount of industrial wastewater and with it–surfactants (Production of green surfactants: Market prospects | Elsevier Enhanced Reader; Akbari et al., 2018; Felzenszwalb et al., 2019; Tovar-Sanchez et al., 2020). Therefore, there is a need for continuous monitoring of their impact on organisms living in soil and groundwaters (Ebele et al., 2017; Rathi et al., 2021). The usefulness of nematodes representatives is manifested in a fast life cycle, easy multiplication and obtaining a large number of individuals in subsequent generations, the possibility of long–term storage of larvae and eggs in laboratory conditions. They do not require continuous breeding, and the procedure for synchronizing the life cycles of individuals in a population is simple. In addition, *Caenorhabditis elegans* feed on an easily available source of food–bacteria *E. coli*. The most important from the human point of view, is the presence of simple organ systems: nervous (nerve ring), blood, protonfridial, gonads, and the ability to assess not only the size of the population under the microscope, but also the ability to actively move individuals in the population. Therefore, nematodes can be indirect

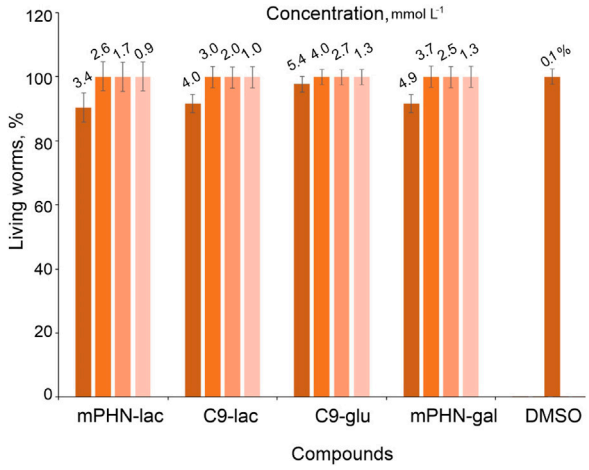

FIGURE 4
Toxicity of the sugar esters against *Caenorhabditis elegans* after 48 h exposure.

bioindicators of the influence of the tested substances on the natural environment (Fagan and Portman, 2014; Hunt, 2017). Having the above in mind, toxicity of the tested sugar esters against *Caenorhabditis elegans* was assessed by observing the nematodes under a microscope after 48 h of exposure. Based on the mobility of *Caenorhabditis elegans* their viability was assessed. Actively moving organisms were considered living, non-moving organisms were considered dead, and barely moving organisms were considered alive as well (having in mind, that the compounds could have a negative effect on worms) (Figure 4).

Observations of the nematodes allowed us to conclude that the obtained SFAEs do not pose a major threat to *Caenorhabditis elegans* at the given time of exposure. Only the highest concentrations

(2.0 mg ml^{-1}) of the mixtures reduced nematodes populations up to 15% but 1.5 mg ml^{-1} was already not effective. The concentrations of the esters per the well ranged from 0.0625 to 2.0 mg ml^{-1} which correspond to their molar concentrations of: C9-glu 0.186.14–5.69 mmol L^{-1}; C9-gal 0.162–5.312 mmol L^{-1}; C9-lac 0.125–4.0 mmol L^{-1}; mPHN-glu 0.142–4.544 mmol L^{-1}; mPHN-gal 0.148–4.744 mmol L^{-1}; mPHN-lac 0.119–3.816 mmol L^{-1}, respectively. We have previously reported that SFAE esters based on nonanoic acid and PHN monomers show anticancer potential. The reported consternations (IC_{50}) of these compounds that were found to be effective against certain cancer lines (In Search of Effective Anticancer Agents—Novel Sugar Esters Based on Polyhydroxyalkanoate Monomers-W. Snoch et al., 2021. pdf) are at the levels of being non-toxic to *Caenorhabditis elegans*. For example, the effective IC_{50} for Du145 and HTB140 cell lines after 24 h exposures to all tested SFAE were below 0.25 mg ml^{-1} (i.e. IC_{50} range respectively 0.09–1.5 mmol $L^{-1}$for cancer cells and 0.5–2.5 mmol L^{-1}, respectively for reference healthy cells).

Sugar esters belong to the group of non-ionic surfactants. The presence of a hydrophobic fatty acid tail and a hydrophilic sugar head give them an amphiphilic character. The chemical structure itself does not, in general, pose a direct threat to the entire organism of nematode. However, this amphiphilicity and the ability of compounds to lower the surface tension of solutions may permeabilize cell membranes (Tuvia et al., 2014; McCartney et al., 2019). On the other hand, the presence of long carbon chains (such as c18 steric acid) increases the solubility of individual compounds in water (e.g. in industrial wastewaters) (Vinarov et al., 2018). All this together causes the entry of undesirable substances from the environment into the cells, an increase in the concentration of H^+ ions, free oxygen radicals, herbicides, pesticides or salts (which can cause an osmotic shock), which in turn may direct the cells to the apoptotic pathway (Shao et al., 2018; Cavanagh et al., 2019; Appah et al., 2020; Liu et al., 2021; Martins-Gomes et al., 2022). In addition, the hydrophobic components of the SFAE tested do not exceed 9 carbon atoms, which may be another advantage compared to other commonly used esters based on acids with a chain length of c12, c16 or c18 (e.g. Span 20, Span 80, PEG 20– Sorbitan monolaurate (SPEG), Tween 20, Tween 80). Since increasing the chain length of the hydrophobic component also increases the toxicity of SFAE (Bunchongprasert and Shao, 2020). For comparison, the toxicity of other structurally similar allose-based esters to *Caenorhabditis elegans* with various carbon chain lengths n = 2, 4, 6, 8 was in the between 0.2 and 1.0 mmol L^{-1} (Sakoguchi et al., 2019).

In addition, every cosmetic or drug carrier potentially used in the industry must be thoroughly tested in terms of toxicology, before it goes to preclinical research (the smallest, largest harmful dose, and chronic administration of the compound), at every possible stage, not only cellular, but also more complex living organisms (Dent et al., 2018; Bopp et al., 2019). The highest tested levels of the SFAE (2.0 mg ml^{-1} around 6.0 mmol L^{-1}) that reduced *Caenorhabditis elegans* populations ~15% were near to CMC values. At the same time, the range of surfactants concentrations used in the water phase, to design model emulsion systems, were 0.5–10-fold CAC. Information obtained about minor negative effects of the esters on tested nematode in this concentration range opens the possibility for further application trials. However, it should be remembered that the SFAE molecules building micelles have a different concentration and organization than those dispersed in the buffers in which the *Caenorhabditis elegans* were used. They may behave differently and show a different level of toxicity, therefore more detailed investigation is foreseen for the future (Khamkar, 2011; Kaur et al., 2016; Rusanov, 2018; Bunchongprasert and Shao, 2020).

Conclusion

The physicochemical properties of the obtained sugar esters were characterized which enabled their application potential evaluation. The obtained CAC and surface tension values correspond to compounds with a similar structure from the literature (such as SM-800, lactose caprate, or glucose monodecanoate). Also, the ability to create water–oil systems based on popular cosmetic ingredients, such as squalene and the commercial skincare oil confirmed application potential of the tested esters. However, the process of forming and testing these emulsions should be further optimized. It would be necessary to test a series of different oil components, as well as co-surfactants, in order to compare their emulsion stability indexes, size of the micelles formed and their behaviour.

In future prospective, it is worthy to focus on assessing the toxicity of not only the compounds themselves, but entire SFAEs based stable emulsion systems. Extending these experiments to such aspects as influence the of SFAE on increasing the vulnerability of *Caenorhabditis elegans* for these emulsion systems and repeat it in unfavourable water and soil conditions (presence of pesticides, inorganic salts, low pH, osmotically active substances). Even assessing susceptibility to opportunistic organisms would be valuable. From pharmaceutical and medical points of view, a key step is to answer questions about the mechanisms of the esters interaction with cells and/or model organisms, including the permeabilization of cells and intracellular membranes, and the ability to reversibly modulate endothelial electrical resistance (TEER), would be of great value. (Lucarini et al., 2018) Nematodes should be examined in more detail in terms of the impact of SFAE, and emulsion systems stabilized by them, on their internal organs, such as the endocrine and nervous systems, and also the ability to reproduce. (Ebele et al., 2017; Alfhili et al., 2018)

Data availability statement

The original contributions presented in the study are included in the article/Supplementary Material, further inquiries can be directed to the corresponding author.

Author contributions

WS—synthesis of PHN polymer, production of its monomers, synthesis, purification, determination of all SFAE in the analytical (UHPLC-MS) and preparative quantity, carrying out some of the toxicity experiments on *Caenorhabditis elegans*, surface tensions measurements, pH, emulsion stability measurements, coordination of the team's work, preparation a draft of the manuscript, applying corrections, editing Figure 1, Figure 4 and all tables. EJ—Infrared spectra confirming structures of the SFAE, measurements of surface tensions, emulsion stability measurements, edition and understanding of surface tension results and determination of equilibrium tensions, kinetics, CAC, Figure 2 and Figure 3, writing a part of the discussion. DM—major toxicity experiments performed on *Caenorhabditis elegans*

JNR—content consultation, editing Figure 4, introducing corrections to the manuscript, editing a part of the discussion. MG—setting up the research topic, introducing corrections to the manuscript, coordination of the team's work, communication in the team. All authors have approved for the publication.

Funding

This work was supported by the National Centre of Research and Development grant TANGO-V-A/0013/2021. This project was partially funded from the Ministry of Education, Science and Technological Development of the Republic of Serbia (Agreement No. 451-03-68/2022-14/200042).

Acknowledgments

WS acknowledges the support of InterDokMed project no. POWR.03.02.00-00-I013/16. We thank Marzena Noworyta[1] for repeating pH and interfacial tension measurements and conductivity measurements.

Conflict of interest

The authors declare that the research was conducted in the absence of any commercial or financial relationships that could be construed as a potential conflict of interest.

Publisher's note

Supplementary material

The Supplementary Material for this article can be found online at: https://www.frontiersin.org/articles/10.3389/fbioe.2023.1112053/full#supplementary-material

References

Akbari, S., Abdurahman, N. H., Yunus, R. M., Fayaz, F., and Alara, O. R. (2018). Biosurfactants—a new frontier for social and environmental safety: A mini review. *Biotechnol. Res. Innov.* 2, 81–90. doi:10.1016/j.biori.2018.09.001

Alfhili, M. A., Yoon, D. S., Faten, T. A., Francis, J. A., Cha, D. S., Zhang, B., et al. (2018). Non-ionic surfactants antagonize toxicity of potential phenolic endocrine-disrupting chemicals, including triclosan in *C. elegans*. *Mol. Cells* 41, 1052–1060. doi:10.14348/molcells.2018.0378

Ali, A., and El-Ashry, R. (2021). Potential effect of the nematicide oxamyl and surfactant combinations on root-knot nematode *Meloidogyne incognita* infecting tomato plants. *Egypt. Acad. J. Biol. Sci. F. Toxicol. Pest Control* 13, 159–176. doi:10.21608/eajbsf.2021.153353

An, D., Zhang, X., Liang, F., Xian, M., Feng, D., and Ye, Z. (2019). Synthesis, surface properties of glucosyl esters from renewable materials for use as biosurfactants. *Colloids Surfaces A Physicochem. Eng. Asp.* 577, 257–264. doi:10.1016/j.colsurfa.2019.05.079

Ansorge-Schumacher, M. B., and Thum, O. (2013). Immobilised lipases in the cosmetics industry. *Chem. Soc. Rev.* 42, 6475–6490. doi:10.1039/c3cs35484a

Appah, S., Jia, W., Ou, M., Wang, P., and Asante, E. A. (2020). Analysis of potential impaction and phytotoxicity of surfactant-plant surface interaction in pesticide application. *Crop Prot.* 127, 104961. doi:10.1016/j.cropro.2019.104961

Blanc, L. (2015). What drives EU exports of pharmaceuticals? Available at: http://www.efpia.eu/uploads/Modules/Documents/the-pharmaceutical-industry-in-a-global-economy-_-what-drives-eu-exports-of-pharmaceuticals-overseas-2.pdf%5Cnhttps://www.coleurope.eu/sites/default/files/research-paper/beer31.pdf.

Bopp, S. K., Kienzler, A., Richarz, A. N., van der Linden, S. C., Paini, A., Parissis, N., et al. (2019). Regulatory assessment and risk management of chemical mixtures: Challenges and ways forward. *Crit. Rev. Toxicol.* 49, 174–189. doi:10.1080/10408444.2019.1579169

Bunchongprasert, K., and Shao, J. (2020). Effect of fatty acid ester structure on cytotoxicity of self-emulsified nanoemulsion and transport of nanoemulsion droplets. *Colloids Surfaces B Biointerfaces* 194, 111220. doi:10.1016/j.colsurfb.2020.111220

Cavanagh, R. J., Smith, P. A., and Stolnik, S. (2019). Exposure to a nonionic surfactant induces a response akin to heat-shock apoptosis in intestinal epithelial cells: Implications for excipients safety. *Mol. Pharm.* 16, 618–631. doi:10.1021/acs.molpharmaceut.8b00934

Dent, M., Amaral, R. T., Da Silva, P. A., Ansell, J., Boisleve, F., Hatao, M., et al. (2018). Principles underpinning the use of new methodologies in the risk assessment of cosmetic ingredients. *Comput. Toxicol.* 7, 20–26. doi:10.1016/j.comtox.2018.06.001

Dini, I., and Laneri, S. (2021). The new challenge of green cosmetics: Natural food ingredients for cosmetic formulations. *Molecules* 26, 3921. doi:10.3390/molecules26133921

Djapovic, M., Milivojevic, D., Ilic-Tomic, T., Lješević, M., Nikolaivits, E., Topakas, E., et al. (2021). Synthesis and characterization of polyethylene terephthalate (PET) precursors and potential degradation products: Toxicity study and application in discovery of novel PETases. *Chemosphere* 275, 130005. doi:10.1016/j.chemosphere.2021.130005

Ebele, A. J., Abou-Elwafa Abdallah, M., and Harrad, S. (2017). Pharmaceuticals and personal care products (PPCPs) in the freshwater aquatic environment. *Emerg. Contam.* 3, 1–16. doi:10.1016/j.emcon.2016.12.004

Fabbron-Appas, C. T., Pandey, P., Parekh, H. S., Sales, C. C., Duque, M. D., Andréo-Filho, N., et al. (2021). Impact of different emollient esters on body emulsions: Sensory, physicochemical, and biometrological characterization. *J. Sens. Stud.* 36. doi:10.1111/joss.12660

Fagan, K. A., and Portman, D. S. (2014). Sexual modulation of neural circuits and behavior in *C. elegans*. *Semin. Cell Dev. Biol.* 33, 3–9. doi:10.1016/j.semcdb.2014.06.007

Farias, C. B. B., Almeida, F. C. G., Silva, I. A., Souza, T. C., Meira, H. M., and Soares da Silva, R. de C. F. (2021). Production of green surfactants: Market prospects. *Electron. J. Biotechnol.* 51, 28–39. doi:10.1016/j.ejbt.2021.02.002

Felzenszwalb, I., Fernandes, A. da S., Brito, L. B., Oliveira, G. A. R., Silva, P. A. S., Arcanjo, M. E., et al. (2019). Toxicological evaluation of nail polish waste discarded in the environment. *Environ. Sci. Pollut. Res.* 26, 27590–27603. doi:10.1007/s11356-018-1880-y

Feng, J., Valkova, Z., Lin, E. E., Nourafkan, E., Wang, T., Tcholakova, S., et al. (2022). Minimum surfactant concentration required for inducing self-shaping of oil droplets and competitive adsorption effects. *Soft Mat.* 18, 6729–6738. doi:10.1039/d1sm01326b

Garofalakis, G., Murray, B. S., and Sarney, D. B. (2000). Surface activity and critical aggregation concentration of pure sugar esters with different sugar headgroups. *J. Colloid Interface Sci.* 229, 391–398. doi:10.1006/jcis.2000.7035

Gaudin, T., Lu, H., Fayet, G., Berthauld-Drelich, A., Rotureau, P., Pourceau, G., et al. (2019). Impact of the chemical structure on amphiphilic properties of sugar-based surfactants: A literature overview. *Adv. Colloid Interface Sci.* 270, 87–100. doi:10.1016/j.cis.2019.06.003

Griffin, W. C. (1954). Calculation of HLB values of non-ionic surfactants. *J. Soc. Cosmet. Chem.* 1, 311–326. doi:10.1002/jps.2600581203

Hill, K., and Rhode, O. (1999). Sugar-based surfactants for consumer products and technical applications. *Lipid - Fett* 101, 25–33. doi:10.1002/(SICI)1521-4133(19991)101:1<25::AID-LIPI25>3.0.CO;2-N

Hollenbach, R., Völp, A. R., Höfert, L., Rudat, J., Ochsenreither, K., Willenbacher, N., et al. (2020). Interfacial and foaming properties of tailor-made glycolipids—influence of the hydrophilic head group and functional groups in the hydrophobic tail. *Molecules* 25, 3797. doi:10.3390/molecules25173797

Hunt, P. R. (2017). The *Caenorhabditis elegans* model in toxicity testing. *J. Appl. Toxicol.* 37, 50–59. doi:10.1002/jat.3357

Hyde, A., Saiuchi, K., Sonobe, S., Shibata, Y., Asakuma, Y., and Phan, C. (2021). Influence of microwave pulsing patterns on oil/water interfacial behavior. *Colloids Surf. A Physicochem Eng. Asp.* 631, 127660. doi:10.1016/j.colsurfa.2021.127660

Judy, J. D., Williams, M., Gregg, A., Oliver, D., Kumar, A., Kookana, R., et al. (2019). Microplastics in municipal mixed-waste organic outputs induce minimal short to long-term toxicity in key terrestrial biota. *Environ. Pollut.* 252, 522–531. doi:10.1016/j.envpol.2019.05.027

Kairaliyeva, T., Aksenenko, E. V., Mucic, N., Makievski, A. V., Fainerman, V. B., and Miller, R. (2017). Surface tension and adsorption studies by drop profile analysis tensiometry. *J. Surfactants Deterg.* 20, 1225–1241. doi:10.1007/s11743-017-2016-y

Kaur, P., Garg, T., Rath, G., Murthy, R. S. R., and Goyal, A. K. (2016). Surfactant-based drug delivery systems for treating drug-resistant lung cancer. *Drug Deliv.* 23, 717–728. doi:10.3109/10717544.2014.935530

Khamkar, G. S. (2011). Self Micro Emulsifying Drug Delivery System (SMEED) o/w microemulsion for BCS class II drugs: An approach to enhance an oral bioavailability. *Int. J. Pharm. Pharm. Sci.* 3, 1–3.

Khan, N. R., and Rathod, V. K. (2015). Enzyme catalyzed synthesis of cosmetic esters and its intensification: A review. *Process Biochem.* 50, 1793–1806. doi:10.1016/j.procbio.2015.07.014

Koursari, N., Johnson, P., Parsa, M., Schneider, M., Trybala, A., and Starova, V. M. (2020). Modelling of foamed emulsion drainage. *Colloids Surf. A Physicochem. Eng. Asp.* 600, 124915. doi:10.1016/j.colsurfa.2020.124915

Kumar, S. (2005). Exploratory analysis of global cosmetic industry: Major players, technology and market trends. *Technovation* 25, 1263–1272. doi:10.1016/j.technovation.2004.07.003

Lanzerstorfer, P., Sandner, G., Pitsch, J., Mascher, B., Aumiller, T., and Weghuber, J. (2021). Acute, reproductive, and developmental toxicity of essential oils assessed with alternative *in vitro* and *in vivo* systems. *Arch. Toxicol.* 95, 673–691. doi:10.1007/s00204-020-02945-6

Larsson, J., Sanchez-Fernandez, A., Mahmoudi, N., Barnsley, L. C., Wahlgren, M., Nylander, T., et al. (2019). Effect of the anomeric configuration on the micellization of hexadecylmaltoside surfactants. *Langmuir* 35, 13904–13914. doi:10.1021/acs.langmuir.9b01960

Lee, S.-M., Wagh, A., Sandhu, G., and Walsh, M. K. (2018). Emulsification properties of lactose fatty acid esters. *Food Nutr. Sci.* 09, 1341–1357. doi:10.4236/fns.2018.912096

Lémery, E., Briançon, S., Chevalier, Y., Bordes, C., Oddos, T., Gohier, A., et al. (2015). Skin toxicity of surfactants: Structure/toxicity relationships. *Colloids Surfaces A Physicochem. Eng. Asp.* 469, 166–179. doi:10.1016/j.colsurfa.2015.01.019

Li, G.-Z., and Friberg, S. E. (1982). Surfactant/cosurfactant association and emulsion stability. *J. Am. Oil Chem. Soc.* 59, 569–572. doi:10.1007/BF02636326

Li, Y., and Xiang, D. (2019). Stability of oil-in-water emulsions performed by ultrasound power or high-pressure homogenization. *PLoS One* 14, 02131899–e213214. doi:10.1371/journal.pone.0213189

Liu, B., Fan, Y., Li, H., Zhao, W., Luo, S., Wang, H., et al. (2021). Control the entire journey of pesticide application on superhydrophobic plant surface by dynamic covalent trimeric surfactant coacervation. *Adv. Funct. Mat.* 31, 2006606. doi:10.1002/adfm.202006606

Łopaciuk, A., and Łoboda, M. (2013). "Global beauty industry trends in the 21st century," in Knowl. Manag. Innov. Knowl. Learn., Zadar, Croatia, 19-21 June 2013, 1079–1087.

Lucarini, S., Fagioli, L., Campana, R., Cole, H., Duranti, A., Baffone, W., et al. (2016). Unsaturated fatty acids lactose esters: Cytotoxicity, permeability enhancement and antimicrobial activity. *Eur. J. Pharm. Biopharm.* 107, 88–96. doi:10.1016/j.ejpb.2016.06.022

Lucarini, S., Fagioli, L., Cavanagh, R., Liang, W., Perinelli, D. R., Campana, M., et al. (2018). Synthesis, structure–activity relationships and *in vitro* toxicity profile of lactose-based fatty acid monoesters as possible drug permeability enhancers. *Pharmaceutics* 10, 81–18. doi:10.3390/pharmaceutics10030081

Martins-Gomes, C., Silva, T. L., Andreani, T., and Silva, A. M. (2022). Glyphosate vs. Glyphosate-based herbicides exposure: A review on their toxicity. *J. Xenobiotics* 12, 21–40. doi:10.3390/jox12010003

Masen, M. (2020). Evaluating lubricant performance to reduce COVID-19 PPE-related skin injury. *PLoS One* 15 (9), e0239363. doi:10.1371/journal.pone.0239363

McCartney, F., Rosa, M., and Brayden, D. J. (2019). Evaluation of sucrose laurate as an intestinal permeation enhancer for macromolecules: *Ex vivo* and *in vivo* studies. *Pharmaceutics* 11, 565. doi:10.3390/pharmaceutics11110565

McClements, D. J., and Jafari, S. M. (2018). Improving emulsion formation, stability and performance using mixed emulsifiers: A review. *Adv. Colloid Interface Sci.* 251, 55–79. doi:10.1016/j.cis.2017.12.001

Nilsson, F., and So, O. (1998). Physical - chemical properties of C 9 G 1 and C 10 G 1 - alkylglucosides. *Phase Diagrams Aggreg. Size/Struct.* 7463, 4050–4058.

Nilsson, F., Söderman, O., and Johansson, I. (1998). Four different C8G1 alkylglucosides. Anomeric effects and the influence of straight vs branched hydrocarbon chains. *J. Colloid Interface Sci.* 203, 131–139. doi:10.1006/jcis.1998.5487

Pappalardo, V. M., Boeriu, C. G., Zaccheria, F., and Ravasio, N. (2017). Synthesis and characterization of arabinose-palmitic acid esters by enzymatic esterification. *Mol. Catal.* 433, 383–390. doi:10.1016/j.mcat.2017.02.029

Para, G., Jarek, E., and Warszynski, P. (2006). The Hofmeister series effect in adsorption of cationic surfactants-theoretical description and experimental results. *Adv. Colloid Interface Sci.* 122, 39–55. doi:10.1016/j.cis.2006.06.017

Patruno, C., Fabbrocini, G., Stingeni, L., and Napolitano, M. (2020). The role of occupational dermatology in the COVID-19 outbreak. *Contact Dermat.* 83, 174–175. doi:10.1111/cod.13568

Pe, B., Anankanbil, S., and Guo, Z. (2017). Synthesis of sugar fatty acid esters and their industrial utilizations. *Fat. Acids* 2017, 329–354. doi:10.1016/B978-0-12-809521-8.00010-6

Place, M. (2020). *In vivo* eco-toxicological assessment of some cationic and amphoteric surfactants in transgenic *Caenorhabditis elegans* CICÎRMA Marius 1,2*. *POMERAI David 3* 25, 19–32.

Rathi, B. S., Kumar, P. S., and Vo, D. V. N. (2021). Critical review on hazardous pollutants in water environment: Occurrence, monitoring, fate, removal technologies and risk assessment. *Sci. Total Environ.* 797, 149134. doi:10.1016/j.scitotenv.2021.149134

Riecan, M., Paluchova, V., Lopes, M., Brejchova, K., and Kuda, O. (2022). Branched and linear fatty acid esters of hydroxy fatty acids (FAHFA) relevant to human health. *Pharmacol. Ther.* 231, 107972. doi:10.1016/j.pharmthera.2021.107972

Rusanov, A. I. (2018). Theory of surfactant diffusion in micellar systems with variable aggregation numbers. *Colloids Surfaces A Physicochem. Eng. Asp.* 551, 158–164. doi:10.1016/j.colsurfa.2018.04.065

Sakoguchi, H., Shintani, T., Ishiyama, H., Yanagita, R. C., Kawanami, Y., and Sato, M. (2019). Nematocidal activity of 6-O-octanoyl- and 6-O-octyl-D-allose against larvae of *C. elegans*. *Biosci. Biotechnol. Biochem.* 83, 2194–2197. doi:10.1080/09168451.2019.1648206

Shao, S., Shi, Y., Wu, Y., Bian, L., and Zhu, Y. (2018). Lipase-Catalyzed synthesis of sucrose monolaurate and its antibacterial property and mode of action. *Molecules* 23 (5), 1118. doi:10.3390/molecules23051118

Sharma, S., and Sarangdevot, K. (2012). Nanoemulsions for cosmetics. *IJARPB* 2, 408–415.

Snoch, W., Wnuk, D., Witko, T., Staroń, J., Bojarski, A. J., Jarek, E., et al. (2021). In Search of effective anticancer agents—novel sugar esters based on polyhydroxyalkanoate monomers. *Int. J. Mol. Sci.* 22 (13), 7238. doi:10.3390/ijms22137238

Snoch, W., Stępień, K., Prajsnar, J., Staroń, J., Szaleniec, M., and Guzik, M. (2019). Influence of chemical modifications of polyhydroxyalkanoate-derived fatty acids on their antimicrobial properties. *Catalysts* 9, 510. doi:10.3390/catal9060510

Staroń, J., Dąbrowski, J. M., Cichoń, E., and Guzik, M. (2018). Lactose esters: Synthesis and biotechnological applications. *Crit. Rev. Biotechnol.* 38, 245–258. doi:10.1080/07388551.2017.1332571

Steinbiichel, A., and Steinbiichel, A. (1995). Diversity of bacterial polyhydroxyalkanoic acids. *FEMS Microbiol. Lett.* 128, 219–228. doi:10.1016/0378-1097(95)00125-O

Stiernagle, T. (2006). Maintenance of *Caenorhabditis elegans*. *WormBook* 2006, 1–11. doi:10.1895/wormbook.1.101.1

Tang, L., Zhang, Y., Li, C., Zhou, Z., Nie, X., Chen, Y., et al. (2022). Biological stability of water-based cutting fluids: Progress and application. *Chin. J. Mech. Eng.* 35, 3. doi:10.1186/s10033-021-00667-z

Taha, A., Ahmed, E., Ismaiel, A., Ashokkumar, M., Xua, X., Pana, S., et al. (2020). Ultrasonic emulsification: An overview on the preparation of different emulsifiers-stabilized emulsions. *Trends Food Sci. Technol.* 105, 363–377. doi:10.1016/j.tifs.2020.09.024

Tortilla, G., Market, C., Chips, T., Size, M., Distribution, B., Forecasts, S., et al. (2019). Report coverage & deliverables key companies & market share insights. 1–6.

Tovar-Sanchez, A., Sparaventi, E., Gaudron, A., and Rodriguez-Romero, A. (2020). A new approach for the determination of sunscreen levels in seawater by ultraviolet absorption spectrophotometry. *PLoS One* 15, e0243591. doi:10.1371/journal.pone.0243591

Tuvia, S., Pelled, D., Marom, K., Salama, P., Levin-Arama, M., Karmeli, I., et al. (2014). A novel suspension formulation enhances intestinal absorption of macromolecules via transient and reversible transport mechanisms. *Pharm. Res.* 31, 2010–2021. doi:10.1007/s11095-014-1303-9

van Kempen, S. E. H. J., Schols, H. A., van der Linden, E., and Sagis, L. M. C. (2014). Effect of variations in the fatty acid chain on functional properties of oligofructose fatty acid esters. *Food Hydrocoll.* 40, 22–29. doi:10.1016/j.foodhyd.2014.01.031

Van Kempen, S. E. H. J., Schols, H. A., Van Der Linden, E., and Sagis, L. M. C. (2013). The effect of diesters and lauric acid on rheological properties of air/water interfaces stabilized by oligofructose lauric acid monoesters. *J. Agric. Food Chem.* 61, 7829–7837. doi:10.1021/jf4018355

Velásquez-Cock, J., Serpa, A. M., Gomez-Hoyos, C., Ganan, P., Romero-Saez, M., Velez, L. M., et al. (2021). Influence of a non-ionic surfactant in the microstructure and rheology of a pickering emulsion stabilized by cellulose nanofibrils. *Polymers* 13 (21), 3625. doi:10.3390/polym13213625

Vinarov, Z., Katev, V., Radeva, D., Tcholakova, S., and Denkov, N. D. (2018). Micellar solubilization of poorly water-soluble drugs: Effect of surfactant and solubilizate molecular structure. *Drug Dev. Ind. Pharm.* 44, 677–686. doi:10.1080/03639045.2017.1408642

Watanabe, T., Kawai, T., and Nonomura, Y. (2018). Effects of fatty acid addition to oil-in-water emulsions stabilized with sucrose fatty acid ester. *J. Oleo. Sci.* 67 (3), 307–313. doi:10.5650/jos.ess17097

Wittkowski, P., Marx-Stoelting, P., Violet, N., Fetz, V., Schwarz, F., Oelgeschläger, M., et al. (2019). *Caenorhabditis elegans* as a promising alternative model for environmental chemical mixture effect assessment - a comparative study. *Environ. Sci. Technol.* 53, 12725–12733. doi:10.1021/acs.est.9b03266

Ye, R., Hayes, D. G., Burton, R., Liu, A., Harte, F. M., and Wang, Y. (2016). Solvent-free lipase-catalyzed synthesis of technical-grade sugar esters and evaluation of their physicochemical and bioactive properties. *Catalysts* 6, 78. doi:10.3390/catal6060078

Zhang, X., Wei, W., Cao, X., and Feng, F. (2015). Characterization of enzymatically prepared sugar medium-chain fatty acid monoesters. *J. Sci. Food Agric.* 95, 1631–1637. doi:10.1002/jsfa.6863

Zhou, Z. H., Zhang, Q., Liu, Y., Wang, H. Z., Cai, H. Y., Zhang, F., et al. (2014). Effect of fatty acids on interfacial tensions of novel sulfobetaines solutions. *Energy Fuels* 28, 1020–1027. doi:10.1021/ef402416j

"Physicochemical studies of novel sugar fatty acid esters based on (*R*)-3-hydroxylated acids derived from bacterial polyhydroxyalkanoates and their potential environmental impact"

Wojciech Snoch [1], Ewelina Jarek[1], Dusan Milivojevic[2], Jasmina Nikodinovic-Runic[2], Maciej Guzik[1*]

[1] Jerzy Haber Institute of Catalysis and Surface Chemistry, Polish Academy of Sciences, Niezapominajek 8, 30-239 Kraków, Poland

[2] Institute of Molecular Genetics and Genetic Engineering (IMGGE) University of Belgrade

*** Correspondence:**
Maciej Guzik
maciej.guzik@ikifp.edu.pl; Tel.: +48-12-6395-159

Keywords: polyhydroxyalkanoates, sugar esters, cosmetic industry, Nematoda, environmental impact

SUPPLEMENTARY

Table S1. Purity, efficiency and yields of the obtained SFAE.

Compound name:	Mas of the obtained ester [g]	Purity [%]	Mass expected if 100% was monoester [g]	Yield 1 [%]	Mass expected if 100% was diester	Yield 2 [%]
C9-glu	0.328	84.78	2.779	10.01	3.995	6.96
C9-gal	0.278	84.45	2.779	8.44	3.995	5.87
C9-lac	0.135	94.59	2.092	6.10	2.700	4.73
mPHN-glu	0.593	87.73	1.25	41.53	3.124	16.65
mPHN-gal	0.6	89.05	1.25	42.67	3.124	17.10
mPHN-lac	0.118	93.86	1.87	5.93	2.436	4.55

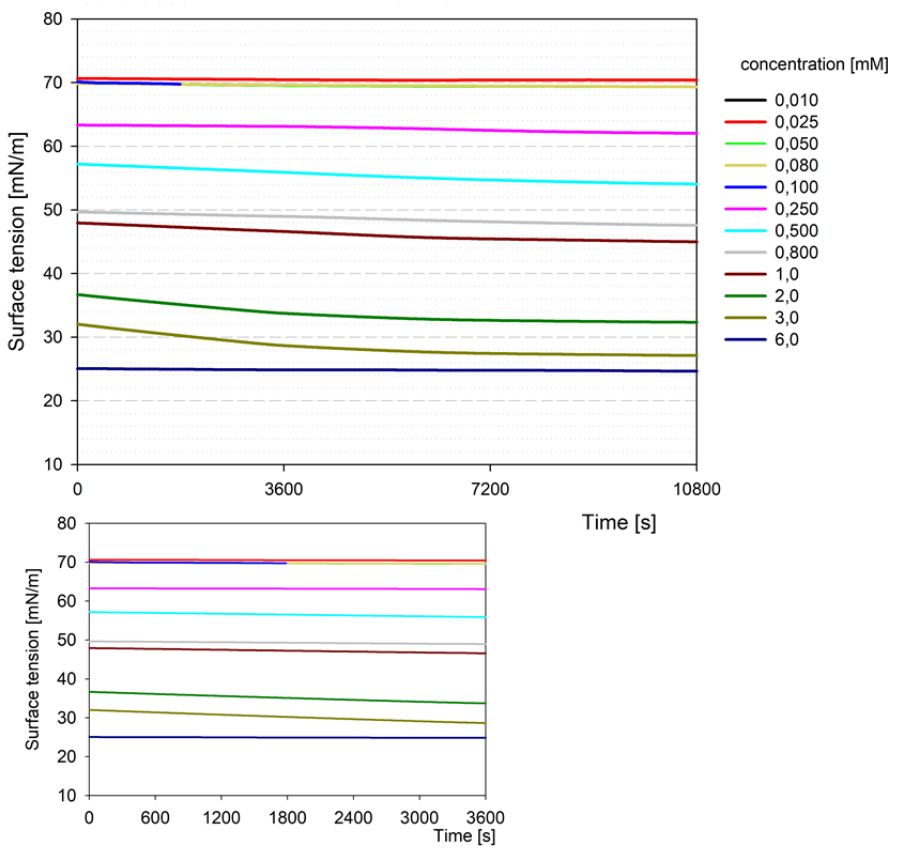

a) C9-glu

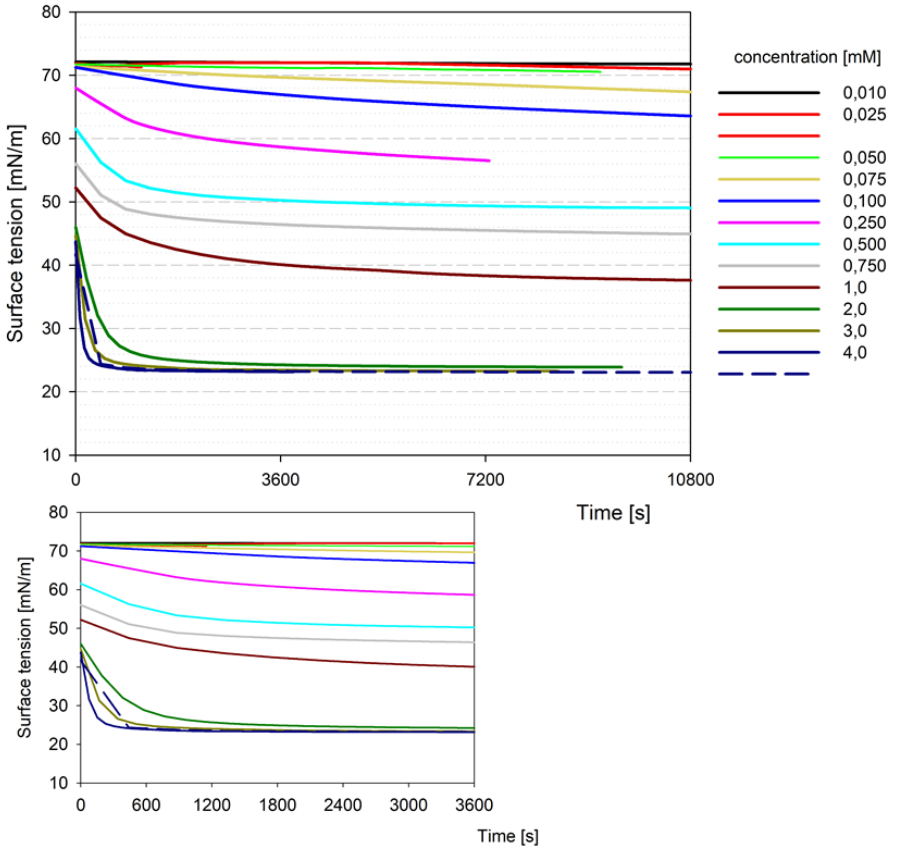

b) C9-gal

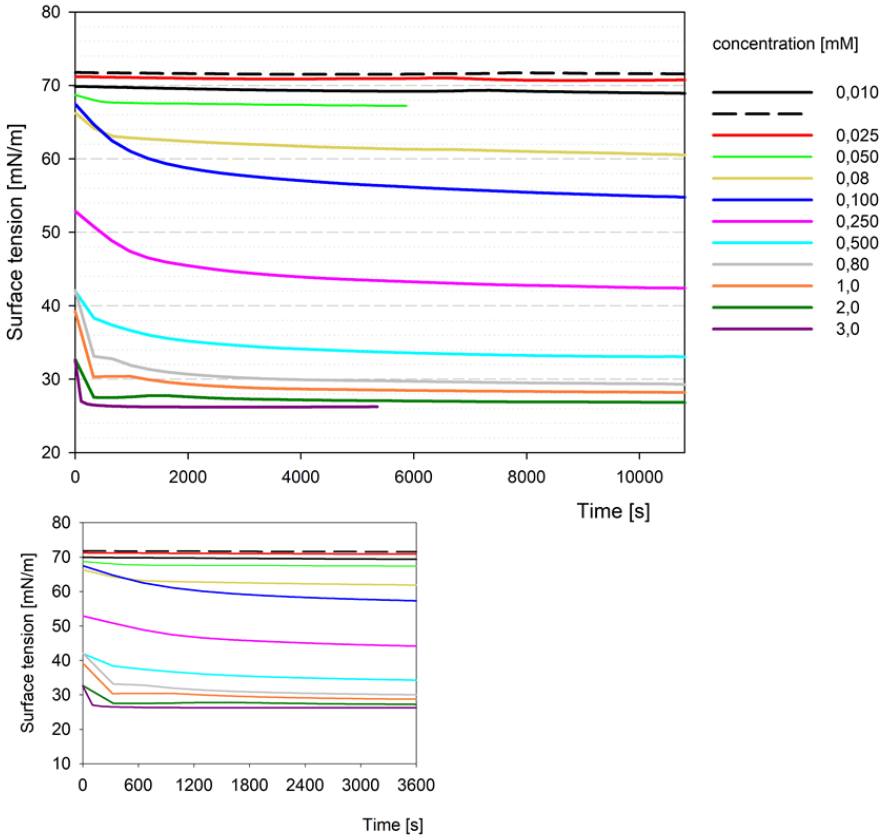

c) C9-lac

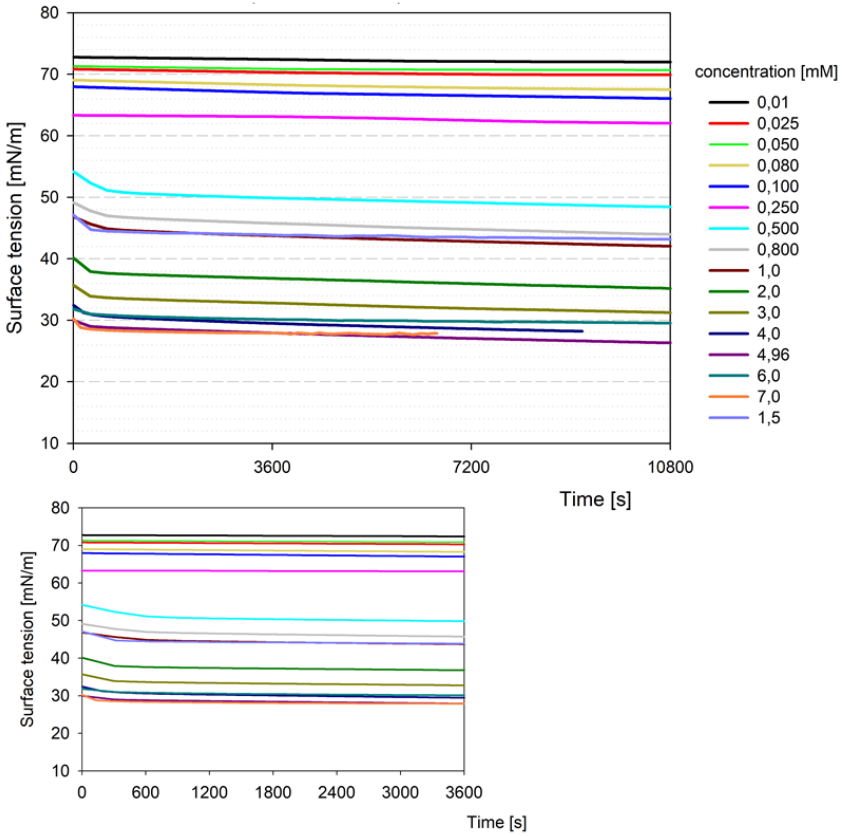

d) mPHN-glu

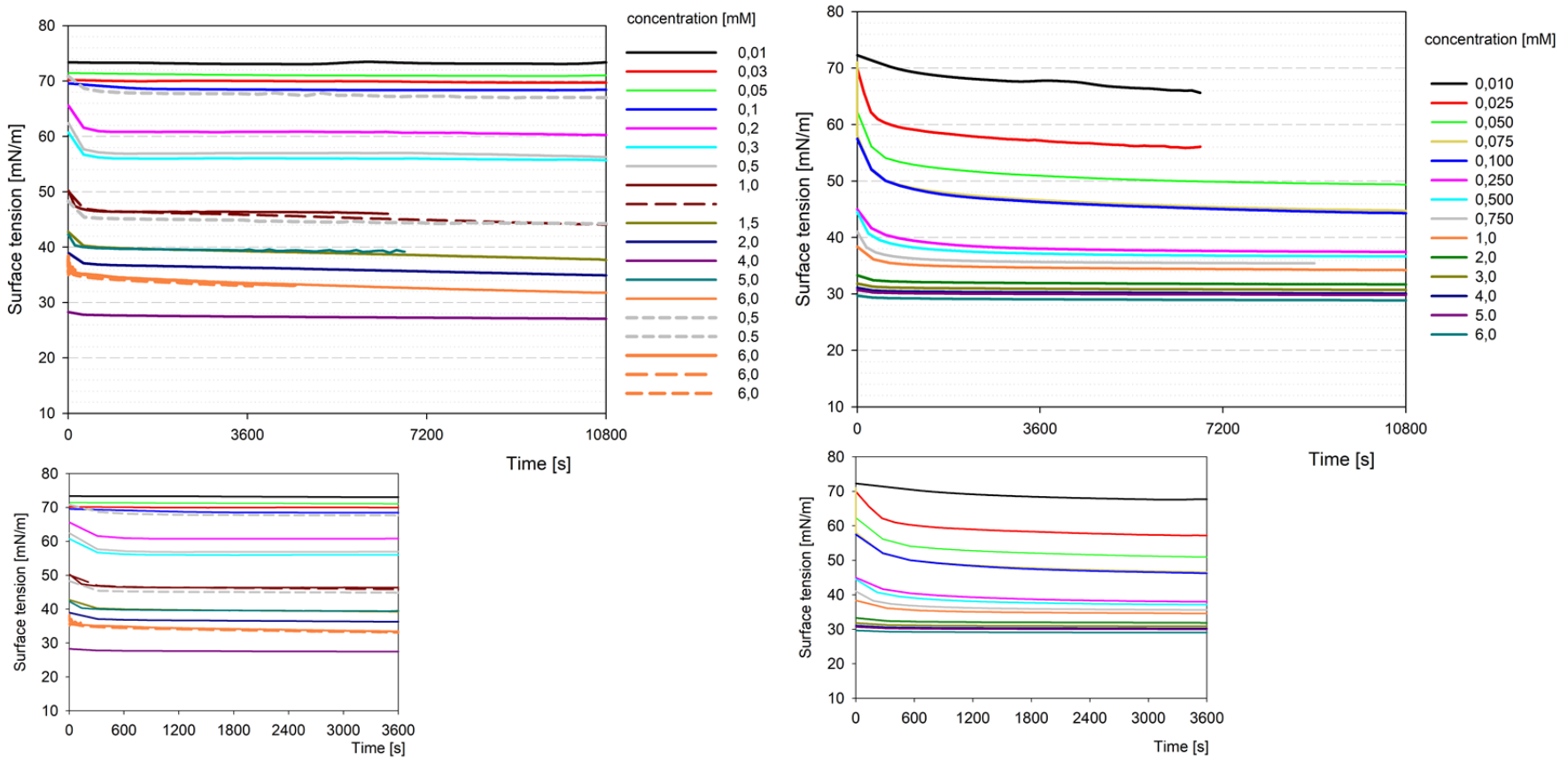

e) mPHN-gal

f) mPHN-lac

Fig S1. Interfacial tension changes in time depending on sugar ester concentration

0	1	2	3	4
	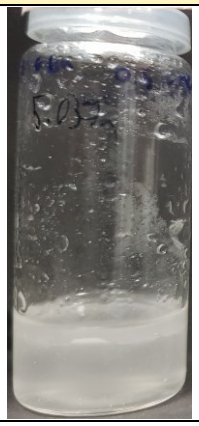		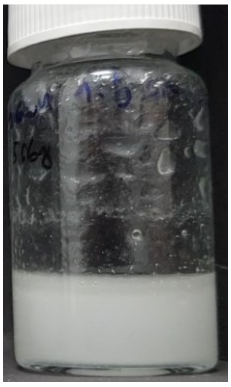	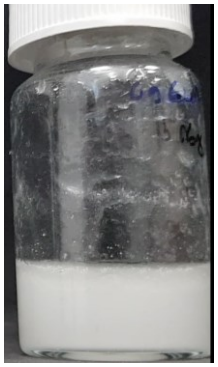
C9-glu squalane- before start making emulsion	C9-glu squalene, 30 min, 0.5 × CAC	C9-glu squalene, 5min, 0.5 × CAC	C9-glu olive 1min, 1.5 × CAC	C9-glu olive 0min, just after mixing, 1.5 × CAC
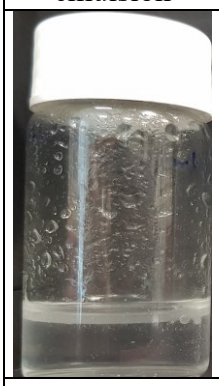				
mPHN-lac squalane- after 24h	mPHN-lac squlane 30 min, 1.0 × CAC	mPHN-lac squalene 5 min 1.5 × CAC	mPHN-lac squalane 0 min	mPHN-lac olive 0 min

Figure S2. Exemplary photos of the formed emulsions stabilized by SFAE